MULTI-PULSE HOMOCLINIC PHENOMENA IN RESONANT HAMILTONIAN SYSTEMS

Thesis by

György Haller

In Partial Fulfillment of the Requirements

for the degree of

Doctor of Philosophy

California Institute of Technology

Pasadena, California

1994

(Submitted July 7, 1993)

To my family:
Anyu, Apu, Laci and Andi

Acknowledgements

First, I would like to thank my advisor, Professor Stephen Wiggins, for continuous guidance, encouragement and support over the past three years. His close attention and criticism helped a great deal in developing the ideas of this thesis. Next, special thanks go to Professor Gábor Stépán of TUB, Hungary, for the many things he taught me and for his continued friendship. I would also like to thank Professors Péter Moson and Miklós Farkas of TUB, Hungary, for introducing me to the subject of dynamical systems and helping in many ways. I am grateful to Professor Jerry Marsden for his attention to this work and for his useful comments.

Besides academic help, I greatly benefited from the friendship of many people during my stay at Caltech. Most importantly, I would like to thank Igor Mezić for the good time we spent together sharing the same office, and for his willingness to help. The love, support, and kindness of my parents and my brother always made it easier for me to overcome difficulties and remain enthusiastic. Finally, I would like to thank my wife for her patience and love which made all this possible.

Abstract

In this thesis we develop a global perturbation method to detect homoclinic orbits which arise in perturbations of manifolds of equilibria with a homoclinic structure in two-degree-of-freedom Hamiltonian systems. Our *energy-phase method* gives conditions for the existence of multiple-pulse and "jumping" orbits asymptotic to different invariant sets within a slow manifold of the perturbed system. The perturbations we consider are either Hamiltonian or weakly dissipative, and the orbits created by these perturbations are generic in both cases. The geometric criterion we derive requires simple algebraic manipulations and detects orbits which are not amenable to Melnikov-type methods, even if those methods are combined with geometric singular perturbation theory. We apply the energy-phase method to the analysis of three-degree-of-freedom resonant Hamiltonian normal forms and prove the existence of *non-exponentially small* splittings of separatrices connecting invariant tori. These structures, together with *double-pulse homoclinic tori*, exist arbitrarily close to resonant elliptic equilibria in a class of Hamiltonian systems. As another application, we consider a two-mode truncation of the driven nonlinear Schrödinger equation and establish the existence of chaotic multiple-pulse "jumping orbits" which can be arranged in a *fractal structure*. We confirm the predictions of the energy-phase method by numerical simulation and visualization of intersecting multi-pulse orbit cylinders.

Contents

Chapter 1

Introduction

One of the most vigorously developing fields in the theory of dynamical systems is Hamiltonian dynamics. The reason is that many physical processes with a conserved energy-type quantity can be put in the Hamiltonian framework, i.e., can be described by a set of ordinary differential equations which directly derive from the conserved quantity. Naturally, most macroscopic systems are subject to various forms of dissipative effects which counteract with the conservation of energy. Still, if the magnitude of the dissipation is small, one can view the dissipative model as a small perturbation of a Hamiltonian limit. The motivation for such an approach is the fact that Hamiltonian systems usually admit much more structure in their phase space and are amenable to efficient geometric methods.

This dissertation is concerned with one aspect of Hamiltonian systems, namely, the analysis of hyperbolic manifolds of equilibria. One's immediate feeling about this subject is probably some doubt whether such a nongeneric situation (i.e., the presence of a whole manifold of fixed points) deserves any study at all. Yet, manifolds of equilibria frequently appear in the study of physical models. One encounters them in laser optics, the theory of water waves, molecular dynamics, nonlinear vibrations of plates, shells, and archs,

just to name a few. The underlying physical situation is quite different in each case but there is one common element in these problems which lies behind the appearence of manifolds of (relative) equilibria: the presence of a *resonance*. Since resonances are ubiquitous in dynamical systems, it seems useful to study this structure, a manifold of equilibria, which is so closely tied up with them.

Resonances have long been known to cause irregular or chaotic behavior. Their peculiarity is demonstratated by plenty of experimental and numerical evidence, as well as by the fact that their mathematical analysis usually requires special methods. Many of these methods are yet to be developed, especially for higher-degree-of-freedom Hamiltonian systems. We hope to contribute to this program by a careful study of a special class of chaotic phenomena arising from perturbations of manifolds of equilibria.

First, let us discuss through two examples why manifolds of equilibria, or briefly *resonant manifolds*, are so common in the study of resonant Hamiltonians. As a first example, one may think of Hamiltonian systems with a rotational or S^1 symmetry. Under certain conditions the presence of such a symmetry makes it possible to reduce the number of degrees of freedom in the problem by one and analyze this lower dimensional Hamiltonian system. One can immediately recover motions in the full system based on the knowledge of trajectories in the reduced system. In particular, a fixed point or *relative equilibrium* of the reduced problem indicates the presence of a periodic orbit for the full system. As an important example, we mention that the truncated normal forms of resonant Hamiltonians (see chapter 3) always have an *internal S^1 symmetry* (i.e., a symmetry resulting from the construction of the normal form) hence relative equilibria appear in their analysis. In addition, these normal forms frequently have additional *external symmetries*, i.e., symmetries originating from the properties of the

underlying physical problem. A sufficient number of these symmetries is enough to make the reduced system integrable, which of course implies integrability for the full truncated normal form. A general feature of integrable Hamiltonians is that their periodic solutions appear in families. In a large class of resonances (see, e.g., those discussed in chapter 3) a subset of this family consists of orbits *of the same period.* For these systems the presence of one relative equilibrium implies the presence of a *family of relative equilibria* in the reduced system. This family of fixed points typically has a manifold structure, hence we obtain a *manifold of relative equilibria* for the reduced system.

Another example for resonant manifolds is provided by Hamiltonians with an explicit periodic time-dependence. Such Hamiltonians arise in the description of many conservative systems subject to parametric forcing. The most efficient way of approaching these problems is to apply some form of *averaging* with respect to time and study the averaged equations. Similarly to the above example, a fixed point of the averaged equation indicates that the full system has a periodic orbit with a period which is some multiple of the period of the forcing, at least up to the precision characteristic of the averaging method. In other words, the system has a periodic orbit *in resonance* with the parametric forcing. Again, if the averaged problem is integrable, its periodic orbits occur in families. If, in addition, the unforced problem itself contains some internal resonance (say of the type considered in the first example), a subset of these families may contain orbits of the same period. This, in analogy with our first example, leads to the existence of a whole manifold of equilibria in the averaged equations, which represent a family of resonant periodic orbits for the full system.

In both of these examples the full Hamiltonian system contains a family of periodic orbits, which are in resonance either with the action of a symmetry group or with some

external forcing. Both examples can be generalized: the Hamiltonian system may possess higher dimensional invariant structures (e.g., n-tori) which are in resonance with the action of a multi-parameter symmetry group and appear as a manifold of relative equilibria after a reduction with respect to that symmetry group. Similarly, one can imagine a quasiperiodic forcing in resonance with a family of quasiperiodic motions in the unforced system, which yields a manifold of equilibria in the multi-frequency-averaged equations.

The weak point of these examples is that they assume the integrability of the reduced and averaged equations, respectively. One can, however, replace this requirement with the physically more realistic assumption of *near-integrability*. In this case the averaged or reduced equations will generically not contain resonant manifolds but will be small perturbations of systems which do admit such structures. Surprisingly many problems can be cast in this form (see section 1.1 for a brief review), a fact which gives strong enough motivation for a perturbation theory for resonant manifolds.

When one starts thinking about perturbation issues, the very first thing to clarify is the stability type of the object to be perturbed. In the Hamiltonian framework, apart from singular cases, one may have elliptic manifolds, hyperbolic manifolds, or manifolds with both elliptic and hyperbolic directions. Elliptic stability is usually harder to deal with, but there is a more practical reason why we will be interested in hyperbolic manifolds in this thesis. Our goal is to investigate geometric structures in the phase space carrying the source of irregularity which resonances are noted for. *Elliptic manifolds of equilibria* are surrounded by regular invariant structures, the majority of which are robust under perturbation. Thus elliptic resonant manifolds will not have a characteristic effect on the global dynamics of the phase space of a resonant system, whatever happens to them under perturbation. *Resonant manifolds of elliptic-hyperbolic-type* are more inter-

esting because in an integrable problem they admit *homoclinic* or *heteroclinic* manifolds. These latter manifolds extend over a larger domain of the phase space and therefore have some global influence on the dynamics. Yet, by the presence of elliptic directions, these homoclinic or heteroclinic structures do not have the largest dimension possible, hence their effect will be tangible only for certain families of trajectories. Hence, although they may be considered important for future research, their significance is definitely less in applications than that of *normally hyperbolic resonant manifolds.* These manifolds may participate in *codimension-one* homoclinic or heteroclinic structures of the reduced or averaged phase space, which have a decisive influence on the overall nature of motions. This is especially true after perturbation which typically causes global *homoclinic chaos* with its attendant chaotic *transport* near these structures. Therefore, if one is interested in finding the possible sources of irregularity in resonances, hyperbolic resonant manifolds appear to be promising candidates. It also turns out that they perturb into objects with much more complex chaotic behavior than what may exist in perturbations of hyperbolic *non*-resonant manifolds.

In view of the above discussion, the main theme of this thesis is a perturbation theory for Hamiltonian resonant manifolds. Since all forthcoming chapters contain detailed introductions, here we only sketch the topic of each chapter. First, in chapter 2, we establish a general theory for two-degree-of-freedom Hamiltopnians, the *energy-phase method*, which gives predictions of the fate of normally hyperbolic resonant manifolds, as well as their homoclinic/heteroclinic structures. To apply the method to a given problem, one needs to calculate an *energy-difference function.* This function can be obtained just by restricting the perturbed Hamiltonian to the original resonant manifold. In particular, the derivation of the energy-difference function does not involve evaluation of improper integrals, which is an inconvenient feature of the most widely used global perturbation

technique, the Melnikov-method. The energy-difference function can be used to detect *multi-pulse transverse homoclinic and heteroclinic orbits* which are asymptotic to invariant sets in a *slow manifold* perturbing from the resonant manifold. In most cases the multi-pulse orbits are doubly asymptotic to periodic orbits of the slow manifold which immediately implies the existence of chaotic dynamics related to Smale-horseshoes near the slow manifold. One can also identify certain *resonant internal orbits* on the slow manifold which serve as boundaries between regions with different pulse-numbers. More precisely, the resonant internal orbits separate regions such that in each region the orbits have multi-pulse homoclinic orbits with the same number of pulses for all the orbits in the region. We also analyze the case when there are two separate homoclinic manifolds connecting a resonant hyperbolic manifold to itself. For this situation the energy-difference function can be used to predict the existence of *multiple-pulse jumping homoclinic orbits.* These jumping orbits make several excursions before they settle onto their limit sets and these excursions involve passages near both of the broken homoclinic manifolds. At the end of chapter 2 we extend the results to the case of additional weak dissipation and construct some special orbits (e.g., multi-pulse Silnikov-type orbits).

In chapter 3 we analyze a class of three-degree-of-freedom resonant Hamiltonians in the same spirit as we described earlier in this introduction. We study the corresponding cubic Birkhoff normal form and find an invariant 3-sphere (filled with periodic solutions) on each energy surface. Appropriate subsets of these spheres are normally hyperbolic and admit homoclinic structures. After a symplectic reduction the periodic solutions of a sphere (all of them of the same frequency) appear as relative equilibria interconnected through heteroclinic orbits. We use a *heteroclinic version of the energy-phase method* to show the existence of transverse homoclinic tori and double-pulse homoclinic tori in the truncated normal form. We also visualize these structures iterating the invariant

manifolds of a 4D symplectic map.

In chapter 4 we study a two-mode truncation of the driven nonlinear Schrödinger equation derived by Bishop *et al.* [7]. This truncation can be written in the form of a two-degree-of-freedom Hamiltonian system which, for zero forcing, has a normally hyperbolic invariant manifold with two homoclinic manifolds. This hyperbolic manifold contains a *circle of fixed points* which can be blown up to an *annulus of fixed points.* Following the techniques of section 2.4, one can analyze this hyperbolic manifold of equilibria and use the energy-phase method to show the existence of transverse jumping multi-pulse homoclinic orbits. We also show that these orbits can be organized into layers which together form a *fractal structure.*

We believe that the theory presented here is fairly self-contained and ready for further applications. However, the analysis of the two examples we consider here will only be complete if the sophisticated phase-space structures found through the energy-phase method are properly related to the underlying physical problems. In the case of three-degree-of-freedom resonances (chapter 3), one can use the results presented here to explain the phenomenon of *chaotic irreversible energy-transfer* in systems of three resonant coupled oscillators. As far as the two-mode truncation of the NLS is considered (chapter 4), one can use the results to argue about the nature of *jumping chaos* (i.e., chaotic time-evolution of a spatially localized solitary wave) found in numerical studies of the full partial differential equation. All this is subject to current research and will appear elsewhere.

Chapter 2

The energy-phase method

2.1 Motivation and notation

In most of this chapter we will be concerned with two-degree-of-freedom Hamiltonian systems of the form

$$\begin{aligned} \dot{x} &= J_2 D_x H_0(x, I; \mu) + \varepsilon J_2 D_x H_1(x, I, \phi; \mu, \varepsilon), \\ \dot{I} &= -\varepsilon D_\phi H_1(x, I, \phi; \mu, \varepsilon), \\ \dot{\phi} &= D_I H_0(x, I; \mu) + \varepsilon D_I H_1(x, I, \phi; \mu, \varepsilon), \end{aligned} \tag{2.1.1}$$

defined on the phase space $\mathcal{P} = \mathbb{R}^2 \times \mathbb{R} \times S^1$ equipped with the symplectic form $\omega = dx_1 \wedge dx_2 + d\phi \wedge dI$. We will refer to the individual equations in (2.1.1) as $(2.1.1)^x$, $(2.1.1)^I$ and $(2.1.1)^\phi$, respectively. In (2.1.1) μ is a p-dimensional vector of parameters taken from some open set $W \subset \mathbb{R}^p$, and

$$J_2 = \begin{pmatrix} 0 & 1 \\ -1 & 0 \end{pmatrix}.$$

The corresponding Hamiltonian $H = H_0 + \varepsilon H_1$ is assumed to be C^{r+1} smooth in its arguments ($r \geq 3$). Setting $\varepsilon = 0$ in (2.1.1) (denoted as $(2.1.1)_{\varepsilon=0}$) we obtain an integrable unperturbed system with Hamiltonian $H_0(x, I; \mu)$. We make the following assumption on this integrable system:

(H1) *There exist* $I_1, I_2 \in \mathbb{R}$, $I_1 < I_2$ *such that for any* $(I,\mu) \in [I_1, I_2] \times W$ $(2.1.1)^x_{\varepsilon=0}$ *has a hyperbolic fixed point* $\bar{x}_0(I;\mu)$ *connected to itself by a homoclinic trajectory* $x^h(t, I; \mu)$.

For every fixed $\mu \in W$ assumption (H1) implies the existence of a normally hyperbolic invariant 2-manifold (with boundary) $\mathcal{A}_0$ for system $(2.1.1)_{\varepsilon=0}$ in the form

$$\mathcal{A}_0 = \{ (x, I, \phi) \in \mathcal{P} \mid x = \bar{x}^0(I;\mu),\, I \in [I_1, I_2],\, \phi \in S^1 \}, \tag{2.1.2}$$

which can be considered as the image of the annulus $A = [I_1, I_2] \times S^1$ under the embedding

$$\begin{aligned} g_0 \colon A &\to \mathcal{P}, \\ (I, \phi) &\mapsto (\bar{x}^0(I;\mu), I, \phi). \end{aligned} \tag{2.1.3}$$

Note that both $\mathcal{A}_0$ and g_0 depend on μ but this will be suppressed for notational simplicity.

It is easy to see that $\mathcal{A}_0$ has a three dimensional stable manifold $W^s(\mathcal{A}_0)$ and a three dimensional unstable manifold $W^u(\mathcal{A}_0)$ which coincide in the homoclinic manifold W_0 (see Fig. 2.1). The solutions of $(2.1.1)_{\varepsilon=0}$ on W_0 can be written in the form

$$y_0(t, I, \phi_0; \mu) = \begin{pmatrix} x^h(t, I; \mu) \\ I \\ \phi_0 + \int_0^t D_I H_0(x^h(\tau, I; \mu), I; \mu)\, d\tau \end{pmatrix}. \tag{2.1.4}$$

Since $\mathcal{A}_0$ is a compact normally hyperbolic invariant manifold, for small $\varepsilon > 0$ system (2.1.1) has a two dimensional invariant manifold $\mathcal{A}_\varepsilon$ which is C^r ε-close to $\mathcal{A}_0$, and hence still a C^r embedding of the annulus A through a map

$$\begin{aligned} g_\varepsilon \colon A &\to \mathcal{P}, \\ (I, \phi) &\mapsto (\bar{x}^\varepsilon(I, \phi; \mu), I, \phi) = (\bar{x}^0(I;\mu) + \varepsilon x^1(I, \phi; \mu, \varepsilon), I, \phi). \end{aligned} \tag{2.1.5}$$

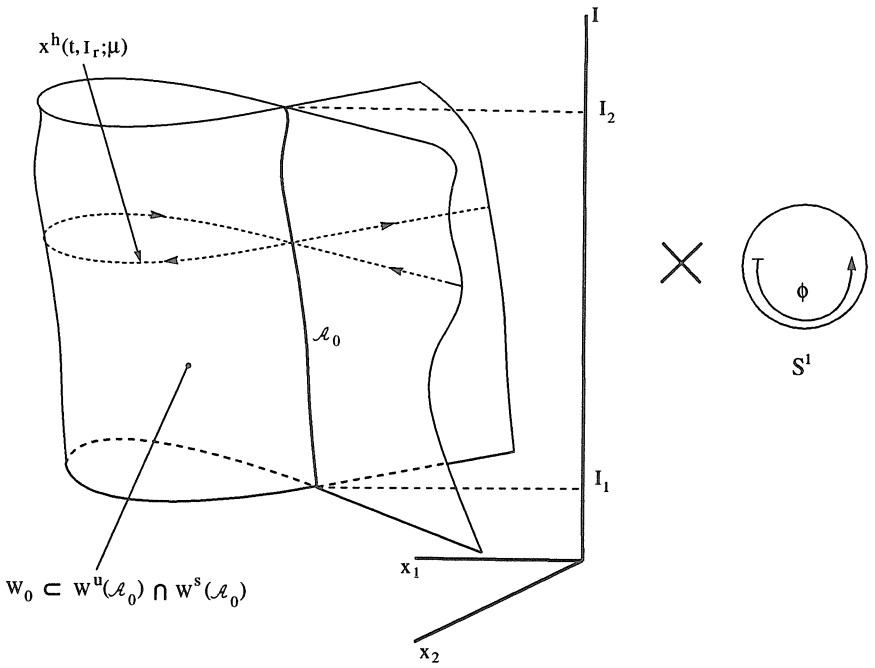

Figure 2.1: The manifolds $\mathcal{A}_0$ and W_0

Let $i_\varepsilon\colon \mathcal{A}_\varepsilon \hookrightarrow \mathcal{P}$ be the inclusion map of $\mathcal{A}_\varepsilon$ with $\varepsilon \geq 0$. Then it can be shown (see Haller and Wiggins [28]) that for small $\varepsilon \geq 0$ $(\mathcal{A}_\varepsilon, i_\varepsilon^*\omega)$ is a symplectic 2-manifold with

$$i_\varepsilon^*\omega = (1 + \mathcal{O}(\varepsilon))d\phi \wedge dI, \tag{2.1.6}$$

on which the vector field of (2.1.1) derives from the *restricted Hamiltonian*

$$\mathcal{H}_\varepsilon = H|\mathcal{A}_\varepsilon = i_\varepsilon^* H. \tag{2.1.7}$$

For small nonzero ε we also have two persisting locally invariant 3-manifolds $W^s_{loc}(\mathcal{A}_\varepsilon)$ and $W^u_{loc}(\mathcal{A}_\varepsilon)$ C^r ε-close to $W^s_{loc}(\mathcal{A}_\varepsilon)$ and $W^u_{loc}(\mathcal{A}_\varepsilon)$, respectively.

Systems of the form (2.1.1) with assumption (H1) have been studied by Holmes and Marsden [31] and Wiggins [74]. These authors also assumed that the manifold

$\mathcal{A}_0$ is foliated by a one parameter family of periodic solutions given by $I = const.$, $\dot{\phi} = D_I H_0(x, I; \mu) \neq 0$. The periodic solutions have two dimensional stable and unstable manifolds coinciding in two dimensional homoclinic submanifolds of W_0. An easy check shows that these submanifolds are isotropic, i.e., the symplectic form ω vanishes restricted to them. Since they also have a dimension half of that of the phase space, they are *Lagrangian submanifolds* of $\mathcal{P}$.

Since periodic orbits on $(\mathcal{A}_\varepsilon, i_\varepsilon^* \omega)$ are structurally stable under small changes in ε, $\mathcal{A}_\varepsilon$ is also foliated by a one parameter family of periodic orbits which are close to their unperturbed counterparts in $\mathcal{A}_0$, and have two dimensional stable and unstable manifolds within $W^s(\mathcal{A}_\varepsilon)$ and $W^u(\mathcal{A}_\varepsilon)$, respectively. The perturbation theory for Lagrangian submanifolds developed in Weinstein [72] implies that for small $\varepsilon \neq 0$ the stable and unstable manifolds of the persisting periodic orbits must still intersect. Using a Melnikov-type analysis Holmes and Marsden [31] gave conditions under which these intersections are transverse within the corresponding level sets

$$E_\varepsilon(h) = \{ (x, I, \phi) \in \mathcal{P} \,|\, H(x, I, \phi; \varepsilon) = h \} \tag{2.1.8}$$

of the Hamiltonian H. This implies the presence of Smale-horseshoes near the perturbed periodic orbits which means chaotic dynamics and nonintegrability for system (2.1.1) (see, e.g., Moser [59]).

Recently Haller and Wiggins reconsidered system (2.1.1) (see [28]) and assumed that either some isolated periodic orbits or all the periodic orbits on $\mathcal{A}_0$ degenerate into circles of equilibria. More precisely, they assumed that *exactly one of the following holds for system (2.1.1)*:

(H2a) *There exists* $I_r \in (I_1, I_2)$ *such that*

$$D_I H_0(\bar{x}_0(I_r;\mu), I_r;\mu) = 0,$$

$$m(I_r;\mu) = D_I^2[H_0(\bar{x}_0(I;\mu), I;\mu)]|_{I=I_r} \neq 0.$$

(H2b) *For every* $I \in [I_1, I_2]$

$$D_I H_0(\bar{x}_0(I;\mu), I;\mu) = 0.$$

In the case of (H2a) we have a circle of equilibria which is surrounded by periodic orbits within $\mathcal{A}_0$ and has coinciding two dimensional stable and unstable manifolds within W_0. In the case of hypothesis (H2b) $\mathcal{A}_0$ itself is a two dimensional normally hyperbolic manifold of equilibria. Since in both cases the presence of equilibria is due to the vanishing frequency $D_I H_0$, one may refer to these manifolds of equilibria as *resonant manifolds*. An important fact is that these resonant manifolds are *isoenergetic*, i.e., the unperturbed Hamiltonian H_0 restricted to them is constant (see the definition of $\mathcal{A}_0$ in (2.1.2) together with the first part of (H2a) and (H2b)). Since, by assumption (H1), the resonant manifold $\mathcal{A}_0$ is hyperbolic, it survives small perturbations and gives rise to a nearby *slow manifold* $\mathcal{A}_\varepsilon$ (see below). Another immediate consequence of the resonance is that the *phase shift*, i.e., the net change of ϕ along orbits on W_0 given by

$$\Delta\phi(I;\mu) = \int_{-\infty}^{+\infty} D_I H_0(x^h(t, I;\mu), I;\mu)\, dt, \tag{2.1.9}$$

is finite either for $I = I_r$ (assumption (H2a)) or for every $I \in [I_1, I_2]$ (assumption (H2b)), see Figs. 2.2a-b. Systems satisfying hypothesis (H2a) arise in the Hamiltonian limit of a number of problems. For example, one encounters circles of equilibria of this kind in the study of parametrically excited plates and shells, surface waves, and shallow archs (see Feng and Sethna [19]-[21], Feng and Wiggins [22], Yang and Sethna [75], and Tien

and Namachchivaya [67]). The driven nonlinear Schrödinger equation of Bishop *et al.* [7]-[8] also satisfies hypothesis (H2a) and served as our main example in [28]. Hyperbolic 2-manifolds of equilibria (hypothesis (H2b)) appear in resonant surface wave problems (Holmes [32]) and in the analysis of a wide class of three-degree-of-freedom Hamiltonian resonances discussed in chapter 3 of this thesis.

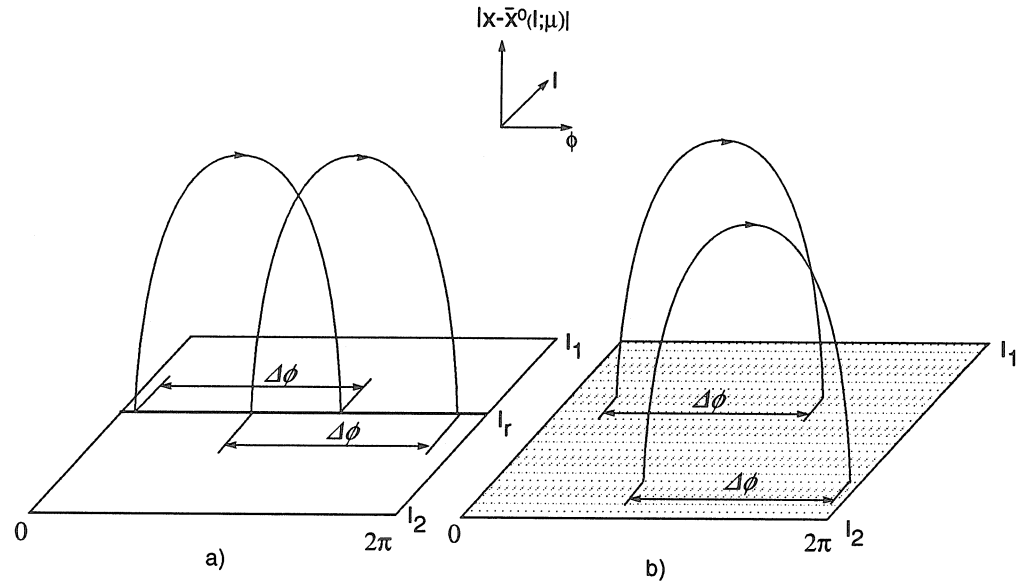

Figure 2.2: The geometric meaning of the phase shift $\Delta\phi$ in the case of hypotheses $(H2a)$ and $(H2b)$, respectively

It is shown in [28] that using methods from regular and singular perturbation theory one can make predictions of what happens in the vicinity of the resonant manifolds above for small nonzero ε. In particular, we established a simple criterion to prove the existence of orbits homoclinic or heteroclinic to various objects on $\mathcal{A}_\varepsilon$. Some of the results for hypothesis (H2a) were also obtained independently by Kovačič [45] with an

application in Kovačič [47].

It turns out, however, that these results give only a partial picture of the complex dynamics which is present near perturbed resonant manifolds. This is the consequence of the fact that the Melnikov-type method, which is used in [28] to tackle the regular perturbation part of the problem, is not particularly well suited to the singular perturbation part of the analysis for three main reasons:

1. The Melnikov-method only gives information about orbits homoclinic to a set $\mathcal{S}_\varepsilon$ of orbits in $\mathcal{A}_\varepsilon$. The set $\mathcal{S}_\varepsilon$ is open and may not cover all of $\mathcal{A}_\varepsilon$; in fact, $\mathcal{S}_\varepsilon$ can be quite small for certain ranges of the parameter μ (see, e.g., the example in [28] or [45]). Moreover, in the case of hypothesis (H2a), one would be more interested to see what happens to the stable and unstable manifolds of periodic orbits which lie near the "core" of the resonance (by core we mean elliptic equilibria generically created in the break-up of the circle of equilibria). However, for typical parameter values this core and its neighborhood does not lie in the set $\mathcal{S}_\varepsilon$ (see again [28] or [45]).

2. Multiple-pulse homoclinic or heteroclinic orbits are not accessible to Melnikov-type methods, but numerical evidence suggests that they exist and the orbits making the same number of pulses form *one-parameter families* (see, e.g., the numerical results presented in chapters 3 and 4 of this thesis).

3. The Melnikov-type method which can be used to study system (2.1.1) concentrates on individual homoclinic or heteroclinic orbits and does not give information about the geometry of the intersecting submanifolds of $W^s(\mathcal{A}_\varepsilon)$ and $W^u(\mathcal{A}_\varepsilon)$, which contain these orbits. In applications, however, this latter kind of information may even be more important if one wants to understand the effect of horseshoes on typical

nearby trajectories.

In this chapter we establish a new global perturbation technique, the *energy-phase method.* This method is different from Melnikov-type methods and is generally applicable to detect orbits homoclinic to perturbed resonant manifolds in two-degree-of-freedom Hamiltonian systems. In contrast to the Melnikov method, it relies on manipulations with simple algebraic or trigonometric equations and does not require evaluation of improper integrals. It is capable of detecting simple transverse or non-transverse homoclinic orbits, as well as transverse or non-transverse *N-pulse homoclinic orbits* to the manifold $\mathcal{A}_\varepsilon$. By N-pulse homoclinic orbit to $\mathcal{A}_\varepsilon$, we mean an orbit negatively asymptotic to some invariant set in $\mathcal{A}_\varepsilon$ which enters and leaves a small neighborhood of $\mathcal{A}_\varepsilon$ N-times to finally return and approach an invariant set of $\mathcal{A}_\varepsilon$ asymptotically. We also show in section 2.5 how the energy-phase method extends to the case of *non-Hamiltonian perturbations* of system (2.1.1).

We give details on the geometry of the multiple-pulse connections and also present a set of unperturbed orbits which can be used to "shadow" a given N-pulse orbit. Moreover, we extend our basic construction to a case when we know more about the geometry of system $(2.1.1)_{\varepsilon=0}$. In particular, we will assume the presence of two manifolds of orbits, W_0^- and W_0^+, homoclinic to the resonant manifold $\mathcal{A}_0$. Under certain conditions we will be able to show the existence of *jumping N-pulse homoclinic orbits* to the slow manifold $\mathcal{A}_\varepsilon$. These are special N-pulse orbits which keep "jumping" between W_0^+ and W_0^-: they may follow W_0^+ during some of their pulses then switch to W_0^- for a while, etc. To describe this complicated motion, one can determine a sequence of two symbols, again, based on the simple analysis of a one-degree-of-freedom problem. Finally, we identify a set of *resonant internal orbits* in $\mathcal{A}_\varepsilon$. These orbits separate regions filled with orbits

which have the same pulse number (i.e., the orbits asymptotic to them make the same number of pulses). All our results can be easily extended to perturbations of manifolds of equilibria which are connected through *heteroclinic manifolds.* This is discussed in chapter 3 in connection with three-degree-of-freedom Hamiltonian resonances.

The exposition of this chapter is as follows. First, in section 2.2 we recollect some general results on invariant manifolds in a form suited to our set-up and perform some estimates to describe the local dynamics around these manifolds. The estimates are stronger than what is actually needed for the purposes of the energy-phase method and may be of independent interest in both the analytical and numerical study of the passage of trajectories near Hamiltonian slow manifolds. In sections 2.3 and 2.4 we establish our main results about nonsimple, i.e., multiple-pulse homoclinic orbits arising in the perturbation of $\mathcal{A}_0$, $W^s(\mathcal{A}_0)$, and $W^u(\mathcal{A}_0)$. We also discuss the detection of jumping N-pulse orbits and the resonant internal orbits mentioned above. In section 2.5 we present an extension of the energy-phase method to weakly dissipative perturbations of system (2.1.1). Finally, in section 2.6 we compare our method to other existing techniques for the detection of multiple-pulse homoclinic orbits.

2.2 Dynamics within and near the invariant manifolds $\mathcal{A}_\varepsilon$, $W^s(\mathcal{A}_\varepsilon)$, and $W^u(\mathcal{A}_\varepsilon)$

From this point we assume that hypothsesis (H2b) holds. The results we derive will be shown to be valid for the case of hypothesis (H2a) in section 2.4. First, we list some features of the invariant manifolds $\mathcal{A}_\varepsilon$, $W^s(\mathcal{A}_\varepsilon)$, and $W^u(\mathcal{A}_\varepsilon)$ introduced in the previous section. We do not deal with their very existence, only refer the reader to the well-known persistence and smoothness results of Fenichel [23] as spelled out for system (2.1.1) in

Haller and Wiggins [28]. We will, however, discuss certain facts about the dynamics on $\mathcal{A}_\varepsilon$, the internal structure of $W^s(\mathcal{A}_\varepsilon)$ and $W^u(\mathcal{A}_\varepsilon)$, as well as the nature of the flow $F_t^\varepsilon(.)$ of (2.1.1) in a neighborhood of $\mathcal{A}_\varepsilon$.

As we noted in the previous section, for small ε $\mathcal{A}_\varepsilon$ is a symplectic manifold on which the *restricted Hamiltonian* $\mathcal{H}_\varepsilon = H|\mathcal{A}_\varepsilon$ generates a vectorfield satisfying

$$\begin{pmatrix} \dot{\phi} \\ \dot{I} \end{pmatrix} = i_\varepsilon^* \omega^\sharp (D_{(\phi,I)} \mathcal{H}_\varepsilon) = \varepsilon J_2 D_{(\phi,I)} \mathcal{H} + \mathcal{O}(\varepsilon^2), \tag{2.2.1}$$

with $i_\varepsilon^* \omega^\sharp : T\mathcal{A}_\varepsilon^* \to T\mathcal{A}_\varepsilon$, $\langle (i_\varepsilon^* \omega^\sharp)^{-1}[p](u), v \rangle = i_\varepsilon^* \omega[p](u,v)$ for all $p \in \mathcal{A}_\varepsilon$, $u, v \in T_p \mathcal{A}_\varepsilon$. The *reduced Hamiltonian* $\mathcal{H}$ in (2.2.1) can be written as

$$\mathcal{H}(I, \phi; \mu) = H_1(\bar{x}^0(I; \mu), I, \phi; \mu, 0), \tag{2.2.2}$$

as shown in [28]. It is related to the restricted Hamiltonian $\mathcal{H}_\varepsilon$ through

$$\mathcal{H}_\varepsilon = h_0 + \varepsilon \mathcal{H} + \mathcal{O}(\varepsilon^2), \tag{2.2.3}$$

with $h_0 = H_0|\mathcal{A}_0 = const.$ (see hypothesis (H2b)). By a slight abuse of notation we will consider $\mathcal{H}(I, \phi; \mu)$ defined on the annulus $A = [I_1, I_2] \times S^1$. Eq. (2.2.3) shows that a structurally stable orbit $\gamma \subset A$ of $\mathcal{H}$ gives rise to an orbit $\gamma_\varepsilon \subset \mathcal{A}_\varepsilon$ of $\mathcal{H}_\varepsilon$ such that $g_\varepsilon^{-1}(\gamma_\varepsilon)$ and γ_0 are C^r ε-close in A. One of our goals will be to find out about the orbits of $\mathcal{H}_\varepsilon$ based on our knowledge of $\mathcal{H}$.

We will say that an orbit $\gamma \subset A$ of some Hamiltonian defined on A is an *internal orbit* if it is either a periodic orbit or an orbit homoclinic to a hyperbolic fixed point, *and* it is bounded away from ∂A. Similarly, an orbit $\gamma_\varepsilon \in \mathcal{A}_\varepsilon$ of the resctricted Hamiltonian $\mathcal{H}_\varepsilon$ is called an internal orbit if ${g_\varepsilon}^{-1}(\gamma_\varepsilon)$ is an internal orbit of the Hamiltonian ${g_\varepsilon}^* \mathcal{H}_\varepsilon$ on $(A, {g_\varepsilon}^* \omega)$. By definition, internal orbits are structurally stable, hence for small ε the internal orbits of the reduced Hamiltonian $\mathcal{H}$ give rise to C^r ε-close internal orbits of ${g_\varepsilon}^* \mathcal{H}_\varepsilon$.

In what follows we will be interested in orbits of (2.1.1) in $\mathcal{P}$ which are asymptotic to internal orbits in $\mathcal{A}_\varepsilon$. The sets of orbits positively (negatively) asymptotic to an internal orbit $\gamma_\varepsilon \subset \mathcal{A}_\varepsilon$ will be denoted by $W^s(\gamma_\varepsilon)$ ($W^u(\gamma_\varepsilon)$). In the case when γ_ε is periodic, this yields the usual definition of stable and unstable manifolds for periodic orbits. If γ_ε is a homoclinic orbit to a fixed point p_ε, we obtain $W^s(\gamma_\varepsilon) = W^s(p_\varepsilon)$ and $W^u(\gamma_\varepsilon) = W^u(p_\varepsilon)$, where $W^s(p_\varepsilon)$ and $W^u(p_\varepsilon)$ are the two dimensional "full" stable and unstable manifolds of p_ε lying in the phase space $\mathcal{P}$.

Our next proposition is a reformulation of the results of Fenichel [24] on the foliation of stable and unstable manifolds (see also [28]). Fenichel was able to relate incoming orbits in $W^s(\mathcal{A}_\varepsilon)$ to their $\omega-$limit sets in $\mathcal{A}_\varepsilon$ in the following way. He showed the existence and persistence of a smooth family of curves, called *fibers*, which foliate $W^s_{loc}(\mathcal{A}_\varepsilon)$. The fibers of the family are usually not invariant individually under the flow but the family itself is invariant, i.e., fibers are mapped into fibers by the underlying flow. Each fiber intersects $\mathcal{A}_\varepsilon$ in a unique point, which we call the *basepoint of the fiber*, and fibers of the unperturbed problem deform smoothly into fibers of the perturbed problem. Most importantly, a solution starting on a fiber of $W^s_{loc}(\mathcal{A}_\varepsilon)$ will be asymptotic to the trajectory in $\mathcal{A}_\varepsilon$ which runs through the basepoint of the fiber, as long as the latter one stays in $\mathcal{A}_\varepsilon$. Similar statements hold for $W^u_{loc}(\mathcal{A}_\varepsilon)$ but, for brevity, we will not list them. To formulate the results precisely, we fix some δ with $\varepsilon << \delta << 1$ and define a closed tubular set U_δ around $\mathcal{A}_0$ by

$$U_\delta = \{(x, I, \phi) \in \mathcal{P} \,|\, |x - \bar{x}^0(I;\mu)| \leq \delta, (I, \phi) \in A\}. \tag{2.2.4}$$

We then have the following result which is a direct application of the general results of Fenichel [24] to system (2.1.1) (see [28] for details.)

Proposition 2.2.1 *There exist* $0 < \varepsilon_0 << \delta_0 << 1$ *such that for every* $\varepsilon \in [0, \varepsilon_0]$

there exists a two parameter family $\mathcal{F}^s_\varepsilon = \cup_{p\in\mathcal{A}_\varepsilon} f^s_\varepsilon(p)$ *of* C^r *smooth curves* $f^s_\varepsilon(p)$ *(with boundary), such that the following hold:*

(*i*) $\mathcal{F}^s_\varepsilon = (W^s_{loc}(\mathcal{A}_\varepsilon) \cup \mathcal{A}_\varepsilon) \cap U_{\delta_0}$ *and* $f^s_\varepsilon(p) \cap \mathcal{A}_\varepsilon = p$.

(*ii*) $\mathcal{F}^s_\varepsilon$ *is* C^{r-1} *in* p *and in* ε.

(*iii*) $\mathcal{F}^s_\varepsilon$ *is a positively invariant family, i.e.,* $F^\varepsilon_t(f^s_\varepsilon(p)) \subset f^s_\varepsilon(F^\varepsilon_t(p))$ *for any* $t \geq 0$ *and* $p \in \mathcal{A}_\varepsilon$ *with* $F^\varepsilon_t(p) \in \mathcal{A}_\varepsilon$.

(*iv*) *There exist* $C_s, \lambda_s > 0$ *such that if* $y \in f^s_\varepsilon(p)$ *then*

$$|F^\varepsilon_t(y) - F^\varepsilon_t(p)| < C_s e^{-\lambda_s t}$$

for any $t \geq 0$ *with* $F^\varepsilon_t(p) \in \mathcal{A}_\varepsilon$.

(*v*) *For any* $p \neq p'$ $f^s_\varepsilon(p) \cap f^s_\varepsilon(p') = \emptyset$.

(*vi*)*For any* $p \neq p'$ *and* $y \in f^s_\varepsilon(p)$, $y' \in f^s_\varepsilon(p')$ *we have*

$$\lim_{t\to\infty} \frac{|F^\varepsilon_t(y) - F^\varepsilon_t(p)|}{|F^\varepsilon_t(y') - F^\varepsilon_t(p)|} = 0.$$

We now turn our attention to the description of the flow near the hyperbolic manifold $\mathcal{A}_\varepsilon$ to obtain some characterization of the trajectories not lying in the local stable and unstable manifolds of $\mathcal{A}_\varepsilon$. The following proposition provides a normal form in a neighborhood of the perturbed manifold, following the basic idea of local normalization sketched in Fenichel [24]. In contrast to his formulation, we do not require analyticity of the vectorfield and give more details on the terms in the normal form. Also, for our specific system (2.1.1) we are able to perform the normalization globally, i.e., in a neighborhood of the whole manifold $\mathcal{A}_\varepsilon$. We do not perform Fenichel's last step in

the construction since it would impose more stringent smoothness hypotheses on system (2.1.1) without a substantial improvment on the normal form. Similar but less specific normalized equations also appeared in the general singular perturbation context of Jones and Kopell [38].

Lemma 2.2.2 *There exist* $0 < \varepsilon_0 << \delta_0 << 1$ *such that for* $\varepsilon \leq \varepsilon_0$ *there is a* C^{r-2} *change of coordinates* $T^\varepsilon: U_{\delta_0} \to \mathbb{R}^2 \times A$, $(x, I, \phi) \mapsto (z, I, \phi)$ *such that* T^ε *is* C^{r-2} *in* ε, *and in the* (z, I, ϕ) *coordinates the flow of (2.1.1) satisfies the equations*

$$\begin{aligned} \dot{z} &= \Lambda(z, I, \phi; \varepsilon) z, \\ \dot{I} &= \varepsilon k_I(z, I, \phi; \varepsilon), \\ \dot{\phi} &= z^T B(z, I, \phi; \varepsilon) z + \varepsilon k_\phi(z, I, \phi; \varepsilon), \end{aligned} \tag{2.2.5}$$

with

$$\Lambda = \begin{pmatrix} \lambda + \langle q_1, z \rangle + \varepsilon k_1 & 0 \\ 0 & -\lambda + \langle q_2, z \rangle + \varepsilon k_2 \end{pmatrix}, \tag{2.2.6}$$

where $\lambda: \mathbb{R} \to \mathbb{R}^+$ *is* C^{r-1}, $k_1, k_2, k_I, k_\phi: \mathbb{R}^2 \times A \times [0, \varepsilon_0] \to \mathbb{R}$ *are* C^{r-2}, $B: \mathbb{R}^2 \times A \times [0, \varepsilon_0] \to \mathbb{R}^{2\times 2}$ *is symmetric and* C^{r-2}, *and* $q_1, q_2: \mathbb{R}^2 \times A \times [0, \varepsilon_0] \to \mathbb{R}^2$ *are* C^{r-3} *functions of their arguments. On* $(\mathcal{P}, T_*^\varepsilon \omega)$ *system (2.2.5) derives from the Hamiltonian* $T_*^\varepsilon H$.

Proof: We know from the persistence theorem of Fenichel [23] that for $\varepsilon \leq \varepsilon_0'$ $\mathcal{A}_\varepsilon$ is a C^r graph over the (I, ϕ) variables with $\varepsilon_0' > 0$ sufficiently small. We first pass from the variable x to $y \in \mathbb{R}^2$ letting

$$x = \bar{x}^\varepsilon(I, \phi; \mu) + y, \tag{2.2.7}$$

where the C^r function $\bar{x}^\varepsilon$ is defined in (2.1.5) for $\varepsilon \leq \varepsilon_0'$. In the new variables (2.1.1)

reads

$$\begin{aligned} \dot{y} &= f_y(y, I, \phi, \varepsilon), \\ \dot{I} &= \varepsilon f_I(y, I, \phi; \varepsilon), \\ \dot{\phi} &= f_\phi(y, I, \phi; \varepsilon), \end{aligned} \tag{2.2.8}$$

where the functions f_y, f_I, and f_ϕ are C^r smooth, and their μ-dependence is suppressed for notational simplicity. Furthermore, they satisfy the equations

$$f_y(0, I, \phi; \varepsilon) = 0, \tag{2.2.9}$$

$$f_\phi(0, I, \phi; 0) = 0, \tag{2.2.10}$$

$$D_y f_\phi(0, I, \phi; 0) = 0. \tag{2.2.11}$$

Here (2.2.9) follows from the invariance of $\mathcal{A}_\varepsilon$, (2.2.10) reflects the fact that $\mathcal{A}_0$ consists of equilibria, and (2.2.11) describes that in $(2.1.1)_{\varepsilon=0}$ the trajectories in $W^s_{loc}(\mathcal{A}_0)$ and $W^u_{loc}(\mathcal{A}_0)$ are asymptotic to $\phi = const.$ planes in positive and negative time, respectively (hence the infinitesimal change of $\dot{\phi}$ is zero for $\varepsilon = 0$ in directions vertical to the manifold $\mathcal{A}_0$). Using (2.2.9) we can write

$$\begin{aligned} f_y(y, I, \phi; \varepsilon) &= \int_0^1 \frac{\partial}{\partial \alpha} f_y(\alpha y, I, \phi; \varepsilon) d\alpha = [\int_0^1 D_y f_y(\alpha y, I, \phi; \varepsilon) d\alpha] y \\ &= L(y, I, \phi; \varepsilon) y = [L_0(I, \phi; \varepsilon) + L_1(y, I, \phi; \varepsilon) y] y, \end{aligned} \tag{2.2.12}$$

where $L_0 \colon A \times [0, \varepsilon_0'] \to \mathbb{R}^{2\times 2}$ is C^{r-1}, and L_1 is a C^{r-2} 3-tensor. Similarly, (2.2.10) and (2.2.11) imply

$$\begin{aligned} f_\phi(y, I, \phi; \varepsilon) &= \int_0^1 \frac{\partial}{\partial \alpha} f_\phi(\alpha y, I, \phi; \alpha\varepsilon) d\alpha = [\int_0^1 D_y f_\phi(\alpha y, I, \phi; \alpha\varepsilon) d\alpha] v \\ &\quad + \varepsilon \int_0^1 D_\varepsilon f_\phi(\alpha y, I, \phi; \alpha\varepsilon) d\alpha \end{aligned}$$

$$= y^T [\int_0^1 \int_0^1 \alpha D_y^2 f_\phi(\alpha\beta y, I, \phi; \alpha\beta\varepsilon) d\alpha d\beta] y$$

$$+\varepsilon[\int_0^1 \alpha D_\varepsilon D_y f_\phi(\alpha\beta y, I, \phi; \alpha\beta\varepsilon) d\alpha d\beta] y + \varepsilon \int_0^1 D_\varepsilon f_\phi(\alpha y, I, \phi; \alpha\varepsilon) d\alpha$$
$$= y^T M(y, I, \phi; \varepsilon) y + \varepsilon g_\phi(y, I, \phi; \varepsilon), \tag{2.2.13}$$

where the functions $M: \mathbb{R}^2 \times A \times [0, \varepsilon_0'] \to \mathbb{R}^{2\times 2}$ and g_ϕ are C^{r-2}.

By the normal hyperbolicity of $\mathcal{A}_0$, $L_0(0, I, \phi; 0) \equiv L_0(0, I; 0)$ has one dimensional stable and unstable eigenspaces which, in fact, only depend on I in a C^{r-1} fashion. Also, by hypothesis (H1) and the Hamiltonian nature of (2.1.1), the corresponding eigenvalues are real and add up to zero. Therefore, a C^{r-1} transformation of the form $v = S(I)y$ with $S: [I_1, I_2] \to \mathbb{R}^{2\times 2}$ puts system (2.2.8) in the form

$$\begin{aligned} \dot{v} &= [N_0(I) + N_1(v, I, \phi, \varepsilon)v + \varepsilon N_2(v, I, \phi)]v, \\ \dot{I} &= \varepsilon h_I(v, I, \phi; \varepsilon), \\ \dot{\phi} &= v^T P(v, I, \phi; \varepsilon)v + \varepsilon h_\phi(v, I, \phi; \varepsilon), \end{aligned} \tag{2.2.14}$$

where $N_0(I) = \mathrm{diag}\,(\lambda(I), -\lambda(I))$ is C^{r-1} with $\lambda(I) > 0$, $N_1 = S^T L_1 S$, $P = S^T M S$, $N_2: \mathbb{R}^2 \times A \times [0, \varepsilon_0'] \to \mathbb{R}^{2\times 2}$ and h_ϕ are C^{r-2} and the function h_I is C^{r-1}.

We now make use of the fact that, according to Fenichel [23], the local stable and unstable manifolds of $\mathcal{A}_\varepsilon$ in system (2.2.14) are given by two C^{r-2} graphs $v_2 = u_2(v_1, I, \phi; \varepsilon)$ and $v_1 = u_1(v_2, I, \phi; \varepsilon)$, respectively. For $\varepsilon \le \varepsilon_0'' \le \varepsilon_0'$ and in a closed tubular set $\tilde{U}(\varepsilon_0'')$ around $v = 0$ (which can be taken the image of U_{δ_0} of Lemma 2.2.1 under the transformation (2.2.7)) we now apply a C^{r-2} change of variables given by $z = v - u(v, I, \phi; \varepsilon)$. In the (z, I, ϕ) variables we can cast system (2.2.14) in the form

$$\begin{aligned} \dot{z}_1 &= \lambda_1(I) z_1 + z^T Q^1(z, I, \phi, \varepsilon) z + \varepsilon k_1(z, I, \phi; \varepsilon) z_1, \\ \dot{z}_2 &= -\lambda_1(I) z_2 + z^T Q^2(z, I, \phi, \varepsilon) z + \varepsilon k_2(z, I, \phi; \varepsilon) z_2, \\ \dot{I} &= \varepsilon k_I(z, I, \phi; \varepsilon), \end{aligned} \tag{2.2.15}$$

$$\dot{\phi} \;=\; z^T B(z,I,\phi;\varepsilon)z + \varepsilon k_\phi(z,I,\phi;\varepsilon),$$

where $Q^1, Q^2 \colon \mathbb{R}^2 \times A \times [0,\varepsilon_0''] \to \mathbb{R}^{2\times 2}$ are symmetric and C^{r-2} in their arguments, and B, k_1 k_2,k_I, and k_ϕ are those appearing in the statement of the lemma. This justifies equations $(2.2.5)^I$-$(2.2.5)^\phi$.

By the the local invariance of the local stable and unstable manifolds, (2.2.15) must also satisfy

$$\dot{z}_1|_{z_1=0} = 0, \quad \dot{z}_2|_{z_2=0} = 0,$$

which implies

$$q^1_{22}(0,z_2,I,\phi;\varepsilon)z_2^2 = 0, \quad q^2_{11}(z_1,0,I,\phi;\varepsilon)z_1^2 = 0. \tag{2.2.16}$$

Then (2.2.15), (2.2.16) and the same calculation as in (2.2.12) yields equations $(2.2.5)^z$ and (2.2.6) with

$$\begin{aligned} q_1(z,I,\phi;\varepsilon) &= (q^1_{11}(z,I,\phi;\varepsilon)\ ,\ 2q^1_{12}(z,I,\phi;\varepsilon) + z_2\int_0^1 D_{z_1}q^1_{22}(\alpha z_1,z_2,I,\phi;\varepsilon)d\alpha), \\ q_2(z,I,\phi;\varepsilon) &= (2q^2_{12}(z,I,\phi;\varepsilon) + z_1\int_0^1 D_{z_2}q^2_{11}(z_1,\alpha z_2,I,\phi;\varepsilon)d\alpha\ ,\ q^2_{22}(z,I,\phi;\varepsilon)), \end{aligned}$$

and with the smoothness properties stated in the lemma. The coordinate transformation $T^\varepsilon \colon (x,I,\phi) \mapsto (z,I,\phi)$ is constructed as a sequence of diffeomorphisms hence the Hamiltonian nature of (2.2.5), as stated in the lemma, follows immediately. □

The significance of the linearization presented above is that it flattens out the local dynamics around $\mathcal{A}_\varepsilon$. In particular, $\mathcal{A}_\varepsilon$ is described by the equation $z = 0$, and its local stable and unstable manifolds satisfy $z_1 = 0$ and $z_2 = 0$, respectively. This enables us to estimate the time certain trajectories spend in a neighborhood of $\mathcal{A}_\varepsilon$. In the following (x_p, I_p, ϕ_p) will refer to the coordinates of a point $p \in \mathcal{P}$ and $T^\varepsilon_\rho(p)$ will denote the

(dummy) ρ coordinate of the image of p under T^ε. We will also use the notation

$$\partial_1 U_\delta = \{p \in \partial U_\delta \mid I_p \in (I_1, I_2)\}.$$

Lemma 2.2.3 *Let us fix a number $0 < \alpha \leq \frac{1}{2}$ and let $w_\varepsilon(t) = (x(t), I(t), \phi(t))$, $t \in \mathbb{R}$, be a trajectory of (2.1.1). Assume that for $\varepsilon < \tilde{\varepsilon}_0$, fixed $\vartheta > 0$, and $\delta(\varepsilon) = \vartheta\varepsilon^\alpha$, $w_\varepsilon(t)$ enters $U_{\delta(\varepsilon)}$ (as defined in (2.2.4)) at a point $p_\varepsilon \in \partial_1 U_{\delta(\varepsilon)}$ and leaves it at $q_\varepsilon \in \partial_1 U_{\delta(\varepsilon)}$. Let us also assume that the distance of the point p_ε from the local stable manifold $W^s_{loc}(\mathcal{A}_\varepsilon)$ obeys the estimate*

$$d(p_\varepsilon, W^s_{loc}(\mathcal{A}_\varepsilon)) > K\varepsilon^{1-\alpha} \tag{2.2.17}$$

for some $K > 0$. Then there exists $0 < \bar{\varepsilon}_0 \leq \tilde{\varepsilon}_0$ such that for $0 < \varepsilon \leq \bar{\varepsilon}_0$ we have the estimates

$$\begin{aligned} |I_{q_\varepsilon} - I_{p_\varepsilon}| &\leq K_I\varepsilon^{1-\alpha}, \\ |\phi_{q_\varepsilon} - \phi_{p_\varepsilon}| &\leq K_\phi\varepsilon^{\alpha}, \end{aligned} \tag{2.2.18}$$

where K_I and K_ϕ are positive constants (see Fig. 2.3 for geometry).

Proof: We first let

$$\hat{\varepsilon}_0 = \min(\varepsilon_0, \tilde{\varepsilon}_0, \left(\frac{\delta_0^2}{\vartheta}\right)^{\frac{1}{\alpha}}),$$

where $\varepsilon_0, \delta_0 > 0$ are the same as in the statement of Lemma 2.2.2. Then for $\varepsilon < \hat{\varepsilon}_0$ we know that $w_\varepsilon(t)$ enters $U_{\delta(\varepsilon)}$ within which, according to Lemma 2.2.2, system (2.1.1) is C^{r-2} conjugate to system (2.2.5). The subspace $z_2 = const.$, $z_1 = 0$ in the phase space of (2.2.5) is a graph over the (I, ϕ) variables, hence there exists $s_\varepsilon \in W^s_{loc}(\mathcal{A}_\varepsilon)$ such that

$$I_{p_\varepsilon} = I_{s_\varepsilon}, \quad \phi_{p_\varepsilon} = \phi_{s_\varepsilon}, \quad T^\varepsilon_{z_2}(p_\varepsilon) = T^\varepsilon_{z_2}(s_\varepsilon), \quad |T^\varepsilon_{z_1}(p_\varepsilon)| > |T^\varepsilon_{z_1}(s_\varepsilon)| = 0, \tag{2.2.19}$$

where T^ε is the transformation contructed in Lemma 2.2.2 (recall that T^ε is the identity map for the (I, ϕ) coordinates). Further, since T^ε is a C^{r-2} diffeomorphism, we can

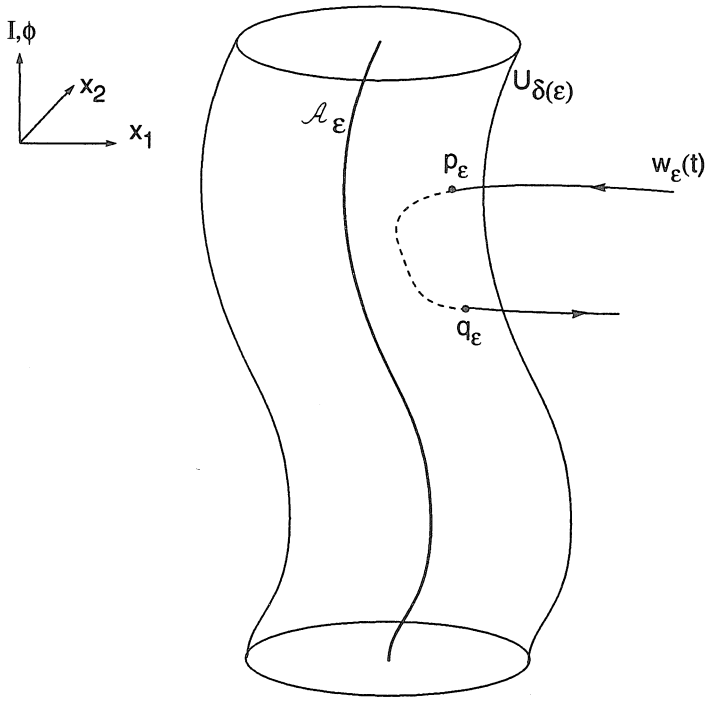

Figure 2.3: Geometry for Lemma 2.2.3

select $L > 0$ such that

$$\|DT_\varepsilon^{-1}\| \leq L \tag{2.2.20}$$

in $\tilde{U}(\hat{\varepsilon}_0) \subset \mathbb{R}^2 \times A$ (defined in the proof of Lemma 2.2.2). Then (2.2.17),(2.2.19)-(2.2.20), and the Mean Value Inequality imply

$$K\varepsilon^{1-\alpha} < |p_\varepsilon - s_\varepsilon| \leq L|T^\varepsilon(p_\varepsilon) - T^\varepsilon(s_\varepsilon)| = L|T^\varepsilon_{z_1}(p_\varepsilon)| \implies |T^\varepsilon_{z_1}(p_\varepsilon)| > \frac{K}{L}\varepsilon^{1-\alpha}. \tag{2.2.21}$$

We now let $r_\varepsilon = g_\varepsilon(I_{q_\varepsilon}, \phi_{q_\varepsilon}) \in \mathcal{A}_\varepsilon$ (see (2.1.5)) and, under the assumptions of the lemma, obtain

$$|T^\varepsilon_z(q_\varepsilon)| = |T^\varepsilon(q_\varepsilon) - T^\varepsilon(r_\varepsilon)| \leq L|q_\varepsilon - r_\varepsilon| = L\delta(\varepsilon). \tag{2.2.22}$$

Let t_ε denote the time the trajectory $w_\varepsilon(t)$ spends between the points p_ε and q_ε. For simplicity, we will assume that $T^\varepsilon_{z_1}(p_\varepsilon) > 0$, which implies $T^\varepsilon_{z_1}(q_\varepsilon) > 0$ by the invariance

of the $z_1 = 0$ hyperplane under the dynamics of system (2.2.5). Then, using our normal form (2.2.5) and eq. (2.2.6), for any $t \leq t_\varepsilon$ we can write

$$\begin{aligned} T^\varepsilon_{z_1}(w_\varepsilon(t)) &= T^\varepsilon_{z_1}(p_\varepsilon) + \int_0^t (\lambda + \langle q_1, z\rangle + \varepsilon k_1) z_1|_{T^\varepsilon(w_\varepsilon(\tau))} d\tau \\ &\geq T^\varepsilon_{z_1}(p_\varepsilon) + \int_0^t (c_1 - c_2|T^\varepsilon_z(w_\varepsilon(\tau)| - c_3\varepsilon) T^\varepsilon_{z_1}(w_\varepsilon(\tau)) d\tau \\ &\geq T^\varepsilon_{z_1}(p_\varepsilon) + \int_0^t (c_1 - c_2\frac{\delta(\varepsilon)}{L} - \varepsilon c_3) T^\varepsilon_{z_1}(w_\varepsilon(\tau)) d\tau, \end{aligned} \tag{2.2.23}$$

where, within $\tilde{U}(\hat{\varepsilon}_0)$, $c_1 > 0$ is a lower bound for λ, and $c_2, c_3 > 0$ are upper bounds for $|q_1|$ and $|k_1|$, respectively. Fixing some $0 < \nu < 1$ (to be determined in Lemma 2.2.5 based on later considerations) and setting

$$\bar{\varepsilon}_0 = \min(\hat{\varepsilon}_0, [\frac{c_1(1-\nu)L}{2c_2\vartheta}]^{\frac{1}{\alpha}}, [\frac{c_2\vartheta}{Lc_3}]^{\frac{1}{1-\alpha}}), \tag{2.2.24}$$

we obtain that, for $\varepsilon \leq \bar{\varepsilon}_0$, $c_1\nu > 0$ is a lower bound for the first factor in the integrand of (2.2.23). Then, using an inverse Gronwall-inequality and substituting $t = t_\varepsilon$, we arrive at the expression

$$T^\varepsilon_{z_1}(q_\varepsilon) \geq T^\varepsilon_{z_1}(p_\varepsilon) e^{c_1\nu t_\varepsilon},$$

from which we obtain the estimate

$$t_\varepsilon \leq \frac{1}{c_1\nu} \log \frac{T^\varepsilon_{z_1}(q_\varepsilon)}{T^\varepsilon_{z_1}(p_\varepsilon)} \leq \frac{1}{c_1\nu} \log \frac{L^2\vartheta}{K\varepsilon^{1-2\alpha}}, \tag{2.2.25}$$

where we have also used (2.2.21) and (2.2.22).

We will now estimate the change of the I coordinate while the trajectory $w_\varepsilon(t)$ passes from p_ε to q_ε. Using eqs. $(2.2.5)^I$ and (2.2.25) we have

$$|I_{q_\varepsilon} - I_{p_\varepsilon}| \leq \varepsilon \int_0^{t_\varepsilon} |k_I|_{T^\varepsilon(w_\varepsilon(\tau))} d\tau \leq \varepsilon c_4 t_\varepsilon \leq \varepsilon \frac{c_4}{c_1\nu} \log \frac{L^2\vartheta}{K\varepsilon^{1-2\alpha}}, \tag{2.2.26}$$

where $c_4 > 0$ is an upper bound for $|k_I|$ in $\tilde{U}(\bar{\varepsilon}_0)$. Since

$$\lim_{\varepsilon\to 0} \frac{\varepsilon \log \frac{L^2\vartheta}{K\varepsilon^{1-2\alpha}}}{\varepsilon^{1-\alpha}} = \lim_{\varepsilon\to 0} \varepsilon^\alpha = 0,$$

based on (2.2.26) we can choose $K_I > 0$ to satisfy the first inequality in (2.2.18) for sufficiently small $\varepsilon > 0$. As for the second inequality of (2.2.18), eq. $(2.2.5)^\phi$ gives rise to the estimate

$$\begin{aligned} |\phi_{q_\varepsilon} - \phi_{p_\varepsilon}| &\leq \int_0^{t_\varepsilon} |z^T B z + \varepsilon k_\phi|_{T^\varepsilon(w_\varepsilon(\tau))} d\tau \\ &\leq (\varepsilon^{2\alpha}\frac{\vartheta^2}{L^2}c_5 + \varepsilon c_6)t_\varepsilon \leq \varepsilon^{2\alpha}\frac{1}{c_1\nu}(\frac{\vartheta^2}{L^2}c_5 + c_6)\log\frac{L^2\vartheta}{K\varepsilon^{1-2\alpha}}, \quad (2.2.27) \end{aligned}$$

where $c_5, c_6 > 0$ are upper bounds for $\|B\|$ and $|k_\phi|$ in $\tilde{U}(\bar{\varepsilon}_0)$, respectively. Again, since

$$\lim_{\varepsilon\to 0}\frac{\varepsilon^{2\alpha}\log\frac{L^2\vartheta}{K\varepsilon^{1-2\alpha}}}{\varepsilon^\alpha} = \lim_{\varepsilon\to 0}\varepsilon^\alpha = 0,$$

(2.2.27) shows that for $0 < \varepsilon < \bar{\varepsilon}_0$ we can choose $K_\phi > 0$ to satisfy the second inequality in (2.2.18). □

In the following we will study certain Poincaré maps related to the local dynamics around $\mathcal{A}_\varepsilon$ and the global perturbed dynamics near W_0. We will construct approximations for these maps which will turn out to be accurate enough to detect families of N-pulse homoclinic orbits. From now on $\tilde{W}^s_{loc}(\mathcal{A}_\varepsilon)$ and $\tilde{W}^u_{loc}(\mathcal{A}_\varepsilon)$ will denote the connected components of $W^s_{loc}(\mathcal{A}_\varepsilon)$ and $W^u_{loc}(\mathcal{A}_\varepsilon)$, respectively, which are C^r ε-close to appropriate subsets of W_0. By the normal hyperbolicity of $\mathcal{A}_\varepsilon$, each of $W^s_{loc}(\mathcal{A}_\varepsilon)$ and $W^u_{loc}(\mathcal{A}_\varepsilon)$ has precisely one more connected component, but hypothesis (H1) tells nothing about the geometry of the corresponding global invariant manifolds. In section 2.3 we will include these other components in our analysis under supplementary assumptions.

Let us first define a family of Poincaré sections for system (2.1.1) in the vicinity of $\mathcal{A}_\varepsilon$. We fix some (yet undetermined) $\vartheta > 0$ and on every energy surface $E_\varepsilon(h)$ (see (2.1.8)) introduce the set

$$\Sigma_\varepsilon(h) = \partial_1 U_{\delta(\varepsilon)} \cap E_\varepsilon(h),$$

where $\delta(\varepsilon)$ is defined as in Lemma 2.2.3. Note that for $\varepsilon = 0$ $\Sigma_\varepsilon(h)$ becomes singular. We now give conditions under which it is a (nonempty) tractable geometric object for $\varepsilon > 0$.

Lemma 2.2.4 *Let us fix the constants $\kappa > 0$ and $0 < \alpha \leq \frac{1}{2}$. Then there exist $\bar{\varepsilon}_0$ such that for $0 < \varepsilon < \bar{\varepsilon}_0$, and $|h - h_0| < \kappa\varepsilon$ (see (2.2.3)):*

(*i*) *$E_\varepsilon(h)$ and $E_0(h_0)$ are C^1 $\varepsilon^{1-\alpha}$-close within $\bar{U}(\vartheta, \varepsilon) = \overline{U_{\delta_0} - U_{\delta(\varepsilon)/2}}$, where δ_0 is that of Lemma 2.2.2.*

(*ii*) *Suppose that condition (2.2.35) below is satisfied. Then two of the connected components of $\Sigma_\varepsilon(h)$, denoted by $\Sigma^s_\varepsilon(h)$ and $\Sigma^u_\varepsilon(h)$, are C^1 $\varepsilon^{1-\alpha}$-close to $\Pi^s_\varepsilon = \partial_1 U_{\delta(\varepsilon)} \cap \tilde{W}^s_{loc}(\mathcal{A}_0)$ and $\Pi^u_\varepsilon = \partial_1 U_{\delta(\varepsilon)} \cap \tilde{W}^u_{loc}(\mathcal{A}_0)$, respectively (see Fig. 2.4). Moreover, $(\Sigma^s_\varepsilon(h), \bar{\omega})$ and $(\Sigma^u_\varepsilon(h), \bar{\omega})$ with $\bar{\omega} = d\phi \wedge dI$ are symplectic two-manifolds (with boundary) and embeddings of the annulus A through two C^r maps $e^s_\varepsilon \colon A \to \mathcal{P}$ and $e^u_\varepsilon \colon A \to \mathcal{P}$, respectively.*

Proof: First note that $E_0(h_0) \cap U_{\delta_0} \supset W_0 \cap U_{\delta_0} \neq \emptyset$ and the intersection is transversal, hence for $\varepsilon > 0$ small enough $E_\varepsilon(h) \cap U_{\delta_0} \neq \emptyset$ holds. We decrease $\bar{\varepsilon}_0$ of Lemma 2.2.3 to achieve this and select $p_0 \in E_0(h_0) \cap \bar{U}(\vartheta, \varepsilon)$ and $p_\varepsilon \in E_\varepsilon(h) \cap \bar{U}(\vartheta, \varepsilon)$, both from a fixed submanifold $I = I_0$, $\phi = \phi_0$. Such a choice is possible since $|D_x H_0|$ (as well as $|D_x H|$) is at least of $\mathcal{O}(\varepsilon^\alpha)$ (i.e., strictly nonzero for $\varepsilon > 0$) in $\bar{U}(\vartheta, \varepsilon)$ (hypothesis (H1)) hence any energy surface can locally be written in the form $x_i = f(x_j, I, \phi; \varepsilon)$. From hypothesis $(H1)$ we also have

$$D_x H(\bar{x}^0(I_0; \mu), I_0, \phi_0; 0) = 0,$$

from which an argument similar to (2.2.12) or (2.2.13) gives

$$D_x H(x, I, \phi; \varepsilon) \;=\; M_1(x, I, \phi; \varepsilon)(x - \bar{x}^0(I_0; \mu)) + m_2(x, I, \phi; \varepsilon)(I - I_0)$$

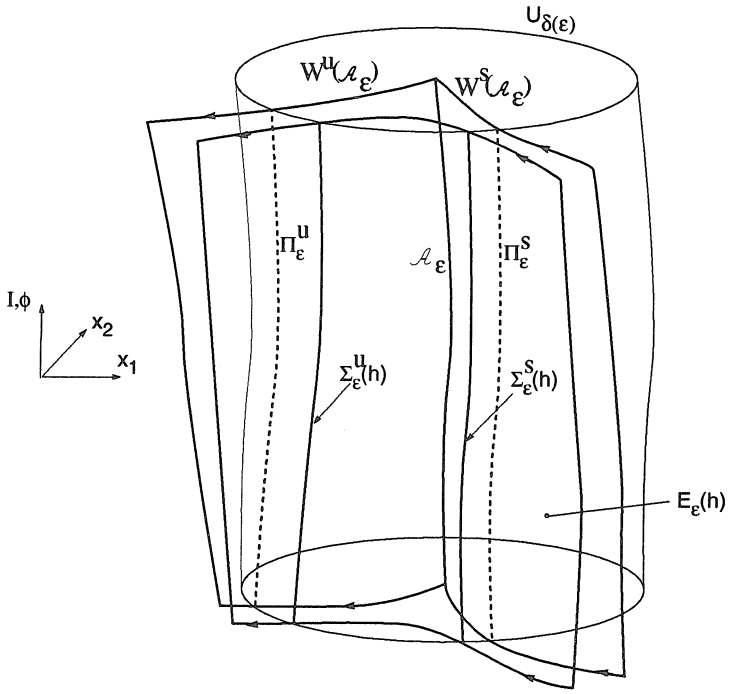

Figure 2.4: Statement (ii) of Lemma 2.2.4

$$+m_3(x, I, \phi; \varepsilon)(\phi - \phi_0) + \varepsilon m_4(x, I, \phi; \varepsilon), \tag{2.2.28}$$

where the matrix M_1 and the functions m_2, m_3, and m_4 are C^{r-1} in their arguments. Now note that on the line $l_{p_0,p_\varepsilon} \subset \bar{U}(\vartheta, \varepsilon)$ connecting p_ε and p_0 (2.2.28) simplifies to

$$D_x H(x, I_0, \phi_0; \varepsilon) = M_1(x, I_0, \phi_0; \varepsilon)(x - \bar{x}^0(I_0; \mu)) + \varepsilon m_4(x, I_0, \phi_0; \varepsilon). \tag{2.2.29}$$

Since (for small $\varepsilon > 0$ and appropriate p_ε) l_{p_0,p_ε} does not intersect $U_{\delta(\varepsilon)/2}$, (2.2.29) gives rise to the estimate

$$|DH||_{l_{p_0,p_\varepsilon}} \geq |D_x H||_{l_{p_0,p_\varepsilon}} > c_7 \frac{\vartheta \varepsilon^\alpha}{2} - c_8 \varepsilon > c_7 \frac{\vartheta \varepsilon^\alpha}{4}, \tag{2.2.30}$$

where $c_7 > 0$ is a lower bound within U_{δ_0} for the positive eigenvalue of

$$M_1(x, I_0, \phi_0; \varepsilon) = \int_0^1 D_x^2 H(\bar{x}^0(I_0; \mu) + s(x - \bar{x}^0(I_0; \mu)), I_0, \phi_0; \mu, \varepsilon) ds,$$

and $c_8 > 0$ is an upper bound for $|m_4|$ in U_{δ_0}. By assumption, we also have

$$\begin{aligned} \kappa\varepsilon &> |H_0|_{p_0} - H|_{p_\varepsilon}| > |H_0|_{p_0} - H_0|_{p_\varepsilon}| - |H_0|_{p_\varepsilon} - H|_{p_\varepsilon}| = |H_0|_{p_0} - H_0|_{p_\varepsilon}| - \varepsilon|H_1|_{p_\varepsilon}| \\ &> c_7\frac{\vartheta\varepsilon^\alpha}{4}|p_0 - p_\varepsilon| - c_9\varepsilon > c_7\frac{\vartheta\varepsilon^\alpha}{8}|p_0 - p_\varepsilon|, \end{aligned} \tag{2.2.31}$$

where we have used the Mean Value Theorem together with (2.2.30) and further diminished $\bar{\varepsilon}_0$ is necessary ($c_9 > 0$ is an upper bound for $|H_1|$ in U_{δ_0}). Thus, based on (2.2.31), we have

$$|p_0 - p_\varepsilon| < \frac{8\kappa}{c_7\vartheta}\varepsilon^{1-\alpha}. \tag{2.2.32}$$

Similarly, we obtain that

$$|DH_0|_{p_0} - DH|_{p_\varepsilon}| \leq |DH_0|_{p_0} - DH_0|_{p_\varepsilon}| + \varepsilon|DH_1|_{p_\varepsilon}| < c_{10}|p_0 - p_\varepsilon| + c_{11}\varepsilon < \frac{16\kappa c_{10}}{c_7\vartheta}\varepsilon^{1-\alpha}, \tag{2.2.33}$$

where $c_{10}, c_{11} > 0$ are upper bounds within U_{δ_0} for $\|D^2H\|$ and $|DH_1|$, respectively. But (2.2.32) and (2.2.33) together prove the first statement of the lemma.

Let us now make the specific choice $p_0 \in \partial U_{\delta(\varepsilon)/2}$. Then

$$|p_0 - p_\varepsilon| < \frac{\vartheta}{2}\varepsilon^\alpha \tag{2.2.34}$$

would ensure that $E_\varepsilon(h)$ intersects $\partial_1 U_{\delta(\varepsilon)}$. Using (2.2.32), (2.2.34) is satisfied if we choose

$$\begin{aligned} \varepsilon &< (\frac{c_7\vartheta^2}{16\kappa})^{\frac{1}{1-2\alpha}}, \quad \text{if} \quad \frac{2}{5} \leq \alpha < \frac{1}{2}, \\ \vartheta &\geq \vartheta^* = 4\sqrt{\frac{\kappa}{c_7}}, \quad \text{if} \quad \alpha = \frac{1}{2}. \end{aligned} \tag{2.2.35}$$

Further, the intersection of $E_\varepsilon(h)$ and $\partial_1 U_{\delta(\varepsilon)}$ is transversal for $\varepsilon > 0$ small enough, since $E_0(h_0)$ and $\partial_1 U_{\delta(\varepsilon)}$ intersect transversally and $E_\varepsilon(h)$ and $E_0(h_0)$ are C^1 $\varepsilon^{1-\alpha}$-close. Hence $\Sigma_\varepsilon(h) = E_\varepsilon(h) \cap \partial_1 U_{\delta(\varepsilon)}$ has two connected components which are manifolds and

are C^1 $\sqrt{\varepsilon}$-close to Π^s_ε and Π^u_ε, respectively. In that case they are graphs over the annulus A as claimed in statement (ii) of the lemma. Since on $\partial_1 U_{\delta(\varepsilon)}$ locally either x_1 is a function of x_2 or vica versa, the symplectic form ω of $\mathcal{P}$ restricts to the closed two form $\bar{\omega}$ on $\partial_1 U_{\delta(\varepsilon)}$. Let us introduce the inclusions $i^s_\varepsilon\colon \Sigma^s_\varepsilon(h) \hookrightarrow \mathcal{P}$ and $i^u_\varepsilon\colon \Sigma^u_\varepsilon(h) \hookrightarrow \mathcal{P}$ (both the embeddings and the inclusions of $\Sigma^s_\varepsilon(h)$ and $\Sigma^u_\varepsilon(h)$ do depend on the energy h). Since both e^s_ε and e^u_ε are diffeomorphisms, $i^{u*}_\varepsilon\omega = \bar{\omega}$ and $i^{s*}_\varepsilon\omega = \bar{\omega}$ are nondegenerate, hence $(\Sigma^s_\varepsilon(h), \bar{\omega})$ and $(\Sigma^u_\varepsilon(h), \bar{\omega})$ are symplectic manifolds (with boundary). This concludes the proof of the lemma. □

We will be interested in following trajectories that intersect both $\Sigma^s_\varepsilon(h)$ and $\Sigma^u_\varepsilon(h)$. To this end, on appropriate open sets $R^s_\varepsilon(h) \subset \Sigma^s_\varepsilon(h)$ and $R^u_\varepsilon(h) \subset \Sigma^u_\varepsilon(h)$ we define the *local map* L^h_ε and the *global map* G^h_ε, respectively, by

$$\begin{array}{ll} L^h_\varepsilon\colon R^s_\varepsilon(h) \to \Sigma^u_\varepsilon(h), & G^h_\varepsilon\colon R^u_\varepsilon(h) \to \Sigma^s_\varepsilon(h), \\ p \mapsto F^\varepsilon_{t^\varepsilon_L(p)}(p), & p \mapsto F^\varepsilon_{t^\varepsilon_G(p)}(p), \end{array}$$

with

$$t^\varepsilon_L(p) = \inf\{t > 0 | F^\varepsilon_t(p) \in \Sigma^u_\varepsilon(h)\}, \quad t^\varepsilon_G(p) = \inf\{t > 0 | F^\varepsilon_t(p) \in \Sigma^s_\varepsilon(h)\}.$$

We also define the auxiliary maps $\mathcal{G}^h_\varepsilon$ and $\mathcal{L}^h_\varepsilon$ through the commutative diagrams

$$\begin{array}{ccc} R^s_\varepsilon(h) & \xrightarrow{L^h_\varepsilon} & \Sigma^u_\varepsilon(h) \\ {\scriptstyle e^s_\varepsilon}\uparrow & & \uparrow{\scriptstyle e^u_\varepsilon} \\ (e^s_\varepsilon)^{-1}(R^s_\varepsilon(h)) & \xrightarrow[\mathcal{L}^h_\varepsilon]{} & A \end{array} \qquad \begin{array}{ccc} R^u_\varepsilon(h) & \xrightarrow{G^h_\varepsilon} & \Sigma^s_\varepsilon(h) \\ {\scriptstyle e^u_\varepsilon}\uparrow & & \uparrow{\scriptstyle e^s_\varepsilon} \\ (e^u_\varepsilon)^{-1}(R^u_\varepsilon(h)) & \xrightarrow[\mathcal{G}^h_\varepsilon]{} & A \end{array} \tag{2.2.36}$$

Lemma 2.2.5 *Let us fix the constants $\kappa > 0$ and $\frac{1}{2} \geq \alpha > 0$. Then for $0 < \varepsilon < \bar{\varepsilon}_0$ and $|h - h_0| < \kappa\varepsilon$*

(i) the two dimensional maps L^h_ε, G^h_ε, $\mathcal{L}^h_\varepsilon$, and $\mathcal{G}^h_\varepsilon$ are symplectic.

(ii) Under condition (2.2.35) the global map G^h_ε can be defined on $R^u_\varepsilon(h) = \Sigma^u_\varepsilon(h)$ and its conjugate map $\mathcal{G}^h_\varepsilon$ is C^1 $\varepsilon^{1-\alpha}$-close to the rotation map

$$\mathcal{R}\colon A \quad \to A,$$

$$(I,\phi) \qquad \mapsto (I,\phi+\Delta\phi(I;\mu)), \tag{2.2.37}$$

where the phase shift $\Delta\phi(I;\mu)$ *is defined in (2.1.9).*

(*iii*) *Suppose that* $\frac{2}{5} \le \alpha < \frac{1}{2}$ *holds. Then for any compact set* $S^s_\varepsilon(h) \subset R^s_\varepsilon(h) \subset \Sigma^s_\varepsilon(h)$ *satisfying*

$$d(S^s_\varepsilon(h), W^s_{loc}(\mathcal{A}_\varepsilon)) > K\varepsilon^{1-\alpha}, \tag{2.2.38}$$

with some $K > 0$, *the map* $\mathcal{L}^h_\varepsilon$ *is* C^1 $\varepsilon^{\frac{\alpha}{3}}$*-close on* $(e^u_\varepsilon)^{-1}(S^s_\varepsilon(h))$ *to the identity map of* A. *For the case* $\alpha = \frac{1}{2}$ *this statement can be strengthened to* C^1 $\sqrt{\varepsilon}$*-closeness provided* $0 < K < \vartheta$.

Proof: Throughout the proof we will use the notation of the earlier lemmas without explicit reference. We will prove (*i*) only for the maps G^h_ε and $\mathcal{G}^h_\varepsilon$ since the same argument works for L^h_ε and $\mathcal{L}^h_\varepsilon$. Let us select a smooth closed curve $\gamma \subset R^u_\varepsilon(h)$. We note that the interior of γ in $R^u_\varepsilon(h)$ (denoted as $Int(\gamma) \subset R^u_\varepsilon(h)$) is simply connected since $R^u_\varepsilon(h)$ is a graph over an open subset of A. Since the flow map $F(.)^\varepsilon_t$ of (2.1.1) is a C^r diffeomorhism and $\Sigma^s_\varepsilon(h)$ is a local transversal to the flow, $\gamma' = G^h_\varepsilon(\gamma) \subset \Sigma^s_\varepsilon(h)$ is a smooth closed curve. Let us consider the cylinder $C_\gamma \in \mathcal{P}$ whose generators are trajectories of (2.1.1) connecting points of γ and γ'. Clearly C_γ is a smooth orientable manifold with boundary $\partial C_\gamma = \gamma - \gamma'$. By the Poincaré-Cartan theorem (see, e.g., Arnold [2]) we can write

$$\int_\gamma x_2 dx_1 + I d\phi - H dt = \int_{\gamma'} x_2 dx_1 + I d\phi - H dt. \tag{2.2.39}$$

Now $\gamma, \gamma' \subset E_\varepsilon(h)$, thus (2.2.39) and Stokes' theorem imply

$$\int_\gamma \omega = \int_{\gamma'} \omega. \tag{2.2.40}$$

Note that we also have

$$\int_{Int(\gamma)} \omega = \int_{Int(\gamma)} i_\varepsilon^{u*}\omega = \int_{Int(\gamma)} \bar{\omega}, \qquad \int_{Int(\gamma')} \omega = \int_{Int(\gamma')} i_\varepsilon^{s*}\omega = \int_{Int(\gamma')} \bar{\omega} = \int_{Int(\gamma)} G_{\varepsilon *}^h \bar{\omega}. \tag{2.2.41}$$

Since γ was arbitrary, (2.2.39)-(2.2.41) yield

$$G_{\varepsilon *}^h \bar{\omega} = \bar{\omega}, \tag{2.2.42}$$

i.e., G_ε^h is symplectic. The fact that $\mathcal{G}_\varepsilon^h$ is symplectic now follows easily since, based on (2.2.36) and (2.2.42), we have

$$\mathcal{G}_{\varepsilon *}^h \bar{\omega} = (e_\varepsilon^s)_*^{-1} G_{\varepsilon *}^h e_{\varepsilon *}^u \bar{\omega} = (e_\varepsilon^s)_*^{-1} G_{\varepsilon *}^h \bar{\omega} = (e_\varepsilon^s)_*^{-1} \bar{\omega} = \bar{\omega}.$$

We now proceed with the proof of (ii) of the lemma. As we noted in Lemma 2.2.4 the energy surface $E_\varepsilon(h)$ intersects $\partial_1 U_{\delta(\varepsilon)}$ transversally in two components. By the nature of the perturbed flow F_t^ε near W_0 and the continuity of $E_\varepsilon(h)$, every trajectory starting from the first component $\Sigma_\varepsilon^u(h)$ is guided to the second component $\Sigma_\varepsilon^s(h)$, which proves the first statement on the global map in (ii). We now turn to the proof of the statement on the map $\mathcal{G}_\varepsilon^h$.

From statement (ii) of Lemma 2.2.4 we know that $\Sigma_\varepsilon^s(h)$ and $\Sigma_\varepsilon^u(h)$ are C^1 $\varepsilon^{1-\alpha}$ close to Π_ε^s and Π_ε^u, respectively. By the smooth dependence of Poincaré maps on parameters (here ε and the energy h) the map

$$\begin{aligned} G_\varepsilon \colon \Pi_\varepsilon^u &\to \Pi_\varepsilon^s, \\ p &\mapsto F_{\tau_\varepsilon(p)}^\varepsilon(p), \end{aligned}$$

with

$$\tau_\varepsilon(p) = \inf\{t > 0 | F_t^\varepsilon(p) \in \Pi_\varepsilon^s\},$$

is C^1 $\varepsilon^{1-\alpha}$-close to G_ε^h for ε sufficiently small. Let us introduce the map $\mathcal{G}_\varepsilon\colon A \to A$ which is C^r conjugate to G_ε and is defined analogously to $\mathcal{G}_\varepsilon^h$ (see (2.2.36)). As a consequence of this, $\mathcal{G}_\varepsilon$ is C^1 $\varepsilon^{1-\alpha}$-close to $\mathcal{G}_\varepsilon^h$. Now observe that $\bar{G}_0 = g_0 \circ \mathcal{R} \circ g_0^{-1}$ (see (2.1.3)) maps α-limit points of unperturbed homoclinic trajectories to their ω-limit points, hence it is a smooth "geometric" extension of the map G_ε at $\varepsilon^\alpha = 0$. It follows from (ii) of Proposition 2.2.1 that $\bar{\mathcal{G}}_0 \equiv \mathcal{R}$ is a C^{r-1} smooth extension of $\mathcal{G}_\varepsilon$ at $\varepsilon^\alpha = 0$. Therefore, $\mathcal{G}_\varepsilon$ and $\mathcal{R}$ are C^{r-1} $\varepsilon^{2\alpha}$ close. Since $\mathcal{G}_\varepsilon$ and $\mathcal{G}_\varepsilon^h$ are C^1 $\varepsilon^{1-\alpha}$-close, this completes the proof of (ii).

Statement (iii) does not allow a similar geometric argument because one cannot define a C^1 $\varepsilon^{1-\alpha}$-close conjugate map $\mathcal{L}_\varepsilon$ in the way above which would extend smoothly to $\varepsilon^\alpha = 0$. Instead, we will make use of the normal form of Lemma 2.2.2 and the estimates of Lemma 2.2.3. First note that the initial conditions of trajectories starting from $S_\varepsilon^s(h)$ satisfy the distance condition (2.2.17), hence the C^0 ε^α-closeness of $\mathcal{L}_\varepsilon^h$ to the identity follows immediately from Lemma 2.2.2. Therefore, using the notation of that lemma, we only have to show that for some constant $\bar{K} > 0$

$$\|\frac{\partial(I_{q_\varepsilon}, \phi_{q_\varepsilon})}{\partial(I_{p_\varepsilon}, \phi_{p_\varepsilon})} - \mathrm{Id}_2\| < \bar{K}\sqrt{\varepsilon}, \qquad \text{for} \quad \alpha = \frac{1}{2}, \tag{2.2.43}$$

and

$$\|\frac{\partial(I_{q_\varepsilon}, \phi_{q_\varepsilon})}{\partial(I_{p_\varepsilon}, \phi_{p_\varepsilon})} - \mathrm{Id}_2\| < \bar{K}\varepsilon^{\frac{\alpha}{3}}, \qquad \text{for} \quad \frac{2}{5} \le \alpha < \frac{1}{2}, \tag{2.2.44}$$

where $\mathrm{Id}_2 \in \mathbb{R}^{2\times 2}$ is the identity matrix. Let $C_\varepsilon > 0$ be a Lipshitz constant in $T^\varepsilon(U_{\delta(\varepsilon)})$ for the right hand side of system (2.2.5). We now make a little digression on the choice of C_ε because later we will need to choose it as small as possible. Let $V_\varepsilon\colon \mathbb{R}^2 \times A \to \mathbb{R}^4$ denote the right hand side of (2.2.5), and consider two points $w_0, w_0' \in T^\varepsilon(U_{\delta(\varepsilon)})$. Using (2.2.5) we can write

$|V_\varepsilon(w_0) - V_\varepsilon(w_0')| \le$

$$|\Lambda|_{w_0} z_0 - \Lambda|_{w_0'} z_0'| + \varepsilon |k_I|_{w_0} - k_I|_{w_0'}| + |z_0^T B|_{w_0} z_0 - (z_0')^T B|_{w_0'} z_0'| + \varepsilon |k_\phi|_{w_0} - k_\phi|_{w_0'}|$$
$$\leq |(\Lambda|_{w_0} - \Lambda|_{w_0'}) z_0| + |\Lambda|_{w_0'}(z_0 - z_0')| + \varepsilon C_1 |w_0 - w_0'| + |(z_0^T B|_{w_0} - (z_0')^T B|_{w_0}) z_0|$$
$$+ |(z_0')^T B|_{w_0}(z_0 - z_0')| + |(z_0')^T (B|_{w_0} - B|_{w_0'}) z_0'| + \varepsilon C_2 |w_0 - w_0'|, \tag{2.2.45}$$

where $C_1, C_2 > 0$ are Lipshitz-constant for k_I and k_ϕ, respectively, within $\tilde{U}(\bar{\varepsilon}_0)$. In the same domain, let $C^* > 0$ an upper bound on $|\Lambda_{ii}|$, $N_B > 0$ an upper bound on $\|B\|$, and $C_\Lambda, C_B > 0$ ε-independent Lipschitz-constants for the maps $\Lambda\colon \mathbb{R}^2 \times A \to \mathbb{R}^{2\times 2}$ and $B\colon \mathbb{R}^2 \times A \to \mathbb{R}^{2\times 2}$. Then (2.2.45) implies the inequality

$$|V_\varepsilon(w_0) - V_\varepsilon(w_0')| \leq (C_\Lambda L \vartheta \varepsilon^\alpha + C^* + \varepsilon C_1 + 2\vartheta \varepsilon^\alpha N_B + \vartheta^2 \varepsilon^{2\alpha} C_B) |w_0 - w_0'|. \tag{2.2.46}$$

If w_0 and w_0' are taken from a neighborhood of a trajectory $w_\varepsilon(t)$ of Lemma 2.2.3 within $U_{\delta(\varepsilon)}$, then by (2.2.18) there exists $I_0 \in (I_1, I_2)$ such that in this neigborhood, for appropriate $c_{12} > 0$, $\lambda(I)$ obeys the upper estimate

$$\lambda(I) < \lambda(I_0) + c_{12}\varepsilon^{1-\alpha},$$

with $c_{12} > 0$ being a bound on $|d\lambda/dI|$. But this, together with (2.2.6), shows that

$$C^* < \lambda(I_0) + c_{12}\varepsilon^{1-\alpha} + c_2 \frac{\vartheta}{L} \varepsilon^\alpha + \varepsilon c_3, \tag{2.2.47}$$

where $c_2, c_3 > 0$ were defined in relation with (2.2.23). Then (2.2.6), (2.2.46), and (2.2.47) imply

$$|V_\varepsilon(w_0) - V_\varepsilon(w_0')| \leq C_\varepsilon |w_0 - w_0'|, \tag{2.2.48}$$

with

$$C_\varepsilon = (C_\Lambda L \vartheta \varepsilon^\alpha + \lambda(I_0) + c_{12}\varepsilon^{1-\alpha} + c_2 \frac{\vartheta}{L} \varepsilon^\alpha + \varepsilon c_3 + \varepsilon C_1 + 2\vartheta \varepsilon^\alpha N_B + \vartheta^2 \varepsilon^{2\alpha} C_B). \tag{2.2.49}$$

Decreasing $\bar{\varepsilon}_0$, if necessary, (2.2.49) yields the choice

$$C_\varepsilon < \lambda(I_0) + c_{13}\varepsilon^\alpha. \tag{2.2.50}$$

A similar argument reveals that the constant c_1 of Lemma 2.2.3 can be chosen such that

$$c_1 > \lambda(I_0) - c_{14}\varepsilon^{\alpha}, \tag{2.2.51}$$

with an appropriate constant $c_{14} > 0$.

We now continue the proof of (ii) of the lemma. For the deviation of two trajectories $w_\varepsilon(t)$ and $w'_\varepsilon(t)$ of (2.2.6) (satisfying the conditions of Lemma 2.2.3) we have the usual Gronwall-estimate

$$|I_\varepsilon(t) - I'_\varepsilon(t)| \leq |w_\varepsilon(t) - w'_\varepsilon(t)| \leq |w_0 - w'_0|e^{C_\varepsilon t}, \tag{2.2.52}$$

where $w_\varepsilon(0) = w_0 \neq w'_\varepsilon(0) = w'_0$, and $I_\varepsilon(t)$ and $I'_\varepsilon(t)$ denote the I coordinate of the corresponding solutions. Dividing both sides of (2.2.52) by $|w_0 - w'_0|$ and taking the limit as $w'_0 \to w_0$ we obtain that

$$|D_{w_0} I_\varepsilon(t)| \leq 2e^{C_\varepsilon t}. \tag{2.2.53}$$

Since estimates similar to (2.2.53) hold for the time evolution of the other three coordinates of $w_\varepsilon(t)$ and $w'_\varepsilon(t)$, we can also write

$$|D_{w_0} z_{1\varepsilon}(t)|, |D_{w_0} z_{2\varepsilon}(t)|, |D_{w_0}\phi_\varepsilon(t)| \leq 2e^{C_\varepsilon t}. \tag{2.2.54}$$

Then (2.52) and (2.53) give rise to the inequality

$$\|D_{w_0} w_\varepsilon(t)\| \leq 4e^{C_\varepsilon t}, \tag{2.54}$$

where, as before, $\|.\|$ denotes the Euclidian matrix norm.

Consider now the I coordinate of the solution $w_\varepsilon(t)$ of (2.2.5) given by

$$I_\varepsilon(t) = I_{p_\varepsilon} + \varepsilon \int_0^t k_I|_{w_\varepsilon(\tau)} d\tau, \tag{2.2.55}$$

the differentiation of which with respect to I_{p_ε} yields

$$\frac{dI_\varepsilon(t)}{dI_{p_\varepsilon}} = 1 + \varepsilon \int_0^t \langle Dk_I|_{w_\varepsilon(\tau)}, D_{I_{p_\varepsilon}} w_\varepsilon(\tau)\rangle d\tau. \tag{2.2.56}$$

Since $w_0 = T^\varepsilon(p_\varepsilon)$, (2.2.54) and (2.2.56) lead to the estimate

$$|\frac{dI_\varepsilon(t)}{dI_{p_\varepsilon}} - 1| \le \varepsilon \int_0^t 4c_{15} e^{C_\varepsilon \tau} d\tau = \varepsilon \frac{4c_{15}}{C_\varepsilon} e^{C_\varepsilon t}, \tag{2.2.57}$$

where $c_{15} > 0$ is an upper bound for $|Dk_I|$ on $\tilde{U}(\bar{\varepsilon}_0)$. Substituting $t = t_\varepsilon$ and using (2.2.25) gives

$$|\frac{dI_{q_\varepsilon}}{dI_{p_\varepsilon}} - 1| = |\frac{dI_\varepsilon(t_\varepsilon)}{dI_{p_\varepsilon}} - 1| \le \varepsilon \frac{4c_{15}}{C_\varepsilon} (\frac{L^2\vartheta}{K\varepsilon^{1-2\alpha}})^{\frac{C_\varepsilon}{c_1\nu}} < K_1 \varepsilon^{(1-\frac{C_\varepsilon(1-2\alpha)}{c_1\nu})}, \tag{2.2.58}$$

with appropriate $K_1 > 0$. Starting from (2.2.55) one obtains the same way that

$$|\frac{dI_{q_\varepsilon}}{d\phi_{p_\varepsilon}}| \le K_1 \varepsilon^{(1-\frac{C_\varepsilon(1-2\alpha)}{c_1\nu})}. \tag{2.2.59}$$

Also, applying the same argument to

$$\phi_\varepsilon(t) = \phi_{p_\varepsilon} + \int_0^t [z^T B(z, I, \phi; \varepsilon) z + \varepsilon k_\phi(z, I, \phi; \varepsilon)]|_{w_\varepsilon(\tau)} d\tau,$$

one arrives at the expressions

$$|\frac{d\phi_{q_\varepsilon}}{d\phi_{p_\varepsilon}} - 1|, |\frac{d\phi_{q_\varepsilon}}{dI_{p_\varepsilon}}| \le K_2 \varepsilon^{(\alpha - \frac{C_\varepsilon(1-2\alpha)}{c_1\nu})} + K_3 \varepsilon^{(1-\frac{C_\varepsilon(1-2\alpha)}{c_1\nu})}, \tag{2.2.60}$$

with $K_2, K_3 > 0$. If $\alpha = 1/2$ then (2.2.58), (2.2.59), and (2.2.60) imply (2.2.43) for $\bar{K} = \sqrt{2K_1^2 + K_2^2 + K_3^2}$. To show (2.2.44) we let

$$\varepsilon < \min(\Big(\frac{\lambda(I_0)}{9c_{13}}\Big)^{\frac{1}{\alpha}}, \Big(\frac{\lambda(I_0)}{9c_{14}}\Big)^{\frac{1}{\alpha}}), \tag{2.2.61}$$

in which case, using the assumption $\alpha \ge \frac{2}{5}$ and (2.2.50)-(2.2.51), we can write

$$\alpha - \frac{C_\varepsilon(1-2\alpha)}{c_1\nu} = \alpha - \frac{(\lambda(I_0) + c_{13}\varepsilon^\alpha)(1-2\alpha)}{(\lambda(I_0) - c_{14}\varepsilon^\alpha)\nu} > \alpha(1 - \frac{5}{4}\frac{1-2\alpha}{\alpha}\frac{1}{\nu}) \ge \alpha(1 - \frac{5}{4}\frac{1}{2}\frac{1}{\nu}) = \frac{1}{3}\alpha, \tag{2.2.62}$$

provided we select

$$\nu = \frac{15}{16}.$$

Thus for ε smaller than the minimum of $\bar{\varepsilon}_0$, the bound of (2.2.24) with $\nu = 15/16$ and the bound of (2.2.61), (2.2.58)-(2.2.62) prove the estimate (2.2.44) with the same choice of $\bar{K}$ as for $\alpha = 1/2$. □

2.3 The existence of N-pulse homoclinic orbits: the energy-phase method

With the estimates and construction of the previous section at hand we now formulate our main result. First, for any $n \in \mathbb{Z}^+$ we define the *n-th order energy-difference function* $\Delta^n\mathcal{H}: A \to \mathbb{R}$ as

$$\begin{aligned} \Delta^n\mathcal{H}(I,\phi;\mu) &= \mathcal{H}(I,\phi;\mu) - \mathcal{H}(I,\phi - n\Delta\phi(I;\mu);\mu) \qquad (2.3.1)\\ &= H_1(\bar{x}^0(I;\mu),I,\phi;\mu,0) - H_1(\bar{x}^0(I;\mu),I,\phi - n\Delta\phi(I;\mu);\mu,0), \end{aligned}$$

and its zero set

$$V_+^n = \{\ (I,\phi) \in A \mid \Delta^n\mathcal{H}(I,\phi;\mu) = 0\ \}. \qquad (2.3.2)$$

Note that $\Delta^n\mathcal{H}$ contains *energy*-type information from the perturbed problem and *phase*-type information from the unperturbed problem.

We will be particularly interested in the transverse zeros of $\Delta^n\mathcal{H}$ which are contained in the set

$$Z_+^n = \{\ (I,\phi) \in V_+^n \mid D\Delta^n\mathcal{H}(I,\phi;\mu) \neq (0,0)\ \}, \qquad (2.3.3)$$

where D denotes the gradient operator w.r.t. the (I,ϕ) variables. We will also need the $-n\Delta\phi(I;\mu)$ translate of these sets in the ϕ coordinate direction, so we define

$$V_-^n = \mathcal{R}^{-n}(V_+^n), \qquad Z_-^n = \mathcal{R}^{-n}(Z_+^n), \qquad (2.3.4)$$

where the map $\mathcal{R}$ is defined in Lemma 2.2.5. Note that all the sets defined in (2.3.2)-(2.3.4) depend on the parameter μ.

In the following we will establish a "graphical" criterion to predict N-pulse homoclinic orbits to the manifold $\mathcal{A}_\varepsilon$. The criterion will require the knowledge of the orbit structure of the (one-degree-of-freedom) reduced Hamiltonian $\mathcal{H}$ (defined in (2.2.2)) on $(A, \bar{\omega})$. In particular, we will need to look for internal orbits of $\mathcal{H}$ (see section 2.1 for definition) which intersect Z_+^n or Z_-^n transversally. Under certain conditions such orbits will perturb to nearby internal orbits of $\mathcal{A}_\varepsilon$ which will be the ω- or α-limit sets of n-pulse homoclinic orbits to $\mathcal{A}_\varepsilon$. These orbits are *homoclinic to the manifold* $\mathcal{A}_\varepsilon$ but they are not necessarily asymptotic to the same invariant set within $\mathcal{A}_\varepsilon$ in positive and negative time. To describe them accurately, for any internal orbit $\gamma \subset A$ of $\mathcal{H}$ we introduce the *pulse number*

$$N(\gamma;\mu) = \min\{\ n \geq 1 \mid V_-^k \cap \gamma = \emptyset,\ k = 1, ..., n-1,\quad Z_-^n \pitchfork \gamma\ \}, \tag{2.3.5}$$

where the symbol $\pitchfork$ refers to *nonempty transversal intersection.* We then have the following main result.

Theorem 2.3.1 *Assume that hypotheses (H1) and (H2b) hold. Suppose that for an internal orbit $\gamma_0^- \subset A$ of the reduced Hamiltonian $\mathcal{H}$*

(A1) $N \equiv N(\gamma_0^-;\mu) < \infty$,

(A2) Let $b_- \in Z_-^N \cap \gamma_0^-$ *and* $b_+ = \mathcal{R}^N(b_-)$. *Assume that the orbit* $\gamma_0^+ \subset A$ *of the reduced Hamiltonian* $\mathcal{H}$ *which contains* b_+ *is an internal orbit with* $Z_+^N \pitchfork \gamma_0^+$ *(see Fig. 2.5).*

(A3) If $D_x H_0$ *points outwards on* W_0, *we assume that*

$$h_0^- = \mathcal{H}|\gamma_0^- < \mathcal{H}|\mathcal{R}^k(\gamma_0^-), \quad k = 1, ..., N-1.$$

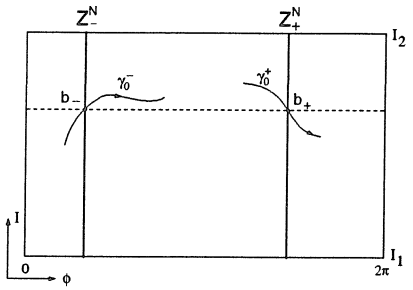

Figure 2.5: Assumption $(A2)$ of Theorem 2.3.1

If $D_x H_0$ points inwards on W_0, we assume that

$$h_0^- = \mathcal{H}|\gamma_0^- > \mathcal{H}|\mathcal{R}^k(\gamma_0^-), \quad k = 1, ..., N-1.$$

Then there exists $\varepsilon_0 > 0$ such that for $0 < \varepsilon < \varepsilon_0$

(i) $\mathcal{A}_\varepsilon$ has an N-pulse homoclinic orbit y_ε^N which is positively asymptotic to an internal orbit $\gamma_\varepsilon^+ \subset \mathcal{A}_\varepsilon$ and negatively asymptotic to an internal orbit $\gamma_\varepsilon^- \subset \mathcal{A}_\varepsilon$. Moreover, $g_\varepsilon^{-1}(\gamma_\varepsilon^+)$ and γ_0^+ are C^r ε-close, $g_\varepsilon^{-1}(\gamma_\varepsilon^+)$ and γ_0^+ are C^0 ε-close. If γ_0^+ is periodic, this latter statement can be strengthened to "C^r ε-close."

(ii) y_ε^N lies in the intersection of $W^u(\gamma_\varepsilon^-)$ and $W^s(\gamma_\varepsilon^+)$ which is transversal within the energy surface $E_\varepsilon(h)$ with $h = H|\gamma_\varepsilon^+ = H|\gamma_\varepsilon^-$.

(iii) Outside a neighborhood of $\mathcal{A}_\varepsilon$ y_ε^N is C^1 $\sqrt{\varepsilon}$-close to the set

$$Y^N = \cup_{i=1}^N y^i,$$

where $y^i \subset W_0$ is an unperturbed orbit of $(2.1.1)_{\varepsilon=0}$ asymptotic to the points $g_0 \circ \mathcal{R}^{i-1}(b_-)$ and $g_0 \circ \mathcal{R}^i(b_-)$ in negative and positive time, respectively, with $\mathcal{R}^0 \equiv Id$ (see Fig. 2.6 for a sketch of the geometry for $N = 3$).

Proof: First, we fix $\alpha = \frac{1}{2}$. Throughout the proof, when we refer to the results of section 2.2, this value of α will be used. We also select some $\vartheta > \vartheta^{(0)} \equiv \vartheta^*$ (see (2.2.35)) to ensure the applicability of (ii) of Lemma 2.2.4. Finally, we introduce the symbol $\overset{s,\varepsilon^\beta}{\sim}$ for C^s ε^β-closeness of sets and maps.

Let us start by letting $h_0^- = \mathcal{H}|\gamma_0^-$. Note that by the compactness of A and the smoothness of $\mathcal{H}$ (see (2.2.2)), there exists $\kappa > 0$ such that

$$\|h_0^-\| < \frac{\kappa}{2}. \tag{2.3.6}$$

Our second observation is that, as it follows immediately from the definition of Z_-^N, $\gamma_0^- \pitchfork Z_-^N$ implies

$$\mathcal{R}^k(\gamma_0^-) \cap \gamma_0^+ = \emptyset, \quad k = 1, ..., N-1, \qquad \mathcal{R}^N(\gamma_0^-) \pitchfork \gamma_0^+, \qquad \mathcal{H}|\gamma_0^+ = h_0^-. \tag{2.3.7}$$

Since γ_0^- is an internal orbit, for small ε, $\mathcal{A}_\varepsilon$ will contain an internal orbit γ_ε^- of $\mathcal{H}_\varepsilon$ such that

$$g_\varepsilon^{-1}(\gamma_\varepsilon^-) \overset{r,\varepsilon}{\sim} \gamma_0^-. \tag{2.3.8}$$

Let

$$h = H|\gamma_\varepsilon^- = \mathcal{H}_\varepsilon|\gamma_\varepsilon^- = h_0 + \varepsilon h_0^- + \mathcal{O}(\varepsilon^2), \tag{2.3.9}$$

with h_0 defined in (2.2.3). Since γ_0^+ is also an internal orbit, $D\mathcal{H}|\gamma_0^+ \neq 0$ (if γ_0^+ is a homoclinic orbit in A, this statement is not true on its closure). If γ_0^+ is a periodic orbit (i.e., a member of a family of periodic orbits of $\mathcal{H}$), by the implicit function theorem, there exists a periodic internal orbit γ_ε^+ such that $g_\varepsilon^{-1}(\gamma_\varepsilon^+) \overset{r,\varepsilon}{\sim} \gamma_0^+$ and

$$H|\gamma_\varepsilon^+ = \mathcal{H}_\varepsilon|\gamma_\varepsilon^+ = h. \tag{2.3.10}$$

If γ_0^+ is a homoclinic orbit, it perturbs to a nearby homoclinic orbit, but that does not necessarily have energy h. However, since there are internal periodic orbits arbitrarily

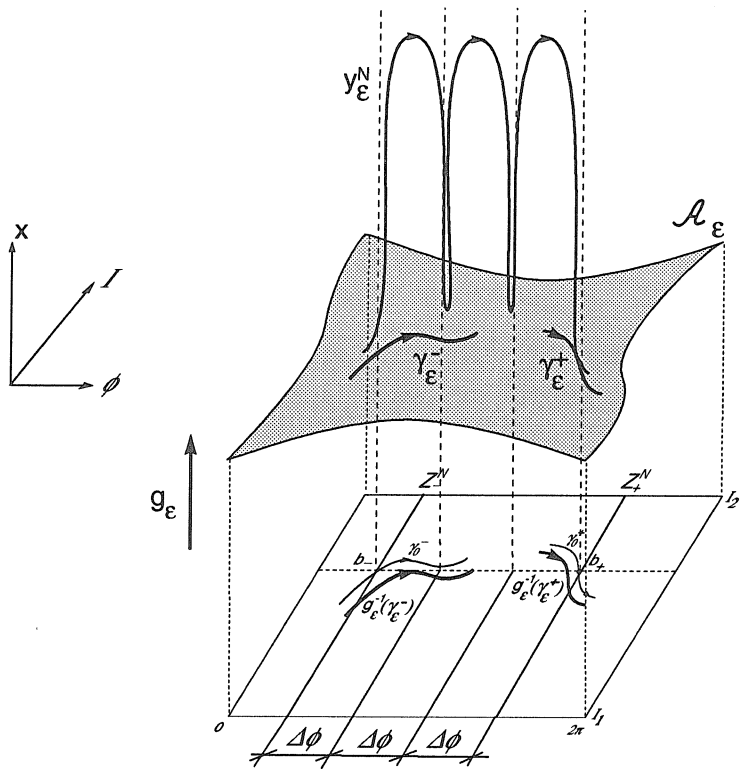

Figure 2.6: An example of the statement (iii) of Theorem 2.3.1 for $N = 3$

close to γ_0^+, we can guarantee the following: there exists an internal orbit γ_ε^+ such that

$$g_\varepsilon^{-1}(\gamma_\varepsilon^+) \overset{1,\varepsilon}{\sim} \gamma_0^+, \tag{2.3.11}$$

inside a fixed neighborhood of Z_+^N and (2.3.10) still holds. Then, for ε small enough, (2.3.7), (2.3.8), and (2.3.11) imply

$$\mathcal{R}^k(g_\varepsilon^{-1}(\gamma_\varepsilon^-)) \cap g_\varepsilon^{-1}(\gamma_\varepsilon^+) = \emptyset, \quad k = 1, ..., N-1, \qquad \mathcal{R}^N(g_\varepsilon^{-1}(\gamma_\varepsilon^-)) \pitchfork g_\varepsilon^{-1}(\gamma_\varepsilon^+). \tag{2.3.12}$$

Furthermore, we see from (2.3.6), (2.3.9), and (2.3.10) that for small $\varepsilon > 0$

$$\|h - h_0\| = \|H|\gamma_\varepsilon^+ - h_0\| = \|H|\gamma_\varepsilon^- - h_0\| = \varepsilon\|h_0^- + \mathcal{O}(\varepsilon)\| < \varepsilon\kappa, \tag{2.3.13}$$

which will make it possible to apply Lemmas 2. and 2.2.5.

By Proposition 2.2.1 (see also Haller and Wiggins [28]) γ_ε^- has a C^{r-1} local unstable manifold $W^u_{loc}(\gamma_\varepsilon^-) \subset W^u_{loc}(\mathcal{A}_\varepsilon)$, which consists of a subfamily of fibers f^u_ε (i.e., a smooth subset of the family $\mathcal{F}^s_\varepsilon$) with their basepoints contained in γ_ε^-. In the usual way $W^u_{loc}(\gamma_\varepsilon^-)$ can be extended to an injectively immersed global manifold $W^u(\gamma_\varepsilon^-) \subset E_\varepsilon(h)$. Now by (2.3.13) and (n) of Lemma 2.2.4, for small $\varepsilon > 0$, $\Sigma^u_\varepsilon(h)$ is a two dimensional graph over A. Since it is also a local transversal to the flow in $E_\varepsilon(h)$, it will be intersected transversally (within $E_\varepsilon(h)$) by $W^u_{loc}(\gamma_\varepsilon^-)$ in a curve $\mathcal{C}^{(1)}_u \subset \Sigma^u_\varepsilon(h)$ (the reader can use Fig. 2.7 to follow this and later steps in our construction). By Proposition 2.2.1

$$\rho_\varepsilon^- = (e^u_\varepsilon)^{-1}(\mathcal{C}^{(1)}_u) \overset{1,\sqrt{\varepsilon}}{\sim} g_\varepsilon^{-1}(\gamma_\varepsilon^-). \tag{2.3.14}$$

By (n) of Lemma 2.2.5, the global map G^h_ε map is defined on $\mathcal{C}^{(1)}_u$. Let us define $\mathcal{C}^{(1)}_s = G^h_\varepsilon(\mathcal{C}^{(1)}_u)$ and note that from (2.2.36) and (2.3.14) we have $(e^s_\varepsilon)^{-1}(\mathcal{C}^{(1)}_s) = \mathcal{G}^h_\varepsilon(\rho_\varepsilon^-)$. Similarly, $W^s_{loc}(\gamma_\varepsilon^+)$ intersects $\Sigma^s_\varepsilon(h)$ in a curve $\mathcal{D}_s \subset \Sigma^s_\varepsilon(h)$. We define $\rho_\varepsilon^+ = (e^s_\varepsilon)^{-1}(\mathcal{D}_s)$ and conclude from Proposition 2.2.1 that

$$\rho_\varepsilon^+ \overset{1,\sqrt{\varepsilon}}{\sim} g_\varepsilon^{-1}(\gamma_\varepsilon^+). \tag{2.3.15}$$

Then (2.3.7) and (2.3.14)-(2.3.15) imply

$$\mathcal{R}^k(\rho_\varepsilon^-) \cap \rho_\varepsilon^+ = \emptyset, \quad k = 1, ..., N-1, \qquad \mathcal{R}^N(\rho_\varepsilon^-) \pitchfork \rho_\varepsilon^+. \tag{2.3.16}$$

For future reference we now introduce the tracking map $\mathcal{T}^h_{\varepsilon,N}: A \to A$ by

$$\mathcal{T}^h_{\varepsilon,N} = \mathcal{G}^h_\varepsilon \circ \underbrace{(\mathcal{L}^h_\varepsilon \circ \mathcal{G}^h_\varepsilon) \circ ... \circ (\mathcal{L}^h_\varepsilon \circ \mathcal{G}^h_\varepsilon)}_{N-1}, \tag{2.3.17}$$

which (if well-defined) will be used to track the graph-projections of subsequent intersections of $W^u(\gamma_\varepsilon^-)$ with the manifold $\Sigma^s_\varepsilon(h)$.

Let us suppose that $N = 1$. Then for small $\varepsilon > 0$ (2.3.16), (2.3.17), and $(ii) - (iii)$ of Lemma 2.2.5 imply

$$\mathcal{T}^h_{\varepsilon,1}(\rho^-_\varepsilon) \pitchfork \rho^+_\varepsilon, \tag{2.3.18}$$

which, by the commutative diagrams of (2.2.36) proves that $\mathcal{C}^{(1)}_s \pitchfork \mathcal{D}_s$ within $\Sigma^s_\varepsilon(h)$ (e^s_ε is a diffeomorphism). But this in turn implies $W^u(\gamma^-_\varepsilon) \pitchfork W^s(\gamma^+_\varepsilon)$ within $E_\varepsilon(h)$, as claimed in (ii) of the lemma. Also, (iii) follows from the size of $U_{\delta(\varepsilon)}$ and the fact that $g_0 \circ \mathcal{R} \circ g_0^{-1}$ maps α-limit points of unperturbed homoclinic trajectories to their ω-limit points.

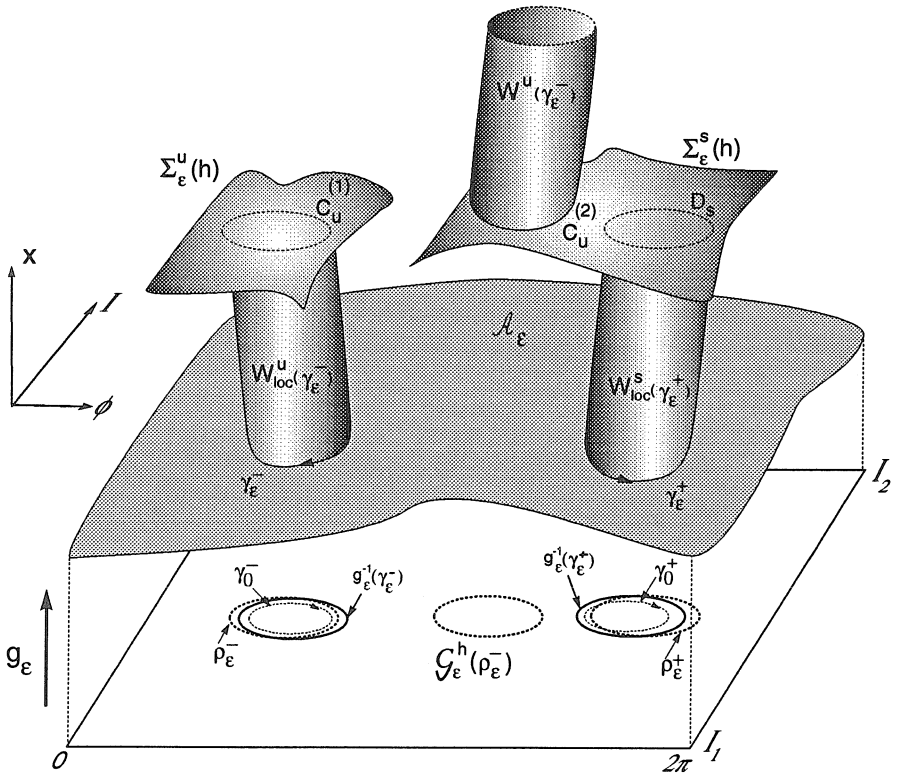

Figure 2.7: The main construction in the proof of Theorem 2.3.1

Let us now suppose that $N = 2$. From what we have discussed up till now it follows that in this case, for small ε, $\mathcal{C}^{(1)}_s \cap \mathcal{D}_s = \emptyset$, hence the trajectories of (2.1.1) enter $U_{\delta(\varepsilon)}$

without intersecting $\tilde{W}^s_{loc}(\mathcal{A}_\varepsilon)$. Using (2.2.20) we know that for small ε $T^\varepsilon(U_{\delta(\varepsilon)})$ is contained in a tubular neighborhood of the manifold $z = 0$ in the phase space of (2.2.5) which is a subset of $\tilde{U}(\bar{\varepsilon}_0)$. This means that the above trajectories missing $\mathcal{D}_s$ enter a neighborhood of $\mathcal{A}_\varepsilon$ in which their behavior is described by the normal form (2.2.5). Consequently, in compliance with the normal hyperbolicity of $\mathcal{A}_\varepsilon$, they will make a near-saddle type passage and leave a neigborhood of $\mathcal{A}_\varepsilon$. We want them to exit along $\tilde{W}^u_{loc}(\mathcal{A}_\varepsilon)$ (see the discussion after Lemma 2.2.3) which we know about from hypothesis (H1). In particular, let us suppose that for $\varepsilon = 0$ the $z_1, z_2 > 0$ "quadrant" of the phase space of (2.2.5) contains trajectories which lie inside the homoclinic manifold W_0. Then, for the local analysis of the perturbed system, we would like the incoming trajectories to have positive z_1 and z_2 coordinates so that when they leave a neighborhood of $\mathcal{A}_\varepsilon$ they would traverse in a neighborhood of W_0. At this point we only know that the trajectories starting from $\mathcal{C}^{(1)}_s$ miss $\mathcal{D}_s$ and enter with positive z_2 coordinate. It is this point where we use assumption (A3). Note that, based on Proposition 2.2.1, $W^s_{loc}(\mathcal{A}_\varepsilon) \cap \partial_1 U_{\delta(\varepsilon)}$ is foliated by curves which are the intersections of the local stable manifolds of orbits in $\mathcal{A}_\varepsilon$ with $\partial_1 U_{\delta(\varepsilon)}$. As Π^s_u, $\tilde{W}^s_{loc}(\mathcal{A}_\varepsilon) \cap \partial_1 U_{\delta(\varepsilon)}$ is given by a graph $g_{W^s}: A \to \mathcal{P}$ over A, too, and by Proposition 2.2.1 the graph-projections of its foliating curves are C^1 $\sqrt{\varepsilon}$-close in A to the graph-projections of the corresponding curves of $\mathcal{A}_\varepsilon$. This implies that near $\mathcal{C}^{(1)}_s$ $\tilde{W}^s_{loc}(\mathcal{A}_\varepsilon) \cap \partial_1 U_{\delta(\varepsilon)}$ is locally foliated by curves whose graph-projections on A are C^1 $\sqrt{\varepsilon}$-close in A to level curves of $g^*_\varepsilon \mathcal{H}_\varepsilon$ which intersect $\rho^{(1)}_\varepsilon$. By assumption (A1), for small ε, $\rho^{(1)}_\varepsilon$ is intersected by level curves which have energies higher than h provided $D_x H$ points outward on $W^s_{loc}(\mathcal{A}_\varepsilon)$. This means that $\mathcal{C}^{(1)}_s$ (and the trajectories through it) lie in the "inner side" of the hypersurface $W^s_{loc}(\mathcal{A}_\varepsilon)$. More precisely, their image under T^ε lies in the $z_1, z_2 > 0$ region of the phase space of (2.2.5). One reaches a similar conclusion under assumption (A3) in the case when $D_x H_0$ is assumed to point outside on W_0.

Knowing the basic character of passage near $\mathcal{A}_\varepsilon$ of the trajectories starting from $\mathcal{C}_s^{(1)}$, we expect to be able to track them via the local map L_ε^h. By Lemma 2.2.5, we have a good approximation for the conjugate map $\mathcal{L}_\varepsilon^h$ provided the distance condition (2.2.38) is satisfied for an appropriate $0 < K < \vartheta$. Since $cl(\gamma_0^-)$ is compact and, by assumption (A1), it is separated from Z_-^N, assumption (A3) implies the existence of a positive number $K^{(1)} > 0$ such that

$$\|h_0^- - \mathcal{H}|\mathcal{R}(\gamma_0^-)\| > 2K^{(1)}. \tag{2.3.19}$$

Based on the above discussion on the foliation of $\tilde{W}^s_{loc}(\mathcal{A}_\varepsilon) \cap \partial_1 U_{\delta(\varepsilon)}$ and on the C^1 $\sqrt{\varepsilon}$ closeness of the objects involved, we conclude from (2.3.9) and (2.3.19) that if $p_c \in \mathcal{C}_s^{(1)}$ and $p_w \in \tilde{W}^s_{loc}(\mathcal{A}_\varepsilon)$ are two points with the same (I, ϕ) coordinates, then

$$\begin{aligned} \|H|_{p_c} - H|_{p_w}\| &= \|h - [h_0 + \varepsilon\mathcal{H}|W_\varepsilon^{-1}(p_w) + \mathcal{O}(\varepsilon\sqrt{\varepsilon})]\| \\ &= \|h_0 + \varepsilon h_0^- + \mathcal{O}(\varepsilon\sqrt{\varepsilon}) - [h_0 + \varepsilon\mathcal{H}|_{p_w^0} + \mathcal{O}(\varepsilon\sqrt{\varepsilon})]\| \\ &= \varepsilon\|h_0^- - \mathcal{H}|_{p_w^0} + \mathcal{O}(\sqrt{\varepsilon})\| > K^{(1)}\varepsilon, \end{aligned} \tag{2.3.20}$$

where $p_w^0 \in \mathcal{R}(\gamma_0^-)$ is a point $\sqrt{\varepsilon}$-close to $W_\varepsilon^{-1}(p_w)$. For an appropriate $c_{16} > 0$ let $c_{16}\vartheta\sqrt{\varepsilon}$ be an upper bound for $\|DH\|$ in $U_{\delta(\varepsilon)}$ (see (2.2.29) and compare (2.2.30)). Then the Mean Value Theorem and (2.3.20) imply

$$\varepsilon K^{(1)} < \|H|_{p_c} - H|_{p_w}\| \leq c_{16}\vartheta\sqrt{\varepsilon}\|p_c - p_w\|,$$

which yields

$$\|p_c - p_w\| \geq \frac{K^{(1)}}{c_{16}\vartheta}\sqrt{\varepsilon}. \tag{2.3.21}$$

Then, setting $S_\varepsilon^s(h) \equiv cl(\mathcal{C}_s^{(1)})$, the conditions of (ii) of Lemma 2.2.5 for $\alpha = \frac{1}{2}$ are satisfied provided we choose

$$0 < \frac{K^1}{c_{16}\vartheta} < \vartheta, \qquad \Rightarrow \qquad \vartheta > \vartheta^{(1)} = \max(\vartheta^{(0)}, \sqrt{\frac{K^{(1)}}{c_{16}}}).$$

So, by (iii) of Lemma 2.2.5, for $\varepsilon > 0$ sufficiently small, the trajectories starting from $\mathcal{C}_s^{(1)}$ will intersect $\Sigma_\varepsilon^u(h)$ in a curve $\mathcal{C}_u^{(2)} = L_\varepsilon^h(\mathcal{C}_s^{(1)})$. Moreover, by (ii) of Lemma 2.2.5 they will later reintersect $\Sigma_\varepsilon^s(h)$ in a curve $\mathcal{C}_s^{(2)}$ with

$$\mathcal{C}_s^{(2)} = G_\varepsilon^h(\mathcal{C}_u^{(2)}) = G_\varepsilon^h \circ L_\varepsilon^h \circ G_\varepsilon^h(\mathcal{C}_u^{(1)}). \tag{2.3.22}$$

Also, Lemma 2.2.5, the commutative diagrams of (2.2.36), (2.3.17), and (2.3.22) show that

$$\mathcal{T}_{\varepsilon,2}^h(\rho_\varepsilon^-) \overset{1,\sqrt{\varepsilon}}{\sim} \mathcal{R}^2(\rho_\varepsilon^-). \tag{2.3.23}$$

Then, as in the case of $N = 1$, (2.3.16), (2.3.15) and (2.3.23) imply

$$\mathcal{T}_{\varepsilon,2}^h(\rho_\varepsilon^-) \pitchfork \rho_\varepsilon^+.$$

From this, by the same argument as in the case $N = 1$, we conclude statements $(i)-(iii)$ of the theorem for $N = 2$ and for some ε_0 bound on ε.

On can now repeat the above construction for any $N > 2$. Assumption (A3) ensures a repeated "nice" passage of the orbits of $W^u(\gamma_\varepsilon^-)$ near $\mathcal{A}_\varepsilon$. At the j-th passage $(j < N)$ we find an appropriate constant $K^{(j)} \geq K^{(j-1)} > 0$ (see (2.3.20)) to describe the energy-difference between orbits in $W^u(\gamma_\varepsilon^-)$ and nearby orbits of $\tilde{W}^s(\mathcal{A}_\varepsilon)$. This provides us with an estimate of the form (2.3.21) for the local distance of the two manifolds. To follow the passage via the local map L_ε^h, we select the size of $U_{\delta(\varepsilon)}$ by setting

$$\vartheta = \vartheta^{(j)} = \max(\vartheta^{(j-1)}, \sqrt{\frac{K^{(j)}}{c_{15}}}).$$

We define $\mathcal{C}_u^{(j+1)} = L_\varepsilon^h(\mathcal{C}_s^{(j)})$, and apply the global map G_ε^h to $\mathcal{C}_u^{(j+1)}$. We define the curve

$$\mathcal{C}_s^{(j+1)} = G_\varepsilon^h(\mathcal{C}_u^{(j)}),$$

which is the $j+1$-st intersection (in forward time) of $W^u(\gamma_\varepsilon^-)$ with $\Sigma_\varepsilon^s(h)$. Note that by Lemma 2.2.5

$$\mathcal{T}_{\varepsilon,j+1}^h(\rho_\varepsilon^-) = (e_\varepsilon^s)^{-1}(\mathcal{C}_s^{(j+1)}) \overset{1,\sqrt{\varepsilon}}{\sim} \mathcal{R}^{j+1}(\rho_\varepsilon^-). \tag{2.3.24}$$

If $j+1=N$ then (2.3.16), (2.3.15), and (2.3.24) imply

$$\mathcal{T}^h_{\varepsilon,N}(\rho^-_\varepsilon) \pitchfork \rho^+_\varepsilon,$$

which proves the theorem the same way as in the case $N=2$. If $j+1<N$ we repeat the above construction recursively until we reach N. In every step we possibly need to decrease the current bound $\varepsilon_0^{(j)}>0$ on ε to be able to proceed further. Since N is finite, we can finally select $\varepsilon_0 \equiv \varepsilon_0^{(N)}>0$ so that the statements of the theorem hold. □

An immediate consequence of Theorem 2.3.1 is the following:

Theorem 2.3.2 *Let us assume that hypotheses (H1) and (H2b) are satisfied and assumptions (A1)-(A3) of Theorem 2.3.1 hold. Let us further assume that $\gamma_0^+ = \gamma_0^-$ of Theorem 2.3.1 is a periodic orbit in A. Then*

(*i*) *The statements of Theorem 2.3.1 hold with $\gamma_\varepsilon = \gamma_\varepsilon^+ = \gamma_\varepsilon^-$ and there exists one more N-pulse transverse homoclinic orbit $\tilde{y}^N_\varepsilon$ with properties similar to those of $\tilde{y}^N_\varepsilon$ (but with corresponding "base-points" $\tilde{b}_+ \neq b_+$ and $\tilde{b}_- \neq b_-$).*

(*ii*) *System (2.1.1) has Smale-horseshoes near γ_ε on energy surfaces sufficiently close to $E_\varepsilon(h)$.*

Proof: Statement (*i*) follows from the fact that the oriented self-intersection number of a curve homeomorphic to the circle is 0, hence if $\mathcal{T}^h_{\varepsilon,N}(\rho^-_\varepsilon)$ and $\rho^-_\varepsilon = \rho^+_\varepsilon$ intersect transversally, then they intersect in at least two points. Since we now have a periodic orbit γ_ε with transverse homoclinic orbits, statement (*ii*) follows from the Smale-Birkhoff homoclinic theorem (see Smale [66]) and the structural stability of horseshoes. □

The statement of Theorem 2.3.2 is sketched in Fig. 2.8 for the case $N=3$. We now supplement Theorems 2.3.1 and 2.3.2 with the following remarks.

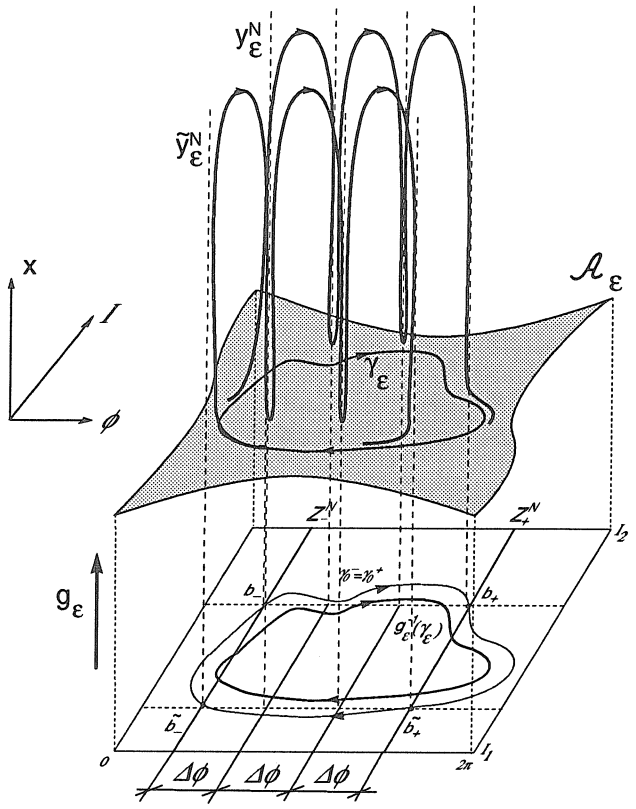

Figure 2.8: The statement of Theorem 2.3.2 for $N = 3$

Remark 2.3.1 Generically, γ_0^- and Z_-^N will intersect transversally in more than one points and each intersection point will give rise to a transverse N-pulse orbit which is negatively asymptotic to γ_ε^-.

Remark 2.3.2 In the case $N = 1$ Theorem 2.3.1 gives a result similar to that of Haller and Wiggins [28]. In that reference, however, we obtained better smoothness results for the distance of y_ε^1 and the set Y^1. The reason is that to detect simple (i.e., one-pulse) homoclinic orbits to the manifold $\mathcal{A}_\varepsilon$, one does not have to deal with the complications related to the long-time passage near $\mathcal{A}_\varepsilon$ (see the definition of the tracking map in (2.3.17) for $N = 1$). Consequently, one can select a fixed tubular neigborhood U_{δ_0} around $\mathcal{A}_\varepsilon$

to work with. This results in a finite time of flight (i.e., bounded by a constant which is independent of ε) for the trajectories travelling from $\mathcal{C}_u^{(1)}$ to $\mathcal{C}_s^{(1)}$. Then, by simple Gronwall-estimates (compare Lemma 2.2.5), $\mathcal{R}$ is C^r ε-close to the conjugate global map $\mathcal{G}_\varepsilon^h$, and the above analysis is essentially equivalent to the Melnikov-type analysis of [28].

Remark 2.3.3 Statement (ii) of Theorem 2.3.1 has an asymmetry: it does not always guarantee the C^r ε closeness of $g_\varepsilon^{-1}(\gamma_\varepsilon^+)$ and γ_0^+. This is the consequence of the fact that we based our construction on γ_0^- and chose $h = H|\gamma_\varepsilon^-$ to be the "reference-energy." As we pointed out in the proof, if γ_0^+ is a homoclinic internal orbit, it will give rise to a perturbed orbit $\tilde{\gamma}_\varepsilon^+$ such that $g_\varepsilon^{-1}(\tilde{\gamma}_\varepsilon^+)$ and γ_0^+ are C^r ε-close, but in general $\tilde{h} = H|\tilde{\gamma}_\varepsilon^+ \neq h$, hence $\tilde{\gamma}_\varepsilon^+ \neq \gamma_\varepsilon^+$. However, by the same argument, one can guarantee that there exists an orbit $\tilde{\gamma}_\varepsilon^-$ with $g_\varepsilon^{-1}(\tilde{\gamma}_\varepsilon^-)$ C^0 ε-close to γ_0^-, such that $\tilde{\gamma}_\varepsilon^-$ and $\tilde{\gamma}_\varepsilon^+$ are connected by an N-pulse orbit $\tilde{y}_\varepsilon^N$ (hence $H|\tilde{\gamma}_\varepsilon^- = \tilde{h}$). Also, $\tilde{y}_\varepsilon^N$ is easily seen to obey statement (iii) of Theorem 2.3.1. This resolves the asymmetry mentioned above.

Remark 2.3.4 Regarding statement (iii) of Theorem 2.3.1, notice that the C^1 $\sqrt{\varepsilon}$ closeness of trajectories may not be optimal for the purposes of numerical simulation. Repeating the proof of Theorem 2.3.1 with the choice $\alpha = \frac{2}{5}$, one can obtain C^0 $\varepsilon^{\frac{3}{5}}$ closeness in the I coordinates. This may be particularly important in relation with the upcoming results of section 2.4 where one wants to keep the change of the I coordinate during one pulse much less in order than $\mathcal{O}(\sqrt{\varepsilon})$. The lesser this change is the higher bound on ε we can choose, to still be able to predict and detect homoclinic orbits with a fixed pulse number.

Remark 2.3.5 As in Haller and Wiggins [28], we point out that if γ_0^- and γ_0^+ are distinct periodic orbits of the reduced Hamiltonian, then transverse N-pulse *heteroclinic*

connections between their perturbed counterparts can be destroyed by arbitrarily small further perturbation. However, since both of them are embedded in families of periodic orbits, and subsets of these families intersect Z_-^N and Z_+^N, respectively, transversally, the *family of heteroclinic connections* between the two sets of periodic orbits *is stable.* If γ_0^- and γ_0^+ are identical periodic solutions (as in the set-up of Theorem 2.3.2), sufficiently small perturbation will preserve the *homoclinic* connection between them.

Theorem 2.3.1 contains the basic construction of N-pulse homoclinic orbits to the manifold $\mathcal{A}_\varepsilon$. For brevity, conditions (A1)-(A3) assume the most simple situation possible, but we now give modifications of the basic results for two special cases arising in applications. The first one weakens assumptions (A2) and (A3) in order to detect orbits homoclinic to *resonant internal orbits.* These internal orbits are invariant under some iterate of the rotation map $\mathcal{R}$ and play a crucial role in the identification of regions in $\mathcal{A}_\varepsilon$ containing orbits with the same pulse number. The second modification of Theorem 2.3.1 assumes a more detailed knowledge of the global geometry of system (2.1.1) together with a symmetry. Again, for the sake of simple exposition, we will not deal with the most general case. However, we are confident that using the ideas of Theorem 2.3.1 the reader can easily "customize" the theorems of the remainder of this section to the specific needs of a given problem.

Let us suppose that for an internal orbit γ of $\mathcal{H}$ $\mathcal{R}^m(\gamma) = \gamma$ holds with some $m \geq 1$. This implies that γ has a nontransversal intersection with V_-^m. If, in addition, $V_-^m = Z_-^m$ and

$$\gamma = V_-^j \cap \gamma = \emptyset, \qquad j = 1, ..., m-1$$

hold then by (2.3.5) we will clearly have $N(\gamma;\mu) = \infty$, hence Theorem 2.3.1 is not applicable to γ. However, with a slight modification one can still predict the existence

of N-pulse homoclinic orbits asymptotic to γ *without guaranteeing their transversality.* Internal orbits tangent to Z_+^n and Z_-^n arise frequently in the applications we know of, and they separate regions in A with orbits having the same (finite) pulse numbers (see, e.g., chapter 4).

We now introduce the *resonant pulse number*

$$N_R(\gamma;\mu) = \min\{\ n \geq 1 \mid V_-^k \cap \gamma = \emptyset,\ k = 1, ..., n-1,\ \ \mathcal{R}^n(\gamma) = \gamma\}. \qquad (2.3.25)$$

To make our previous discussion more precise, we will call an internal orbit γ_0 *resonant* if $N_R(\gamma_0, \mu) < \infty$ holds.

Theorem 2.3.3 *Assume that hypotheses (H1) and (H2b) hold. Suppose further that for an internal orbit $\gamma_0 \subset A$ of the reduced Hamiltonian $\mathcal{H}$*

(A1) $N \equiv N_R(\gamma_0;\mu) < \infty$ (γ_0 is resonant),

(A2) Assumption (A3) of Theorem 2.3.1 holds with $\gamma_0 = \gamma_0^-$.

Then there exists $\varepsilon_0 > 0$ such that for $0 < \varepsilon < \varepsilon_0$

(i) $\mathcal{A}_\varepsilon$ has two N-pulse homoclinic orbits, y_ε^N and $\tilde{y}_\varepsilon^N$, which are asymptotic in positive and negative time to an internal orbit $\gamma_\varepsilon \subset \mathcal{A}_\varepsilon$. The orbits γ_0 and $g_\varepsilon^{-1}(\gamma_\varepsilon)$ are C^r ε-close in A.

(ii) There exists two points $b_-, \tilde{b}_- \in \gamma_0$ such that outside a neighborhood of $\mathcal{A}_\varepsilon$ y_ε^N ($\tilde{y}_\varepsilon^N$) is C^1 $\sqrt{\varepsilon}$-close to the set

$$Y^N = \cup_{i=1}^N y^i, \qquad (\tilde{Y}^N = \cup_{i=1}^N \tilde{y}^i,)$$

where $y^i \subset W_0$ ($\tilde{y}^i \subset W_0$) is an unperturbed orbit of $(2.1.1)_{\varepsilon=0}$ asymptotic to the

points $g_0 \circ \mathcal{R}^{i-1}(b_-)$ *(*$g_0 \circ \mathcal{R}^{i-1}(\tilde{b}_-)$*) and* $g_0 \circ \mathcal{R}^i(b_-)$ *(*$g_0 \circ \mathcal{R}^i(\tilde{b}_-)$*) in negative and positive time, respectively. (*$\mathcal{R}^0 \equiv Id$*).*

Proof: The only significant difference compared to the proof of Theorem 2.3.1 that instead of (2.3.7) we now have the relations

$$\mathcal{R}^k(\gamma_0) \cap \gamma_0 = \emptyset, \quad k = 1, ..., N-1, \quad \mathcal{R}^N(\gamma_0) = \gamma_0. \tag{2.3.26}$$

As in the proof of Theorem 2.3.3, (2.3.26) leads to (cf. (2.3.16) and (2.3.17))

$$\mathcal{T}^h_{\varepsilon,N}(\rho^-_\varepsilon) \overset{1,\sqrt{\varepsilon}}{\sim} \rho^+_\varepsilon, \tag{2.3.27}$$

with

$$\rho^-_\varepsilon = (e^u_\varepsilon)^{-1}(W^u_{loc}(\gamma_\varepsilon) \cap \Sigma^u_\varepsilon(h)), \quad \rho^+_\varepsilon = (e^s_\varepsilon)^{-1}(W^s_{loc}(\gamma_\varepsilon) \cap \Sigma^s_\varepsilon(h)).$$

Now recall that according to (i) of Lemma 2.2.5, $\mathcal{G}^h_\varepsilon$ and $\mathcal{L}^h_\varepsilon$ preserve the symplectic form $d\phi \wedge dI$, thus the tracking map $\mathcal{T}^h_{\varepsilon,N}$ of (2.3.17) is area preserving for any $N \geq 1$. Consequently, if ρ^-_ε is a closed curve, then, by (2.3.27), $\mathcal{T}^h_{\varepsilon,N}(\rho^-_\varepsilon)$ must intersect ρ^+_ε in at least two points. For the same reason, if ρ^-_ε is not a closed curve (it originates from an internal orbit γ_0 homoclinic to $p_0 \in A$), $cl(\mathcal{T}^h_{\varepsilon,N}(\rho^-_\varepsilon))$ and $cl(\rho^+_\varepsilon)$ must intersect in at least two points. In this case, one point in the intersection may give rise to an N-pulse orbit $\tilde{y}^N_\varepsilon$ which is homoclinic to a fixed point $p_\varepsilon \in \mathcal{A}_\varepsilon$ with $g^{-1}_\varepsilon(p_\varepsilon)$ ε-close to p_0 in A. Then the statement of the theorem follows the same way as in the proof of Theorem 2.3.1. □

Our second modification of Theorem 2.3.1 deals with the case when there is one more homoclinic manifold to $\mathcal{A}_0$ to start with. We will concentrate on the case when both homoclinic manifolds admit the same phase shift. This is satisfied in all the applications we know of involving two homoclinic manifolds, and it can be explained by the presence of

a discrete symmetry in these problems. In Theorem 2.3.4 we will give conditions for the existence of *jumping N-pulse homoclinic orbits* to the manifold $\mathcal{A}_\varepsilon$. These orbits make N departures and returns, as the N-pulse homoclinic orbits of Theorem 2.3.1, but they also keep changing the unperturbed homoclinic manifold which they temporarily follow. This kind of behavior can be best described in terms of symbol sequences. To make the exposition simpler, we will also assume that $D_x H_0$ points *inwards* on both homoclinic manifolds. One can remove this restriction to obtain somewhat more complicated statements with the same proof.

We first change our initial hypothesis (H1) to

(H1') There exist $I_1, I_2 \in \mathbb{R}$, $I_1 < I_2$ such that for any $(I,\mu) \in [I_1, I_2] \times W$ $(2.1.1)^x_{\varepsilon=0}$ has a hyperbolic fixed point $\bar{x}_0(I;\mu)$ connected to itself by two homoclinic trajectories $x^{h+}(t,I;\mu)$ and $x^{h-}(t,I;\mu)$. Moreover, $D_x H_0$ points inwards on both homoclinic trajectories.

As in section 2.1, (H1') implies the existence of two homoclinic manifolds W_0^+ and W_0^- (see Fig. 2.9), which contain solutions $y_0^+(t,I,\phi_0;\mu)$ and $y_0^-(t,I,\phi_0;\mu)$ of $(2.1.1)_{\varepsilon=0}$ (compare (2.1.4) and substitute $x^{h+}(t,I;\mu)$ and $x^{h-}(t,I;\mu)$, respectively). As we indicated above, our next major assumption is

(H3) For all $I \in [I_1, I_2]$

$$\Delta\phi(I;\mu) = \int_{-\infty}^{+\infty} D_I H_0(x^{h+}(t,I;\mu), I;\mu)\, dt \equiv \int_{-\infty}^{+\infty} D_I H_0(x^{h-}(t,I;\mu), I;\mu)\, dt.$$

We then have the following result on jumping N-pulse homoclinic orbits.

Theorem 2.3.4 *Assume that hypotheses (H1'),(H2b), and (H3) hold. Suppose that for an internal orbit $\gamma_0^- \subset A$ of the reduced Hamiltonian $\mathcal{H}$*

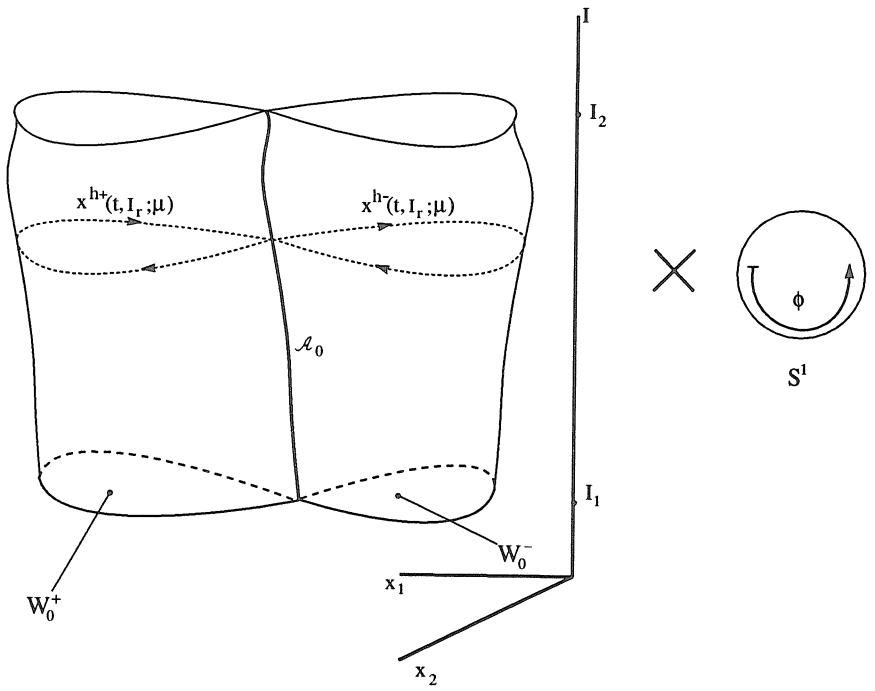

Figure 2.9: Hypothesis ($H1'$)

(A1) $N \equiv N(\gamma_0^-;\mu) < \infty$,

(A2) Assumption (A2) of Theorem 2.3.1 holds,

(A3) Let $\chi_{j+1} = \text{sign}\,(h_0^- - \mathcal{H}|\mathcal{R}^j(\gamma_0^-))\chi_j$, $j = 1,...,N$, *with* $\chi_1 \in \{-1,+1\}$ *to be specified below.*

Then there exists $\varepsilon_0 > 0$ *such that for* $0 < \varepsilon < \varepsilon_0$*:*

(i) $\mathcal{A}_\varepsilon$ *has two* N*-pulse homoclinic orbit* y_ε^{N+} *and* y_ε^{N-} *which are positively asymptotic to an internal orbit* $\gamma_\varepsilon^+ \subset \mathcal{A}_\varepsilon$ *and negatively asymptotic to an internal orbit* $\gamma_\varepsilon^- \subset \mathcal{A}_\varepsilon$. *Moreover,* $g_\varepsilon^{-1}(\gamma_\varepsilon^+)$ *and* γ_0^- *are* C^r ε*-close,* $g_\varepsilon^{-1}(\gamma_\varepsilon^+)$ *and* γ_0^+ *are* C^0 ε*-close. If* γ_0^+ *is periodic, this latter statement can be strengthened to "*C^r ε*-close."*

(*ii*) y_ε^{N+} *and* y_ε^{N-} *lie in the intersection of* $W^u(\gamma_\varepsilon^-)$ *and* $W^s(\gamma_\varepsilon^+)$ *which is transversal within the energy surface* $E_\varepsilon(h)$ *with* $h = H|\gamma_\varepsilon^+ = H|\gamma_\varepsilon^-$.

(*iii*) *Let us set* $\chi_1 = +1$. *Then outside a neighborhood of* $\mathcal{A}_\varepsilon$ y_ε^{N+} *is* C^1 $\sqrt{\varepsilon}$*-close to the set*

$$Y^{N+} = \cup_{i=1}^N y^i(\chi_i), \tag{2.3.28}$$

where

$$y^i(\chi_i) \subset \begin{cases} W_0^+ & \text{if } \chi_i = +1, \\ W_0^- & \text{if } \chi_i = -1, \end{cases} \tag{2.3.29}$$

is an unperturbed orbit of $(2.1.1)_{\varepsilon=0}$ *asymptotic to the points* $g_0(\mathcal{R}^{i-1}(b_-))$ *and* $g_0(\mathcal{R}^i(b_-))$ *in negative and positive time, respectively* ($\mathcal{R}^0 \equiv Id$). *Setting* $\chi_1 = -1$ *we obtain a similar statement on the relation of the orbit* y_ε^{N-} *to the set* Y^{N-} *(defined the same way as in (2.3.28)-(2.3.29)).*

Proof: The proof is the application of the proof of Theorem 2.3.1 to the perturbation of W_0^+ and W_0^-, individually. This time, however, we do not have to worry about keeping the trajectories passing near $\mathcal{A}_\varepsilon$ "on the same side" (see the discussion of the $N = 2$ case in the proof of Theorem 2.3.1). We only keep track continuously where the passing trajectories end up: if after the j-th local passage they remain near the homoclinic manifold they followed during the j-th pulse, we set the sign of χ_{j+1} to the sign of χ_j. If not, we reverse the sign of χ_{j+1} compared to χ_j. In view of this the statements of the theorem follow. □

An example of the possible cases covered by Theorem 2.3.4 is sketched in Fig. 2.10 for $N = 3$ and with the "jump sequence" $\chi_2 = -\chi_1$, and $\chi_3 = -\chi_2$ (the intersection of the jumping homoclinic orbits with the slow manifold is of course an artifact of the projection from $\mathcal{P}$).

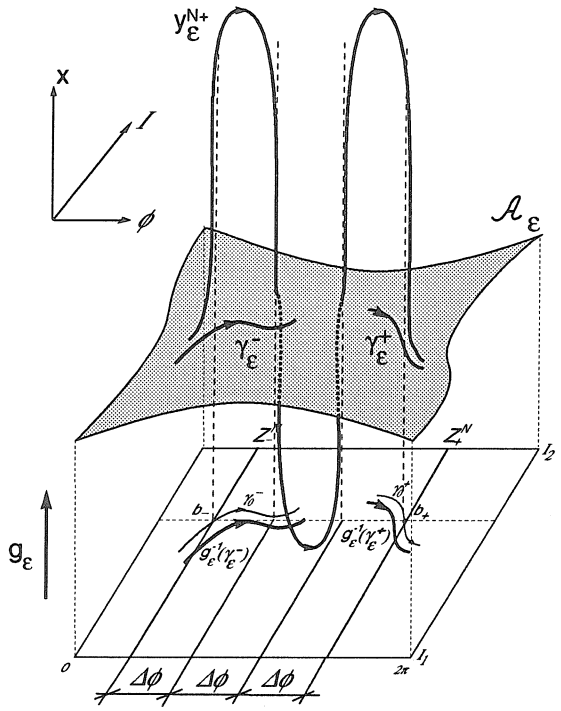

Figure 2.10: An example of the statement of Theorem 2.3.4 for $N = 3$ and "jump sequence" $\chi_2 = -\chi_1$, $\chi_3 = -\chi_2$

2.4 An application: N-pulse orbits homoclinic to resonance bands

In this section, as we indicated in the introduction, we will examine the existence of N-pulse homoclinic orbits in the case covered by hypothesis (H2a). Namely, we will assume the presence of an isolated circle of equilibria within the unperturbed normally hyperbolic manifold $\mathcal{A}_0$ and focus on the consequences of the break-up of this circle under perturbation. The key idea in studying this is blowing up the circle into a "thin" manifold of equilibria or *resonance band* (see Kovačič and Wiggins [44]). This resonance band appears as a two dimensional manifold of equilibria for a system which we will call the *standard form* (see eqs. (2.4.1)). Consequently, the analysis of N-pulse orbits

homoclinic to resonance bands simplifies to the application of the more general results of section 2.3.

Our program will be to apply the energy-phase method of section 2.2 to the standard form and then transform the results back to system (2.1.1). For clarity, we will put a hat on the quantities pertaining to the standard form to distinguish them from quantities directly related to our original system (2.1.1). For a detailed derivation of the equations used in this section and for more geometry the reader is referred to [28]. Throughout this section the Hamiltonian function H of system (2.1.1) will be assumed C^{r+1} smooth with $r \geq 5$.

First, we restrict the variable I to an ε-dependent neighborhood of the resonant value $I = I_r$ by letting

$$I = I_r + \eta\sqrt{\varepsilon}, \quad \eta \in [-\eta_0, \eta_0],$$

with $\eta_0 > 0$ to be determined later. In this "slice" of the phase space $\mathcal{P}$, we can Taylor-expand the right-hand-side of eq. (2.1.1) to obtain the *standard form*

$$\begin{aligned} \dot{x} &= J_2 D_x H_0(x, I_r; \mu) + \sqrt{\varepsilon} J_2 D_x D_I H_0(x, I_r; \mu)\eta + \mathcal{O}(\sqrt{\varepsilon}^2), \\ \dot{\eta} &= -\sqrt{\varepsilon} D_\phi H_1(x, I_r, \phi; \mu, 0) + \mathcal{O}(\sqrt{\varepsilon}^2), \\ \dot{\phi} &= D_I H_0(x, I_r; \mu) + \sqrt{\varepsilon} D_I^2 H_0(x, I_r; \mu)\eta + \mathcal{O}(\sqrt{\varepsilon}^2). \end{aligned} \tag{2.4.1}$$

For $\varepsilon > 0$ system (2.4.1) is Hamiltonian on the space $(\hat{\mathcal{P}}, \hat{\omega})$ with

$$\begin{aligned} \hat{\mathcal{P}} &= \mathbb{R}^2 \times [-\eta_0, \eta_0] \times S^1, \\ \hat{\omega} &= dx_1 \wedge dx_2 + \frac{1}{\sqrt{\varepsilon}} d\phi \wedge d\eta, \end{aligned}$$

and with the corresponding Hamiltonian

$$\hat{H}(x, \eta, \phi; \mu, \sqrt{\varepsilon}) = H(x, I_r + \sqrt{\varepsilon}\eta, \phi; \mu, \varepsilon) = H_0(x, I_r; \mu) + \sqrt{\varepsilon}\hat{H}_1(x, \eta, \phi; \mu, \sqrt{\varepsilon}). \tag{2.4.2}$$

Note that in (2.4.2) the function

$$\hat{H}_1(x,\eta,\phi;\mu,\varepsilon) = D_I H_0(x,I_r;\mu)\eta + \sqrt{\varepsilon}[\frac{1}{2}D_I^2 H_0(x,I_r;\mu)\eta^2 + H_1(x,I_r,\phi;\mu,0)] + \mathcal{O}(\sqrt{\varepsilon}^2)$$

is only C^{r-1} smooth, and accordingly, the right-hand-side of (2.4.1) is only C^{r-2}. For $\varepsilon > 0$ we can define the energy surface with energy h for the standard form (2.4.1) as

$$\hat{E}_{\sqrt{\varepsilon}}(h) = \{(x,\eta,\phi) \in \hat{\mathcal{P}} \mid \hat{H}(x,\eta,\phi;\mu,\sqrt{\varepsilon}) = h\}.$$

System (2.4.1) can be considered as an $\mathcal{O}(\sqrt{\varepsilon})$ perturbation of the system

$$\begin{aligned} \dot{x} &= J_2 D_x H_0(x,I_r;\mu), \\ \dot{\eta} &= 0, \\ \dot{\phi} &= D_I H_0(x,I_r;\mu), \end{aligned} \tag{2.4.3}$$

which is not Hamiltonian but *integrable* with the two independent integrals $H_0(x,I_r;\mu)$ and η. Therefore, for a given h it makes sense to define a (quasi) energy surface for system (2.4.3) in the form

$$\hat{E}_0(h) = \{(x,\eta,\phi) \in \hat{\mathcal{P}} | H_0(x,I_r;\mu) = \hat{H}(x,\eta,\phi;\mu,0) = h\}.$$

This hypersurface relates the same way to $\hat{E}_{\sqrt{\varepsilon}}(h)$ as $E_0(h)$ to $E_\varepsilon(h)$ in the previous sections. One also finds that $\hat{E}_0(\hat{h}_0) \supset \hat{\mathcal{A}}_0 \cup \hat{W}_0$ (see (2.4.4) below), in analogy with the previous sections.

Based on hypothesis (H1), for system (2.4.3) (or $(2.4.1)_{\varepsilon=0}$) we again have a normally hyperbolic invariant two-manifold of equilibria given by

$$\hat{\mathcal{A}}_0 = \{(x,\eta,\phi) \in \hat{\mathcal{P}} \mid x = \bar{x}^0(I_r;\mu),\ \eta \in [-\eta_0,\eta_0], \phi \in S^1\}, \tag{2.4.4}$$

which is a graph over the annulus

$$\hat{A} = [-\eta_0,\eta_0] \times S^1.$$

Furthermore, $\mathcal{A}_0$ has a three dimensional homoclinic manifold $\hat{W}_0$, which contains trajectories of the form

$$\hat{y}_0(t,\eta,\phi_0;\mu) = \begin{pmatrix} x^h(t,I_r;\mu) \\ \eta \\ \phi_0 + \int_0^t D_I H_0(x^h(\tau,I_r;\mu),I_r;\mu)\,d\tau \end{pmatrix}. \tag{2.4.5}$$

Again, for $\varepsilon > 0$ system (2.4.1) has a C^{r-2} $\sqrt{\varepsilon}$-close hyperbolic manifold $\hat{\mathcal{A}}_\varepsilon$ given by the embedding

$$\hat{g}_\varepsilon \colon \hat{A} \to \hat{\mathcal{P}},$$

$$(\eta,\phi) \mapsto (\hat{x}^\varepsilon(\eta,\phi;\mu),\eta,\phi) = (\bar{x}^0(I_r;\mu) + \sqrt{\varepsilon}\hat{x}^1(\eta,\phi;\mu,\sqrt{\varepsilon}),\eta,\phi).$$

Also, $(\hat{\mathcal{A}}_\varepsilon, \hat{i}_\varepsilon^*\hat{\omega})$ is a C^{r-2} symplectic manifold with

$$\hat{i}_\varepsilon^* \colon \hat{\mathcal{A}}_\varepsilon \hookrightarrow \hat{\mathcal{P}},$$

$$\hat{i}_\varepsilon^*\hat{\omega} = (\frac{1}{\sqrt{\varepsilon}} + \mathcal{O}(\sqrt{\varepsilon}^2))d\phi \wedge d\eta.$$

As in the case of hypothesis (H2b), we can define the *restricted Hamiltonian*

$$\hat{\mathcal{H}}_\varepsilon = \hat{H}|\hat{\mathcal{A}}_\varepsilon = \hat{i}_\varepsilon^*\hat{H},$$

which generates a restricted Hamiltonian flow on $\hat{\mathcal{A}}_\varepsilon$ satisfying

$$\begin{pmatrix} \dot{\phi} \\ \dot{\eta} \end{pmatrix} = \hat{i}_\varepsilon^*\hat{\omega}^\sharp(D_{(\phi,\eta)}\hat{\mathcal{H}}_\varepsilon) = \sqrt{\varepsilon}J_2 D_{(\phi,\eta)}\hat{\mathcal{H}} + \mathcal{O}(\sqrt{\varepsilon}^2).$$

Here the *reduced Hamiltonian* $\hat{\mathcal{H}} \colon \hat{A} \to \mathbb{R}$ takes the form

$$\hat{\mathcal{H}}(\eta,\phi;\mu) = \frac{1}{2}m(I_r;\mu)\eta^2 + H_1(\bar{x}^0(I_r;\mu),I_r,\phi;0), \tag{2.4.6}$$

with $m(I_r;\mu)$ defined in hypothesis (H2a). $\hat{\mathcal{H}}$ is related to the restricted Hamiltonian $\hat{\mathcal{H}}_\varepsilon$ through

$$\hat{\mathcal{H}}_\varepsilon = \hat{h}_0 + \sqrt{\varepsilon}^2\hat{\mathcal{H}} + \mathcal{O}(\sqrt{\varepsilon}^3),$$

with

$$\hat{h}_0 = H_0(\bar{x}^0(I_r;\mu), I_r;\mu).$$

Note that the reduced Hamiltonian of (2.4.6) is always the sum of kinetic and potential energy-type terms. Any $\hat{\gamma}_0 \subset \hat{A}$ internal orbit of $\hat{\mathcal{H}}$ gives rise to an internal orbit $\hat{\gamma}_\varepsilon \subset \hat{\mathcal{A}}_\varepsilon$ such that $\hat{\gamma}_0$ and $\hat{g}_\varepsilon^{-1}(\hat{\gamma}_\varepsilon)$ are C^{r-1} $\sqrt{\varepsilon}$-close in $\hat{A}$.

Introducing the tubular set

$$\hat{U}_\delta = \{(x,\eta,\phi) \in \hat{\mathcal{P}} \mid |x - \bar{x}^0(I_r;\mu)| \leq \delta,\ (\eta,\phi) \in \hat{A}\},$$

one can redo the estimates of section 2.2 for system (2.4.1) substituting $\sqrt{\varepsilon}$ for ε, η for I, and $r-2$ for r in all the statements and proofs (one also has to put a hat on all the functions and quantities we introduced). Therefore, our main construction of a local map $\hat{L}^h_{\sqrt{\varepsilon}}$ to track trajectories inside $\hat{U}_{\delta(\sqrt{\varepsilon})}$ (with $\delta(\sqrt{\varepsilon}) = \vartheta\sqrt{\varepsilon}^\alpha$) and a global map $\hat{G}^h_{\sqrt{\varepsilon}}$ to follow them outside $\hat{U}_{\delta(\sqrt{\varepsilon})}$ holds without modification.

As in section 2.3, we define the *n-th order energy-difference function* $\Delta^n\hat{\mathcal{H}}\colon \hat{A} \to \mathbb{R}$ by

$$\begin{aligned} \Delta^n\hat{\mathcal{H}}(\phi;\mu) &= \hat{\mathcal{H}}(\eta,\phi;\mu) - \hat{\mathcal{H}}(\eta,\phi - n\Delta\phi(I_r;\mu);\mu) \qquad (2.4.7)\\ &= H_1(\bar{x}^0(I_r;\mu), I_r, \phi;\mu,0) - H_1(\bar{x}^0(I_r;\mu), I_r, \phi - n\Delta\phi(I_r;\mu);\mu,0). \end{aligned}$$

Note that $\Delta^n\hat{\mathcal{H}}$ does not depend on η; hence the corresponding zero sets

$$\hat{V}^n_+ = \{\ (\eta,\phi) \in \hat{A} \mid \Delta^n\hat{\mathcal{H}}(\phi;\mu) = 0\ \}, \qquad (2.4.8)$$

$$\hat{Z}^n_+ = \{\ (\eta,\phi) \in V^n_+ \mid D_\phi\Delta^n\hat{\mathcal{H}}(\phi;\mu) \neq 0\ \}, \qquad (2.4.9)$$

and

$$\hat{V}^n_- = \hat{\mathcal{R}}^{-n}(\hat{V}^n_+), \qquad \hat{Z}^n_- = \hat{\mathcal{R}}^{-n}(\hat{Z}^n_+), \qquad (2.4.10)$$

generically consist of $\phi = const.$ lines of the annulus $\hat{A}$. We note that the rotation map

$$\begin{aligned} \hat{\mathcal{R}}: \hat{A} &\rightarrow \hat{A}, \\ (\eta, \phi) &\mapsto (\eta, \phi + \Delta\phi(I_r; \mu)) \end{aligned}$$

has no explicit η-dependence either. As in (2.3.5), for any internal orbit $\hat{\gamma} \subset \hat{A}$ of $\hat{\mathcal{H}}$ we define the *pulse number*

$$\hat{N}(\hat{\gamma}; \mu) = \min\{\ n \geq 1 \mid \hat{V}_-^k \cap \hat{\gamma} = \emptyset, k = 1, ..., n-1, \quad \hat{Z}_-^n \pitchfork \hat{\gamma}\ \}.$$

Finally, for $\varepsilon, \eta_0 > 0$ we introduce the blow-up map

$$\begin{aligned} \mathcal{B}_\varepsilon: A &\rightarrow \hat{A}, \\ (I, \phi) &\mapsto (\eta, \phi) = (\frac{I - I_r}{\sqrt{\varepsilon}}, \phi), \end{aligned}$$

which will be used to relate internal orbits of $\hat{\mathcal{H}}$ in $\hat{A}$ to internal orbits of $\hat{\mathcal{H}}_\varepsilon$ on $\hat{\mathcal{A}}_\varepsilon$ under assumption (H2a). We can now prove the following basic result on N-pulse orbits homoclinic to resonances bands:

Theorem 2.4.1 *Assume that hypotheses (H1) and (H2a) hold. Suppose that for an internal orbit $\hat{\gamma}_0^- \subset \hat{A}$ of the reduced Hamiltonian $\hat{\mathcal{H}}$*

(A1) $N \equiv \hat{N}(\hat{\gamma}_0^-; \mu) < \infty$,

(A2) Let $b_- \in \hat{Z}_-^N \cap \hat{\gamma}_0^-$ *and* $b_+ = \hat{\mathcal{R}}^N(b_-)$. *Assume that the orbit* $\hat{\gamma}_0^+ \subset \hat{A}$ *of the reduced Hamiltonian* $\hat{\mathcal{H}}$ *which contains* b_+ *is an internal orbit with* $\hat{Z}_+^N \pitchfork \hat{\gamma}_0^+$.

(A3) If $D_x H_0$ *points outwards on* W_0, *we assume that*

$$\hat{h}_0^- = \hat{\mathcal{H}}|\hat{\gamma}_0^- < \hat{\mathcal{H}}|\hat{\mathcal{R}}^k(\hat{\gamma}_0^-), \quad k = 1, ..., N-1.$$

If $D_x H_0$ *points inwards on* W_0, *we assume that*

$$\hat{h}_0^- = \hat{\mathcal{H}}|\hat{\gamma}_0^- > \hat{\mathcal{H}}|\hat{\mathcal{R}}^k(\hat{\gamma}_0^-), \quad k = 1, ..., N-1.$$

Then there exists $\varepsilon_0 > 0$ *such that for* $0 < \varepsilon < \varepsilon_0$

(*i*) $\mathcal{A}_\varepsilon$ *has an* N*-pulse homoclinic orbit* y_ε^N *which is positively asymptotic to an internal orbit* $\gamma_\varepsilon^+ \subset \mathcal{A}_\varepsilon$ *and negatively asymptotic to an internal orbit* $\gamma_\varepsilon^- \subset \mathcal{A}_\varepsilon$. *Moreover,* $g_\varepsilon^{-1}(\gamma_\varepsilon^+)$ *and* $\mathcal{B}_\varepsilon^{-1}(\hat{\gamma}_0^-)$ *are* C^{r-2} $\sqrt{\varepsilon}$*-close,* $g_\varepsilon^{-1}(\gamma_\varepsilon^+)$ *and* $\mathcal{B}_\varepsilon^{-1}(\hat{\gamma}_0^+)$ *are* C^0 $\sqrt{\varepsilon}$*-close. If* $\hat{\gamma}_0^+$ *is periodic, this latter statement can be strengthened to "*C^{r-2} $\sqrt{\varepsilon}$*-close."*

(*ii*) y_ε^N *lies in the intersection of* $W^u(\gamma_\varepsilon^-)$ *and* $W^s(\gamma_\varepsilon^+)$ *which is transversal within the energy surface* $E_\varepsilon(h)$ *with* $h = H|\gamma_\varepsilon^+ = H|\gamma_\varepsilon^-$.

(*iii*) *Outside a neighborhood of* $\mathcal{A}_\varepsilon$ y_ε^N *is* C^1 $\sqrt{\varepsilon}$*-close to the set*

$$Y^N = \cup_{i=1}^N y^i,$$

where $y^i \subset W_0$ *is an unperturbed orbit of* $(2.1.1)_{\varepsilon=0}$ *asymptotic to the points* $g_0 \circ \mathcal{R}^{i-1} \circ \mathcal{B}_\varepsilon^{-1}(b_-)$ *and* $g_0 \circ \mathcal{R}^i \circ \mathcal{B}_\varepsilon^{-1}(b_-)$ *in negative and positive time, respectively* ($\mathcal{R}^0 \equiv Id$).

Proof: We first apply Theorem 2.3.1 to the standard form (2.4.1) substituting $\sqrt{\varepsilon}$ for ε in the statement of that theorem. Then we relate back the results on system (2.4.1) to system (2.1.1) using the map $\mathcal{B}_\varepsilon$. Note that objects of the standard form which are C^s ε^β-close in $\hat{\mathcal{P}}$ are mapped by the map $(x, \eta, \phi) \mapsto (x, \mathcal{B}_\varepsilon^{-1}(\eta, \phi))$ into objects of system (2.1.1) which are C^s ε^β-close in $\mathcal{P}$. Based on this fact the statements of theorem follow.

□

Remark 2.4.1 It is important to note that although we can locate the orbits γ_ε^+ and γ_ε^- with $\mathcal{O}(\sqrt{\varepsilon})$ precision, we can still guarantee that they fall in the $\mathcal{O}(\sqrt{\varepsilon})$-thick resonance band in which system (2.1.1) is equivalent to the standard form (2.4.1). This comes

about as follows. Let $\hat{\gamma}_\varepsilon^+$ be the orbit on $\hat{A}_\varepsilon$ which is obtained by the application of Theorem 2.3.1 to system (2.4.1). Then $\hat{g}_\varepsilon^{-1}(\hat{\gamma}_\varepsilon^+)$ and $\hat{\gamma}_0^+$ are C^{r-2} $\sqrt{\varepsilon}$-close in $\hat{A}$. As we indicated above in the proof of Theorem 2.4.1, the map $\mathcal{B}_\varepsilon^{-1}$ maps $\hat{g}_\varepsilon^{-1}(\hat{\gamma}_\varepsilon^+)$ and $\hat{\gamma}_0^+$ to the orbits $g_\varepsilon^{-1}(\gamma_\varepsilon^+)$ and $\gamma_0^+ \equiv \mathcal{B}_\varepsilon^{-1}(\hat{\gamma}_0^+)$, respectively, which are C^{r-2} $\sqrt{\varepsilon}$-close in A. However, their I-projections are only $\mathcal{O}(\varepsilon)$ apart, as it is easily seen from the definition of $\mathcal{B}_\varepsilon$. Since γ_0^+ lies in the resonance band defined by $I \in [I_r - \sqrt{\varepsilon}\eta_0, I_r - \sqrt{\varepsilon}\eta_0]$, so does γ_ε^+, as shown in Fig. 2.11. For the same reason, the deviation of the orbit y_ε^N *in the* I *coordinate* from the shadowing orbits y^i of statement (iii) above is actually only $\mathcal{O}(\varepsilon^{\frac{3}{4}})$.

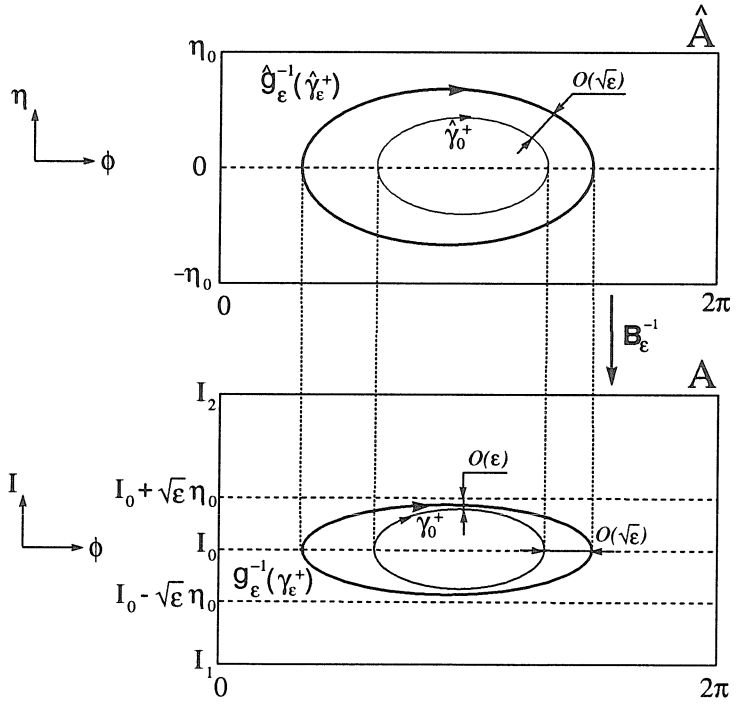

Figure 2.11: The relation between the internal orbits of the standard form (2.4.1) and system (2.1.1) under hypothesis (H2a)

For the case of N-pulse orbits which are actually homoclinic to a periodic orbit of $\mathcal{A}_\varepsilon$ we again have the following theorem.

Theorem 2.4.2 *Let us assume that hypotheses (H1) and (H2a) are satisfied and assumptions (A1)-(A3) of Theorem 2.4.1 hold. Let us further assume that* $\hat{\gamma}_0^+ = \hat{\gamma}_0^-$ *of Theorem 2.4.1 is a periodic orbit in* $\hat{A}$. *Then*

(*i*) *The statements of Theorem 2.4.1 hold with* $\gamma_\varepsilon = \gamma_\varepsilon^+ = \gamma_\varepsilon^-$ *and there exists one more* N*-pulse transverse homoclinic orbit* $\tilde{y}_\varepsilon^N$ *with properties similar to those of* $\tilde{y}_\varepsilon^N$ *(but with corresponding "base-points"* $\tilde{b}_+ \neq \hat{b}_+$ *and* $\tilde{b}_- \neq \hat{b}_-$*).*

(*ii*) *System (2.1.1) has Smale-horseshoes near* γ_ε *on energy surfaces sufficiently close to* $E_\varepsilon(h)$.

Proof: See the proof of Theorem 2.3.2. □

The remarks of section 2.3 are valid with the appropriate modifications. We can also deal with *resonant internal orbits.* Again, we call an internal orbit $\hat{\gamma}$ resonant if $\hat{N}_R(\hat{\gamma};\mu) < \infty$, where the *resonant pulse number* $\hat{N}_R$ is defined by

$$\hat{N}_R(\hat{\gamma};\mu) = \min\{\ n \geq 1 \mid \hat{V}_-^k \cap \hat{\gamma} = \emptyset,\ k = 1,...,n-1,\ \ \hat{\mathcal{R}}^n(\hat{\gamma}) = \hat{\gamma}\}.$$

Theorem 2.4.3 *Assume that hypotheses (H1) and (H2a) hold and* $\hat{\gamma}_0 \subset \hat{A}$ *is an internal orbit of the reduced Hamiltonian* $\hat{\mathcal{H}}$ *such that*

(A1) $N \equiv \hat{N}_R(\hat{\gamma}_0,\mu) < \infty$ *(*$\hat{\gamma}_0$ *is resonant),*

(A2) Assumption (A3) of Theorem 2.4.1 holds.

Then there exists $\varepsilon_0 > 0$ *such that for* $0 < \varepsilon < \varepsilon_0$

(*i*) $\mathcal{A}_\varepsilon$ *has two* N*-pulse homoclinic orbits,* y_ε^N *and* $\tilde{y}_\varepsilon^N$*, which are asymptotic in positive and negative time to an internal orbit* $\gamma_\varepsilon \subset \mathcal{A}_\varepsilon$. *The orbits* $\mathcal{B}_\varepsilon^{-1}(\hat{\gamma}_0)$ *and* $g_\varepsilon^{-1}(\gamma_\varepsilon)$ *are* C^{r-2} $\sqrt{\varepsilon}$*-close in* A.

(*ii*) *There exists two points* $b_-, \tilde{b}_- \in \hat{\gamma}_0$ *such that outside a neighborhood of* $\mathcal{A}_\varepsilon$, y_ε^N ($\tilde{y}_\varepsilon^N$) *is* C^1 $\sqrt{\varepsilon}$*-close to the set*

$$Y^N = \cup_{i=1}^N y^i, \qquad (\tilde{Y}^N = \cup_{i=1}^N \tilde{y}^i,)$$

where $y^i \subset W_0$ ($\tilde{y}^i \subset W_0$) *is an unperturbed orbit of* $(2.1.1)_{\varepsilon=0}$ *asymptotic to the points* $g_0 \circ \mathcal{R}^{i-1} \circ \mathcal{B}_\varepsilon^{-1}(b_-)$ ($g_0 \circ \mathcal{R}^{i-1} \circ \mathcal{B}_\varepsilon^{-1}(\tilde{b}_-)$) *and* $g_0 \circ \mathcal{R}^i \circ \mathcal{B}_\varepsilon^{-1}(b_-)$ ($g_0 \circ \mathcal{R}^i \circ \mathcal{B}_\varepsilon^{-1}(\tilde{b}_-)$) *in negative and positive time, respectively.* ($\mathcal{R}^0 \equiv Id$).

Proof: The same as the proof of Theorem 2.3.3 with the results related back to system (2.1.1). □

We close this section by establishing a result analogous to Theorem 2.3.4: Theorem 2.4.4 below gives conditions for the existence of *jumping N-pulse orbits homoclinic to a resonance band.* Such orbits arise, e.g., in the modal truncation of the nonlinear Schrödinger equation, which we will study in chapter 4.

We adapt hypothesis (H1') of section 2.3 and also assume that

(H3')

$$\Delta\phi(I_r;\mu) = \int_{-\infty}^{+\infty} D_I H_0(x^{h+}(t, I_r;\mu), I_r;\mu)\, dt \equiv \int_{-\infty}^{+\infty} D_I H_0(x^{h-}(t, I_r;\mu), I_r;\mu)\, dt.$$

Note that hypoyhesis (H3') is less restrictive than (H3) since it requires the two phase shifts to be equal only for the resonant value $I = I_r$.

Theorem 2.4.4 *Assume that hypotheses (H1'),(H2a), and (H3') hold. Suppose that for an internal orbit* $\hat{\gamma}_0^- \subset \hat{A}$ *of the reduced Hamiltonian* $\hat{\mathcal{H}}$

(A1) $N \equiv \hat{N}(\hat{\gamma}_0^-;\mu) < \infty$.

(A2) Let $b_- \in \hat{Z}_-^N \cap \hat{\gamma}_0^-$ *and* $b_+ = \hat{\mathcal{R}}^N(b_-)$. *Assume that the orbit* $\hat{\gamma}_0^+ \subset \hat{A}$ *of the reduced Hamiltonian* $\hat{\mathcal{H}}$ *which contains* b_+ *is an internal orbit with* $\hat{Z}_+^N \pitchfork \hat{\gamma}_0^+$.

(A3) Let $\hat{\chi}_{j+1} = \text{sign}\,(\hat{h}_0^- - \hat{\mathcal{H}}|\hat{\mathcal{R}}^k(\hat{\gamma}_0^-))\hat{\chi}_j$, $j = 1, ..., N$, *with* $\hat{\chi}_1 \in \{-1, +1\}$ *to be specified below.*

Then there exists $\varepsilon_0 > 0$ *such that for* $0 < \varepsilon < \varepsilon_0$

(i) $\mathcal{A}_\varepsilon$ *has two* N*-pulse homoclinic orbit* y_ε^{N+} *and* y_ε^{N-} *which are positively asymptotic to an internal orbit* $\gamma_\varepsilon^+ \subset \mathcal{A}_\varepsilon$ *and negatively asymptotic to an internal orbit* $\gamma_\varepsilon^- \subset \mathcal{A}_\varepsilon$. *Moreover,* $g_\varepsilon^{-1}(\gamma_\varepsilon^+)$ *and* $\mathcal{B}_\varepsilon^{-1}(\hat{\gamma}_0^-)$ *are* C^{r-2} $\sqrt{\varepsilon}$*-close,* $g_\varepsilon^{-1}(\gamma_\varepsilon^+)$ *and* $\mathcal{B}_\varepsilon^{-1}(\hat{\gamma}_0^+)$ *are* C^0 $\sqrt{\varepsilon}$*-close. If* $\hat{\gamma}_0^+$ *is periodic, this latter statement can be strengthened to "*C^{r-2} $\sqrt{\varepsilon}$*-close."*

(ii) y_ε^{N+} *and* y_ε^{N-} *lie in the intersection of* $W^u(\gamma_\varepsilon^-)$ *and* $W^s(\gamma_\varepsilon^+)$ *which is transversal within the energy surface* $E_\varepsilon(h)$ *with* $h = H|\gamma_\varepsilon^+ = H|\gamma_\varepsilon^-$.

(iii) Let us set $\hat{\chi}_1 = +1$. *Then outside a neighborhood of* $\mathcal{A}_\varepsilon$ y_ε^{N+} *is* C^1 $\sqrt{\varepsilon}$*-close to the set*

$$Y^{N+} = \cup_{i=1}^N y^i(\hat{\chi}_i), \tag{2.4.11}$$

where

$$y^i(\hat{\chi}_i) \subset \begin{cases} W_0^+ & \text{if } \hat{\chi}_i = +1, \\ W_0^- & \text{if } \hat{\chi}_i = -1, \end{cases} \tag{2.4.12}$$

is an unperturbed orbit of $(2.1.1)_{\varepsilon=0}$ *asymptotic to the points* $g_0 \circ \mathcal{R}^{i-1} \circ \mathcal{B}_\varepsilon^{-1}(b_-)$ *and* $g_0 \circ \mathcal{R}^i \circ \mathcal{B}_\varepsilon^{-1}(b_-)$ *in negative and positive time, respectively* ($\mathcal{R}^0 \equiv Id$). *Setting* $\hat{\chi}_1 = -1$ *we obtain a similar statement on the relation of the orbit* y_ε^{N-} *to the set* Y^{N-} *(defined the same way as in (2.4.11)-(2.4.12)).*

Proof: Again, the theorem follows from the application of Theorem 2.3.4 to the standard form (2.4.1) (see the discussion in the proof of Theorem 2.4.3 above). □

We remark that for Theorems 2.4.2-2.4.4 Remark 2.4.1 again applies and explains why C^{r-2} $\sqrt{\varepsilon}$-precision is enough to locate orbits in the resonance band of width $\mathcal{O}(\sqrt{\varepsilon})$.

2.5 Extension of the results to weakly dissipative perturbation

In this section we show how the energy-phase method extends to the case when one adds additional non-Hamiltonian perturbation to system (2.1.1). This question is particularly relevant in possible applications of our results to certain engineering problems (see, e.g., [19]-[22], [32], [67], [75], etc.) if the dissipation is small but not negligible. In such systems the asymptotic behavior of solutions is characteristically dissipative, but the short-term behavior of trajectories is amenable to Hamiltonian perturbation methods. It is exactly this feature that makes it possible to adapt the main construction of the previous sections to weakly dissipative systems.

The equations we study can be written in the form

$$\begin{aligned}
\dot{x}_1 &= D_{x_2}H_0(x,I;\mu) + \varepsilon[D_{x_2}H_1(x,I,\phi;\mu,\varepsilon) + \nu_{x_1}g_{x_1}(x,I,\phi;\mu,\varepsilon)],\\
\dot{x}_2 &= -D_{x_1}H_0(x,I;\mu) - \varepsilon[D_{x_1}H_1(x,I,\phi;\mu,\varepsilon) + \nu_{x_2}g_{x_2}(x,I,\phi;\mu,\varepsilon)],\\
\dot{I} &= -\varepsilon[D_{\phi}H_1(x,I,\phi;\mu,\varepsilon) + \nu_I g_I(x,I,\phi;\mu,\varepsilon)], \qquad (2.5.1)\\
\dot{\phi} &= D_I H_0(x,I;\mu) + \varepsilon[D_I H_1(x,I,\phi;\mu,\varepsilon) + \nu_\phi g_\phi(x,I,\phi;\mu,\varepsilon)],
\end{aligned}$$

again defined in the phase space $\mathcal{P}$. Here g_x, g_I, and g_ν are C^r functions, $H = H_0 + \varepsilon H_1$ is again assumed to be C^{r+1} with $r \geq 3$, and $\nu = (\nu_x, \nu_I, \nu_\phi) \in \mathbb{R}^4$ is a vector of parameters which will be chosen small in norm. We will assume that hypotheses (H1)

and (H2b) hold for system (2.5.1). Based on section 2.4, the upcoming results of this section can immediately be applied to *resonance bands* (assumption (H2a)). Since it does not involve any new ideas, we will not pursue this question here. A study of a different kind of multiple-pulse behavior near resonance bands appears in the recent work of Kaper and Kovačič [40] which we review briefly in section 2.6.

Under (H1)-(H2b) system $(2.5.1)_{\varepsilon=0}$ has a normally hyperbolic invariant manifold $\mathcal{A}_0$ of the form (2.1.2) which perturbs to a C^r ε close manifold $\mathcal{A}_\varepsilon$ for small $\varepsilon > 0$ (see (2.1.5)). On this manifold the dynamics is now described by the *restricted system*

$$\begin{aligned} \dot{\phi} &= \varepsilon[\ D_I\mathcal{H}(I,\phi;\mu) + \nu_\phi g_\phi(\bar{x}_0(I;\mu),I,\phi;\mu,0)] + \mathcal{O}(\varepsilon^2), \\ \dot{I} &= \varepsilon[-D_\phi\mathcal{H}(I,\phi;\mu) - \nu_I g_I(\bar{x}_0(I;\mu),I,\phi;\mu,0)] + \mathcal{O}(\varepsilon^2), \end{aligned} \tag{2.5.2}$$

which is generally not Hamiltonian for $\nu_\phi, \nu_I \neq 0$, but contains a Hamiltonian part generated by the reduced Hamiltonian $\mathcal{H}$ of (2.2.2). Rescaling the time by ε and setting $\varepsilon = 0$ in (2.5.2) we obtain the *reduced system*

$$\begin{aligned} \dot{\phi} &= D_I\mathcal{H}(I,\phi;\mu) + \nu_\phi g_\phi(\bar{x}_0(I;\mu),I,\phi;\mu,0), \\ \dot{I} &= -D_\phi\mathcal{H}(I,\phi;\mu) - \nu_I g_I(\bar{x}_0(I;\mu),I,\phi;\mu,0), \end{aligned} \tag{2.5.3}$$

which we consider defined on the annulus A. The relation between the orbits of the restricted and reduced systems is similar to what we had in section 2.2: if $\gamma_0 \subset A$ is a structurally stable orbit of the reduced system, then for small ε the restricted system has an orbit $\gamma_\varepsilon \subset \mathcal{A}_\varepsilon$ such that γ_0 and $g_\varepsilon^{-1}(\gamma_\varepsilon)$ are C^r ε-close on appropriate compact subsets of A.

It is important to note that in a general dissipative system of the form (2.5.3), there may be no orbits other than fixed points, which are isolated from ∂A. This is related to the fact that for non-Hamiltonian perturbations, $\mathcal{A}_0$ usually perturbs into an overflowing

or inflowing invariant manifold $\mathcal{A}_\varepsilon$ whose stable and unstable manifolds are only locally invariant. For this reason, we will generally not speak about internal orbits for the restricted and reduced systems (2.5.2)-(2.5.3). Correspondingly, we will establish the existence of N-pulse orbits which are only asymptotic to $\mathcal{A}_\varepsilon$ in one time-direction and approach an orbit σ_ε partially lying in $\mathcal{A}_\varepsilon$ in the other time-direction. These orbits still have a characteristic influence on the perturbed dynamics near $\mathcal{A}_\varepsilon$ through the N pulses they make before leaving $W^s(\mathcal{A}_\varepsilon) \cap W^u(\mathcal{A}_\varepsilon)$.

When we speak about *N-pulse orbits* in this section, we will mean orbits which leave and then enter a neigborhood of $\mathcal{A}_\varepsilon$ N-times and before the first pulse and after the last pulse they follow orbits in $\mathcal{A}_\varepsilon$ in positive and negative time, respectively, as long as these latter orbits stay in $\mathcal{A}_\varepsilon$. More precisely, we will say that an N-pulse orbit y_ε^N with $W^s(\mathcal{A}_\varepsilon) \cap y_\varepsilon^N \neq \emptyset$ *positively approaches* another orbit σ_ε^+ with $\sigma_\varepsilon^+ \cap \mathcal{A}_\varepsilon \neq \emptyset$ if y_ε^N intersects a stable fiber $f_\varepsilon^s(p) \subset W_{loc}^s(\mathcal{A}_\varepsilon)$ with basepoint $p \in \sigma_\varepsilon^+$ (see (iii) of the Proposition 2.2.1 and Fig. 2.12 for the implications of this). Similarly, one can speak about an orbit y_ε^N *negatively approaching* another orbit σ_ε^- if it approaches σ_ε^- positively in reverse time. If $F_t^\varepsilon(p) \in \mathcal{A}_\varepsilon$ holds for any $t \geq 0$, then "positively approching" is equivalent to "positively asymptotic." Similarly, if $F_t^\varepsilon(p) \in \mathcal{A}_\varepsilon$ holds for any $t \leq 0$, then "negatively approching" is equivalent to "negatively asymptotic." Using the same quantities as defined in (2.3.1)-(2.3.5), we can now state the following theorem.

Theorem 2.5.1 *Let us suppose that hypothesis (H1) and (H2b) are satisfied for system (2.5.1) and assumptions (A1)-(A3) of Theorem 2.3.1 hold for the internal orbits $\gamma_0^+, \gamma_0^- \subset A$ of the reduced Hamiltonian $\mathcal{H}$. Then there exist $\varepsilon_0, \nu_0 > 0$ such that for $0 < \varepsilon < \varepsilon_0$ and $0 < \|\nu\| < \nu_0$*

(i) system (2.5.1) has an N-pulse orbit y_ε^N which is positively approaching an orbit σ_ε^+

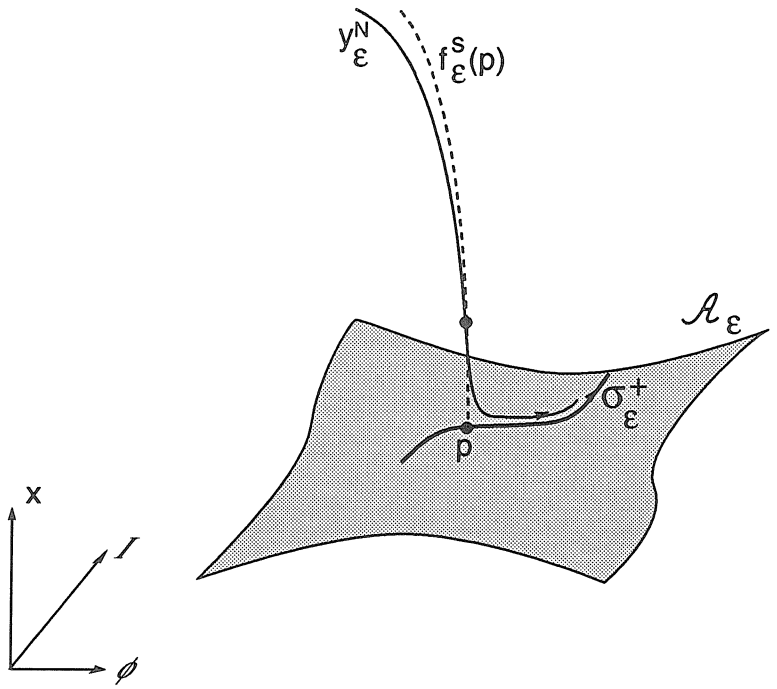

Figure 2.12: An N-pulse orbit y^N_ε positively approaching σ^+_ε

and negatively approaching an orbit σ^-_ε of system (2.5.1). Further, $\sigma^+_\varepsilon \cap \mathcal{A}_\varepsilon \neq \emptyset$ and $\sigma^-_\varepsilon \cap \mathcal{A}_\varepsilon \neq \emptyset$.

(*ii*) *Suppose that σ^-_0 and σ^+_0 are structurally stable orbits of the reduced system (2.5.3) intersecting Z^N_- and Z^N_+ transversally at the points b_- and b_+, respectively. Suppose further that $\mathcal{N} \subset A$ is a compact set not containing α- or ω-limit points of σ^-_0. Then $g^{-1}_\varepsilon(\sigma^-_\varepsilon) \cap \mathcal{N}$ and $\sigma^-_0 \cap \mathcal{N}$ are C^r ε-close in A. If σ^-_0 is a periodic orbit, then $g^{-1}_\varepsilon(\sigma^-_\varepsilon)$ and σ^-_0 are C^r ε-close in A. Similar statements hold for the relation of σ^+_ε to σ^+_0.*

(*iii*) *For finite times y^N_ε is contained in a two dimensional manifold W^N_ε which lies in the transversal intersection of $W^s(\mathcal{A}_\varepsilon)$ with $W^u(\mathcal{A}_\varepsilon)$.*

(*iv*) *If assumption (A3) of Theorem 2.3.1 is satisfied, then statement* (*iii*) *of the same theorem holds for* y_ε^N.

(*v*) *If hypotheses (H1') and (H4), and assumption (A3) of Theorem 2.3.4 are satisfied, then there exists another* N*-pulse orbit* $\tilde{y}_\varepsilon^N$ *with the same properties as* y_ε^N *above. Moreover,* y_ε^N *and* $\tilde{y}_\varepsilon^N$ *are jumping* N*-pulse orbits satisfying* (*iii*) *of Theorem 2.3.4.*

Proof: The proof is based on the following simple idea. One can first set $\nu = 0$ and, using Theorem 2.3.1, show the existence of multiple pulse homoclinic orbits to $\mathcal{A}_\varepsilon$, which form a two dimensional manifold W_ε^N. If this manifold lies in the *transversal* intersection of $W^s(\mathcal{A}_\varepsilon)$ and $W^u(\mathcal{A}_\varepsilon)$, then it persists for small ν. Furthermore, the basepoints of the stable and unstable fibers contained in W_ε^N perturb smoothly in ν (see Proposition 2.2.1) and hence form C^{r-1} curves which are C^{r-1} ε-close to $g_\varepsilon(Z_+^N)$ and $g_\varepsilon(Z_-^N)$, respectively. Then all statements of Theorem 2.5.1 follow from Theorem 2.3.1 and Proposition 2.2.1.

Therefore, to prove this theorem, we only have to show that for $\nu = 0$ and sufficiently small $\varepsilon > 0$, the N-pulse homoclinic orbit y_ε^N obtained from Theorem 2.3.1 is contained in a two dimensional manifold W_ε^N, which lies in the transversal intersection of $W^s(\mathcal{A}_\varepsilon)$ and $W^u(\mathcal{A}_\varepsilon)$. As it is shown in Haller and Wiggins [28], if γ_ε^+ is an internal orbit of the restricted Hamiltonian $\mathcal{H}_\varepsilon$ with $\mathcal{H}_\varepsilon|\gamma_\varepsilon^+ = h_\varepsilon$, then $E_\varepsilon(h_\varepsilon)$ intersects $W^s(\mathcal{A}_\varepsilon)$ transversally along $W^s(\gamma_\varepsilon^+)$. Similarly, if γ_ε^- is an internal orbit of the restricted Hamiltonian $\mathcal{H}_\varepsilon$ with $\mathcal{H}_\varepsilon|\gamma_\varepsilon^+ = h_\varepsilon$, then $E_\varepsilon(h_\varepsilon)$ intersects $W^u(\mathcal{A}_\varepsilon)$ transversally along $W^u(\gamma_\varepsilon^-)$. Now under the assumptions of the theorem, for $\nu = 0$, $W^s(\gamma_\varepsilon^+) \pitchfork W^u(\gamma_\varepsilon^-)$ holds within the energy surface $E_\varepsilon(h_\varepsilon)$ as it is guaranteed by (*ii*) of Theorem 2.3.1. In other words, if $p_\varepsilon \in W^s(\gamma_\varepsilon^+) \cap W^u(\gamma_\varepsilon^-)$, then

$$T_{p_\varepsilon}(W^s(\mathcal{A}_\varepsilon) \cap E_\varepsilon(h_\varepsilon)) + T_{p_\varepsilon}(W^u(\mathcal{A}_\varepsilon) \cap E_\varepsilon(h_\varepsilon)) = T_{p_\varepsilon}(E_\varepsilon(h_\varepsilon));$$

hence $T_{p_\varepsilon}(W^s(\mathcal{A}_\varepsilon))$ has a one dimensional subspace not contained in $T_{p_\varepsilon}(W^u(\mathcal{A}_\varepsilon))$. Since both $W^s(\mathcal{A}_\varepsilon)$ and $W^u(\mathcal{A}_\varepsilon)$ are codimension one manifolds in $\mathcal{P}$, this proves that they intersect transversally at $p_\varepsilon \in W^N_\varepsilon$ for $\nu = 0$. □

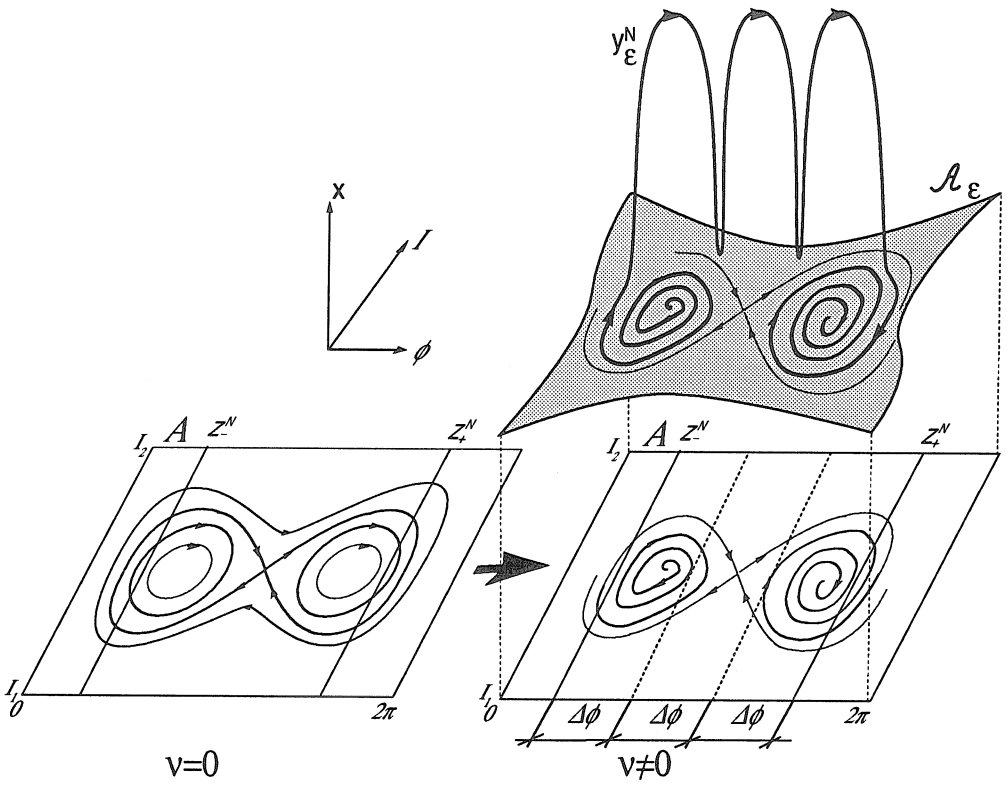

Figure 2.13: Example I of the statement of Theorem 2.5.1 for $N = 3$.

Some cases of the application of Theorem 2.5.1 are sketched in Figs. 2.13-2.15. These examples show that in the presence of equilibria or a limit cycle and an equilibrium (of opposite stability types), one obtains N-pulse orbits which are in fact N-pulse homoclinic orbits to $\mathcal{A}_\varepsilon$. Otherwise, the N pulse orbits are guaranteed to be asymptotic to $\mathcal{A}_\varepsilon$ only in positive or negative time, as we discussed above. This suggests that in the weakly dissipative context of this section, equilibria have a prominent role in creating

recurrent motions near the slow manifold $\mathcal{A}_\varepsilon$. For instance, if the zero set Z_+^N transversally intersects the domain of attraction of a stable fixed point s_ν of (2.5.3), then there exists a family of N-pulse orbits which are positively asymptic to a stable equilibrium of $\mathcal{A}_\varepsilon$ (see Figs. 2.13-2.15). These orbits are in fact N-pulse homoclinic orbits to the

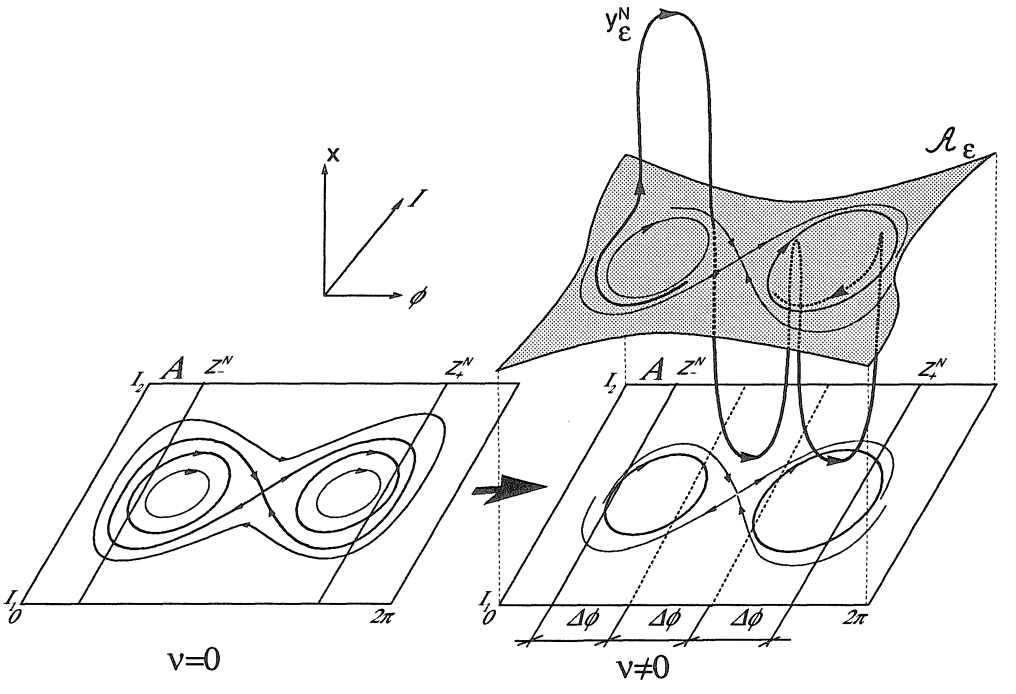

Figure 2.14: Example II of the statement of Theorem 2.5.1 for $N = 3$ and jump sequence $\chi_2 = -\chi_1$, $\chi_3 = \chi_2$

slow manifold $\mathcal{A}_\varepsilon$ if the zero set Z_-^N transversally intersects the domain of "repulsion" of an unstable limit cycle or unstable focus of (2.5.3), as shown in Figs. 2.13-2.15. In many cases, however, the unstable equilibria of (2.5.3) are saddles which have no open domain of attraction in negative time. If for some parameter value μ^* Z_-^N happens to pass through these equilibria, we expect that for some nearby μ value there will be an N pulse homoclinic orbit to $\mathcal{A}_\varepsilon$ which is negatively asymptotic to the saddle.

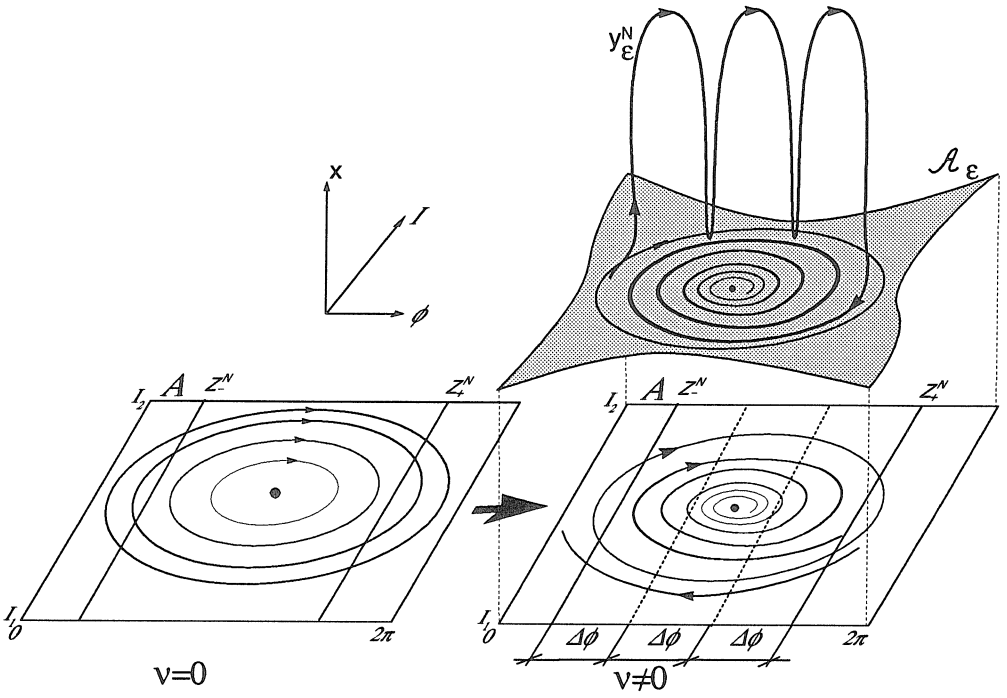

Figure 2.15: Example III of the statement of Theorem 2.5.1 for $N = 3$

In general, one may ask what can be said about N-pulse homoclinic orbits in the case when Z_-^N or Z_+^N contains an equilibrium $s_0(\mu, \nu)$ of the reduced system, and hence the transversality condition in (ii) of Theorem 2.5.1 is not satisfied for $\sigma_0^+ = s_0(\mu, \nu)$. The following theorem provides an answer to this question.

Theorem 2.5.2 *Let us suppose that hypotheses (H1) and (H2b) are satisfied for system (2.5.1) and the following hold:*

(A1) Let M be an open subset of the parameter space $W \times \mathbb{R}^4$. Suppose that for (μ, ν) the reduced system (2.5.3) has a nondegenerate equilibrium $s_0(\mu, \nu)$ (no zero eigenvalues). Moreover, for some $(\mu^*, 0) \in M$ we have $s_0(\mu^*, 0) \equiv b_- \in Z_-^N$ (see, e.g., the part of Fig. 2.15 with $\nu = 0$).

(A2) For $(\mu,\nu) \in M$ Z_+^N *intersects the domain of attraction of a closed set* $S_0(\mu,\nu)$ *of the reduced system (2.5.3) transversally in a neighborhood of the point* $b^+ = \mathcal{R}^N(s_0(\mu^*,0)) \in Z_+^N$. *Moreover, the trajectory* σ_0^+ *containing* b^+ *intersects* Z_+^N *transversally at* b^+ *for* $t = 0$ *and stays in* A *for* $t > 0$ *(see Fig. 2.15).*

(A3) $D_{(\mu,\nu)}\Delta^N\mathcal{H}(s_0(\mu,\nu);\mu)|_{(\mu^*,0)} \neq 0 \in \mathbb{R}^{p+4}$.

Then there exists $\varepsilon_0 > 0$ *and for* $0 < \varepsilon < \varepsilon_0$ *there exists a codimension one surface* $C \subset M$ *near* $(\mu^*,0)$ *such that for any* $(\mu,\nu) \in C$ *the following hold:*

(ii) $\mathcal{A}_\varepsilon$ *has an* N*-pulse homoclinic orbit* y_ε^N *which is positively asymptotic to a set* $S_\varepsilon(\mu,\nu) \subset \mathcal{A}_\varepsilon$ *and negatively asymptotic to an equilibrium* $s_\varepsilon(\mu,\nu) \subset \mathcal{A}_\varepsilon$. *Moreover,* $g_\varepsilon^{-1}(S_\varepsilon(\mu,\nu))$ *and* $S_0(\mu,\nu)$ *are* C^r ε*-close, as well as* $g_\varepsilon^{-1}(s_\varepsilon(\mu,\nu))$ *and* $s_0(\mu,\nu)$.

(iii) If assumption (A3) of Theorem 2.3.1 is satisfied with $s_0(\mu,\nu) = \gamma_0^-$, *then statement (iii) of Theorem 2.3.1 holds with* $b_- = s_0(\mu,\nu)$. *Similarly, if assumption (A3) of Theorem 2.3.4 is satisfied with* $s_0(\mu,\nu) = \gamma_0^-$, *then the part of statement (iii) of Theorem 2.3.4 regarding the orbits shadowing* y_ε^N *holds with* $b_- = s_0(\mu,\nu)$.

Proof: In view of Theorems 2.3.1 and 2.5.1, we only have to show that there exists a codimension one surface C (see above) in the space of the parameters (μ,ν) such that for parameter values taken from C, the basepoints of the unstable fibers lying in the two dimensional intersection manifold W_ε^N form a curve $B_\varepsilon \subset \mathcal{A}_\varepsilon$ containing $s_\varepsilon(\mu,\nu)$ (here s_ε is the equilibrium arising from the perturbation of $s_0(\mu^*,0)$). In this case, by Proposition 2.2.1, there is a unique N pulse orbit y_ε^N negatively asymptotic to $s_\varepsilon(\mu,\nu)$ and positively approaching an orbit σ_ε^+. Since for small ε σ_ε^+ stays in $\mathcal{A}_\varepsilon$ by assumption (A2) above,

y_ε^N is positively asymptotic to the perturbed attractor $S_\varepsilon(\mu,\nu)$ and the statements of the theorem follow.

Since the curve B_ε perturbs from $g_0(Z_-^N)$, by Proposition 2.2.1 in a neighborhood of the point $s_0(\mu,\nu)$ $g_\varepsilon^{-1}(B_\varepsilon)$ satisfies the equation

$$\mathcal{H}(I,\phi;\mu)+\varepsilon\tilde{\mathcal{H}}(I,\phi,\mu,\nu;\varepsilon)=0,$$

with some C^{r-1} function $\tilde{\mathcal{H}}$. Hence the requirement that B_ε contains $s_\varepsilon(\mu,\nu)$ can be expressed as

$$\mathcal{H}(g_\varepsilon^{-1}(s_\varepsilon(\mu,\nu));\mu)+\varepsilon\tilde{\mathcal{H}}(g_\varepsilon^{-1}(s_\varepsilon(\mu,\nu)),\mu,\nu;\varepsilon)=0.$$

Note that by assumption (A1) this equation is solved by $(\mu,\nu,\varepsilon)=(\mu^*,0,0)$. But then, using assumption (A3) and noting that $g_\varepsilon^{-1}(s_\varepsilon(\mu,\nu))|_{\varepsilon=0}=s_0(\mu,\nu)$, we conclude from the implicit function theorem the local existence of the hypersurface C in the set M of the parameter space. □

We would like to make two remarks in connection with Theorem 2.5.2:

Remark 2.5.1 It is easy to see that the above treatment of N-pulse orbits homoclinic to equilibria can be extended to the case of purely Hamiltonian perturbation considered in section 2.3. The conditions of a corresponding theorem would be similar to those of Theorem 2.5.2 above with the quantities involved depending on the parameter μ only. For brevity, we do not formulate the Hamiltonian analogue of Theorem 2.5.2 here.

Remark 2.5.2 If $s_0(\mu,\nu)=S_0(\mu,\nu)$, Theorem 2.5.2 establishes the existence of an N-pulse orbit homoclinic to the equilibrium $s_\varepsilon(\mu,\nu)=S_\varepsilon(\mu,\nu)$. If $s_0(\mu,\nu)$ is a stable focus of the restricted system (2.2.1), then the homoclinic orbit is a Silnikov-type orbit (see Fig. 2.16). The existence of such an orbit *with one pulse* for the case of assumption (H2a)

was studied by Kovačič and Wiggins [44]. As they point out, these orbits satisfy the conditions of Silnikov [65] (see also Wiggins [74]) and hence one can construct horseshoes in their neighborhoods. This is a situation which justifies why one would be sometimes interested in detecting N-pulse orbits homoclinic to $\mathcal{A}_\varepsilon$ which occur on codimension one surfaces in the parameter space: these orbits may create chaotic hyperbolic sets which survive even when the N-pulse orbit breaks, hence they have an effect on the global dynamics of system (2.5.1) on an open set of parameter values.

We close this section by noting that single-pulse versions of the codimension one connections treated in Theorem 2.5.2 also appear in Kovačič [47] where dissipative perturbations of Hamiltonian resonance bands (hypothesis (H2a)) are considered.

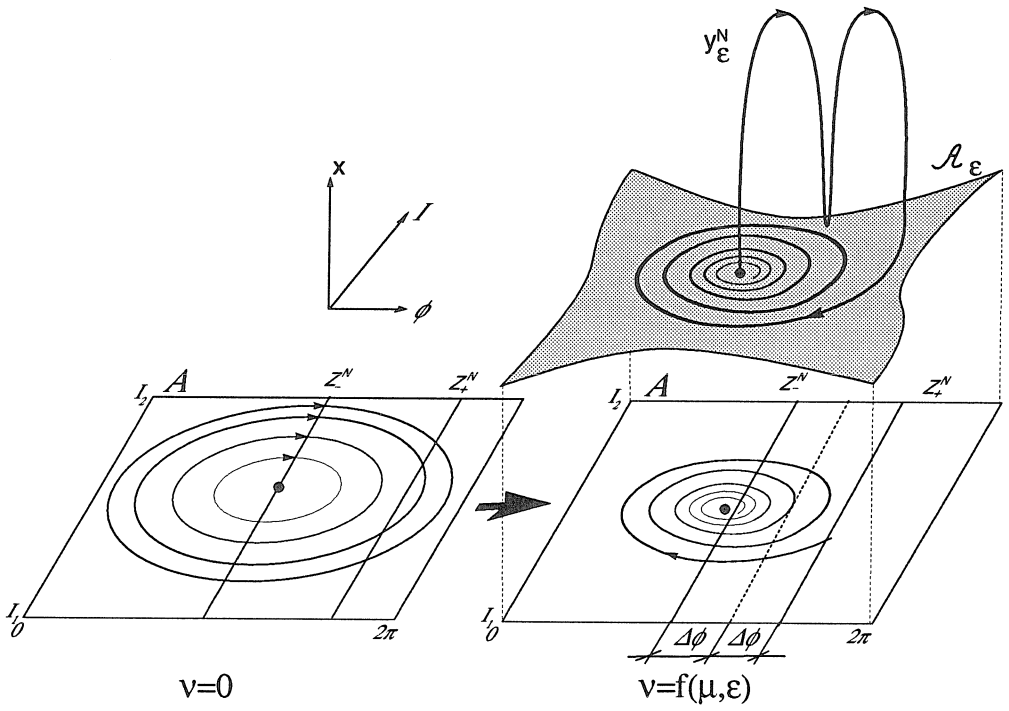

Figure 2.16: Double-pulse Silnikov-type orbit

2.6 Discussion

In the preceeding sections we have proved global perturbation results on the existence and geometry of multiple-pulse orbits in perturbations of certain two-degree-of-freedom integrable Hamiltonian systems. In the following we would like to relate our results to previous and recent work on multiple-pulse orbits.

N-pulse orbits near an unperturbed orbit homoclinic to a saddle-center of a reversible Hamiltonian system were detected in Mielke *et al.* [56]. Similarly to their work, we construct local and global tracking maps describing the excursion of perturbed orbits near the unperturbed homoclinic manifolds. However, we do not base our construction on the solution of variational equations: for a given application one only has to do some simple algebraic manipulations to obtain quick results. Also, our analysis is global in the sense that it deals with a whole manifold of fixed points instead of a single one. For this reason, we cannot use an (integrable) local normal form around a fixed point to describe the local passage of trajectories.

We would also like to mention the work of Jones and Kopell [38] on perturbations of manifolds of equilibria. In the heart of their analysis lies the powerful exchange lemma which they use to track solutions making a long-time passage near the perturbed manifold. As an application they assume that the unperturbed system has a "singular homoclinic orbit," i.e., a cyclic sequence of N heteroclinic orbits such that the ω-limit point of the k-th member of the sequence coincides with the α-limit point of the $k+1$-st member and the first and last members of the sequence are identical. If this singular homoclinic orbit lies in the *transversal* intersection of stable and unstable manifolds and the corresponding singular homoclinic point p_0 perturbs to an equilibrium p_ε which is asymptotically stable *within* the corresponding slow manifold, they are able to show the

existence of a locally unique N-pulse orbit homoclinic to p_ε.

Recently, Jones *et al.* [39] obtained a version of the exchange lemma with exponentially small error which enables one to assume only weak transversality along the singular homoclinic orbit (i.e., the relevant angles of intersection are allowed to vanish with the perturbation parameter ε). Other extensions of the exchange lemma involving higher dimensional manifolds are also available (see Tin [68]). Using these results, Kaper and Kovačič [40] constructed multiple pulse orbits homoclinic to resonance bands (arising from the case described by our hypothesis (H2a)). These multiple-pulse orbits lie in the vicinity of a "skeleton" consisting of single-pulse orbits obtained from a modified Melnikov-analysis and segments of orbits in the slow manifold. In the Hamiltonian case, their multiple-pulse orbits are generically asymptotic to orbits in the set $\mathcal{S}_\varepsilon$ (described in section 2.1), which is bounded away from the core of the resonance. In the dissipative case the multiple-pulse orbits lie in the vicinity of one-pulse orbits constructed by the appropriate Melnikov-type method. Accordingly, the basepoints of the detected multiple-pulse orbits (i.e., the basepoints of the stable and unstable fibers they intersect) are bounded away from the core of the resonance.

Both in Mielke *et al.* [56], Jones and Kopell [38], and the dissipative results of Kaper and Kovačič [40], the existence of N-pulse orbits is a *codimension one phenomenon* in the parameter space. In contrast, our orbits are *generic* in systems satisfying hypothesis (H1) and (H2) without an underlying family of systems (except for the special orbits constructed in Theorem 2.5.2). The reason for genericity in the dissipative context is that our N-pulse orbits are not constructed in the vicinity of 1-pulse orbits homoclinic to $\mathcal{A}_\varepsilon$: for arbitrary high pulse number the energy-phase method tracks multiple-pulse orbits independently of existing lower pulse orbits.

Another new feature of our orbits is related to their observability. The distance of our orbits from the stable and unstable manifolds of $\mathcal{A}_\varepsilon$ is *bounded from below* when they make their intermediate returns to $\mathcal{A}_\varepsilon$. In particular, when they approach $\mathcal{A}_\varepsilon$ for the k-th time ($1 \leq k \leq N-1$), they lie in a subset of $W^u(\mathcal{A}_\varepsilon)$ which *does not intersect* $W^s_{loc}(\mathcal{A}_\varepsilon)$: this intersection only occurs at the final N-th return of the orbits. As a result of this, the intermediate passage times near the slow manifold $\mathcal{A}_\varepsilon$ are bounded from above by a constant (see (2.2.25) with the choice $\alpha = 1/2$). This is to be compared with the passage time $\mathcal{O}(\frac{1}{\sqrt{\varepsilon}})$ which is necessary for the appropriate version of the exchange lemma to apply (see Kaper and Kovačič [40] for the case of a perturbed circle of equilibria). The longer the passage time is, the more error one has to be concerned with in numerical experiments. Moreover, the presence of the slow manifold itself already makes any simulation somewhat more involved because of the presence of two different time scales in the problem. This suggests that multiple pulse orbits constructed through the exchange lemma may easily get out of numerical control in the resonance band of width $\mathcal{O}(\sqrt{\varepsilon})$. Orbits constructed through the energy-phase method, however, do not share this feature. The main idea used in detecting these orbits is precisely that the solution tubes emanating from internal orbits deform only slightly when they repeatedly pass near the slow manifold $\mathcal{A}_\varepsilon$ (see Lemma 2.2.3). As a result, our N-pulse orbits are easily detectable numerically; in fact, most of the research presented in this dissertation was stimulated by numerical experiments on multiple-pulse solution tubes and their intersections (see chapters 3 and 4).

Finally, we would like to note that the energy-phase method provides a classification for multiple-pulse homoclinic orbits near slow manifolds. It turns out that even in relatively simple examples, such as the one we study in chapter 4 of this thesis, the orbits can be ordered in a self-affine *fractal structure* which would be very hard to recognize

based on numerical data alone. This again highlights the complexity in the behavior of systems near resonances even in two degrees of freedom. Generalizations of the energy-phase method to higher dimensions is also possible and will appear elsewhere.

Chapter 3

Whiskered tori in resonant normal forms

In this chapter we apply the energy-phase method to a class of three-degree-of-freedom resonant Hamiltonian normal forms which, when truncated at cubic order, possess hyperbolic manifolds of *relative* equilibria. Our goal will be to find out more about the geometry of the phase space near resonant elliptic fixed points of three-degree-of-freedom Hamiltonians. It turns out that these systems exhibit quite rich local dynamics even if the resonant equilibrium is known to be stable (i.e., the Hamiltonian is definite at the equilibrium). Hence, while the upcoming results illustrate the usage of the energy-phase method for systems with more than two degrees of freedom, they are also interesting in their own right.

3.1 Survey of previous work and outline of the results

Suppose the quadratic part H_2 of a three-degree-of-freedom smooth Hamiltonian $H = H_2 + \tilde{H}$ to be of the form

$$H_2 = \frac{1}{2}\sum_{k=1}^{3} \omega_k (q_k^2 + p_k^2), \tag{3.1.1}$$

which is characterized by the frequency vector $\omega = (\omega_1, \omega_2, \omega_3)$. This frequency is said to be resonant if we can find a nonzero integer vector $n = (n_1, n_2, n_3)$ such that

$$\langle \omega, n \rangle = 0 \tag{3.1.2}$$

is satisfied. We usually speak about a *strong resonance* if there exists an integer vector n verifying (3.1.2) with $|n| = |n_1| + |n_2| + |n_3| \leq 4$. One can also introduce the term *full resonance* (or *multiplicity-two resonance*) which means that there are two linearly independent integer vectors n and $\tilde{n}$ satisfying the relation (3.1.2).

It is well known that the six dimensional phase space of (3.1.1) is foliated by a three parameter family of 3-tori, which best manifest themselves in action-angle variables (see, e.g., Arnold [2]). System (3.1.1) also has three families of distinguished motions, usually called *normal modes*, which are periodic orbits with only one nonvanishing action. As we know from the appropriate version of the KAM theory (see, e.g., [2]-[5]), in a neighborhood of the origin $q = p = 0$ most of the 3-tori typically persist under the effect of the higher order terms in $\tilde{H}$ provided ω is not strongly resonant. In these cases, close to the origin, the observed perturbed dynamics is reminiscent of the unperturbed one, at least for finite times.

As it was soon revealed by computer experiments following the appearance of KAM-type results, the dynamics around a strongly resonant equilibrium may differ significantly from the picture described above (see, e.g., Ford and Waters [25] and Ford and Lunsford [26]). In particular, one can observe significant short-time deviation from the solutions of (3.1.1). Trajectories of H starting close to the linear normal modes of the quadratic part H_2 may leave and return on time scales much shorter than those mentioned above. Moreover, plotting the action values of these trajectories, one experiences irregular patterns in the change of action, which is usually referred to as *energy transfer* between

different modes ([25],[26],[69],[70], etc.) Though this terminology is descriptive, it is not quite accurate since the linear normal modes of H_2 do not necessarily persist as *nonlinear normal modes* under the effect of $\tilde{H}$. Hence, the first natural question one might ask about the nature of full resonances should be about the fate of the linear normal modes and the possible creation of new periodic orbits.

A general answer to this question is given by the work of Weinstein [73] (see also Moser [60] and Ito [37]). If H_2 is definite, his results guarantee the existence of at least three distinct periodic orbits on every energy surface $H = const.$ For more specific results one has to appeal to the method of normal forms (see, e.g., Arnold *et al.* [5], Sanders and Verhulst [63]) and simplify the general Hamiltonian $H = H_2 + \tilde{H}_3$ for the purposes of the analysis. This is achieved through a smooth near-identity change of variables which puts H to the Birkhoff normal form

$$H = H_2 + H_3 + H_4 + ... + H_r + \mathcal{O}(r+1), \tag{3.1.3}$$

where H_j is a homogeneous polynomial of order j in the new coordinates (q', p') with $\{H_2, H_j\} = 0, \{\ ,\ \}$ denoting the Poisson-bracket. If we truncate (3.1.3) at some order less than r to obtain a Hamiltonian $\bar{H}$, the corresponding system has two independent first integrals: $\bar{H}$ and H_2. If ω is not fully resonant, we can always find one more independent integral (see Arnold *et al.* [5]); hence the normal form is integrable if truncated at any finite order. This effectively means that system (3.1.3) exhibits a resonance only between two of the frequencies and can be analyzed by the methods developed for two-degree-of freedom resonant Hamiltonians (see Arnold *et al.* [5], Churchill *et al.* [10]-[11], Sanders and Verhulst [63], and the references cited therein). To obtain inherently three-degree-of-freedom effects, one therefore needs to assume that the frequency ω is fully resonant, in which case the truncated normal form is not automatically integrable.

To describe how complex a given fully resonant normal form is, we may speak about a *genuine k-th order resonance* if (3.1.3) truncated at order $k+2$ (and not below) exhibits full coupling between all the three degrees of freedom (for a precise definition see Sanders and Verhulst [63]). A systematic study of periodic solutions and their stability for genuine first order resonances was carried out in Van der Aa [70] (see also Sanders and Verhulst [63]). Related results for symmetric systems appeared in, e.g., Montaldi *et al.* [57]-[58] and the references therein, which also address the question of persistence of periodic solutions for the full system (3.1.3). Parallel to this, one can also see an increasing interest in the integrability of fully resonant normal forms. The picture arising from the works of Martinet *et al.* [54], Van der Aa and Sanders [69], Van der Aa [70], Van der Aa and Verhulst [71], *et al.* is that genuine first order resonances (truncated at cubic order) do not seem to have a third independent integral in general. Nice exceptions are the 1:2:2 resonance and resonances with discrete symmetries. For these integrable cases the methods of symplectic and Poisson reductions (Abraham and Marsden [1]) gave an insight to the foliation of the phase space (see Cushman [13], Holm [30], and Kummer [48]), making use of related results for two degrees of freedom (Churchill *et al.* [11], Cushman and Rod [14], Kummer [49], Kummer [50], Kirk *et al.* [42]). The work of Kummer [51] extends this point of view to n-degrees of freedom and also gives a persistence theorem for a class of $n-1$ tori arising from the truncated normal form. Recently Hoveijn [35] gave a nice classification of the possible reduced phase spaces of integrable three-degree-of-freedom resonances using the theory of singular reduction. He also proved the existence of invariant spheres in these systems.

As a rule, most of the above results seem to focus on regular behavior (periodic orbits, 2-tori) in three-degree-of-freedom resonances. The first reference pointing towards irregularity appears to be Duistermaat [18] with a proof that the 1:1:2 resonance is typ-

ically nonintegrable. Duistermaat shows an infinite branching of complex continuation of manifolds of periodic orbits with constant frequency, which is known to be an obstruction to integrability (see Arnold *et al.* [5]). He also considers the special case when the two terms of the cubic normal form of this resonance have equal coefficients. In this integrable case he finds a manifold of homoclinic orbits for a relative equilibrium and shows that one Silnikov-type orbit survives the effect of a specific quartic normal form term. He then appeals to the results of Devaney [17] to argue that horseshoes are present in that specific system; hence it cannot possess a third analytic integral (see Moser [59]). A more geometric discussion of another resonance, the 1:2:3 can be found in Hoveijn and Verhulst [34]. Using the methods of Duistermaat, they construct a two dimensional invariant manifold of the cubic normal form which contains a one-parameter family of spiralling homoclinic orbits (the dynamics restricted to this manifold is not Hamiltonian). As in Duistermaat [18], they proceed by considering a given fourth order normal form term and present numerical results showing the survival of one orbit homoclinic to a relative equilibrium. The homoclinic orbit apparently lies in the transversal intersection of the stable and unstable manifolds of the relative equilibrium; hence Devaney's results apply again to suggest the peresence of horseshoes in the normal form truncated at fourth order. Using Melnikov's method Hoveijn [35] completed this study by proving that the stable and unstable manifolds of the relative equilibrium do intersect transversally for a special choice of the quartic normal form terms. His analysis essentially follows that of Duistermaat [18] who established nonintegrability the same way for a special parameter configuration in the 1:1:2 resonance.

In this chapter we would like to go one step further in exploring the mechanism and onset of chaos near three-degree-of-freedom resonant equilibria. We consider fully resonant systems for which the resonance relationship (3.1.2) is satisfied with $|n_1| = 2$,

$|n_2| = 1$. In the usual terminology, we assume that the resonance has a *generator* of the form $\bar{n} = (2, 1, 0)$ or $(2, -1, 0)$. Rescaling the frequencies by ω_1, we then obtain the new frequency vector $\tilde{\omega} = (1, \pm 2, \tilde{\omega}_3)$, where $\tilde{\omega}_3$ is a a nonzero rational number. We want to ensure that the corresponding normal form is integrable when truncated at cubic order and intend to treat higher order normal form terms as perturbations on this integrable structure. To obtain an integrable cubic normal form we may make various assumptions. *Either* we require $|\tilde{\omega}_3| \geq 5$ or $|\tilde{\omega}_3| = 2$ to hold (see hypothesis $(H_2)(i)$ of section 3.2 and Remark 3.3.1) *or* we assume that the full Hamiltonian H is close to being discrete symmetric at cubic order (see $(H_2)(ii)$ of section 3.2). A large number of multiplicity two resonances satisfy one of these assumptions and can be cast in the same type of normal form. In particular, we can treat the genuine first order resonances 1:2:1, 1:2:3, and 1:2:4 with appropriate discrete symmetries, and the 1:2:2 without any symmetry assumed. All the genuine second order resonances with cubic generator $\bar{n}$ also qualify (i.e., the 1:2:6, 2:4:3, 3:6:1, and the 3:6:2), and, we repeat, all resonances of the form $1:2:\omega_3$, $\omega_3 \geq 5$ are covered without symmetry assumptions. Further, in all the cases listed here and above, the signs of individual frequencies may be negative. Although it will not be discussed here, our constructions and results go through for resonances with a generator $\hat{n} = (1, 1, -1)$ (e.g., for the 2:3:5) with similar alternative assumptions which make the cubic normal form integrable. Using somewhat different (simpler) methods but doing more calculations, one can also build up a similar analysis for resonances with a generator $n = (1, \pm 3, 0)$, with assumptions making the corresponding normal forms integrable at quartic order. All this is not persued here and planned for future publication. Our study is based on the global knowledge of the integrable geometry of the cubic normal form. We pay special attention on a family of invariant 3-spheres which (restricted to the energy surface) have normally hyperbolic subsets with corresponding

four dimensional stable and unstable manifolds. Each 3-sphere is filled with a two-parameter family of periodic solutions. In the framework of reduction, this set appears as a conical singularity of the reduced phase space. Fixing only the value of one of the integrals, the degenerate set shows up as a manifold of equilibria in the corresponding two-degree-of-freedom system. This manifold is connected to itself by a two-parameter family of homoclinic orbits. Using an appropriate heteroclinic version of the energy-phase method of chapter 2, we determine what happens to this degenerate structure under the effect of higher order normalization. The predictions we are able to make involve the existence and geometry of various hyperbolic sets, including families of 2-tori with transversally intersecting stable and unstable manifolds (*whiskers*) or tori with double-pulse homoclinic 2-manifolds. The splitting of the asymptotic surfaces mentioned here is of the order of the square of the distance from the origin; in particular, it is *not exponentially small.* We hope that our results can be used to identify the micro-structure of the "stochastic layer" present in the normal form through simple calculations, and also give a global picture of the related geometry.

3.2 Set-up and assumptions

We will be concerned with Hamiltonians of the form

$$H(q,p) = H_2(q,p) + \tilde{H}(q,p), \tag{3.2.1}$$

where (q,p) are canonical coordinates on the phase space $(\mathbb{R}^6,\omega)$ with $\omega = dq \wedge dp$. In (3.2.1) H_2 is a quadratic polynomial and $\tilde{H}$ is a C^4 function with $D\tilde{H}(0) = 0$ and $D^2\tilde{H}(0) = 0$. With the notation $x = (q,p)$ the Hamiltonian equations associated with

(3.2.1) take the form

$$\dot{x} = J_6 DH(x), \quad J_6 = \begin{pmatrix} 0 & Id_3 \\ -Id_3 & 0 \end{pmatrix}, \tag{3.2.2}$$

where $Id_3 \in \mathbb{R}^{3\times 3}$ is the identity matrix. We assume that $x = 0$ is an elliptic fixed point of system (3.2.2) and $J_6 D^2 H_2|_0$ is semisimple, in which case a linear canonical transformation puts H_2 to the form

$$H_2(q,p) = \frac{1}{2}\sum_{k=1}^{3} \omega_k (q_k^2 + p_k^2), \tag{3.2.3}$$

where $\Omega = (\omega_1, \omega_2, \omega_3) \in \mathbb{R}^3 - \{0\}$ is the frequency vector of the linear flow generated by H_2. We now introduce the canonical change of variables

$$z = q - ip, \quad \bar{z} = q + ip, \quad z, \bar{z} \in \mathbb{C}^3, \tag{3.2.4}$$

with its inverse defined as $T_1 : (z, \bar{z}) \mapsto (q, p)$, and consider the transformed system on the phase space $(\mathbb{C}^3, \tilde{\omega})$ with $\omega = \frac{1}{2}\mathrm{Im}(d\bar{z} \wedge dz)$. Letting $z \to \varepsilon z$, $\bar{z} \to \varepsilon \bar{z}$ with $\varepsilon > 0$ small, and dividing (3.2.1) by ε^2, we arrive at the Hamiltonian

$$H(z, \bar{z}; \varepsilon) = H_2(z, \bar{z}) + \varepsilon \tilde{H}(z, \bar{z}; \varepsilon), \tag{3.2.5}$$

with

$$H_2(z, \bar{z}) = \frac{1}{2}\sum_{k=1}^{3} \omega_k |z_k|^2, \quad \tilde{H}(z, \bar{z}; \varepsilon) = \sum_{|l|+|m|\geq 3} \varepsilon^{|l|+|m|-3} h_{lm} z^l \bar{z}^m, \tag{3.2.6}$$

where $h_{lm} = \bar{h}_{ml} \in \mathbb{C}$ with $(l, m) \in \mathbb{N}^3 \times \mathbb{N}^3$and $|l| = l_1 + l_2 + l_3$. In (3.2.6) we used the usual notation $z^p := z_1^{p_1} z_2^{p_2} z_3^{p_3}$. To describe the resonances we will study, let us introduce the resonant module

$$M = \{ n \in \mathbb{Z}^3 \mid \langle \omega, n \rangle = 0 \}. \tag{3.2.7}$$

We then assume that, after a possible reindexing of the variables $z_k, \bar{z}_k$,

(H1) Either $(2,1,0) \in M$ or $(2,-1,0) \in M$ holds *and* $\dim M = 2$.

(H2) If $s \in M$ and $s \notin \text{span}\{(2,1,0),(2,-1,0)\}$ then *one of the following* is satisfied:

(i) $|s| > 4$,

(ii) For any $l, m \in \mathbb{N}^3$ with $|l| + |m| = 3$, $l - m = s$, we have $h_{lm} = 0$.

Here (H1) means that the first two frequencies satisfy the strong resonance relationship $|\omega_1| : |\omega_2| = 1:2$ *and* there is one more independent resonance relationship among the three frequencies. If (H2)(i) holds then $(2, \pm 1, 0)$ is the unique third order generator of the resonant module M. This is satisfied by all resonances of the form $1 : \pm 2 : \omega_3$ with $|\omega_3| \geq 5$, and by a number of other resonances, like the $1:2:6$, $2:4:3$, $3:6:1$, $3:6:2$, $3:6:10$, etc. If, alternatively, (H2)(ii) holds then $(2, \pm 1, 0)$ is not the only third order generator of M. We then require certain coefficients of $\tilde{H}$ to vanish, which usually translates to the assumption that system (3.2.6) is close to having a discrete symmetry at cubic order (one can also assume $h_{lm} = \nu\varepsilon$ which requires the symmetry breaking terms to be less in order than the symmetric cubic terms). We note that all genuine first order resonances in three-degree-of-freedom Hamiltonians (i.e., $1 : \pm 2 : \omega_3$, $|\omega_3| = 1, 2, 3, 4$) with appropriate weakly broken discrete symmetries satisfy hypotheses (H1) and (H2)(ii) (see Sanders and Verhulst [63] for the definition of genuine resonances and discussion on the effect of discrete symmetries).

Based on hypothesis (H1) we can rescale the frequencies by letting

$$\omega_1 = 1, \quad \omega_2 = 2, \quad \omega_3 \to \frac{\omega_3}{\omega_1}, \tag{3.2.8}$$

where we have set the sign of ω_2 positive for convenience. Although the basic results are the same, some of the geometry will be different in the case $\omega_2 = -2$. We believe that, based on the material presented below, it is straightforward to make the necessary

modifications for this case. We finally note that assumption (H1) implies the rescaled frequency ω_3 to be rational. In order to simplify the Hamiltonian (3.2.6) further, we apply a near-identity canonical change of variables which puts our system in Birkhoff normal form up to some order $r \geq 4$ (see Arnold [2] or Sanders and Verhulst [63], etc.). Using (H1)-(H2), the rescaling (3.2.8), and allowing some slight detuning from the exact resonance, we can write the normalized part of the Hamiltonian in the form

$$H = H_2 + \varepsilon H_3 + \varepsilon^2 \tilde{H}_4 + \varepsilon^3 H_5 + \cdots + \varepsilon^{r-2} H_r,$$

$$H_2 = \frac{1}{2}|z_1|^2 + |z_2|^2 + \frac{1}{2}\omega_3 |z_3|^2, \qquad H_3 = \frac{a}{2}\mathrm{Re}\,(z_1^2 \bar{z}_2), \ a \in \mathbb{R}, \qquad \tilde{H}_4 = H_4 + \hat{H}_4, \quad (3.2.9)$$

with

$$\{H_2, H_j\} = 0, \quad 3 \leq j \leq r, \qquad \{H_2, \hat{H}_4\} = 0, \qquad (3.2.10)$$

where $\{\ ,\ \}$ is the canonical Poisson bracket. In (3.2.9) H_j contains resonant terms of the form $z^l \bar{z}^m$ with $|l| + |m| = j$, $l - m \in M$. In general, the normalization procedure leads to the cubic term $H_3 = \mathrm{Re}\,(A z_1^2 \bar{z}_2)$, $A \in \mathbb{C}$ and we have to apply an additional symplectic change of coordinates $z_1 \to \exp(-i\arg(A)/2) z_1$, $\bar{z}_1 \to \exp(-i\arg(A)/2)\bar{z}_1$, to put H_3 in the form of (3.2.9) with $a = 2|A|$ (see Kummer [51]). From this point we will assume that the nondegeneracy condition $a \neq 0$ holds. The expression $\hat{H}_4$ contains some possible unnormalized perturbation of system (3.2.1) Poisson commuting with H_2, as well as cubic terms $h_{lm} z^l \bar{z}^m$ of the normal form with $h_{lm} = \mathcal{O}(\varepsilon)$, which may arise in the case of hypothesis (H2). We finally remark that for $\Omega = (1 : \pm 2 : \pm 2)$ system (3.2.6) can be put in the form (3.2.9) even if (H2) is not satisfied (see Van der Aa and Verhulst [71], Kummer [50], and Cushman [13]).

3.3 Integrability and geometry of the cubic normal form

In this section we briefly discuss the geometry of the normal form (3.2.9) for $r = 3$, i.e., we will study the Hamiltonian

$$H_0 = \frac{1}{2}|z_1|^2 + |z_2|^2 + \frac{1}{2}\omega_3|z_3|^2 + \varepsilon\frac{a}{2}\mathrm{Re}\,(z_1^2\bar{z}_2). \tag{3.3.1}$$

Related results can be found in Kummer [49], Churchill *et al.* [11], and Kirk *et al.* [42] for two-degree-of-freedom resonances, Kummer [48], Cushman [13], and Holm [30] for certain three-degree-of-freedom resonances, and Kummer [51], Hoveijn [35] for n-degree-of-freedom systems. The standard terminology of symplectic reduction can be found in Abraham and Marsden [1].

Let us introduce the notation $P = \mathbb{C}^3$ and consider the action of the Lie group $G = \mathbb{T}^2 = S^1 \times S^1$ on $(P, \tilde{\Omega})$ given by

$$\begin{aligned} \Phi: G \times P &\to P, \\ (g_1, g_2, z_1, z_2, z_3) &\mapsto (e^{-ig_1}z_1, e^{-2ig_1}z_2, e^{-ig_2}z_3). \end{aligned} \tag{3.3.2}$$

We define the mapping

$$\begin{aligned} J: P &\to \mathfrak{g}^* \simeq \mathbb{R}^2, \\ (z_1, z_2, z_3) &\mapsto (\frac{1}{2}|z_1|^2 + |z_2|^2, \frac{1}{2}|z_3|^2), \end{aligned} \tag{3.3.3}$$

where $\mathfrak{g}^*$ denotes the dual of the Lie algebra $\mathfrak{g}$ of G. For any fixed $\xi \in \mathfrak{g}$ we also introduce the map $\hat{J}(\xi): P \to \mathbb{R}^2$, $\hat{J}(\xi)(z) = \langle J(z), \xi \rangle$, where $\langle\ ,\ \rangle$ denotes the natural pairing between elements of $\mathfrak{g}^*$ and $\mathfrak{g}$. Using the definition of J we have

$$\hat{J}(\xi)(z) = (\frac{1}{2}|z_1|^2 + |z_2|^2)\xi_1 + \frac{1}{2}|z_3|^2\xi_2. \tag{3.3.4}$$

Let us also define for any $\xi \in \mathfrak{g}$ the vectorfield $\xi_P: P \to TP$ by

$$\xi_P(z) = \frac{d}{dt}|_{t=0}\Phi(\exp t\xi, z), \quad \xi \in \mathfrak{g},\ z \in P,$$

which is just the infinitesimal generator of the action of the subgroup generated by $\xi \in \mathfrak{g}$. A straightforward calculation shows that

$$\xi_P(z) = (-i\xi_1 z_1, -2i\xi_1 z_2, -i\xi_2 z_3),$$

which together with (3.3.4) yields

$$\imath_{\xi_P(z)}\tilde{\Omega}(z) = d\hat{J}(\xi)(z), \quad z \in P,$$

with $\imath_{\xi_P}\tilde{\Omega}$ denoting the interior product of the vectorfield ξ with the form $\tilde{\Omega}$. Consequently, J is a momentum mapping for the action Φ. Since G is Abelian, J is Ad^* equivariant, i.e., the following diagram commutes:

$$\begin{array}{ccc} P & \xrightarrow{\Phi_g} & P \\ {\scriptstyle J}\uparrow & & \uparrow{\scriptstyle J} \\ \mathfrak{g}^* & \xrightarrow[Ad^*_{g^{-1}}]{} & \mathfrak{g}^* \end{array} \tag{3.3.5}$$

with the map $Ad^*_{g^{-1}}: \mathfrak{g}^* \to \mathfrak{g}^*$, $\langle Ad^*_{g^{-1}}\mu, \xi\rangle = \langle \mu, Ad_g\xi\rangle$, for all $g \in G$, $\mu \in \mathfrak{g}^*$, and $\xi \in \mathfrak{g}$. For any $\mu \in \mathfrak{g}^*$ we would like to obtain a representation of the reduced phase space $P_\mu = J^{-1}(\mu)/G_\mu$, which is well defined based on the Ad^* equivariance of J. Since G is compact, the action of the isotropy subgroup $G_\mu = \{g \in G | Ad^*_{g^{-1}}\mu = \mu\} = G$ is proper on $J^{-1}(\mu)$, but it is not free (G has nonidentity elements leaving $(0, z_2, z_3) \in J^{-1}(\mu)$ fixed). Hence the Marsden-Weinstein reduction theorem does not guarantee that P_μ is a smooth manifold, and it is indeed not, as we will see. Introducing the Euler-variables (see the references above)

$$W_1 = \mathrm{Re}(z_1^2\bar{z}_2), \quad W_2 = \mathrm{Im}(z_1^2\bar{z}_2), \quad W_3 = \frac{1}{2}|z_1|^2, \tag{3.3.6}$$

we observe that

$$W_1^2 + W_2^2 = 4W_3^2(J_1(z) - W_3). \tag{3.3.7}$$

Let $Z_\mu \subset \mathbb{R}^3$ denote the zero set of the function $f_\mu: \mathbb{R}^3 \to \mathbb{R}$ defined as

$$f_\mu(W_1, W_2, W_3) = \frac{1}{2}(W_1^2 + W_2^2 - 8W_3^2(\mu_1 - W_3)). \tag{3.3.8}$$

Introducing the Hopf-map $\pi_W: P \to \mathbb{R}^3$, $z \to W(z)$ (see (3.3.6)) one can verify from (3.3.4)-(3.3.8) that $\pi_W(J^{-1}(\mu)) \subset Z_\mu$ and away from the z_2 plane $\pi_W|J^{-1}(\mu)$ is a surjective submersion. From (3.3.6) and the definition of Φ we readily see that $\pi_W \circ \Phi = \pi_W$. On the other hand, a simple calculation reveals that for any fixed $\mu \in \mathfrak{g}^*$ and $z, z^* \in J^{-1}(\mu)$, $\pi_W(z) = \pi_W(z^*)$ implies the existence of $\tilde{g} \in G$ with $z^* = \Phi(\tilde{g}, z)$. Putting these facts together we conclude that Z_μ can be identified with the orbit-space of the action of Φ on P, i.e., $P_\mu \simeq Z_\mu$.

We now turn to the study of the cubic truncation of the normal form (3.2.9) given by (3.3.1). It is easy to verify that $\phi_g \circ H_0 = H_0$ holds; hence, based on the construction above, H_0 defines an *integrable Hamiltonian system* with H_0, J_1, and J_2 being three independent integrals. As we have found, the reduce phase space for H_0 can be realized as $P_\mu \simeq Z_\mu$, embedded in $\mathbb{R}^3$. It is not hard to see from (3.3.7) that P_μ is homeomorphic to S^2. In fact, Z_μ is a pinched sphere with its pinch at the origin of the W-space, and its axis of rotation is just the W_3 axis. As noted in the references cited at the beginning of the section, the reduced flow of (3.3.1) on P_μ is given by the Euler-like equations

$$\dot{W} = \nabla H_0 \times \nabla f_\mu, \tag{3.3.9}$$

with

$$f_\mu = \frac{1}{2}(W_1^2 + W_2^2 - 8W_3^2(\mu_1 - W_3)).$$

Using the fact for any $\mu \in \mathfrak{g}^*$ $J^{-1}(\mu)$ is a 2-torus bundle over P_μ, we can reconstruct certain invariant structures in the phase space of (3.3.1) based on our knowledge of the orbits of the reduced system (3.3.9). To identify the reduced orbits on P_μ, one can use the fact that the Euler-variable W_1 is constant on these orbits (being a first integral for the cubic normal form (3.3.1)). Hence, following the idea of Kummer [49], we can visualize the orbit structure of (3.3.9) by intersecting the pinched sphere Z_μ with planes $W_1 = const.$ As we show in Fig. 3.1, each such intersection is either a point, or a smooth closed curve, or a continuous closed curve through the pinch of Z_μ at $W = 0$. The closed

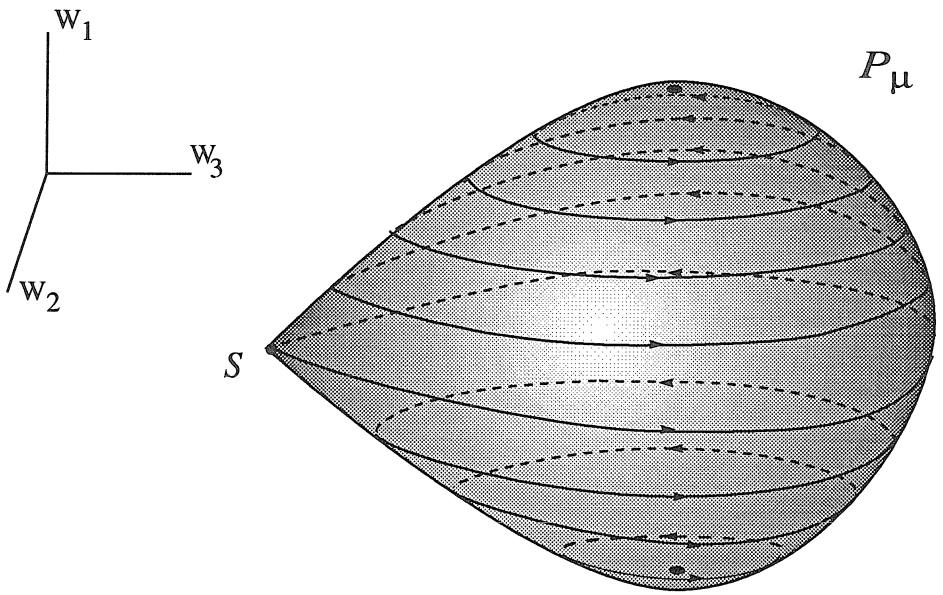

Figure 3.1: The reduced phase space P_μ

curve through the pinch contains a relative equilibrium p_μ at $W = 0$ which is connected to itself by a homoclinic orbit in the reduced phase space satisfying

$$W_1 = 0, \quad W_2 = 2\sqrt{2}W_3\sqrt{\mu_1 - W_3}, \quad W_3 > 0. \tag{3.3.10}$$

As we pointed out, a relative equilibrium or a periodic solution of (3.3.9) indicates the presence of an invariant 2-torus or an invariant 3-torus, respectively, in $J^{-1}(\mu)$. One can ask what happens to these invariant sets under perturbation and, using an appropriate version of the KAM theory, one can show that most of the invariant 3-tori persist in the phase space of (3.2.9). However, this is a phenomenon which one also finds in nonresonant normal forms. In particular, this result does not bring us any closer to an understanding of the source of irregularity in strongly resonant systems. To this end, we will study what happens to the homoclinic structure described by (3.3.10) above.

We start by defining the invariant set $M^h \subset P$ with $h > 0$ as

$$M^h = \cup_{\mu_1+\mu_2=h} \pi_W^{-1}(p_\mu).$$

Clearly, M^h is the set of orbits in a given energy-surface $H_0 = h$ which are mapped into relative equilibria at $W = 0$ in P_μ under the quotient projection $P \to P_\mu$. Using (3.3.6) and (3.2.4), one can immediately see that the image of M^h under the diffeomorhism T_1 (defined after (3.2.4)) satisfies

$$T_1(M^h) = \{ (q,p) \in \mathbb{R}^6 \mid q_1 = p_1 = 0,\ q_2^2 + p_2^2 + \frac{1}{2}\omega_3(q_3^2 + p_3^2) = h\}. \qquad (3.3.11)$$

This shows that for $\omega_3 > 0$ M^h is diffeomorphic to S^3, while for $\omega_3 < 0$ it is a three dimensional hyperbolic surface of revolution. In either case, M^h is connected to itself by a four dimensional homoclinic manifold W^h which lies in the preimage of the set defined in (3.3.10) under π_W.

One can check that for any $h > 0$ M^h is entirely filled with periodic orbits. Two of these closed orbits are distinguished: they are the (nonlinear) *normal modes* of H_0 given by

$$N_2^h \quad = \quad \{ z \in \mathbb{C}^3 \mid z_1 = z_3 = 0,\ |z_2| = \sqrt{h}\,\},$$

$$N_3^h = \{ z \in \mathbb{C}^3 \mid z_1 = z_2 = 0, |z_3| = \sqrt{\frac{2h}{\omega_3}} \}.$$

These two normal modes survive from the quadratic Hamiltonian H_2 under the effect of the cubic terms in (3.3.1). With the exception of N_3^h, all the periodic orbits in $\mathcal{M}^h$ have two-dimensional stable and unstable manifolds which foliate W^h into a two-parameter family of cylindrical surfaces.

Since M^h is a manifold of periodic orbits, the flow of the Hamiltonian (3.3.1) restricted to M^h can be considered as the action of the group S^1 on M^h. We can define $F^h = M^h/S^1$, the quotient space corresponding to this action, with the usual quotient projection $\pi_F: M^h \to F^h$. In other words, F^h is the orbit space of the periodic solutions contained in M^h. From (3.3.11) we see that the set $T_1(M^h) \simeq M^h$ can be considered as the three dimensional energy surface for a Hamiltonian system of two linear oscillators which, by assumption (H1), are in $2{:}\,\omega_3$ resonance. Accordingly, F^h can be viewed as the reduced phase space for these oscillators with respect to the resonant $2{:}\,\omega_3$ action of S^1. As it is shown in, e.g., Churchill *et al.* [11], this reduced phase space is homeomorphic to S^2. Furthermore, if κ_1 and κ_2 are relative prime positive integers with

$$\frac{2}{|\omega_3|} = \frac{\kappa_1}{\kappa_2}, \tag{3.3.12}$$

then F^h will be a pinched sphere with a κ_1-order singularity at its north pole, and with a κ_2-order singularity at its south pole (e.g., $\kappa_1 = 1, 2, 3$ would mean no singularity, conical singularity, and cusp singularity, respectively). We summarize the observations of this section in the following proposition.

Proposition 3.3.1 *Suppose that $\omega_3 > 0$ holds. Then on any energy surface $H_0 = h$ (with $h > 0$) of the integrable Hamiltonian system defined by H_0 there exists an invariant set M^h defined by $z_1 = 0$, which is diffeomorphic to S^3. The set M^h is entirely filled*

with periodic orbits. Furthermore,

(*i*) *Any invariant subset $M_0^h \subset M^h$ not containing the third normal mode N_3^h is normally hyperbolic and connected to itself by a four dimensional homoclinic manifold W^h.*

(*ii*) *The orbit space $F^h = M^h/S^1$ of periodic solutions in M^h is homeomorphic to a 2-sphere with a κ_1-order singularity at its north pole, and with a κ_2 order singularity at its south pole (see (3.3.12)).*

We note that invariant spheres similar to M^h have been found recently in a large class of Hamiltonian resonances by Hoveijn [35]. The methods we use in the following sections can be used to study perturbations of those spheres as well if they admit a homoclinic structure similar to W^h.

3.4 The "blown-up" normal form and the formulation of the perturbation problem

The goal of this section is to introduce coordinates which are suited to the study of what happens to the manifolds M^h and W^h in the normal form (3.2.9) under the perturbative effects of the terms $\varepsilon^2\hat{H}_4 + \cdots \varepsilon^{r-2}H_r$.

Let us first introduce action-angle variables for the quadratic part H_2 of (3.2.9) letting

$$z_k = \sqrt{2I_k}e^{i\phi_k}, \quad \bar{z}_k = \sqrt{2I_k}e^{-i\phi_k}, \qquad k = 1,2,3, \tag{3.4.1}$$

with the inverse change of variables $T_2\colon (I,\phi) \mapsto (z,\bar{z})$. We apply a further canonical change of variables

$$\begin{array}{ll} \psi_1 = \phi_1, & K_1 = I_1 + 2I_2 + \omega_3 I_3, \\ \psi_2 = \phi_3 - \omega_3\phi_1, & K_2 = I_3, \\ x_1 = \sqrt{2I_2}\sin(\phi_2 - 2\phi_1), & x_2 = \sqrt{2I_2}\cos(\phi_2 - 2\phi_1), \end{array} \tag{3.4.2}$$

with the inverse coordinate transformation being $T_3\colon (K, \psi, x) \mapsto (I, \phi)$. In this final set of variables our Hamiltonian (3.3.1) takes the form

$$H_0(x, K, \psi) = K_1 + \varepsilon a(K_1 - \omega_3 K_2 - |x|^2)x_2. \tag{3.4.3}$$

The corresponding Hamiltonian vectorfield is smooth and defined on the set

$$\mathcal{P} = \{(x, K_1, \psi_1, K_2, \psi_2) |\ x \in \mathbb{R}^2, K \in \mathbb{R}^2, \psi \in \mathbb{T}^2\}, \tag{3.4.4}$$

through the symplectic form $\omega = dx_1 \wedge dx_2 + d\psi \wedge dK$, but it is related to system (3.3.1) only in the domain

$$\bar{\mathcal{P}} = \{(x, K_1, \psi_1, K_2, \psi_2) \in \mathcal{P} |\ K_1 - \omega_3 K_2 \geq 0,\ K_2 \geq 0\}. \tag{3.4.5}$$

Our main goal with the sequence of transformations (3.4.1)-(3.4.2) is to "blow up" the singularity of the reduced phase space. This is achieved, as we will see next, by extending the transformations (3.4.1)-(3.4.2) to the domain $I_1 = 0$, in which case (3.4.1) is not a diffeomorhism any longer and the angle variable ϕ_1 is not well defined. Since M^h is characterized by $I_1 = 0$, we have to study the effect of this singular transformation if we want to relate our later results on the perturbation of the blown-up normal form (3.4.3) back to the original normal form (3.2.9).

Proposition 3.4.1 *Suppose that $\omega_3 > 0$ is satisfied. Then the following hold:*

(*i*) $T_3^{-1} \circ T_2^{-1}(M^h) = \mathcal{D}^h \cup \mathcal{M}^h$ *where the set $\mathcal{D}^h$ satisfies*

$$\mathcal{D}^h = \{\, (x, K_1, \psi_1, K_2, \psi_2) \in \mathcal{P} \,|\, |x|^2 + \omega_3 K_2 = h,\ |x_2| > 0,\ K_1 = h,\ \psi \in \mathbb{T}^2 \,\};$$

hence it is diffeomorphic to the disjoint union of two five dimensional open discs. The set $\mathcal{M}^h$ satisfies

$$\mathcal{M}^h = \{\, (x, K_1, \psi_1, K_2, \psi_2) \in \mathcal{P} \,|\, x_2 = 0,\ x_1^2 + \omega_3 K_2 = h,\ K_1 = h,\ \psi \in \mathbb{T}^2 \,\};$$

hence it is diffeomorphic to $S^2 \times S^1$. Furthermore, $\mathcal{M}^h$ is filled with periodic orbits of (3.4.3), while $\mathcal{D}^h$ consists of orbits of (3.4.3) positively and negatively asymptotic to periodic orbits in $\mathcal{M}^h$.

(*ii*) *The manifold $\mathcal{W}^h = T_3^{-1} \circ T_2^{-1}(W^h)$ satisfies*

$$\mathcal{W}^h = \{ (x, K_1, \psi_1, K_2, \psi_2) \in \mathcal{P} \mid x_2 = 0,\ x_1^2 + \omega_3 K_2 < h,\ K_1 = h,\ \psi \in \mathbb{T}^2 \};$$

thus it is diffeomorphic to $B^3 \times S^1$ where B^3 is the open unit ball in $\mathbb{R}^3$. Further, $\mathcal{W}^h$ is filled with a three parameter family of orbits positively and negatively asymptotic to periodic orbits in $\mathcal{M}^h$.

(*iii*) *Let $\pi_{\mathcal{F}}: \mathcal{M}^h \to \mathcal{F}^h = \mathcal{M}^h / S^1$ be the quotient projection from $\mathcal{M}^h$ to its orbit space $\mathcal{F}^h$, and let Q^h be defined through the diagram*

$$\begin{array}{ccc} \mathcal{M}^h & \xrightarrow{T_2 \circ T_3} & M^h \\ {\scriptstyle \pi_{\mathcal{F}}}\downarrow & & \downarrow{\scriptstyle \pi_F} \\ \mathcal{F}^h & \xrightarrow{Q^h} & F^h \end{array}$$

In other words, let Q^h be the map between the quotient spaces induced by $T_2 \circ T_3$. Then $\mathcal{F}^h$ is diffeomorphic to S^2. Moreover, if M_0^h is a compact subset of M^h which does not contain the periodic orbits N_2^h and N_3^h, then $\mathcal{F}^h$ has a compact subset $\mathcal{F}_0^h$ not containing $\mathcal{N}_2^h = (Q^h)^{-1} \circ \pi_F(N_2^h)$ and $\mathcal{N}_3^h = (Q^h)^{-1} \circ \pi_F(N_3^h)$, such that Q^h restricts to a κ_1-fold smooth covering map onto $\pi_F(M_0^h)$ on any of the two connected components of $\mathcal{F}_0^h = \pi_{\mathcal{F}}(\mathcal{M}_0^h)$.

Proof: The proof of statements $(i) - (ii)$ is a direct computation based on the definition of T_2 and T_3, which we omit. To prove (iii) we first note that the change of variables (3.4.1) puts the vectorfield corresponding to (3.3.1) to the form

$$\dot{I}_1 \quad = \quad \varepsilon 2 a I_1 \sqrt{2 I_2} \sin(2\phi_1 - \phi_2),$$

$$\begin{aligned}
\dot{I}_2 &= -\varepsilon a I_1 \sqrt{2I_2}\sin(2\phi_1 - \phi_2), \\
\dot{I}_3 &= 0, \\
\dot{\phi}_1 &= 1 + \varepsilon a\sqrt{2I_2}\cos(2\phi_1 - \phi_2), \\
\dot{\phi}_2 &= 2 + \varepsilon a\frac{I_1}{\sqrt{2I_2}}\cos(2\phi_1 - \phi_2), \\
\dot{\phi}_3 &= \omega_3.
\end{aligned} \tag{3.4.6}$$

Straightforward calculations show that the periodic orbits in $T_2^{-1}(M^h)$ (described by $I_1 = 0$) can be labelled by the two parameters

$$\alpha = I_2 = \frac{1}{2}(q_2^2 + p_2^2) \in [0, \frac{h}{2}], \quad \beta = \omega_3\phi_2 - 2\phi_3 \bmod \omega_3\frac{2\pi}{\kappa_2}, \tag{3.4.7}$$

which, combined with the definition of T_2, gives a parametrization of F^h. The parametrization is singular on $\pi_F(N_3^h)$ and $\pi_F(N_2^h)$: all points of F^h with $\alpha = 0$ should be identified with $\pi_F(N_3^h)$ and all points with $\alpha = h/2$ should be identified with $\pi_F(N_2^h)$ (see Fig. 3.2). Using (3.4.2) and (3.4.7) we can see that on the set $\mathcal{M}^h$ the coordinates (x, K, ψ) and the parameters (α, β) satisfy the following relationships:

$$\begin{array}{ll}
\dot{\psi}_1 = 1, & K_1 = h, \\
\psi_2 = \beta/2 \pm \omega_3\pi/4, & K_2 = (h - 2\alpha)/\omega_3, \\
x_1 = \pm\sqrt{2\alpha}, & x_2 = 0.
\end{array} \tag{3.4.8}$$

Factoring out the uniform rotation in the ψ_1 coordinate in the above equations is equivalent to passing to the quotient space $\mathcal{F}^h$. Performing this, we find from (3.4.8) that $\mathcal{F}^h$ can be identified with the set defined by the equation

$$x_1^2 + \omega_3 K_2 = h. \tag{3.4.9}$$

But (3.4.9) represents a 2-sphere in the (x_1, K_2, ψ_2) space which proves the first statement of (iii). Choosing a compact set M_0^h as in statement (iii) of the proposition, (3.4.7) and (3.4.8) show that $\mathcal{F}_0^h = \pi_{\mathcal{F}}(\mathcal{M}_0^h)$ has two components: one on the northern hemisphere

($x_1 > 0$) and one on the southern hemisphere ($x_1 < 0$) of $\mathcal{F}^h$. We denote these two components by $\mathcal{A}_0^1$ and $\mathcal{A}_0^2$, respectively, and note that both can be globally parametrized by the variables (K_2, ψ_2). From (3.4.2) we in fact obtain a coordinate representation of $Q^h|\mathcal{A}_0^1 \cup \mathcal{A}_0^2$ in the form

$$\begin{aligned} Q_0^h\colon \mathcal{F}_0^h = \mathcal{A}_0^1 \cup \mathcal{A}_0^2 \quad &\longrightarrow \quad \pi_F(M_0^h) \subset F^h, \\ (K_2, \psi_2) \quad &\mapsto \quad (\frac{1}{2}(h - K_2\omega_3), 2\psi_2 - \omega_3 \frac{\pi}{2} \text{sign}\, x_1), \end{aligned} \tag{3.4.10}$$

which, together with (3.3.12) and (3.4.7) implies the second part of statement (*iii*) of the proposition. □

In Fig. 3.2 we show the parametrization of the orbit space $\mathcal{F}^h$ which we constructed in the proof of the above proposition. We now rewrite the full normalized Hamiltonian (3.2.9) in terms of the (x, K, ψ) coordinates to obtain

$$H(x, K, \psi_2; \varepsilon) = H_0(x, K) + \varepsilon^2 \tilde{H}_4(x, K, \psi_2) + \cdots + \varepsilon^{r-2} H_r(x, K, \psi_2). \tag{3.4.11}$$

Note that the quantities listed in (3.4.11) do not depend on ψ_1, which follows from the fact that the symplectic transformations defined in (3.4.1)-(3.4.2) preserve the bracket relations in (3.2.10). The underlying idea of our study will be the following: the Hamiltonian (3.4.11) has an unbroken S^1 symmetry corresponding to rotations in the ψ_1 coordinate which allows a reduction to a two-degree-of-freedom system. For $\varepsilon = 0$ this subsystem can be reduced further using the S^1 symmetry of the Hamiltonian H in the ψ_2 coordinate. Due to the poper choice of our coordinates both reductions can be carried out by fixing the values of the actions K_1 and K_2, respectively. One then obtains that the reduced phase space of the blown-up cubic normal form is just a two-dimensional disk which is obtained by blowing up the pinched sphere of Fig. 3.1 (see Fig. 3.3). We indicate in the figure the important fact that the flow on this new reduced phase space

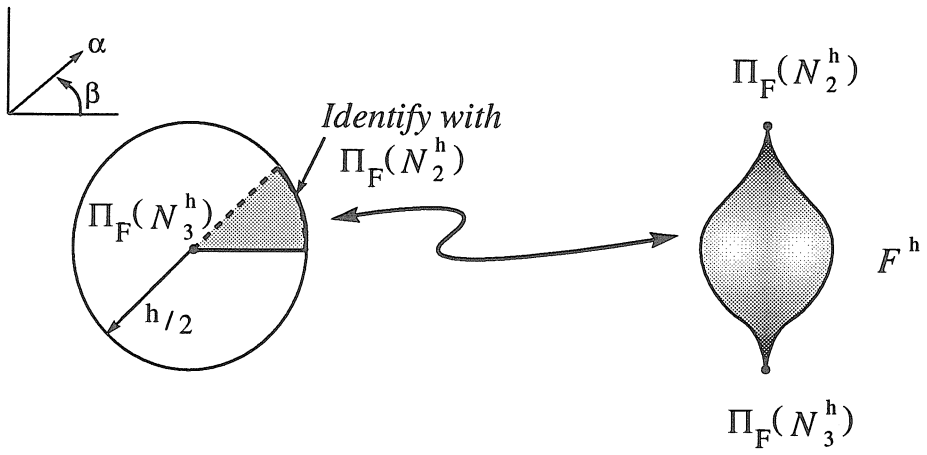

Figure 3.2: Parametrization of the orbit space $\mathcal{F}^h$

extends smoothly to the whole two-dimensional plane. Since for $\varepsilon \neq 0$ the symmetry in the ψ_2 coordinate disappears, for the analysis of the truncated normal form (3.4.11) we only carry out a partial reduction with respect to the S^1 symmetry in the ψ_1 coordinate. This practically means considering the Hamiltonian system which derives from (3.4.11) through the symplectic form

$$\omega_R = dx_1 \wedge dx_2 + d\psi_2 \wedge dK_2, \tag{3.4.12}$$

on the phase space

$$\mathcal{P}^h = \{\, (x, K_2, \psi_2) \,|\, x \in \mathbb{R}^2,\ K_2 \in \mathbb{R}^+,\ \phi_2 \in S^1 \,\}. \tag{3.4.13}$$

For the invariant manifolds $\mathcal{M}^h$ and $\mathcal{W}^h$ this reduction means a passage to the quotient spaces $\mathcal{F}^h$ and $\mathcal{W}^h/S^1$, respectively. Since $\mathcal{M}^h$ is entirely filled with periodic orbits,

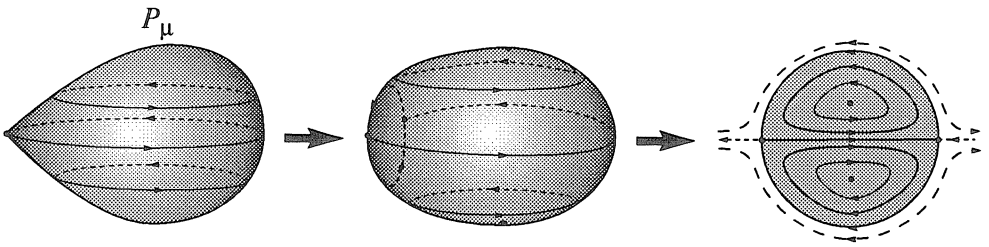

Figure 3.3: The effect of the blow-up transformation on the reduced phase space $\mathcal{P}_\mu$

the two-degree-of-freedom reduced system will have a 2-manifold of equilibria which we identify with $\mathcal{F}^h$. This invariant 2-sphere will be connected to itself by a three dimensional homoclinic manifold which we identify with $\mathcal{W}^h/S^1$. Any subset of $\mathcal{F}^h$ not containing the poles and the equator will therefore appear as a normally hyperbolic 2-manifold of equilibria which is connected to some other subset of $\mathcal{F}^h$ through the appropriate subset of the homoclinic 3-manifold $\mathcal{W}^h/S^1$. Based on (3.4.10), two relative equilibria $p_1 \neq p_2$ in $\mathcal{F}^h \backslash (\pi_F(\mathcal{N}_2^h) \cup \pi_F(\mathcal{N}_3^h))$ represent the same periodic solution in M^h if and only if $Q^h(p_1) = Q^h(p_2)$, i.e., one of the following holds:

1. p_1 and p_2 lie on the same hemisphere of $\mathcal{F}^h$, their K_2 coordinates are the same, and

their ψ_2 coordinates differ by some integer multiple of

$$\tilde{\psi}_2 = \omega_3 \frac{\pi}{\kappa_2} = \frac{2\pi}{\kappa_1}. \tag{3.4.14}$$

2. p_1 and p_2 lie on different hemispheres of $\mathcal{F}^h$, their K_2 coordinates are the same, and their ψ_2 coordinates differ by some integer multiple of

$$\bar{\psi}_2 = \omega_3 \frac{\pi}{2} = \pi \frac{\kappa_2}{\kappa_1}. \tag{3.4.15}$$

We would like to find out what happens to $\mathcal{F}^h$ and $\mathcal{W}^h/S^1$ under the effect of higher order normal form terms in (3.4.11). As the partially reduced problem is a two-degree-of-freedom Hamiltonian system wich has a 2-manifold of relative equilibria with a homoclinic structure, we expect that the energy-phase method of chapter 2 can be applied in this context. However, as it follows from ($\imath$) of Proposition 2.2.1, $\mathcal{F}^h$ is not normally hyperbolic. In order to apply the energy-phase method, we will consider two disjoint normally hyperbolic subsets of $\mathcal{F}^h$ which appear as two 2-manifolds of equilibria with heteroclinic connections in the system defined by (3.4.11) on $\mathcal{P}^h$. We will analyze this system, but first discuss an appropriate heteroclinic version of the energy-phase method in the next section. This will involve no new ideas compared to chapter 2 but the formulation of some of the results will be slightly different.

3.5 The energy-phase method for heteroclinic manifolds

As in chapter 2, we consider two-degree-of-freedom Hamiltonian systems of the form

$$\begin{aligned} \dot{x} &= J_2 D_x H_0(x, I) + \varepsilon J_2 D_x H_1(x, I, \phi; \varepsilon), \\ \dot{I} &= -\varepsilon D_\phi H_1(x, I, \phi; \varepsilon), \\ \dot{\phi} &= D_I H_0(x, I) + \varepsilon D_I H_1(x, I, \phi; \varepsilon), \end{aligned} \tag{3.5.1}$$

on the phase space $\tilde{\mathcal{P}} = \mathbb{R}^2 \times \mathbb{R} \times S^1$ equipped with the symplectic form $\omega = dx_1 \wedge dx_2 + d\phi \wedge dI$. The basic smoothness assumptions on this system are the same as for system (2.1.1) in chapter 2. This time, however, we make the assumptions

(A1) There exist $I_1, I_2 \in \mathbb{R}$, $I_1 < I_2$ such that for any $I \in [I_1, I_2]$ $(3.5.1)^x_{\varepsilon=0}$ has two hyperbolic fixed points, $\bar{x}^1(I)$ and $\bar{x}^2(I)$, connected by a cycle of heteroclinic trajectories, $x^{h1}(t, I)$ and $x^{h2}(t, I)$, with

$$\begin{aligned} \lim_{t \to -\infty} x^{h1}(t, I) &= \lim_{t \to +\infty} x^{h2}(t, I) = \bar{x}^1(I), \\ \lim_{t \to +\infty} x^{h1}(t, I) &= \lim_{t \to -\infty} x^{h2}(t, I) = \bar{x}^2(I). \end{aligned}$$

(A2) For every $I \in [I_1, I_2]$

$$D_I H_0(\bar{x}^j(I), I) = 0, \quad j = 1, 2. \tag{3.5.2}$$

It follows from assumption (A1) that system (3.5.1) possesses two, two dimensional invariant manifolds (with boundary) defined as

$$\mathcal{A}_0^j = \{(x, I, \phi) \in \mathcal{L} |\ x = \bar{x}^j(I), I \in [I_1, I_2], \phi \in S^1\}, \quad j = 1, 2\,. \tag{3.5.3}$$

These sets are the images of the annulus $A = [I_1, I_2] \times S^1$ under the embeddings

$$\begin{aligned} g_0^j \colon A &\to \mathcal{P}, \\ (I, \phi) &\mapsto (\bar{x}^j(I), I, \phi). \end{aligned} \tag{3.5.4}$$

Note that $\mathcal{A}_0^1$ has a three dimensional unstable manifold $W^u(\mathcal{A}_0^1)$ which coincides with the three dimensional stable manifold $W^s(\mathcal{A}_0^2)$ to form a heteroclinic manifold $\mathcal{W}_0^1$. Assumption (A1) also shows that there exists another similar heteroclinic manifold in the phase space, defined as $\mathcal{W}_0^2 = W^s(\mathcal{A}_0^1) \cap W^u(\mathcal{A}_0^2)$. As a consequence of assumption (A2),

the manifolds $\mathcal{A}_0^j$ are entirely filled with equilibria. Solutions of $(3.5.1)_{\varepsilon=0}$ falling in $\mathcal{W}_0^j$ are heteroclinic connections between these equilibria. Again, we define the *phase shifts*

$$\Delta\phi^j(I) = \int_{-\infty}^{+\infty} D_I H_0(x^{h,j}(t,I),I)\,dt, \quad j=1,2. \tag{3.5.5}$$

Since, for $j=1,2$, $\mathcal{A}_0^j$ is a compact normally hyperbolic invariant manifold, for small $\varepsilon > 0$ system (3.5.1) has a two dimensional invariant manifold $\mathcal{A}_\varepsilon^j$, which is C^r ε-close to $\mathcal{A}_0^j$, and is still a C^r embedding of the annulus A through the map

$$g_\varepsilon^j \colon A \to \tilde{\mathcal{P}},$$

$$(I,\phi) \mapsto (\bar{x}_\varepsilon^j(I,\phi),I,\phi) = (\bar{x}^j(I) + \varepsilon\tilde{x}^j(I,\phi;\varepsilon),I,\phi). \tag{3.5.6}$$

As we did in section 2.1, we let $i_\varepsilon^j \colon \mathcal{A}_\varepsilon^j \hookrightarrow \mathcal{P}$ be the inclusion map of $\mathcal{A}_\varepsilon^j$ with $\varepsilon \geq 0$ and note that for small $\varepsilon \geq 0$ and $j=1,2$ $(\mathcal{A}_\varepsilon^j, (i_\varepsilon^j)^*\omega)$ is a symplectic 2-manifold with

$$(i_\varepsilon^j)^*\omega = (1+\mathcal{O}(\varepsilon))d\phi \wedge dI,$$

on which the vector field (3.5.1) derives from the *restricted Hamiltonian*

$$\mathcal{H}_\varepsilon^j = H|\mathcal{A}_\varepsilon^j = (i_\varepsilon^j)^*H = h_0 + \varepsilon\mathcal{H}^j + \mathcal{O}(\varepsilon^2), \tag{3.5.7}$$

with

$$\begin{aligned} h_0 &= H_0|\mathcal{A}_0^j = const., \\ \mathcal{H}^j(I,\phi) &= H_1(\bar{x}^j(I),I,\phi;0). \end{aligned} \tag{3.5.8}$$

We again call $\mathcal{H}^j(I,\phi)$ the *reduced Hamiltonian* corresponding to the manifold $\mathcal{A}_0^j$, and consider it defined on the annulus A. We also adapt the definition of internal orbits from chapter 2.

In the following we will give conditions for the existence of *N-pulse heteroclinic orbits* connecting the two manifolds $\mathcal{A}_\varepsilon^1$ and $\mathcal{A}_\varepsilon^1$ to one another. An N-pulse heteroclinic orbit

is negatively asymptotic to, e.g., $\mathcal{A}_\varepsilon^1$, and it leaves a neighborhood of $\mathcal{A}_\varepsilon^1$ to enter a neighborhood of the slow manifold $\mathcal{A}_\varepsilon^2$, then passes back to a neighborhood of $\mathcal{A}_\varepsilon^1$, etc. Finally, after making $N-1$ $\mathcal{A}_\varepsilon^1-\mathcal{A}_\varepsilon^2-\mathcal{A}_\varepsilon^1$-type excursions, the orbit tends asymptotically to some invariant set in $\mathcal{A}_\varepsilon^2$. We will discuss the existence of such orbits under the simplifying assumption

(A3) For any $\varepsilon > 0$ $W^s(\mathcal{A}_\varepsilon^1) = W^u(\mathcal{A}_\varepsilon^2)$, i.e., $\mathcal{W}_0^2$ possibly deforms but does not break under the perturbation considered.

This symmetry assumption is not necessary for the general theory, but greatly simplifies the statement of the results. Moreover, it will be shown to hold for the perturbation problem outlined in the previous section.

The program of the *heteroclinic energy-phase method* described below is to predict the existence of multiple-pulse connections between the slow manifolds $\mathcal{A}_\varepsilon^1$ and $\mathcal{A}_\varepsilon^2$ using the *n-th order energy-difference function* $\Delta^n\mathcal{H}\colon A \to \mathbb{R}$ defined as

$$\Delta^n\mathcal{H}(I,\phi) = \mathcal{H}^2(I,\phi) - \mathcal{H}^1(I,\phi - n\Delta\phi^1(I) - (n-1)\Delta\phi^2(I))$$

$$= H_1(\bar{x}^2(I),I,\phi;0) - H_1(\bar{x}^1(I),I,\phi - n\Delta\phi^1(I) - (n-1)\Delta\phi^2(I);0). \qquad (3.5.9)$$

As in the homoclinic case, we will need to study the relation of the zero set of (3.5.9) to the orbits of the reduced Hamiltonian (3.5.8). To this end, we introduce the zero set V_+^n of $\Delta^n\mathcal{H}$:

$$V_+^n = \{\ (I,\phi) \in A \mid \Delta^n\mathcal{H}(I,\phi) = 0\ \}, \qquad (3.5.10)$$

and the transversal zero set

$$Z_+^n = \{\ (I,\phi) \in V_+^n \mid D\Delta^n\mathcal{H}(I,\phi) \neq (0,0)\ \}. \qquad (3.5.11)$$

We will also need the $-(n\Delta\phi^1(I)+(n-1)\Delta\phi^2(I))$ translate of these sets defined as

$$V_-^n = \mathcal{R}^{-n}(V_+^n), \qquad Z_-^n = \mathcal{R}^{-n}(Z_+^n). \tag{3.5.12}$$

Here $\mathcal{R}^k\colon A \to A$ denotes the k-th power of the "heteroclinic" rotation map which we define as the composition of "homoclinic" rotation maps (see (2.2.37)) as follows:

$$\mathcal{R}^k = \mathcal{R}_1^k \circ \mathcal{R}_2^{k-1}, \quad k \geq 1, \tag{3.5.13}$$

with

$$\begin{aligned} \mathcal{R}_j\colon A &\to A, \\ (I,\phi) &\mapsto (I, \phi + \Delta\phi^j(I)). \quad j = 1,2 \end{aligned} \tag{3.5.14}$$

It is again understood that $\mathcal{R}^0 \equiv \mathrm{Id}_A\colon (I,\phi) \mapsto (I,\phi)$. For any internal orbit $\gamma^1 \subset A$ of $\mathcal{H}^1$ the definition of the *pulse number* is again

$$N(\gamma^1) = \min\{\, n \geq 1 \mid V_-^k \cap \gamma^1 = \emptyset,\ k = 1,\ldots,n-1,\ Z_-^n \pitchfork \gamma^1 \,\}, \tag{3.5.15}$$

with $\pitchfork$ referring to nonempty transversal intersection. The definition of the *resonant pulse number*

$$N_R(\gamma^1) = \min\{\, n \geq 1 \mid V_-^k \cap \gamma^1 = \emptyset,\ k = 1,\ldots,n-1,\ \gamma^1 \subset V_-^n\} \tag{3.5.16}$$

also follows the definition given in (2.3.25). One can easily verify that if $N \equiv N(\gamma^1) < \infty$ then $\mathcal{R}^N(\gamma^1)$ intersects an orbit γ^2 of $\mathcal{H}^2$ transversally in the annulus A, such that the two orbits are "isoenergetic," i.e., $\mathcal{H}^1|\gamma^1 = \mathcal{H}^2|\gamma_2$. Moreover, $j = N$ is the minimal index for $\mathcal{R}^j$ such that such a transverse isoenergetic intersection occurs. Also note that $N_R \equiv N_R(\gamma^1) < \infty$ implies $N(\gamma^1) = \infty$. In that case $j = N_R(\gamma^1)$ is the minimum index for which $\mathcal{R}^j$ maps γ^1 *onto* an orbit γ^2 of $\mathcal{H}^2$ with the same energy. The heteroclinic version of the energy-phase method predicts intersections of stable and unstable manifolds of

internal orbits of the restricted Hamiltonians $\mathcal{H}^1_\varepsilon$ and $\mathcal{H}^1_\varepsilon$, based on the intersection of $\mathcal{R}^N(\gamma^1)$ or $\mathcal{R}^{N_R}(\gamma^1)$ with γ^2 or γ^1, respectively.

Theorem 3.5.1 *Let us assume that (A1)-(A3) hold. Suppose that for an internal orbit $\gamma^1_0 \subset A$ of the reduced Hamiltonian $\mathcal{H}^1$*

(A4) $N \equiv N(\gamma^1_0) < \infty$,

(A5) *Let $b_1 \in Z^N_- \cap \gamma^1_0$ and $b_2 = \mathcal{R}^N(b_1)$. Assume that the orbit $\gamma^2_0 \subset A$ of the reduced Hamiltonian $\mathcal{H}^2$ which contains b_2 is an internal orbit with $Z^N_+ \pitchfork \gamma^2_0$.*

(A6) *If $D_x H_0$ points outwards on the heteroclinic cycle $\mathcal{W}^1 \cup \mathcal{W}^2$ of manifolds, we assume that*

$$h^1_0 = \mathcal{H}^1|\gamma^1_0 < \mathcal{H}^2|\mathcal{R}^k(\gamma^1_0), \quad k = 1, ..., N-1.$$

If $D_x H_0$ points inwards on $\mathcal{W}^1 \cup \mathcal{W}^2$ we assume that

$$h^1_0 = \mathcal{H}^1|\gamma^1_0 > \mathcal{H}^2|\mathcal{R}^k(\gamma^1_0), \quad k = 1, ..., N-1.$$

Then there exists $\varepsilon_0 > 0$ such that for $0 < \varepsilon < \varepsilon_0$ the following are satisfied:

(i) There exists an N-pulse heteroclinic orbit y^N_ε which is negatively asymptotic to an internal orbit $\gamma^1_\varepsilon \in \mathcal{A}^1_\varepsilon$ and positively asymptotic to an internal orbit $\gamma^2_\varepsilon \in \mathcal{A}^2_\varepsilon$. Moreover, $(g^1_\varepsilon)^{-1}(\gamma^1_\varepsilon)$ and γ^1_0 are $C^{\rho-1}$ ε-close, and $(g^2_\varepsilon)^{-1}(\gamma^2_\varepsilon)$ and γ^2_0 are C^0 ε-close. If γ^2_0 is periodic, this latter statement can be strengthened to "$C^{\rho-1}$ ε-close."

(ii) y^N_ε lies in the intersection of $W^u(\gamma^1_\varepsilon)$ and $W^s(\gamma^2_\varepsilon)$ which is transversal within the energy surface $\{H = h\}$ with $h = H|\gamma^1_\varepsilon = H|\gamma^2_\varepsilon$.

(iii) Outside small neigborhoods of the manifolds $\mathcal{A}^1_\varepsilon$ and $\mathcal{A}^2_\varepsilon$ y^N_ε is C^1 $\sqrt{\varepsilon}$-close to a set

$$Y^N = \cup_{i=1}^{2N-1} y^i, \tag{3.5.17}$$

where y^i are heteroclinic orbits of $(3.5.1)_{\varepsilon=0}$ such that

$$y^i \subset \begin{cases} \mathcal{W}^1 & \text{if } i \text{ is odd,} \\ \mathcal{W}^2 & \text{if } i \text{ is even.} \end{cases} \tag{3.5.18}$$

Furthermore, if $\alpha(y^i)$ and $\omega(y^i)$ denote the α- and ω-limit points of the orbit y^i, then we have the following:

$$\begin{array}{ll} \alpha(y^{2k+1}) = g_\varepsilon^1(\mathcal{R}_1^k \circ \mathcal{R}_2^k(b_1)), & \omega(y^{2k+1}) = g_\varepsilon^2(\mathcal{R}_1^{k+1} \circ \mathcal{R}_2^k(b_1)), \\ \alpha(y^{2k}) = g_\varepsilon^2(\mathcal{R}_1^k \circ \mathcal{R}_2^{k-1}(b_1)), & \omega(y^{2k}) = g_\varepsilon^1(\mathcal{R}_1^k \circ \mathcal{R}_2^k(b_1)), \end{array} \tag{3.5.19}$$

with $\mathcal{R}_j^0 \equiv \mathrm{Id}$.

If, alternatively, we assume that

(A4') $N \equiv N_R(\gamma_0^1) < \infty$,

and $(A1) - (A3)$ and $(A6)$ still hold, then for small $\varepsilon > 0$ we have the following:

(i') *There exist two N-pulse heteroclinic orbits, y_ε^N and $\tilde{y}_\varepsilon^N$, which are asymptotic in negative time to an internal orbit $\gamma_\varepsilon^1 \in \mathcal{A}_\varepsilon^1$ and is positive time to an internal orbit $\gamma_\varepsilon^2 \in \mathcal{A}_\varepsilon^2$. The orbits γ_0^1 and $(g_\varepsilon^1)^{-1}(\gamma_\varepsilon^1)$ are $C^{\rho-1}$ ε-close in A, while the orbits $\gamma_0^2 = \mathcal{R}_N(\gamma_0^1)$ and $(g_\varepsilon^2)^{-1}(\gamma_\varepsilon^2)$ are C^0 ε-close in A. If γ_0^1 is periodic, this latter statement can be strengthened to "$C^{\rho-1}$ ε-close."*

(ii') *y_ε^N and $\tilde{y}_\varepsilon^N$ lie in the intersection of $W^u(\gamma_\varepsilon^1)$ and $W^s(\gamma_\varepsilon^2)$ within the energy surface $H = h$ with $h = H|\gamma_\varepsilon^1 = H|\gamma_\varepsilon^2$.*

(iii') *Statement (iii) above holds for y_ε^N and a similar statement holds for $\tilde{y}_\varepsilon^N$ with an appropriate basepoint $\tilde{b}_1 \in \gamma_0^1$.*

Proof: The proof is based on the same ideas as the proofs of Theorems 2.3.1-2.3.2, hence we will only sketch the main steps.

The results in Lemma 2.2.4 hold for both $\mathcal{A}_\varepsilon^1$ and $\mathcal{A}_\varepsilon^2$ individually. Hence, for fixed energy h one can define two sets of Poincaré sections, $\Sigma_\varepsilon^{s,j}(h)$ and $\Sigma_\varepsilon^{u,j}(h)$, with the global maps

$$\begin{aligned} G_\varepsilon^{h,1} &: R_\varepsilon^{u,1}(h) \to \Sigma_\varepsilon^{s,2}(h), \\ G_\varepsilon^{h,2} &: R_\varepsilon^{u,2}(h) \to \Sigma_\varepsilon^{s,1}(h), \end{aligned}$$

and local maps

$$\begin{aligned} L_\varepsilon^{h,1} &: R_\varepsilon^{s,1}(h) \to \Sigma_\varepsilon^{u,1}(h), \\ L_\varepsilon^{h,2} &: R_\varepsilon^{s,2}(h) \to \Sigma_\varepsilon^{u,2}(h), \end{aligned}$$

which are defined analogously to the corresponding maps in section 2.2. Similarly, one can introduce the conjugate global and local maps,

$$\mathcal{G}_\varepsilon^{h,j}, \mathcal{L}_\varepsilon^{h,j} : A \to A, \quad j = 1, 2$$

to follow the graph-projections of the intersections of $W^u(\gamma_\varepsilon^1)$ with the Poincaré sections mentioned above. Again, these maps are symplectic (Lemma 2.2.4) and for the choice $\alpha = \frac{1}{2}$ we have

$$\mathcal{G}_\varepsilon^{h,j} \overset{1,\sqrt{\varepsilon}}{\sim} \mathcal{R}_j, \qquad \mathcal{L}_\varepsilon^{h,j} \overset{1,\sqrt{\varepsilon}}{\sim} \mathrm{Id}_A, \quad j = 1, 2.$$

This time, we use the tracking map

$$\mathcal{T}_{\varepsilon,N}^h = \mathcal{G}_\varepsilon^{h,1} \circ \underbrace{(\mathcal{L}_\varepsilon^{h,1} \circ \mathcal{G}_\varepsilon^{h,2} \circ \mathcal{L}_\varepsilon^{h,2} \circ \mathcal{G}_\varepsilon^{h,1}) \circ \ldots \circ (\mathcal{L}_\varepsilon^{h,1} \circ \mathcal{G}_\varepsilon^{h,2} \circ \mathcal{L}_\varepsilon^{h,2} \circ \mathcal{G}_\varepsilon^{h,1})}_{N-1}, \tag{3.5.20}$$

to track the graph-projections of subsequent intersections of $W^u(\gamma_\varepsilon^1)$ with the manifold $\Sigma_\varepsilon^{s,2}(h)$. Given all these ingredients, the proof proceeds the same way as the proofs of Theorems 2.3.1-2.3.2. Assumption (A3) ensures that if condition (A6) holds, then after the trajectories in $W^u(\gamma_\varepsilon^1)$ make their local passage near $\mathcal{A}_\varepsilon^2$, they will be guided back to $\Sigma_\varepsilon^{s,1}(h)$ along the unbroken heteroclinic manifold $\mathcal{W}_\varepsilon^2$. □

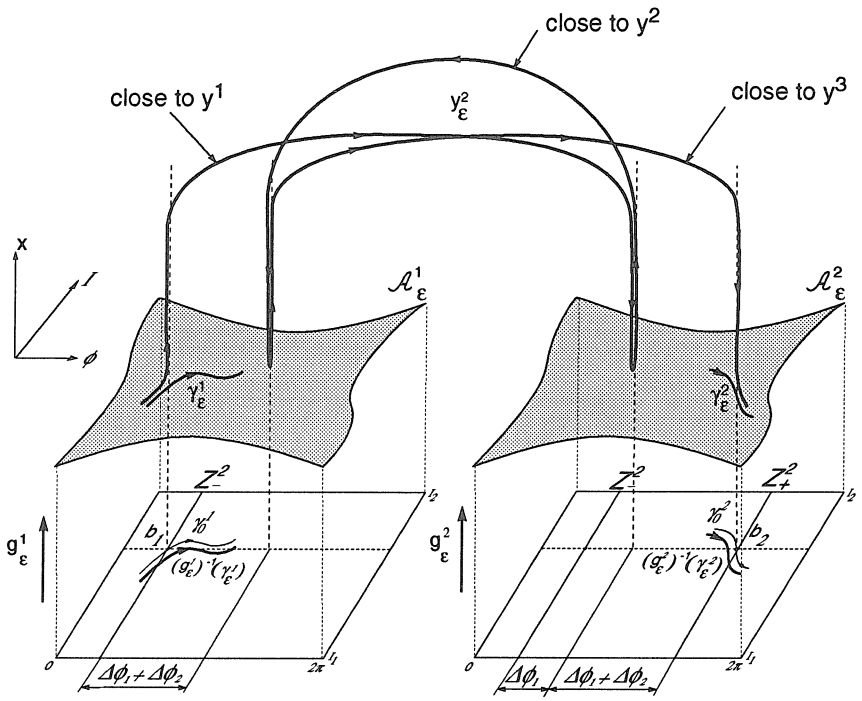

Figure 3.4: Double-pulse heteroclinic orbit between the manifolds $\mathcal{A}_\varepsilon^1$ and $\mathcal{A}_\varepsilon^2$.

In Fig. 3.4 we show statements $(i) - (iii)$ of Theorem 3.5.1 with $N = 2$. As far as the stability of individual heteroclinic connections is concerned, only the family of such connections is structurally stable (see Remark 2.3.5) under general perturbations.

In the next section we return to the normal form Hamiltonian (3.4.11) and show how the heteroclinic energy-phase method described above can be used to study its dynamics.

3.6 Whiskered tori and chaos in the normal form

In accordance with our discussion in section 3.4, we will first analyze the two-degree-of-freedom subsystem

$$\begin{aligned} \dot{x} &= J_2 D_x H_0(x, K_2) + \varepsilon J_2 D_x H_1(x, K_2, \psi_2; \varepsilon), \\ \dot{K}_2 &= -\varepsilon D_{\psi_2} H_1(x, K_2, \psi_2; \varepsilon), \\ \dot{\psi}_2 &= D_{K_2} H_0(x, K_2) + \varepsilon D_I H_1(x, I, \phi; \varepsilon), \end{aligned} \tag{3.6.1}$$

with

$$H_0(x, K_2) = a(K_1 - \omega_3 K_2 - |x|^2)x_2, \tag{3.6.2}$$

$$H_1(x, K_2, \psi_2; \varepsilon) = \tilde{H}_4(x, h, K_2, \psi_2) + \sum_{j=5}^{r} \varepsilon^{j-2} H_j(x, h, K_2, \psi_2), \tag{3.6.3}$$

which derives from (3.4.11) on $(\mathcal{P}^h, \omega_R)$ (see (3.4.12)-(3.4.13) and note that in (3.6.1) we rescaled the time by ε). As we noted in the proof of Proposition 3.4.1, the reduction with respect to the S^1 symmetry in the ψ_1 coordinate reduces $\mathcal{M}^h$ (which is diffeomorphic to $S^2 \times S^1$) to its orbit space $\mathcal{F}^h$ which is diffeomorphic to S^2. Thus system (3.6.1) possesses a two dimensional manifold of equilibria which is a 2-sphere and has a three dimensional homoclinic manifold $\mathcal{W}^h$ attached to it. We will consider two subsets of the southern and northern hemispheres of $\mathcal{F}^h$ which will play the same role as the manifolds of equilibria $\mathcal{A}_0^1$ and $\mathcal{A}_0^2$, respectively, of the previous section. This will enable us to apply the energy phase method and obtain information for $\varepsilon > 0$ small on the dynamics of the system defined by the normal form Hamiltonian (3.4.11).

Fixing some small but arbitrary $\lambda > 0$, one can easily verify that for $K_2 \in [\lambda, h/\omega_3 - \lambda]$ $(3.6.1)^x_{\varepsilon=0}$ has two hyperbolic equilibria

$$\bar{x}^1(K_2) = (-\sqrt{h - K_2\omega_3}, 0), \quad \bar{x}^2(K_2) = (+\sqrt{h - K_2\omega_3}, 0). \tag{3.6.4}$$

Moreover, these equilibria are connected by three heteroclinic trajectories, $x^{h1}(t; K_2)$,

$x^{h2+}(t;K_2)$, and $x^{h2-}(t;K_2)$ with

$$\lim_{t\to-\infty} x^{h1}(t,K_2) = \lim_{t\to+\infty} x^{h2+}(t,K_2) = \lim_{t\to+\infty} x^{h2-}(t,K_2) = \bar{x}^1(K_2),$$
$$\lim_{t\to+\infty} x^{h1}(t,K_2) = \lim_{t\to-\infty} x^{h2-}(t,K_2) = \lim_{t\to-\infty} x^{h2+}(t,K_2) = \bar{x}^2(K_2),$$
$$\{x^{h1}(t,K_2)\}_{t=-\infty}^{\infty} = \{\, x \,|\, |x_1| < \sqrt{h-K_2\omega_3},\ x_2 = 0 \,\},$$
$$\{x^{h2+}(t,K_2)\}_{t=-\infty}^{\infty} = \{\, x \,|\, x_2 > 0,\ x_1^2 + x_2^2 = h - K_2\omega_3 \,\},$$
$$\{x^{h2-}(t,K_2)\}_{t=-\infty}^{\infty} = \{\, x \,|\, x_2 < 0,\ x_1^2 + x_2^2 = h - K_2\omega_3 \,\}.$$

Hence $(3.6.1)_{\varepsilon=0}^{x}$, with its phase plane structure shown in the disk of Fig. 3.3, satisfies assumptions (A1)-(A2) (see also $(3.6.1)^{\psi}$ above) with two possible choices for the heteroclinic trajectory $x^h(I,\phi)$. Consequently, all the sets and quantities of section 3.4 can be defined for system (3.6.1) with the substitution $(I,\phi) \to (K_2,\psi_2)$, and $(\tilde{\mathcal{P}},\omega) \to (\mathcal{P}^h,\omega_R)$. In particular, introducing

$$A = [\lambda, h/\omega_3 - \lambda] \times S^1, \tag{3.6.5}$$

we have two normally hyperbolic 2-manifolds

$$\mathcal{A}_0^1 = \{\, (x,K_2,\psi_2) \in \mathcal{P}_h \,|\, x_1 = -\sqrt{h-\omega_3 K_2},\ x_2 = 0,\ (K_2,\psi_2) \in A \,\},$$
$$\mathcal{A}_0^2 = \{\, (x,K_2,\psi_2) \in \mathcal{P}_h \,|\, x_1 = +\sqrt{h-\omega_3 K_2},\ x_2 = 0,\ (K_2,\psi_2) \in A \,\},$$

connected through the heteroclinic manifolds

$$\mathcal{W}_0^1 = \{\, (x,K_2,\psi_2) \in \mathcal{P}^h \,|\, |x_1| < \sqrt{h-\omega_3 K_2},\ x_2 = 0,\ (K_2,\psi_2) \in A \,\},$$
$$\mathcal{W}_0^{2+} = \{\, (x,K_2,\psi_2) \in \mathcal{P}^h \,|\, x_1^2 + x^2 = h - \omega_3 K_2,\ x_2 > 0\, (K_2,\psi_2) \in A \,\},$$
$$\mathcal{W}_0^{2-} = \{\, (x,K_2,\psi_2) \in \mathcal{P}^h \,|\, x_1^2 + x^2 = h - \omega_3 K_2,\ x_2 < 0\, (K_2,\psi_2) \in A \,\}.$$

We show these invariant manifolds in Fig. 3.5. The phase shifts defined in (3.5.5) can

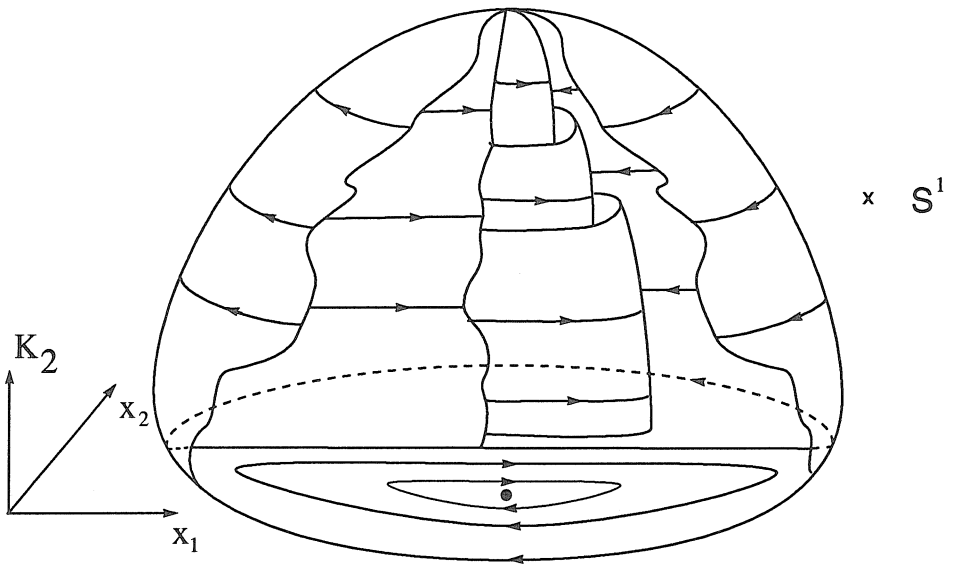

Figure 3.5: The invariant manifolds of system (3.6.1) for $\varepsilon = 0$.

be computed to equal

$$\Delta\psi_2^1(K_2) = 0, \quad \Delta\psi_2^{2\pm}(K_2) = \pm\tilde{\psi}_2 = \pm\omega_3\frac{\pi}{\kappa_2} = \pm\frac{2\pi}{\kappa_1}, \tag{3.6.6}$$

where the + sign is valid for the phase shift on $\mathcal{W}_0^{2+}$, and the − sign is valid on $\mathcal{W}_0^{2-}$. Then the rotation maps in (3.5.13)-(3.5.14) take the form

$$\mathcal{R}_1 = \mathrm{Id}_A, \qquad \mathcal{R}_2^{\pm}(K_2, \psi_2) = (K_2, \psi_2 \pm \frac{2\pi}{\kappa_1}), \qquad \mathcal{R}^k \equiv \mathcal{R}_2^{k-1}, \quad k \geq 1. \tag{3.6.7}$$

The *restricted Hamiltonians* $\mathcal{H}_\varepsilon^j$ defined in (3.5.7) take the form

$$\mathcal{H}_\varepsilon^j(K_2, \psi_2) = (H_0(x, K_2) + \varepsilon H_1(x, K_2, \psi_2; \varepsilon))|\mathcal{A}_\varepsilon^j = h_0 + \varepsilon\mathcal{H}^j(K_2, \psi_2) + \mathcal{O}(\varepsilon^2), \tag{3.6.8}$$

with the *reduced Hamiltonians* being specifically

$$\mathcal{H}^j(K_2, \psi_2) = \tilde{H}_4((-1)^j\sqrt{h - K_2\omega_3}, 0, h, K_2, \psi_2), \quad j = 1, 2. \tag{3.6.9}$$

Note that by our discussion after Proposition 3.4.1 (see (3.4.14)-(3.4.15)), for any $k \in \mathbb{Z}$ we have

$$\mathcal{H}^j(K_2, \psi_2 + k\tilde{\psi}_2) = \mathcal{H}^j(K_2, \psi_2), \quad j = 1, 2, \tag{3.6.10}$$

$$\mathcal{H}^1(K_2, \psi_2) = \mathcal{H}^2(K_2, \psi_2 + k\bar{\psi}_2), \tag{3.6.11}$$

To satisfy assumption (A3) of section 3.4 we require the following.

(A3') The resonant module M has no element of the form $(1, n_2, n_3)$ with $|n_2|+|n_3| = 3$.

An easy calculation shows that assumption (A3') implies the quartic truncation $H^* = H_0 + \varepsilon^2 \tilde{H}_4$ of (3.2.9) to have an invariant 3-sphere M_ε^h which lies in the transversal intersection of the energy surface $H^* = h$ and the subspace $z_1 = 0$. Applying the transformation $T_3^{-1} \circ T_2^{-1}$ to this set, one obtains two sets, $\mathcal{M}_\varepsilon^h$ and $\mathcal{D}_\varepsilon^h$, with the same properties as $\mathcal{M}^h$ and $\mathcal{D}^h$ in Proposition 3.4.1. But $\mathcal{W}^{2+} \cup \mathcal{W}^{2-} = \mathcal{D}^h/S^1$, implying that both $\mathcal{W}^{2+}$ and $\mathcal{W}^{2-}$ persist unbroken under the effect of terms deriving from $\tilde{H}_4 = H_1|_{\varepsilon=0}$, hence (A3) holds for system $(3.6.1)_{\varepsilon=0}$. Note that (A3') is always satisfied if κ_1 is odd.

To apply the energy-phase method we need to compute the heteroclinic energy-difference function as defined in (3.5.9). In the case of system (3.6.1), using (3.4.14)-(3.4.15), (3.6.10)-(3.6.11), and (3.6.6), we can write

$$\Delta^1\mathcal{H}(K_2, \psi_2) = \tilde{H}_4(\sqrt{h - K_2\omega_3}, 0, h, K_2, \psi_2) - \tilde{H}_4(\sqrt{h - K_2\omega_3}, 0, h, K_2, \psi_2 + \frac{\pi\kappa_2}{\kappa_1}), \tag{3.6.12}$$

$$\Delta^2\mathcal{H}(K_2, \psi_2) \equiv 0. \tag{3.6.13}$$

These equations and (3.5.10)-(3.5.12) immediately imply

$$V_+^1 = V_-^1, \quad Z_+^1 = Z_-^1, \quad V_+^2 = V_-^2 = A, \quad Z_+^2 = Z_-^2 = \emptyset. \tag{3.6.14}$$

Then (3.5.15), (3.5.16), and (3.6.14) show that for the pulse numbers N and N_R of any internal orbit $\gamma^1 \subset A$ of $\mathcal{H}^1$, the following hold:

Fact 1 $N(\gamma_1) = 1$ and $N_R(\gamma_1) = \infty$ if $\gamma^1 \pitchfork Z^1_-$,

Fact 2 $N(\gamma_1) = \infty$ and $N_R(\gamma_1) = 2$ if $\gamma^1 \cap Z^1_- = \emptyset$.

Based on the results of section 3.4, this shows that if $Z^1_- = Z^1_+ \neq \emptyset$, then almost all internal orbits in $\mathcal{A}^1_\varepsilon$ and $\mathcal{A}^2_\varepsilon$ will participate either in transverse single-pulse heteroclinic connections or (not necessarily transverse) double-pulse connections.

We are now ready to apply Theorem 3.5.1 to (3.6.1). We will, however, state the results immediately in terms of the full normal form Hamiltonian (3.4.11) defined on $(\mathcal{P}, \omega)$. This can be done using the fact that for $\varepsilon > 0$ any invariant set $\mathcal{S}$ in the phase space $(\mathcal{P}^h, \omega_R)$ indicates the existence of an invariant set $\mathcal{S}^*$ in the $K_1 = h$ hypersurface of the phase space $(\mathcal{P}, \omega)$, such that $\mathcal{S}^*$ is diffeomorphic to $\mathcal{S}^* \times S^1$. Note that for small fixed $\varepsilon > 0$, the normally hyperbolic manifolds $\mathcal{A}^j_\varepsilon \subset \mathcal{P}^h$ of (3.6.1) give rise to normally hyperbolic invariant 4-manifolds $\mathcal{B}^j_\varepsilon \subset \mathcal{P}$ of the full normal form (3.4.11), which are given by the two $C^{\rho-1}$ smooth embeddings

$$\begin{aligned} G^j_\varepsilon : \mathbb{R}^+ \times S^1 \times A &\to \mathcal{P}, \\ (K_1, \psi_1, K_2, \psi_2) &\mapsto (K_1, \psi_1, g^j_\varepsilon(K_2, \psi_2)), \quad j = 1, 2. \end{aligned} \tag{3.6.15}$$

Although it is not hyperbolic, $\mathcal{B}^j_0$ still exists as a smooth limit of manifolds, with the corresponding embedding $G^j_0 : \mathbb{R}^+ \times S^1 \times A \to \mathcal{P}$, $j = 1, 2$. To facilitate the statement of the results, we introduce the set

$$E_\varepsilon(h_1, h_2) = \{ (x, K_1, \psi_1, K_2, \psi_2) \in \mathcal{P} \,|\, K_1 = h_1,\ H(x, K, \psi; \varepsilon) = h_2 \}. \tag{3.6.16}$$

We then have the following theorem as an immediate application of Theorem 3.5.1 to system (3.6.1) with the results interpreted for the full normal form (3.4.11).

Theorem 3.6.1 *Suppose that assumption (A3') is satisfied and for some* $\bar{h} \in \mathbb{R}^+$

(α) $Z_+^1 = Z_-^1 \neq \emptyset$, *where* $Z_+^1 = Z_-^1$ *is the transverse zero set of* $\Delta^1\mathcal{H}$ *defined in (3.6.12).*

(β) γ^1 *and* γ^2 *are internal orbits of the reduced Hamiltonians* $\mathcal{H}^1$ *and* $\mathcal{H}^2$ *(see (3.6.9)), respectively, and both intersect* Z_+^1 *transversally at* $p = (\bar{K}_2, \bar{\psi}_2) \in A$.

Then there exists $\varepsilon_0 > 0$ *and an open set* $U \subset \mathbb{R}^+$ *with* $\bar{h} \in U$ *such that for* $0 < \varepsilon < \varepsilon_0$ *and* $K_1 = h \in U$ *the following are satisfied:*

($\imath$) *Let* $I_\varepsilon^j : \mathcal{B}_\varepsilon^j \to \mathcal{P}$ *be the inclusion map of* $\mathcal{B}_\varepsilon^j$. *Then* $(\mathcal{B}_\varepsilon^j, (I_\varepsilon^j)^*\omega)$ *is a symplectic 4-manifold for* $j = 1, 2$, *on which the (integrable) dynamics is generated by the restricted Hamiltonian* $\mathcal{H}_\varepsilon^j$ *defined in (3.6.8).*

($\imath\imath$) *The Hamiltonian (3.4.11) has two two dimensional invariant manifolds,* $\mathcal{T}_\varepsilon^1$ *and* $\mathcal{T}_\varepsilon^2$. *If* γ^j *is periodic then* $\mathcal{T}_\varepsilon^j$ *is* $C^{\rho-1}$ *diffeomorphic to* $\mathbb{T}^2$, *and is* $C^{\rho-1}$ ε*-close to the set* $G_0^j(\{h\} \times S^1 \times \gamma^j)$. *If* γ^j *is not periodic, one has to replace "*$C^{\rho-1}$ *diffeomorphic" with "homeomorphic" and "*$C^{\rho-1}$ ε*-close" with "*C^0 ε*-close" in the above statement.*

($\imath\imath\imath$) $\mathcal{T}_\varepsilon^1$ *has a three dimensional unstable manifold* $W^u(\mathcal{T}_\varepsilon^1)$, *and* $\mathcal{T}_\varepsilon^2$ *has a three dimensional stable manifold* $W^s(\mathcal{T}_\varepsilon^2)$. $W^u(\mathcal{T}_\varepsilon^1)$ *and* $W^s(\mathcal{T}_\varepsilon^2)$ *are injective immersions of* $\mathbb{R}^+ \times S^1 \times \gamma^1$ *and* $\mathbb{R}^+ \times S^1 \times \gamma^2$, *respectively. Furthermore, they intersect transversally within* $E(h, H|\mathcal{T}_\varepsilon^1)$ *in a two dimensional heteroclinic manifold* Y_ε.

Suppose that assumption (α) *above holds together with*

(β') *γ^1 and γ^2 are internal orbits of the reduced Hamiltonians $\mathcal{H}^1$ and $\mathcal{H}^2$ respectively, with $\mathcal{R}^2(\gamma^1) = \gamma^2$ for some choice of the sign in (3.6.6).*

Then statements ($\imath$) – ($\imath\imath$) still hold. In contrast to ($\imath\imath\imath$), however, there exist two double-pulse heteroclinic manifolds, Y_ε^1 and Y_ε^2 lying in the (not necessarily transversal) intersection of $W^u(\mathcal{T}_\varepsilon^1)$ and $W^s(\mathcal{T}_\varepsilon^1)$.

Proof: The theorem is an immediate application of Theorem 3.5.1. We only note that assumption (A6) of Theorem 3.5.1 is always satisfied for one of the two possible choices for the sign in (3.6.6), i.e., for one of the two possible definitions of the rotation map $\mathcal{R}$ in (3.6.7). □

In most cases the internal orbits γ^1 and γ^2 in assumption (α) of Theorem 3.6.1 are members of families of periodic orbits in A. It may also happen that they map to the same set of points in the orbit space $\mathcal{F}^h$ under the map $T_2 \circ T_3$ (see, e.g., the next section for the case of the 1:2:2 resonance). Thus transverse heteroclinic connections between their perturbed counterparts actually yield transverse homoclinic connections in system (3.2.9). For this case, using Theorem 3.6.1, the Smale-Birkhoff homoclinic theorem (Smale [66]), and a theorem of Moser [59], we obtain a result similar to Theorem 2.3.2.

Corollary 3.6.2 *Let us suppose that the assumptions (α) – (β) of Theorem 3.5.1 hold and γ^1 and γ^2 are periodic orbits with $\mathcal{R}^2(\gamma_1) = \gamma_2$. Then for $\varepsilon > 0$ small enough*

($\imath$) *$\mathcal{T}_\varepsilon^1$ and $\mathcal{T}_\varepsilon^2$ are members of two-parameter families of whiskered 2-tori. The whiskers $W^u(\mathcal{T}_\varepsilon^1)$ and $W^s(\mathcal{T}_\varepsilon^2)$ intersect transversally within $E_\varepsilon(h, H|\mathcal{T}_\varepsilon^1)$.*

($\imath\imath$) *System (3.2.9) does not possess any nontrivial analytic integral other than H and K_1.*

(*ii*) *On energy surfaces* $\mathcal{O}(\varepsilon)$ *close to the surface* $H = \bar{h} \in U$, *an appropriately defined Poincaré-map of system (3.2.9) has invariant Cantor-sets on which it is homeomorphic to a full shift on* N *symbols.*

3.7 An example: the 1:2:2 resonance with detuning

In this final section we show an example to illustrate the results of chapter 3. Our goal is to convince the reader that using our methods one can quickly and easily uncover the geometry of a given problem and gain insight into the diverse structure of chaotic sets in the corresponding Hamiltonian normal form. We will also visualize the objects we find through the numerical simulation of a related four dimensional symplectic map.

3.7.1 The geometry of the normal form

We consider a Hamiltonian system of the form (3.2.1) and assume that the frequency vector in (3.2.3) is $\Omega = (1, 2, 2)$. As we noted earlier this system satisfies assumption $(H1)$ of section 3.2, but it does not satisfy $(H2)$ unless we assume a weak $\mathbf{Z_2}$ symmetry at cubic order in the original coordinates (q_3, p_3). By weak symmetry we mean that the terms breaking this symmetry are less in order of magnitude than those obeying the symmetry (see $(H2)(ii)$ of section 3.2). As we pointed out, however, in the case of the 1:2:2 resonance, one can apply an additional linear canonical change of coordinates to put the Hamiltonian to the form (3.2.9) *without assuming the weak* $\mathbf{Z_2}$ *symmetry mentioned above.* For simplicity, we suppose that the fourth order normalized terms contained in $\tilde{H}_4$ of (3.2.9) vanish, and we employ a weak detuning of the form

$$\hat{H}(z, \bar{z}; \delta) = \delta_1 |z_2|^2 + \delta_2 |z_3|^2, \quad \delta_1, \delta_2 \in \mathbb{R}, \tag{3.7.1}$$

as $\mathcal{O}(\varepsilon^2)$ perturbation (see Van der Aa and Verhulst [70]). Physically, we are interested in what happens to a system of three weakly nonlinear coupled oscillators in 1:2:2 resonance if we slightly change this frequency ratio.

Under the above assumptions, performing the change to complex coordinates as in section 3.2, we arrive at the normalized Hamiltonian

$$H = H_2 + \varepsilon H_3 + \varepsilon^2 \tilde{H}_4 + \varepsilon^3 H_5 + \ldots + \varepsilon^{r-2} H_r,$$

$$H_2 = \frac{1}{2}|z_1|^2 + |z_2|^2 + |z_3|^2, \qquad H_3 = \mathrm{Re}\,(a_1 z_1^2 \bar{z}_2 + a_2 z_1^2 \bar{z}_3), \quad a_1, a_2 \in \mathbb{R}^+,$$

$$\tilde{H}_4 = H_d = \delta_1 |z_2|^2 + \delta_2 |z_3|^2, \quad \delta_1, \delta_2 \in \mathbb{R}. \tag{3.7.2}$$

As in (3.2.9), one usually has to change the phase of the complex variables to make the constants a_1 and a_2 positive real. Following Kummer [50] (see also Cushman [13]) we now introduce a symplectic change of variables $z' = T_4 z$ with

$$T_4^{-1} = \frac{1}{\sqrt{a_1^2 + a_2^2}} \begin{pmatrix} \sqrt{a_1^2 + a_2^2} & 0 & 0 \\ 0 & a_1 & -a_2 \\ 0 & a_2 & a_1 \end{pmatrix}. \tag{3.7.3}$$

Dropping the primes and using (3.7.3), we can rewrite the Hamiltonan (3.7.2) as

$$H = H_2 + \varepsilon H_3 + \varepsilon^2 \tilde{H}_4 + \varepsilon^3 H_5 + \ldots + \varepsilon^{r-2} H_r,$$

$$H_2 = \frac{1}{2}|z_1|^2 + |z_2|^2 + |z_3|^2, \qquad H_3 = \sqrt{a_1^2 + a_2^2}\,\mathrm{Re}\,(z_1^2 \bar{z}_2),$$

$$\tilde{H}_4 = H_d = \frac{1}{a_1^2 + a_2^2}(\delta_1 |a_1 z_2 - a_2 z_3|^2 + \delta_2 |a_2 z_2 + a_1 z_3|^2), \tag{3.7.4}$$

which, as we announced, is of the form (3.2.9) for $a = 2\sqrt{a_1^2 + a_2^2}$. We now apply the transformations listed in (3.4.1)-(3.4.2) to obtain the form (3.6.2)-(3.6.3) for our Hamiltonian with the concrete perturbation term

$$\begin{aligned} \tilde{H}_4(x, K, \psi_2; \delta) &= \frac{1}{a_1^2 + a_2^2}[(a_1^2 \delta_1 + a_2^2 \delta_2)|x|^2 + 2(\delta_1 a_2^2 + \delta_2 a_1^2) K_2 \\ &+ 2a_1 a_2 (\delta_2 - \delta_1)\sqrt{2K_2}(x_1 \sin \psi_2 + x_2 \cos \psi_2)]. \end{aligned} \tag{3.7.5}$$

Everything we have discussed regarding the geometry of system (3.3.1) immediately holds for the Hamiltonian

$$H_0 = \frac{1}{2}|z_1|^2 + |z_2|^2 + |z_3|^2 + \varepsilon\sqrt{a_1^2 + a_2^2}\,\mathrm{Re}\,(z_1^2\bar{z}_2). \tag{3.7.6}$$

In particular, the Hamiltonian system generated by (3.7.6) has invariant 3-spheres on every level set $H_0 = h$ (see Proposition 3.3.1) with corresponding four dimensional homoclinic manifolds. The only thing to point out is that, as a consequence of the transformation (3.7.3), the normal modes N_2^h and N_3^h of (3.7.6) typically do not agree with the normal modes $\tilde{N}_2^h$ and $\tilde{N}_3^h$ of the original Hamiltonian (3.7.4) truncated at cubic order. Using (3.4.1)-(3.4.2),(3.7.3), and the notation of Proposition 3.4.1, we find that for $j = 1, 2$ $\tilde{\mathcal{N}}_2^h \equiv (Q^h)^{-1} \circ \pi_F(\tilde{N}_2^h)$ has a copy in $\mathcal{A}_0^j$ given by

$$\begin{aligned} x_1 &= (-1)^j a_1\sqrt{h}/\sqrt{a_1^2 + a_2^2}, \quad & K_2 &= a_2^2 h/(a_1^2 + a_2^2), \\ x_2 &= 0, & \psi_2 &= (\mathrm{sign}\, x_1)\pi/2, \end{aligned} \tag{3.7.7}$$

and $\tilde{\mathcal{N}}_3^h \equiv (Q^h)^{-1} \circ \pi_F(\tilde{N}_3^h)$ has a copy in $\mathcal{A}_0^j$ given by

$$\begin{aligned} x_1 &= (-1)^j a_2\sqrt{h}/\sqrt{a_1^2 + a_2^2}, \quad & K_2 &= a_1^2 h/(a_1^2 + a_2^2), \\ x_2 &= 0, & \psi_2 &= -(\mathrm{sign}\, x_1)\pi/2. \end{aligned} \tag{3.7.8}$$

Using (3.4.7), (3.4.8), and (3.7.7)-(3.7.8) above, we see that for $a_1 = 0$ we have $\tilde{\mathcal{N}}_2^h = \mathcal{N}_3^h$, $\tilde{\mathcal{N}}_3^h = \mathcal{N}_2^h$, and for $a_2 = 0$ we have $\tilde{\mathcal{N}}_2^h = \mathcal{N}_2^h$, $\tilde{\mathcal{N}}_3^h = \mathcal{N}_3^h$. For general values of a_1 and a_2, however, the normal modes of $H_2 + \varepsilon H_3$ in (3.7.2) are different from the normal modes of (3.7.4). In particular, we can choose $\lambda > 0$ small enough in (3.6.5) such that each of $\tilde{\mathcal{N}}_2^h$ and $\tilde{\mathcal{N}}_3^h$ has one copy in each of the manifolds $\mathcal{A}_0^1$ and $\mathcal{A}_0^2$, respectively.

Since (3.3.12) yields $\kappa_1 = \kappa_2 = 1$ for the 1:2:2 resonance, (*ii*) of Proposition 3.4.1 tells us that each of $\tilde{\mathcal{N}}_2^h$ and $\tilde{\mathcal{N}}_3^h$ has *exactly one* copy in each manifold $\mathcal{A}_0^j$ (Q^h is a diffeomorphism). We also see from (*ii*) of Proposition 3.4.1 that the orbit space $\mathcal{F}^h$ is diffeomorphic to S^2. Finally, one can infer from (3.4.14)-(3.4.15) and (3.7.7)-(3.7.8) that

for $a_1 \neq a_2$, $\tilde{N}_2^h$ and $\tilde{N}_3^h$ form heteroclinic cycles with two other periodic solutions in M_0^h through their stable and unstable manifolds. In the exceptional case of $a_1 = a_2$, they form heteroclinic cycles with each other.

3.7.2 Chaos in the 1:2:2 resonance

We now turn to the application of our results in section 3.6. For this, we first compute the reduced Hamiltonians defined in (3.6.9). Based on (3.7.5), an easy calculation gives

$$\mathcal{H}^j(K_2, \psi_2; h, \delta) = \frac{2(\delta_1 - \delta_2)}{a_1^2 + a_2^2}[(a_2^2 - a_1^2)K_2 + (-1)^j a_1 a_2 \sqrt{2K_2(h - 2K_2)} \sin \psi_2], \quad j = 1, 2, \tag{3.7.9}$$

where we have dropped the constant terms. One can now directly verify the relations (3.6.10)-(3.6.11) for our example with $\tilde{\psi}_2 = 2\pi$ and $\bar{\psi}_2 = \pi$ (see also (3.4.14)-(3.4.15)).

We feel that one of the advantages of the methods we used so far is the simplicity of the calculations and the arising quantities. For instance, it is quite simple to analyze the reduced Hamiltonians given in (3.7.9) and sketch their phase portrait, as we have done this in Fig. 3.6 for fixed parameters $a_1 \neq a_2$, $h \neq 0$, and $\delta_1 \neq \delta_2$. As it follows from (3.6.11), we can obtain the phase portrait of $\mathcal{H}^2$ simply by rotating this figure by $\bar{\psi}_2 = \pi$. The reduced Hamiltonians are not smooth at the center and on the perimeter of the circle $K_2 = h$. The smoothness problem at the center of the circle, which corresponds to the periodic orbit $\mathcal{N}_2^h$, comes from the usage of the polar coordinates (K_2, ψ_2) and of purely technical nature. The lack of smoothness on the boundary is a consequence of the degeneracy of the periodic solution N_3^h, which caused the unperturbed 3-sphere M^h to be nonhyperbolic. We also remark that, as one can verify from (3.7.7)-(3.7.9), the two elliptic equilibria of Fig. 3.6 are just the relative equilibria $\tilde{\mathcal{N}}_2^h$ and $\tilde{\mathcal{N}}_3^h$ which correspond to the "real"normal modes $\tilde{N}_2^h$ and $\tilde{N}_3^h$, respectively.

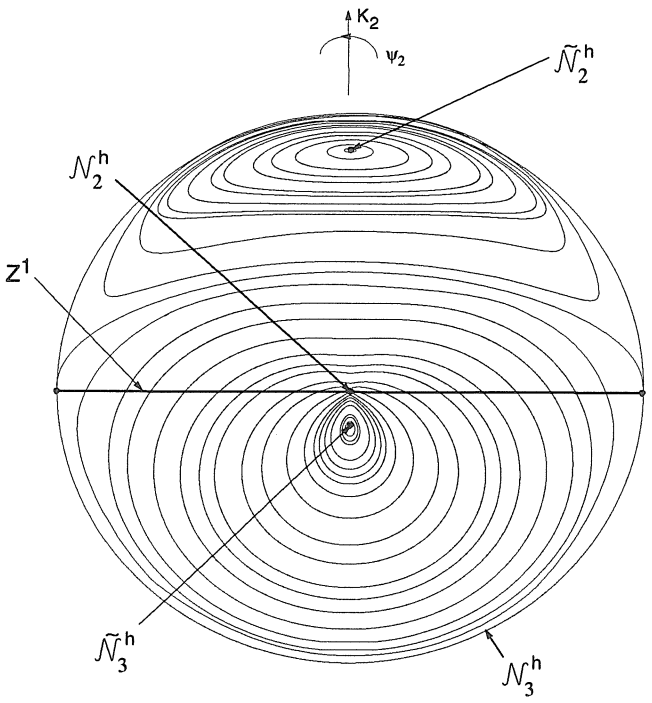

Figure 3.6: The phase portrait of the reduced Hamiltonian $\mathcal{H}^1$ for $a_1 = 3$, $a_2 = 4$, $\delta_1 = 1$ and $\delta_2 = 2$.

To be consistent with section 3.6, we fix a small $\lambda > 0$ and consider the reduced Hamiltonians of (3.7.9) defined on the annulus A defined in (3.6.5). According to our definition given in section 2.2, all orbits in Fig. 3.6 not intersecting the boundaries of A are internal orbits for $\mathcal{H}^j$.

Since elliptic equilibria of one-degree-of-freedom Hamiltonian systems are structurally stable, and the reduced dynamics is a first order approximation of the Hamiltonian dynamics within $\mathcal{A}_\varepsilon^j$, we conclude that the two "real" normal modes of (3.7.4) survive the perturbation caused by the detuning and become elliptic within $\mathcal{B}_\varepsilon^j$ for $h, \varepsilon > 0$ (see (3.6.15)). Also, applying (ii) of Theorem 3.6.1, we obtain that they are surrounded by one-parameter families of 2-tori $\mathcal{T}_\varepsilon^j \in E(h, H|\mathcal{T}_\varepsilon^j)$, which appear as periodic solutions

surrounding the equilibria in Fig. 3.6. This family of tori within $\mathcal{B}_\varepsilon^j$ are bounded by a two dimensional cylindrical homoclinic manifold connecting the relevant copy of the surviving periodic solution N_2^h to itself. Outside this surface, we have another one parameter family of 2-tori in $\mathcal{B}_0^j$ which shrink to the degenerate periodic orbit N_3^h (see Fig. 3.6).

We now explore the geometry associated with the stable and unstable manifolds (guaranteed by Theorem 3.6.1) of internal orbits. Using (3.6.12)-(3.6.13) and (3.7.9), the first and second order energy-difference functions take the form

$$\begin{aligned} \Delta^1\mathcal{H}(K_2,\psi_2;h,\delta) &= \frac{4(\delta_1-\delta_2)a_1a_2}{a_1^2+a_2^2}\sqrt{2K_2(h-2K_2)}\sin\psi_2, \\ \Delta^2\mathcal{H}(K_2,\psi_2;h,\delta) &\equiv 0, \end{aligned} \tag{3.7.10}$$

with the corresponding zero set (see (3.6.14))

$$\begin{aligned} Z^1 &\equiv Z_+^1 = Z_-^1 = V_+^1 = V_-^1 = \{(K_2,\psi_2)\in A | \psi_2 = 0,\pi\}, \quad \delta_1 \neq \delta_2, \\ Z_+^2 &= Z_-^2 = \emptyset, \\ V_+^2 &= V_-^2 = A, \end{aligned} \tag{3.7.11}$$

which are sketched in Fig. 3.6. We see that internal orbits from the outer family of periodic orbits intersect transversally. Any such periodic orbit γ^1 has an identical counterpart γ^2 in the phase portrait of $\mathcal{H}^2$ with

$$\mathcal{R}(\gamma^1) = \mathcal{R}_2(\gamma^1) = \gamma^2. \tag{3.7.12}$$

Furthermore, both γ_0^1 and γ_0^2 intersect Z^1 transversally at the same points in A. Hence, according to Theorem 3.6.1, for fixed $K_1 = h$ we have a *one parameter family of whiskered 2-tori in $\mathcal{B}_\varepsilon^1$ and another such family in $\mathcal{B}_\varepsilon^2$. The stable and unstable manifolds of the members of these families intersect transversally in two dimensional sets Y_ε and Y_ε'*

described in (iii) of Theorem 3.6.1. Using (3.7.12) together with Corollary 3.6.2 we obtain that *in the normal form (3.7.2) there exists a one parameter family of homoclinic whiskered 2-tori with associated Smale-horseshoes, making system (3.7.2) nonintegrable.*

We now fix some $h > 0$ and denote the Poincaré-map of system (3.7.4) for the cross section $K_1 = h, \psi_1 = 0$ by P_ε^h. The invariant manifolds of this map coincide with those of system (3.6.1) with H_1 given in (3.7.5). In Fig. 3.7 we indicate how the intersection of whiskered tori of the full normal form appears in terms of the invariant manifolds of the Poincare-map P_ε^h. From the figure one can readily understand why the zero set Z^1

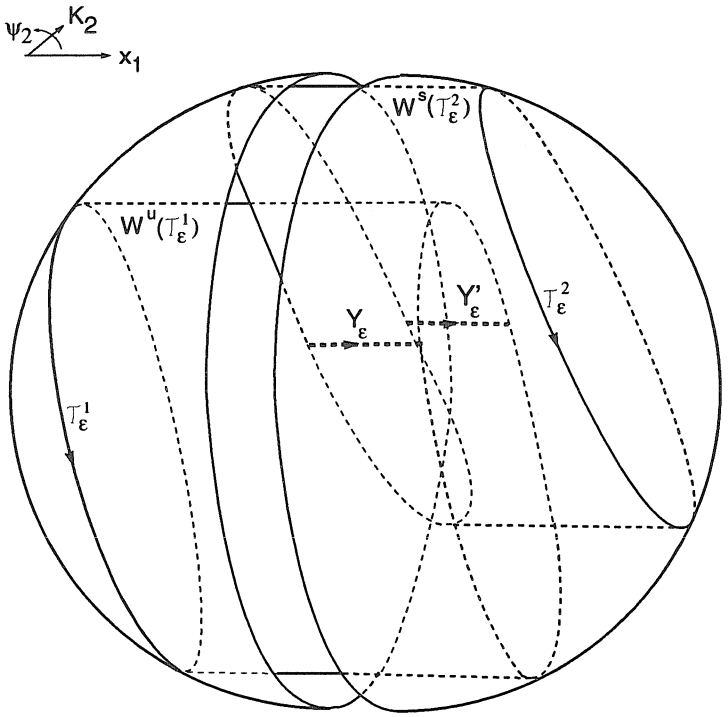

Figure 3.7: Transverse homoclinic orbits for the map P_ε^h

defined in (3.7.11) consists of two disjoint $\psi_2 = const.$ lines. To confirm this, we also present a typical result of the simulation of the map P_ε^h in Fig. 3.8 (based on the iteration of the continuous system (3.6.1)). In Fig. 3.9 we let the manifolds evolve further in time.

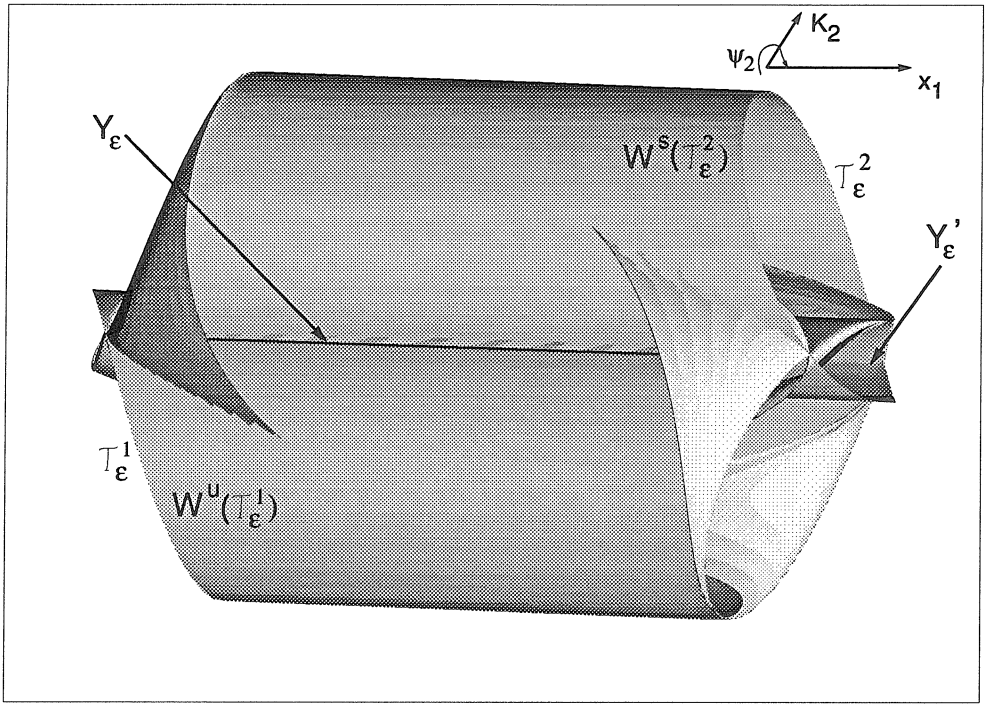

Figure 3.8: Projection of invariant manifolds of the map P_ε^h to the space (x_1, K_2, ψ_2) ($a_1 = 3$, $a_2 = 4$, $\delta_1 = 1$, $\delta_2 = 2$, $\varepsilon = 0.1$. Energy of $\gamma_\varepsilon^1 = 0.082$, energy conservation=$10^{-12}$, number of iterations=6500, stepsize=.001)

Here, of course, the apparent self-intersection of the manifolds is a consequence of the fact that the trajectories intersect the domain on which the projection to the (K_2, ψ_2, x_1) subspace of $\mathcal{P}$ fails to be injective.

Studying further, we notice that the family of internal periodic orbits surrounding the centers do not intersect Z^1 ($\delta_1 \neq \delta_2$). By (3.7.12) above, assumption (β') of Theorem 3.6.1 is satisfied for these orbits; hence we obtain that outside some neighborhood of the "real" normal modes, $\tilde{N}_2^h$ and $\tilde{N}_3^h$, *system (3.7.2) has a one-parameter family (h is fixed) of 2-tori which have two dimensional double-pulse homoclinic manifolds,* Y_ε^1 *and* Y_ε^2, described in Theorem 3.6.1. We did not attempt to draw the full geometry

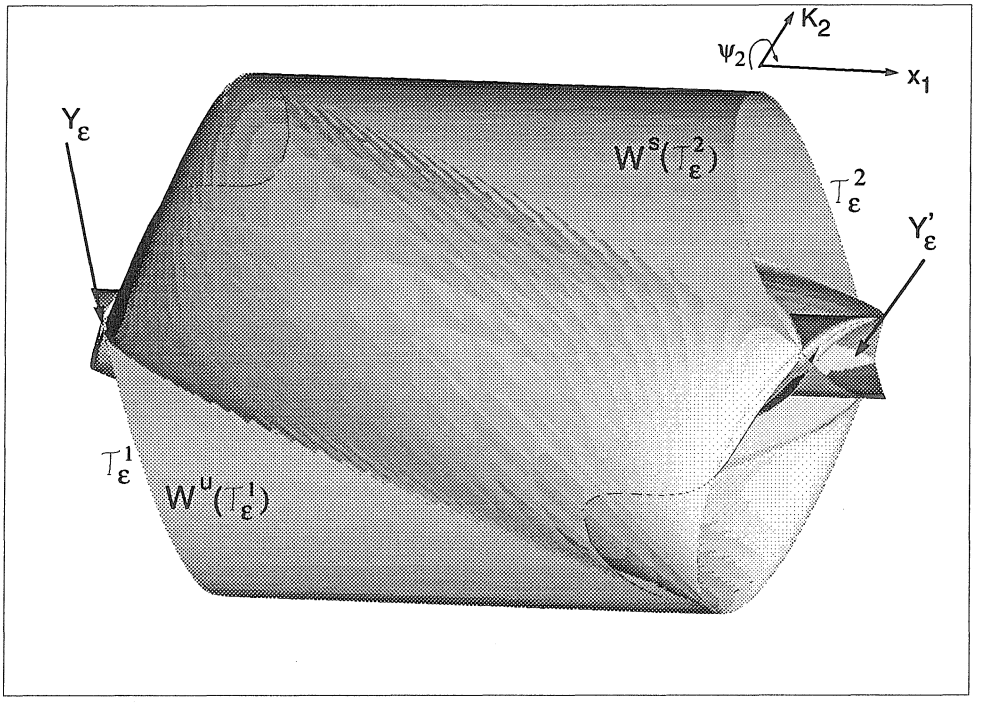

Figure 3.9: Same as Fig. 3.8 with energy conservation=10^{-9} and number of iterations=7500

corresponding to this family, but picked one such torus of the iterated Poincare-map in Fig. 3.10. As one can see, the double-pulse manifolds are apparently results of transversal intersections, which suggests the presence of Smale-horseshoes in their neighborhoods. This illustrates how the missing claim of transversality in Theorem 3.6.1 can be made based on the results of simulation of controlled precision.

To summarize, we have seen that in the case of asymmetric detuning ($\delta_1 \neq \delta_2$), system (3.7.2) exhibits a rather rich dynamical behavior in the neighborhood of the 3-sphere M^h for any $h > 0$. If we start solutions close to the "real" normal modes $\tilde{N}_2^h$ and $\tilde{N}_3^h$, we will experience the effect of the 2-tori with double-pulse homoclinic manifolds. Moving further energetically from the normal modes, we become under the influence of

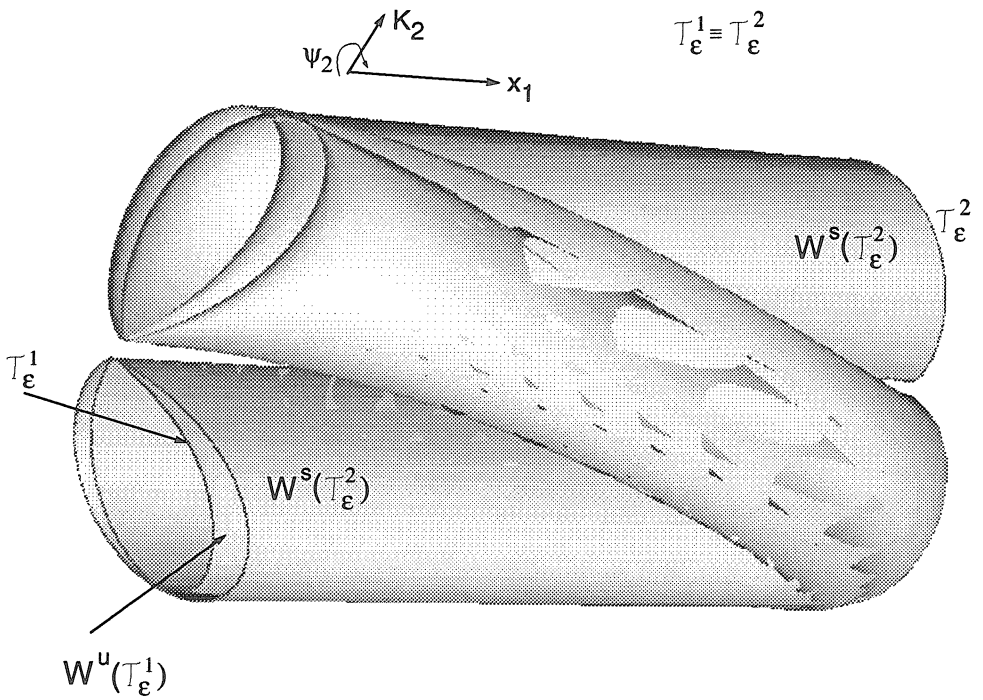

Figure 3.10: The creation of double-pulse homoclinic orbits for the map P_ε^h ($a_1 = 3$, $a_2 = 4$, $\delta_1 = 1$, $\delta_2 = 2$, $\varepsilon = 0.1$. Energy of γ_ε^1=0.139, energy conservation=10^{-9}, stepsize=0.001, number of iterations=7900)

the whiskered 2-tori with simple homoclinic orbits. This gives us information about how the domain of irregular motions of the resonant normal form is structured into regimes with different types of chaos. Passing the homoclinic manifold of N_2^h, which separates these two regimes, we experience a change in the topology of horseshoes, and related to this, an intensification of chaos.

3.8 On the persistence of invariant manifolds under the effect of the "tail" of the normal form

In this chapter we used the energy-phase method to study the dynamics in a wide class of three-degree-of-freedom resonant normal forms. We now make some comments on the

relation of these results to the dynamics of the full unnormalized Hamiltonian system (3.2.1).

Based on the results showing hyperbolic manifolds of 2-tori for the normalized system, one might be tempted to say that since "hyperbolic sets persist under perturbation," all the complex geometry described above is present in the full system (3.2.1). Though we are convinced that the second part of this statement is close to being true, we point out the weakness of the argument given in the first part. The problem is that the "tail" of the normal form (i.e., terms of order bigger than five) embodies a *perturbation of fixed order* on the hyperbolic structures, which themselves are *weakly hyperbolic* only. This means that if the tail is of order $O(\varepsilon^3)$ for small ε, then the contraction and expansion rates near the hyperbolic manifolds of tori we found are of order $O(\varepsilon^2)$. If we want to consider "small" perturbations, we obviously have to decrease ε, but this also decreases the strength of hyperbolicity of the manifolds we would like to see to persist. Therefore, the usual persistence results for normally hyperbolic invariant manifolds of Hirsch *et al.* [29] or Fenichel [23] do not apply immediately. Related problems arise in local bifurcation theory or in the method of averaging when one is interested in the preservation of weakly hyperbolic periodic solutions or tori. The case of periodic solutions can be solved by the application of the implicit function theorem to the fixed point of an appropriate Poincaré-map (see, e.g., Iooss [36], Guckenheimer and Holmes [27], etc.) and one can also gain control over the persisting (weak) stable and unstable manifolds. There are also results available for weakly hyperbolic tori (see Iooss [36], Sacker [62] with an application in Scheurle and Marsden [64], and Kirchgraber [41]). Unfortunately, the tori we construct are not normally hyperbolic, because they lie in families of whiskered tori, thus only the family itself, i.e., the manifold of tori, is hyperbolic. There seems to be little known about general weakly hyperbolic invariant manifolds, although the methods of de la Llave

and Wayne [52] applied to a small "patch" on the manifold of tori should go through to prove the persistence of some of our double-pulse homoclinic tori. We also have to mention the approach of Delshams [15] pointing in this direction, which appeals to a global linearization result of Hirsch *et al.* [29] and, if applied to our family of tori, gives a continuous persistence result with no extra effort. However, we prefer to avoid using this argument because we would loose even differentiability for the surviving objects, and would have no control over transversality of the whiskers anymore. Although it will not be detailed in this thesis, one can solve the problem of persistence using an idea of Kopell [43] giving uniform upper estimates for the Liapunov type numbers of Fenichel [23] which are used in persistence theorems of (strongly) hyperbolic invariant manifolds. Therefore, *the whiskered tori we constructed for the normal form are indeed present in the original system.*

One more question we would like to address briefly is that of the *Arnold-diffusion* (Arnold [4], Arnold *et al.* [5]) in the class of resonant Hamiltonians we considered. Since the whiskered tori we construct on the level surfaces $H_2 = const.$ are energetically isolated from each other, we cannot conclude the existence of transition chains created by the transversal intersection of whiskers of different tori. In the full system this energetical isolation of the surviving whiskered tori does not exist anymore (H_2 is not a first integral anymore), and the whiskers of tori originally lying on different level surfaces of H_2 do intersect generically. However, these secondary intersections (not captured by the normal form) are results of *exponentially small splittings* of asymptotic surfaces. This is not surprising since the drift created through the tangles of these secondary intersections have to obey Nekhorosev's general estimates (Nekhorosev [61], Arnold *et al.* [5]) as worked out in Lochak [53] for perturbations of resonant linear oscillators (see also Benettin and Gallavotti [6] for the case of nonresonant oscillators). But this also means that

establishing the existence of Arnold-diffusion in the full system (3.2.1) requires special methods. Related results exist for rapidly forced one-degree-of freedom systems (Holmes *et al.* [33], Delshams *et al.* [16]) which can be applied to normal forms of two-degree-of-freedom Hamiltonians (Holmes *et al.* [33]). We also mention the paper of Churchill and Rod [11] which proves the existence of homoclinic and heteroclinic orbits in rapidly forced symmetric systems without control over the transversality of these orbits. Besides the fact that these techniques are really worked out only for the case of the rapidly forced pendulum (except for Churchill and Rod [11]), in their present form they do not apply to three degrees of freedom. Hence, the other issue which needs to be worked on, if one wishes to use the results of this paper towards Arnold-diffusion, is that of the treatment of small splittings for multi-degree-of-freedom systems. Some results pointing in this direction were announced recently in Chiercia and Gallavotti [9] for a class of Hamiltonian systems with symmetry consisting of rotators and pendula. See also Lochak [53] for a generalization of the classic example of Arnold [4].

Chapter 4

Multiple-pulse homoclinic orbits in the truncated driven nonlinear Schrödinger equation

In this final chapter we demonstrate another application of the energy-phase method to a two-degree-of-freedom Hamiltonian system arising from a two-mode truncation of the driven nonlinear Schrödinger equation. This problem yields a circle of equilibria which enables us to apply the results of section 2.4 for multiple-pulse phenomena near resonance bands. Using the full power of our method, we will establish the existence of jumping multiple-pulse orbits with arbitrarily high pulse numbers. We will construct a layer-sequence, each layer containing internal orbits of the perturbed system with the same pulse number. As it will turn out, these layers form a fractal structure. This high-pulse homoclinic fractal structure manifests itself as stochastic "jumping" in the phase space in the truncated system, a feature numerically observed in the full PDE.

4.1 Derivation and basic properties of the two-mode truncation

The example we will study originates from the perturbed sine-Gordon equation

$$u_{tt} - u_{xx} + \sin u = \varepsilon(-\hat{\alpha} + \hat{\Lambda} u_{txx} + \hat{\Gamma} \sin \omega t), \tag{4.1.1}$$

with boundary conditions

$$u(x = -\frac{1}{2}L, t) = u(x = \frac{1}{2}L, t), \qquad u(x, t) = u(-x, t). \tag{4.1.2}$$

In eq. (4.1.1) we let $0 < \varepsilon\hat{\alpha} << 1$, $0 < \varepsilon|\hat{\Lambda}| << 1$, $\omega = 1 - \varepsilon\tilde{\omega}$. The constants L and $\tilde{\omega}$, and the perturbation parameter ε are all positive. System (4.1.1) has been the subject of a series of papers started by the study of Bishop *et al.* [7]-[8]. For small amplitudes and frequencies close to 1, one can seek a solution of (4.1.1) in the form

$$u_\varepsilon(x, t) = 2\sqrt{\varepsilon\tilde{\omega}}[B(X, T)e^{i\omega t} + \bar{B}(X, T)e^{-i\omega t}] + \mathcal{O}(\varepsilon), \tag{4.1.3}$$

with $X = \sqrt{2\varepsilon\tilde{\omega}}x$ and $T = \varepsilon\tilde{\omega}t$. Substituting (4.1.3) in (4.1.1) one arrives at the perturbed nonlinear Schrödinger equation

$$-iB_T + B_{XX} + (|B|^2 - 1)B = \varepsilon(i\alpha B - i\Lambda B_{XX} + i\bar{\Gamma}), \tag{4.1.4}$$

with $\hat{\alpha} = 2\varepsilon\tilde{\omega}\alpha$, $\hat{\Lambda} = \Lambda$, and $\hat{\Gamma} = 8\varepsilon^{\frac{3}{2}}\hat{\omega}^{\frac{3}{2}}\bar{\Gamma}$, $X \in [-\frac{1}{2}L_X, \frac{1}{2}L_X]$, and $L_X = \sqrt{2\varepsilon\tilde{\omega}}L$. Based on numerical experiments, Bishop *et al.* found that much of the apparent chaotic behavior of system (4.1.1) is already captured by a two-Fourier-mode truncation of (4.1.4). Inspired by this, they assumed a solution of (4.1.4) of the form

$$B(X, T) = \frac{1}{\sqrt{2}}c(T) + b(T)\cos kX, \qquad k = \frac{2\pi}{L_X},$$

which, after one substitutes it into eq. (4.1.4) and neglects the higher order Fourier-modes, yields the equations

$$-i\dot{c} + (\frac{1}{2}|c|^2 + \frac{1}{2}|b|^2 - 1)c + \frac{1}{2}(c\bar{b} + b\bar{c})b = i\varepsilon\alpha c + i\varepsilon\Gamma,$$

$$-i\dot{b} + (\frac{1}{2}|c|^2 + \frac{3}{4}|b|^2 - (1+k^2))c + \frac{1}{2}(c\bar{b} + b\bar{c})c = i\varepsilon\beta b, \qquad (4.1.5)$$

with $\Gamma = \sqrt{2}\bar{\Gamma}$ and $\beta = \alpha + \Lambda k^2$. This two-mode model carries an essential feature of the underlying PDE: it is integrable for $\varepsilon = 0$. The integrability of (4.1.5) for $\varepsilon = 0$ is best revealed by the coordinate transformation

$$c = Ie^{-i\phi}, \qquad b = (x_1 + ix_2)e^{-i\phi},$$

(used in Kovačič and Wiggins [44]) which puts eqs. (4.1.5) in the form

$$\begin{aligned}
\dot{x}_1 &= -k^2 x_2 - \frac{3}{4}x_1^2 x_2 + \frac{1}{4}x_2^3 - \varepsilon\left[\Gamma\frac{x_2}{\sqrt{2I - x_1^2 - x_2^2}}\sin\phi + \beta x_1\right], \\
\dot{x}_2 &= (k^2 - 2I)x_1 + \frac{7}{4}x_1^3 + \frac{3}{4}x_1 x_2^2 + \varepsilon\left[\Gamma\frac{x_1}{\sqrt{2I - x_1^2 - x_2^2}}\sin\phi - \beta x_2\right], \\
\dot{I} &= -\varepsilon\left[\Gamma\sqrt{2I - x_1^2 - x_2^2}\cos\phi + (\beta - \alpha)(x_1^2 + x_2^2) + 2\alpha I\right], \\
\dot{\phi} &= I - 1 + x_1^2 - \varepsilon\Gamma\frac{1}{\sqrt{2I - x_1^2 - x_2^2}}\sin\phi.
\end{aligned} \qquad (4.1.6)$$

Kovačič and Wiggins [44] studied system (4.1.6) under the assumption $\alpha \neq \beta$ which means unequal damping for different modes ($\Lambda \neq 0$ in (4.1.4)). Using singular perturbation theory and a special Melnikov-type method, they showed that for $\varepsilon > 0$ sufficiently small and

$$\frac{\alpha}{\Gamma} < 0.13, \qquad \frac{\beta}{\Gamma} \approx -7.92\sqrt{1 - 2\frac{\alpha^2}{\Gamma}} - 1.14\frac{\alpha}{\Gamma}, \qquad (4.1.7)$$

system (4.1.6) has a Silnikov-type orbit homoclinic to a fixed point (with corresponding horseshoes) in a *resonance band* (see below). However, their methods indicated no such behavior for the case $\alpha = \beta$ studied by Bishop *et al.* In [28] we took a different viewpoint and considered the Hamiltonian limit $\alpha = \beta = 0$ (no damping). The reason for that was the expectation that the dynamics of the limiting problem is more accessible to geometric methods. Although some of the delicate Hamiltonian structures are destroyed

by dissipative perturbation, for small ε one will still recover motions following their Hamiltonian limits for long times. Also, this way one can give up the restriction $\alpha \neq \beta$ and replace it by the assumption that α and β are sufficiently small, i.e., the damping is small compared to the forcing in eq. (4.1.4).

Following this program, we found various orbits homoclinic to periodic solutions which are *created by the perturbation* near the resonance band mentioned above. These orbits exist generically and, in contrast to (4.1.7), their existence is not confined to a measure zero set of the parameter space. (In other words, one does not need to embed the system in a one parameter family to obtain such orbits.) Moreover, one obtains a two dimensional manifold of transverse homoclinic orbits which has more influence on the near-resonance dynamics of system (4.1.6) than a single homoclinic orbit. The shortcoming of our analyis was that we could not describe the dynamics on all energy levels close to the resonance: our methods did not show homoclinic behavior for a certain set of periodic orbits. This set becomes large for certain ranges of the parameters (see below); hence its effect can not be neglected. In the following we describe what happens near this set to obtain a full picture of the chaotic dynamics of (4.1.6).

4.2 The analysis of the Hamiltonian limit of the truncated problem

First note that for $\alpha = \beta = 0$ system (4.1.6) is of the form (2.1.1) with the parameter $\mu = (k, \Gamma) \in (0, \sqrt{2}) \times \mathbb{R}$ and with the Hamiltonians

$$H_0 = \frac{1}{2}I^2 - I - \frac{7}{16}x_1^4 - \frac{3}{8}x_1^2x_2^2 + \frac{1}{16}x_2^4 + (I - \frac{1}{2}k^2)x_1^2 - \frac{1}{2}k^2x_2^2, \tag{4.2.1}$$

and

$$H_1 = \Gamma\sqrt{2I - x_1^2 - x_2^2}\,\sin\phi. \tag{4.2.2}$$

One can also check that $(4.1.6)^{x}_{\varepsilon=0}$ has a hyperbolic fixed point at $(x_1, x_2) = (0, 0)$ for all $I > \frac{k^2}{2}$, which is connected to itself by a pair of homoclinic orbits with $D_x H_0$ pointing inwards on them. Consequently, system $(4.1.6)_{\varepsilon=0}$ satisfies our hypothesis $(H1')$ in chapter 2 (as well as $(H1)$) and possesses two symmetric three dimensional homoclinic manifolds, W_0^+ and W_0^-' of the type as those of Fig. 2.9 (see [44]). As one can verify from $(4.1.6)_{\varepsilon=0}$, the normally hyperbolic two-manifold

$$\mathcal{A}_0 = \{(x, I, \phi) \in \mathcal{P} | x = \bar{x}^0(I; \mu) = 0,\ I \in [I_1, I_2], \phi \in\ S^1\ \}, \tag{4.2.3}$$

with

$$\frac{k^2}{2} < I_1 < 1 < I_2$$

contains an isolated circle of equilibria satisfying $I = 1$; hence our hypothesis (H2a) in chapter 2 holds for system (4.1.6) with $I_r = 1$. Note that as a result of the discrete symmetry $(x, I, \phi) \to (-x, I, \phi)$, $\mathcal{A}_\varepsilon$ and $\mathcal{A}_0$ are, in fact, identical. This implies that

$$\begin{aligned} g_\varepsilon \equiv g_0 \colon A &\to \mathcal{P}, \\ (I, \phi) &\mapsto (0, I, \phi). \end{aligned} \tag{4.2.4}$$

Furthermore, both homoclinic manifolds W_0^+ and W_0^- admit the same constant phase shift

$$\Delta\phi(k) = \begin{cases} 2\cot^{-1}\left(\frac{k}{\sqrt{2-k^2}}\right) + \frac{2}{\sqrt{7}}\tanh^{-1}\left(\sqrt{\frac{7k^2}{2-k^2}}\right) - \pi, & \text{if } 0 < k < \frac{1}{2}, \\ 2\tan^{-1}\left(\frac{\sqrt{2-k^2}}{k}\right) + \frac{2}{\sqrt{7}}\tanh^{-1}\left(\sqrt{\frac{2-k^2}{7k^2}}\right), & \text{if } \frac{1}{2} < k < \sqrt{2}, \end{cases} \tag{4.2.5}$$

which is plotted in Fig. 4.1 as a function of the parameter k. Consequently, system (4.1.6) also satisfies our hypothesis (H3') is section 2.4, and we expect Theorems 2.4.1-2.4.4 to be applicable.

Using eq. (2.4.6), we obtain from (4.2.1)-(4.2.3) the reduced Hamiltonian

$$\hat{\mathcal{H}}(\eta, \phi; \mu) = \frac{1}{2}\eta^2 + \sqrt{2}\Gamma \sin\phi, \tag{4.2.6}$$

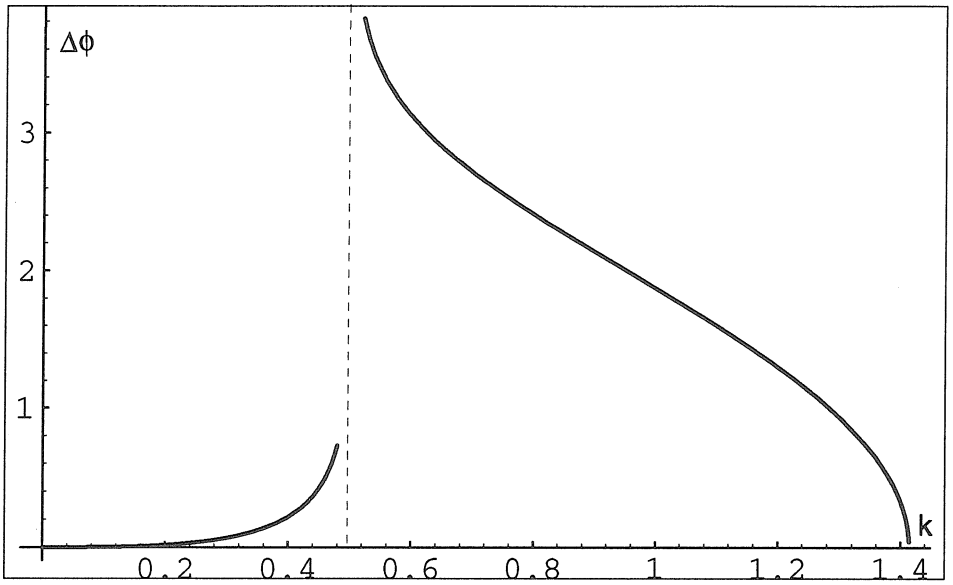

Figure 4.1: The phase shift $\Delta\phi$ for system $(4.1.6)_{\varepsilon=0}$ as a function of the parameter k

which is defined on $(\hat{A}, \hat{\omega})$ with some

$$\eta_0 > 2\sqrt{\sqrt{2}\Gamma}. \tag{4.2.7}$$

Fig. 4.2 shows the level curves of $\hat{\mathcal{H}}$ and explains our choice of η_0 in (4.2.7) to include all the internal orbits associated with the presence of the resonance at $\eta = 0$ $(I = 1)$. Note that the phase portrait of the reduced Hamiltonian is just that of the ordinary pendulum shifted by $-\pi/2$ in ϕ.

From its definition (2.4.7) coupled with (4.2.6), one immediately obtains the n-th order energy-difference function

$$\Delta^n \hat{\mathcal{H}}(\phi; \mu) = \sqrt{2}\Gamma[\ \sin\phi - \sin(\phi - n\Delta\phi(k))\ ], \tag{4.2.8}$$

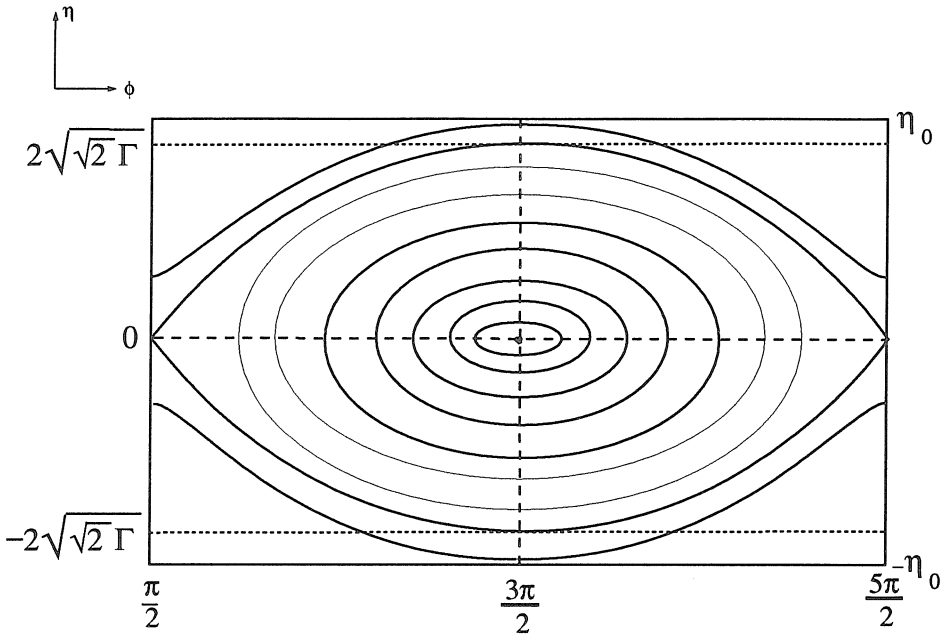

Figure 4.2: The phase portrait of the reduced Hamiltonian $\hat{\mathcal{H}}$

which has the following zero set (see (2.3.2))

$$\hat{V}_+^n = \begin{cases} \hat{A} & \text{if } n\Delta\phi = 2l\pi, \quad (l \in \mathbb{Z}), \\ \{\,(\eta,\phi) \in \hat{A} | \phi \in \{\phi_{n,1}, \phi_{n,2}\}\} & \text{otherwise} \end{cases} \tag{4.2.9}$$

with

$$\phi_{n,1} = \frac{\pi}{2} + n\frac{\Delta\phi}{2}, \qquad \phi_{n,2} = \frac{3\pi}{2} + n\frac{\Delta\phi}{2}. \tag{4.2.10}$$

This shows that $\hat{V}_+^n$ typically has two connected components, $\hat{V}_{+,1}^n$ and $\hat{V}_{+,2}^n$, which are lines with $\phi = \phi_{n,1}$ and $\phi = \phi_{n,2}$, respectively. One also finds that these lines represent transverse zero sets, thus we have (see (2.4.9))

$$\hat{Z}_+^n = \begin{cases} \emptyset & \text{if } n\Delta\phi = 2l\pi, \quad (l \in \mathbb{Z}), \\ \hat{V}_+^n & \text{otherwise.} \end{cases} \tag{4.2.11}$$

From (2.4.10) we also obtain the other two zero sets

$$\hat{V}_-^n = \begin{cases} \hat{A} & \text{if } n\Delta\phi = 2l\pi, \quad (l \in \mathbb{Z}), \\ V_{-,1}^n \cup V_{-,2}^n = \{ (\eta,\phi) \in \hat{A} | \phi \in \{\phi_{n,1} - n\Delta\phi, \phi_{n,2} - n\Delta\phi\}\} & \text{otherwise,} \end{cases} \tag{4.2.12}$$

$$\hat{Z}_-^n = \begin{cases} \emptyset & \text{if } n\Delta\phi = 2l\pi, \quad (l \in \mathbb{Z}), \\ \hat{V}_-^n & \text{otherwise.} \end{cases} \tag{4.2.13}$$

For $n\Delta\phi \neq 2l\pi$ we introduce the components $Z_{+,i}^n = V_{+,i}^n$, $Z_{+,i}^n = V_{+,i}^n$ $(i = 1,2)$. For later reference, let us define the set

$$S_0 = \{(\eta,\phi) \in \hat{A} | -\sqrt{2}\Gamma \leq \hat{\mathcal{H}}(I,\phi;\mu) \leq \sqrt{2}\Gamma, \quad \frac{\pi}{2} \leq \phi \leq \frac{5\pi}{2}\},$$

which is just one copy of the closed region bounded by the separatrices connecting the hyperbolic fixed points of $\hat{\mathcal{H}}$ (see Fig 4.2). We now make some observations based on what we have found so far.

Fact 1. It is easy to see that $\hat{Z}_{+,i}^n$ and $\hat{Z}_{-,i}^n$ can be obtained from each other by a reflection with respect to the line $\phi = 3\pi/2$. Since the orbits of $\hat{\mathcal{H}}$ are also symmetric to $\phi = 3\pi/2$, we find that any internal orbit $\hat{\gamma}_0$ intersecting $\hat{Z}_{-,i}^n$ transversally in a point b_- will also intersect $\hat{Z}_{+,i}^n$ transversally in $b_+ = \hat{\mathcal{R}}^n(b_-)$. Hence, *if we detect an N-pulse orbit homoclinic to the manifold $\mathcal{A}_\varepsilon$, by Theorem 2.4.2, it will also be homoclinic to some set within $\mathcal{A}_\varepsilon$ ($\hat{\gamma}_0^- = \hat{\gamma}_0^+$ implies $\gamma_\varepsilon^- = \gamma_\varepsilon^+$).*

Fact 2. For an internal periodic orbit $\hat{\gamma}_0 \subset S_0$ with $\hat{\mathcal{H}}|\gamma_0 = h_0$, let us suppose that for some fixed $j \geq 1$

$$\hat{\mathcal{R}}^j(\hat{\gamma}_0) \cap \gamma_0 = \emptyset. \tag{4.2.14}$$

Since $\hat{\mathcal{R}}^j(\hat{\gamma}_0)$ and $\hat{\gamma}_0$ have the same area, this is only possible if $\hat{\gamma}_0 \subset S_0 - \text{Int}\,(\gamma_0)$. Now the energy $\hat{\mathcal{H}}$ of the internal orbits increases monotonically from the center to the separatrices, hence (4.2.14) implies

$$\hat{\mathcal{H}}|\hat{\mathcal{R}}^j(\hat{\gamma}_0) > h_0.$$

But this implies that if $\hat{\gamma}_0 = \gamma_0^-$ satisfies assumptions (A1)-(A2) of Theorem 2.4.4, then the sequence defined in assumption (A3) will take the form

$$\hat{\chi}_{j+1} = (-1)^j \hat{\chi}_j. \tag{4.2.15}$$

Consequently, *if we detect an N-pulse orbit homoclinic to the manifold $\mathcal{A}_\varepsilon$, it will be a jumping orbit which makes one pulse near one of the unperturbed homoclinic manifolds and then switches to the other one.*

Fact 3. For $\Delta\phi \neq 2l\pi$ define the set

$$\begin{aligned} A_n(\mu) \;=\; & \{(\eta,\phi) \in S_0 | \min(\hat{\mathcal{H}}(0,\phi_{n,1};\mu), \hat{\mathcal{H}}(0,\phi_{n,2};\mu)) \leq \hat{\mathcal{H}}(\eta,\phi;\mu) \\ & < \max(\hat{\mathcal{H}}(0,\phi_{n,1};\mu), \hat{\mathcal{H}}(0,\phi_{n,2};\mu))\}. \end{aligned} \tag{4.2.16}$$

Despite its formidable definition A_n has a very simple meaning: it is a layer of internal orbits intersecting only that component of $\hat{Z}_+^n$ (and $\hat{Z}_-^n$) which is closer to $\phi = \frac{3\pi}{2}$ (see Fig. 4.3). Similarly,

$$B_n(\mu) = \{(\eta,\phi) \in S_0 | \max(\hat{\mathcal{H}}(0,\phi_{n,1};\mu), \hat{\mathcal{H}}(0,\phi_{n,2};\mu)) \leq \hat{\mathcal{H}}(\eta,\phi;\mu)\}, \tag{4.2.17}$$

contains the internal orbits which intersect both components of $\hat{Z}_+^n$. Note that A_n is bounded from inside by a periodic resonant internal orbit $\hat{\gamma}_n^R$ with $\hat{N}_R(\hat{\gamma}_n^R,\mu) = n$. From outside, it is bounded by a periodic internal orbit $\hat{\gamma}_n$ which is tangent to, but does not coincide with $\hat{\mathcal{R}}^n(\hat{\gamma}_n)$. $\hat{\gamma}_n$ is also the boundary of B_n from inside. Suppose now that

$$A_j \cap A_n = B_j \cap A_n = \emptyset, \qquad j = 1,...,n-1 \tag{4.2.18}$$

holds. Since any internal orbit in A_n intersects Z_-^n (and Z_+^n) transversally in two points, by Theorems 2.4.2 and 2.4.4, *any such orbit gives rise to a periodic internal*

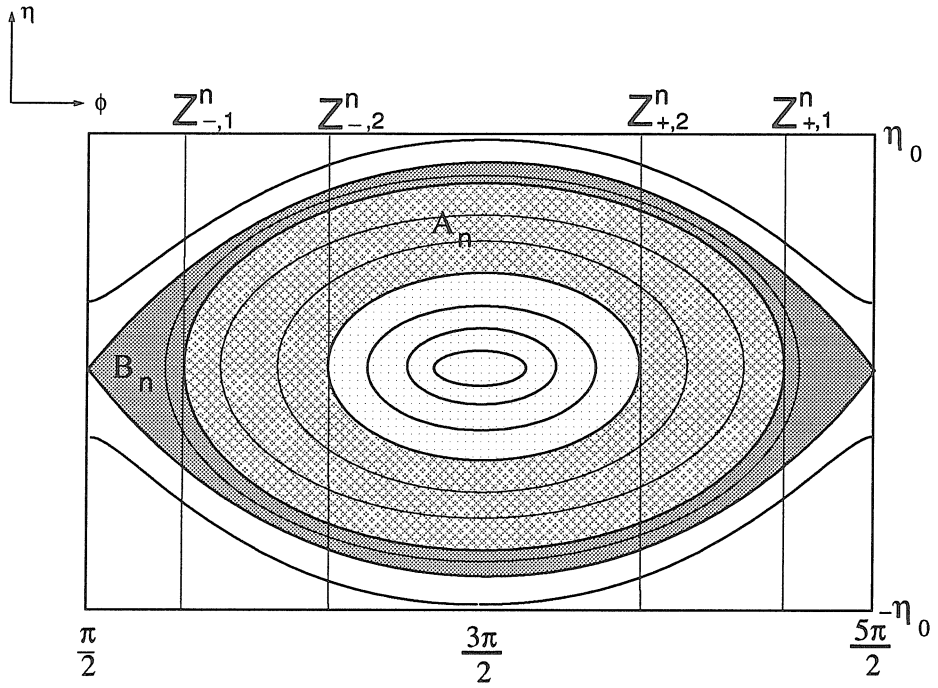

Figure 4.3: The layers A_n and B_n

orbit in $\mathcal{A}_\varepsilon$ with four jumping n-pulse homoclinic orbits (two from the perturbation of W_0^+ and two from W_0^-). Similarly,

$$A_j \cap B_n = B_j \cap B_n = \emptyset, \qquad j = 1, ..., n-1 \tag{4.2.19}$$

would mean that any internal orbit in B_n gives rise to an internal orbit in $\mathcal{A}_\varepsilon$ which has *eight* (jumping) n-pulse homoclinic orbits. Note, however, that $B_1 \cap B_n \neq \emptyset$; hence condition (4.2.19) is satisfied *only* for $n = 1$.

Fact 4. For $n = 1$, $\Delta\phi \neq 2l\pi$ conditions (4.2.18) and (4.2.19) are satisfied. Consequently, *with the exception of $\hat{\gamma}_1^R$, all internal orbits in A_1 perturb to orbits with four single-pulse transverse homoclinic orbits, and all in B_1 perturb to ones with eight single-pulse transverse homoclinic orbits.* This is discussed in Haller and Wig-

gins [28]. By Theorem 2.4.2 $\hat{\gamma}_1^R$ also gives rise to single pulse homoclinic orbits, but we can not claim that they are transversal. In fact, they really *are not*: the transversal intersections become nontransversal in the critical energy surface which is responsible for the disappearence of single-pulse orbits within the region

$$S_1 = \mathrm{Int}\,(\hat{\gamma}_1^R),$$

where the methods of [28] do not apply. The set $g_\varepsilon \circ \mathcal{B}_\varepsilon^{-1}(S_1)$ is C^1 ε-close to the set $\mathcal{S}_\varepsilon \subset \mathcal{A}_\varepsilon$ (mentioned in section 2.1) whose internal orbits *do not admit homoclinic behavior accessible to previous methods.* It is exactly this type of a situation which inspired the analysis in chapter 2.

It is now clear what we have to do to study the structure of the set S_1 in terms of the pulse number of the internal orbits it contains. We increase n from $N_1 = 1$ until we find that for some $N_2 > N_1$ a component of $\hat{Z}_-^{N_2}$ intersects S_1 transversally, i.e., it lies between the line $\phi = \frac{3\pi}{2}$ and the component of Z_-^1 falling closer to $\phi = \frac{3\pi}{2}$. This means that for the internal orbit $\hat{\gamma}_0$ lying in $A_{N_2} \backslash A_{N_1} \subset S_1$ condition (4.2.18) holds; hence $\hat{\gamma}_0$ gives rise to an internal orbit $\gamma_\varepsilon \subset \mathcal{A}_\varepsilon$ (with $g_\varepsilon^{-1}(\gamma_\varepsilon)$ and $\mathcal{B}_\varepsilon^{-1}(\hat{\gamma}_0)$ C^{r-1} ε-close) such that γ_ε has *four* N_2-pulse jumping transverse homoclinic orbits (see Theorem 2.4.4). We then repeat this procedure to find the minimal $N_3 > N_2$ such that a component of $\hat{Z}_-^{N_3}$ intersects

$$S_{N_2} = S_{N_1} \backslash A_{N_2}$$

transversally and conclude the existence of tranverse N_3-pulse homoclinic orbits for internal orbits perturbing from those inside $A_{N_3} \backslash A_{N_2} \subset S_{N_2}$. Clearly, we can repeat this construction inductively.

The sequence $N_1, N_2, ...$ terminates at some $N_j = p$ if

$$p\Delta\phi = 2l\pi, \tag{4.2.20}$$

with p and l relative prime integers, because then the closest component of Z_-^p to the line $\phi = \frac{3\pi}{2}$ is just that line itself and $S_p = \emptyset$. This means that all the orbits within S_{p-1} and outside an $\mathcal{O}(\varepsilon^{\frac{3}{4}})$ neigborhood of the elliptic fixed point at $(\eta, \phi) = (0, \frac{3\pi}{2})$ give rise to periodic orbits in $\mathcal{A}_\varepsilon$ with four p-pulse transverse homoclinic orbits. We have to exclude an $\mathcal{O}(\varepsilon^{\frac{3}{4}})$ neigborhood of the elliptic fixed point because our construction is based on following trajectories of the standard form with $\mathcal{O}(\varepsilon^{\frac{1}{4}})$ precision which translates to an $\mathcal{O}(\varepsilon^{\frac{3}{4}})$ error for system (2.1.1) (see the proof of Theorem 2.4.1).

On the other hand, if (4.2.20) does not hold for any $p \in \mathbb{Z}$, then we can construct an infinite sequence $\{N_i\}_{i=1}^{\infty}$ of pulse numbers with a corresponding sequence of layers $\{A_{N_{i+1}} \backslash A_{N_i}\}_{i=1}^{\infty}$ such that internal orbits in $A_{N_{i+1}} \backslash A_{N_i}$ give rise to periodic orbits of system (4.1.6) with four N_{i+1}-pulse transverse jumping homoclinic orbits. Again, for fixed $\varepsilon > 0$, all this is valid outside an $\mathcal{O}(\varepsilon^{\frac{3}{4}})$ neighborhood of the elliptic fixed point of the reduced Hamiltonian $\hat{\mathcal{H}}$.

4.3 Chaos in the two-mode model

To summarize the informal discussion of the previous section, we introduce the sequence of distances

$$\begin{aligned} d_0 &= \frac{\pi}{2}, \\ d_n &= \min\left(\left|\frac{3\pi}{2} - \phi_{n,1} \bmod 2\pi\right| , \left|\frac{3\pi}{2} - \phi_{n,2} \bmod 2\pi\right|\right) \qquad (4.3.1) \\ &= \min\left(\left|\pi - n\frac{\Delta\phi}{2}\right| \bmod 2\pi , n\frac{\Delta\phi}{2} \bmod 2\pi\right), \qquad (4.3.2) \end{aligned}$$

the sequence of pulse numbers

$$N_1 = 1, \qquad N_k = \min\{\ n\ |N_{k-1} < n < \infty,\ d_n < d_{N_{k-1}}\ \}, \tag{4.3.3}$$

and finally, the sequence of layers

$$L_{N_1} = S_0 \backslash S_1, \qquad L_{N_k} = A_{N_k} \backslash A_{N_{k-1}}. \tag{4.3.4}$$

As we noted earlier, from inside and outside, the layer L_{N_k} is bounded by two level curves of the reduced Hamiltonian, which are just the resonant internal orbits $\hat{\gamma}^R_{N_k}$ and $\hat{\gamma}^R_{N_{k-1}}$, respectively. Using (4.2.6) we have a general formula for the resonant internal orbit $\hat{\gamma}^R_{N_j}$ of the form

$$\hat{\gamma}^R_{N_j} \ = \ \{\ (\eta, \phi) \in \hat{A}\ ||\eta| = \sqrt{2\sqrt{2}\Gamma[\sin(\frac{3\pi}{2} + d_{N_j}) - \sin\phi]}\ \}, \tag{4.3.5}$$

where d_{N_j} is defined in (4.3.1). One can now use (4.3.5) to identify the layers by their boundaries. Based on Theorems 2.4.1-2.4.4 and Facts 1-3 of the previous section, we proved the following result:

Theorem 4.3.1 *Suppose that $\hat{\gamma}_0 \subset \hat{A}$ is periodic orbit of the reduced Hamiltonian $\hat{\mathcal{H}}$ defined in (4.2.6). Suppose further that for some $j > 0$ $\hat{\gamma}_0 \in L_{N_j}$ holds. Let $N \equiv N_j$ and define $b_{-,i} \in \hat{Z}^N_- \cap \hat{\gamma}_0$, $i = 1, 2$, and $b_{+,i} = \hat{\mathcal{R}}^N(b_{-,i})$. ($b_{-,1}$ and $b_{-,2}$ have the same ϕ coordinate and their η coordinates add up to zero). Then there exists $\varepsilon_0 > 0$ such that for $0 < \varepsilon < \varepsilon_0$*

(*i*) *$\mathcal{A}_\varepsilon = \mathcal{A}_0$ (defined in (4.2.3)) has four N-pulse homoclinic orbits $y^{N+}_{\varepsilon,i}$ and $y^{N-}_{\varepsilon,i}$, $i = 1, 2$, which are positively and negatively asymptotic to an internal orbit $\gamma_\varepsilon \in \mathcal{A}_\varepsilon$. Moreover, $g^{-1}_\varepsilon(\gamma_\varepsilon)$ and $\mathcal{B}^{-1}_\varepsilon(\hat{\gamma}_0)$ are C^{r-1} ε-close in $\hat{A}$. If $N = 1$ the number of homoclinic orbits is actually eight with the same properties.*

(*ii*) *y_ε^{N+} and y_ε^{N-} lie in the intersection of $W^u(\gamma_\varepsilon^-)$ and $W^s(\gamma_\varepsilon^+)$. This intersection is transversal within the energy surface $E_\varepsilon(h)$ ($h = H|\gamma_\varepsilon^+ = H|\gamma_\varepsilon^-$) provided $\hat{\gamma}_0 \neq \hat{\gamma}_N^R$.*

(*iii*) *Statement (iii) of Theorem 2.4.4 holds with the embedding $g_\varepsilon = g_0$ defined in (4.2.4), and with the jump-sequence $\hat{\chi}_k$ defined in (4.2.15).*

(*iv*) *System (4.1.6) has Smale-horseshoes near γ_ε on energy surfaces sufficiently close to $E_\varepsilon(h)$.*

From (4.3.1) one can see that the sequence $N_1, N_2, ...$ of pulse numbers is defined recursively through the repeated iteration of the circle map

$$\mathcal{M}: \phi \mapsto \phi + \frac{\Delta\phi}{2}.$$

In particular, we simultaneously start two iterations from $\phi_0 = \frac{\pi}{2}$ and $\phi_0' = \frac{3\pi}{2}$, respectively, and let $d_1 = d_{N_1}$ be the minimal distance of the first iterates from ϕ_0. We then keep iterating simultaneously until for some $N_2 > N_1$ one of the two N_2-iterates falls in the d_{N_1} neighborhood of ϕ_0. We then make a record of N_2 and iterate further until, for some $N_3 > N_2$, one of the two N_3-iterates falls in the $d_{N_2} < d_{N_1}$ neighborhood of $\phi_0 = \frac{\pi}{2}$, and make a record of N_3, etc. If (4.2.20) is satisfied we terminate the iteration at the p-th step because $d_{N_p} = 0$. If, however, (4.2.20) does not hold, we can continue our recursive construction infinitely through the iteration of the map $\mathcal{M}$. Note that in this latter case $\mathcal{M}$ is an irrational rotation of the circle which has two important effects on the structure of the set of layers defined in (4.3.4). First, although the iteration will result in two dense orbits and hence does not terminate, it will take more and more "time" for one of the two simultaneously iterated discrete orbits to hit the current gradually shrinking target, i.e., the d_{N_k} neighborhood of ϕ_0. This will result in a rapid increase in subsequent pulse numbers in the sequence N_j. Hence, approaching the elliptic fixed point of $\hat{\mathcal{H}}$ we must

experience a dramatic increase in the pulse numbers of the related homoclinic orbits on passing the boundary between the layers L_{N_j} and $L_{N_{j+1}}$. Second, $\mathcal{M}$ has a sensitive dependence on parameters, i.e., for a slight change in the parameter k (and hence in the phase shift $\Delta\phi(k)$) high iterates of the map $\mathcal{M}$ will change significantly. So will the sequence of pulse numbers, hence we conclude that the partition of S into layers is *not structurally stable* unless we limit the maximum pulse number considered and choose our bound ε_0 on the perturbation parameter ε accordingly.

To demonstrate the dependence of the pulse number sequence (4.3.3) on the parameters, we chose to vary $\Delta\phi$ instead of k (one can relate these two parameters using (4.2.5) and Fig. 4.1). In Figs. 4.4-4.6 we plotted the pulse number sequence as a function of the phase shift $\Delta\phi$. We chose 650, 100, and 10, respectively, as upper bounds on the pulse numbers. As we predicted above, the figures show a stable pulse-distributaion for low pulses but show an increasing sensitivity of higher and higher pulses for small changes in the phase shift. Note that around $\Delta\phi = \frac{4\pi}{5}$ there is a region which seems quite stable for high pulses, too. This region of the parameter space shows an abundance of transverse homoclinic orbits with a wide spectrum of pulse numbers. At the same time, there are "tounges" in the diagrams where there are very few homoclinic orbits, the strongest tounges being at $\Delta\phi = 0, \pi, 2\pi$. Fig. 4.1 shows that these regions will repeat themselves with an increasing speed as k tends to 0.5 and $\Delta\phi$ sweeps the interval $[0, 2\pi]$ more and more frequently. In Figs. 4.7-4.8 we also show the distance sequence d_{N_j} as a function of the phase shift. The sequence $\{d_{N_j}\}_{j=1}^{\infty}$ gives the angular radii of subsequent resonant internal orbits, or alternatively, describes the half-width of subsequent layers in the layer sequence (4.3.4). To generate the figures we plotted the elements of the distance sequence for which the corresponding pulse number is less than or equal to 10 and 50, respectively. These plots show the striking self-affinity of a fractal structure which grows

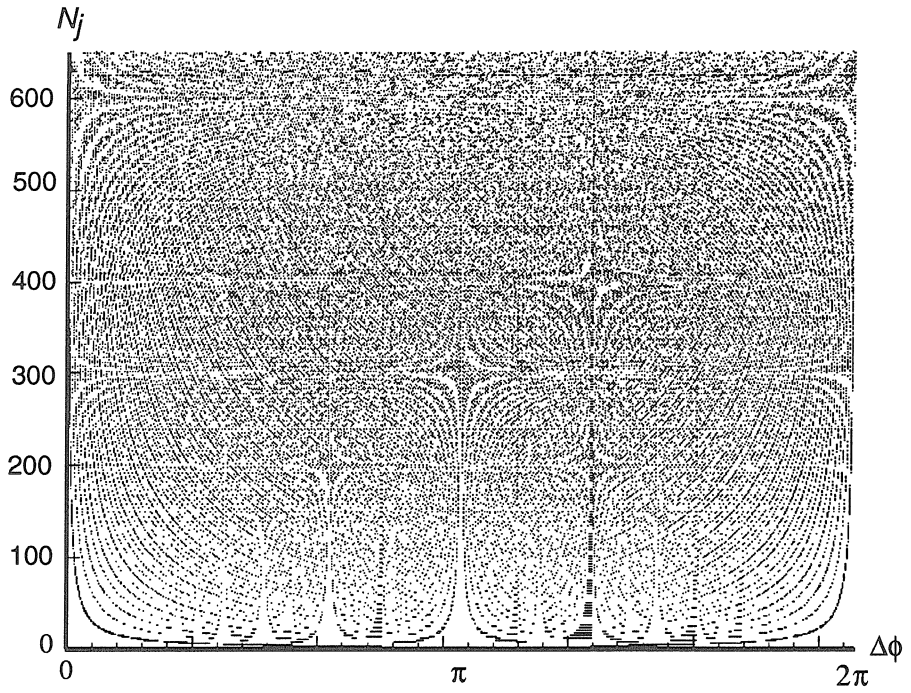

Figure 4.4: The pulse number sequence as a function of the phase shift

as we increase the maximum pulse-number considered. Hence, even if we had better methods and did not have to exclude a neighborhood of the center from the analysis, it would be impossible to describe the exact nature of the homoclinic phenomena associated with the "core" of the resonance, i.e., the elliptic fixed point of $\hat{\mathcal{H}}_\varepsilon$. Instead, one finds a high degree of stochasticity revealing itself in a fractal-type structure of layers containing periodic orbits with the same pulse number. Finally in Figs. 4.10 and 4.11 we present some simulation results. The parameters for Fig. 4.10 are: $\Gamma = 1.$, $k = 0.65$, energy$= -9.3 \times 10^{-6}$, $\sqrt{\varepsilon} = .003$, energy conservation$= 7.9 \times 10^{-9}$, stepsize$= 10^{-4}$. The parameters for Fig. 4.11 are: $\Gamma = 1.$ $k = 1.$, $\sqrt{\varepsilon} = .003$, energy$= -1.1 \times 10^{-5}$, energy conservation$= 5.0 \times 10^{-9}$, stepsize$= 10^{-4}$. We chose to iterate the leading order vectorfield of the standard form (2.4.1) which we computed for system (4.1.6). We picked

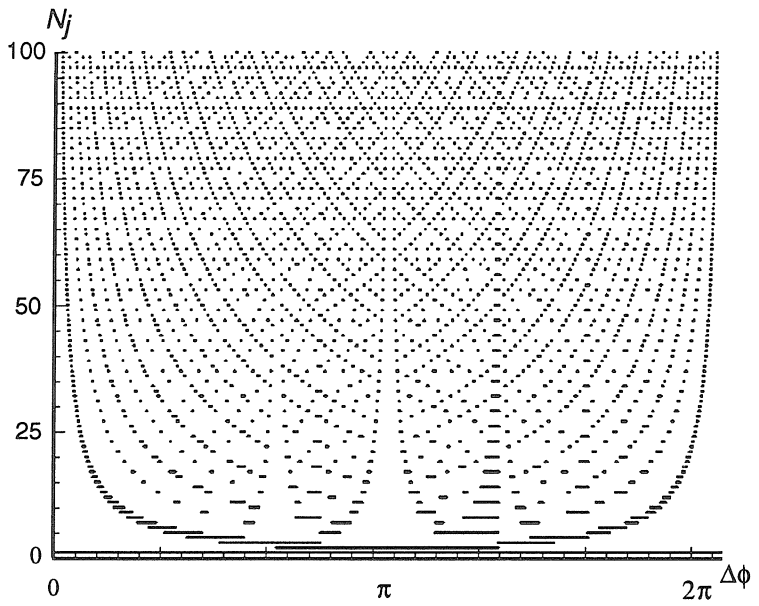

Figure 4.5: The pulse number sequence as a function of the phase shift

internal orbits (shown in the upper-right hand corner of the figures) with pulse numbers $N = 2$ and $N = 3$ in the resonance band, respectively, and iterated their unstable manifolds until they reintersected the corresponding (local) stable manifolds. In the figures we show the "shadowing orbits" which are preticted to be C^1 $\sqrt{\varepsilon}$ approximations for the actual intersection of the orbit-cylinders outside a neighborhood of the slow manifold $\mathcal{A}_\varepsilon$. One can find a good agreement between the theoretical predictions and the numerical results.

We close this final chapter by noting that using the results of section 2.5, one can also investigate the effect of weakly dissipative perturbations on the Hamiltonian limit we analyzed above. The analysis reveals the existence of multiple pulse jumping orbits which are asymptotic to fixed points in the resonance band in one time direction and leave the resonance band in the other time-direction. This establishes a new mechanism

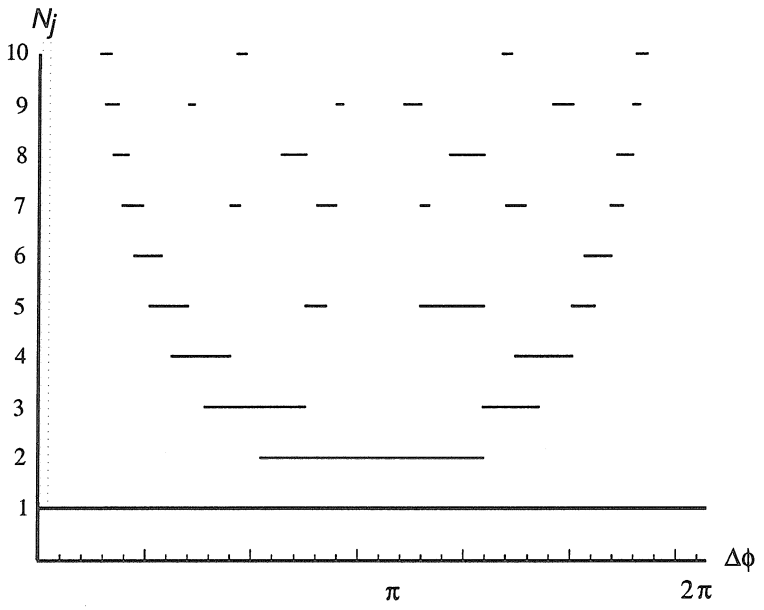

Figure 4.6: The pulse number sequence as a function of the phase shift

for capture in resonance: *jumping into a resonance through multiple pulses.* Since, as predicted by the dissipative version of the energy-phase method, this jumping phenomenon holds not only for individual orbits but families of orbits, it must have a characteristic effect on the near-resonance dynamics of the two-mode model (4.1.6). In particular, one must be able to observe high-pulse "jumping" for the dissipative system. This behavior was already pointed out by Bishop *et al.* [7]-[8] and partially explained for some unphysical parameter configurations in Kovačič and Wiggins [44]. Related results can also be found in McLaughlin *et al.* [55] where a (single-pulse) orbit homoclinic to a saddle in the resonance band is proved to exist for a physically realistic codimension-one set of the parameter space. The authors construct Smale-horseshoes in the vicinity of the homoclinic orbit and also study the truncated system numerically.

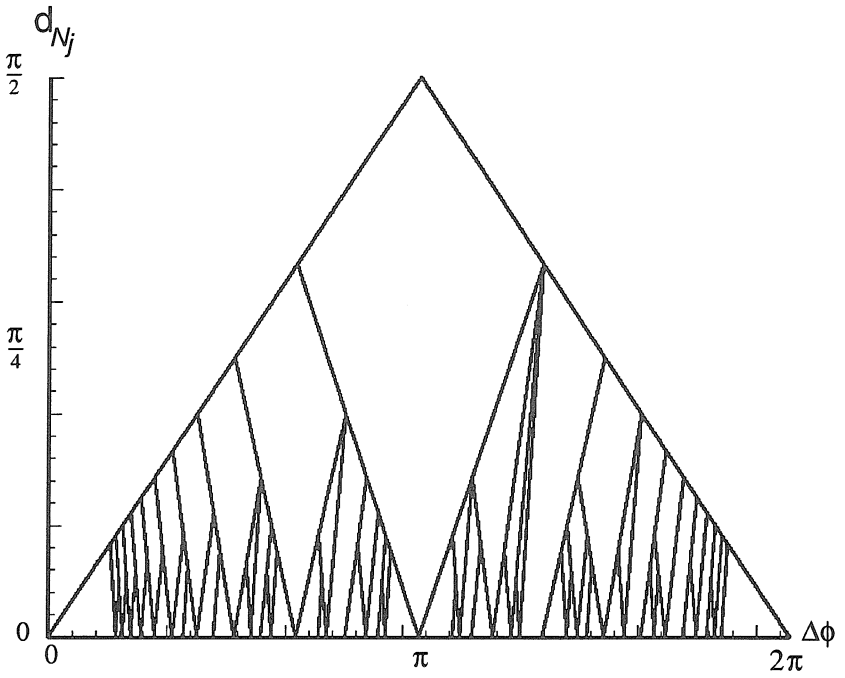

Figure 4.7: The distance sequence d_{N_j} as a function of $\Delta\phi$ for $N_j \leq 10$

We hope that our results contribute to the understanding of the chaotic jumping (between two spatially dependent states) observed in the two-mode model, and highlight some aspects for the future study of the chaotic attractor of the driven-damped nonlinear Schrödinger equation.

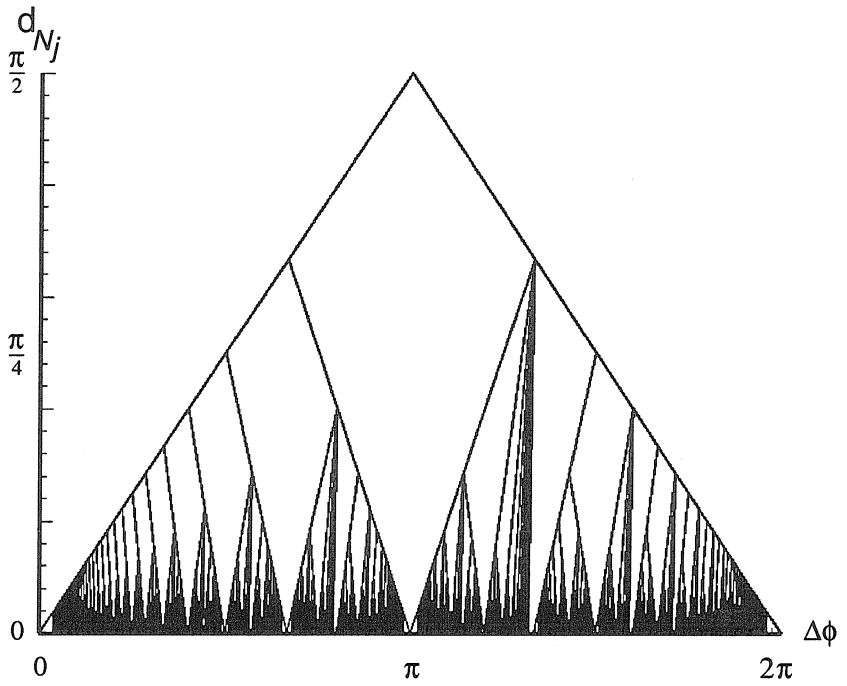

Figure 4.8: The distance sequence d_{N_j} as a function of $\Delta\phi$ for $N_j \leq 50$

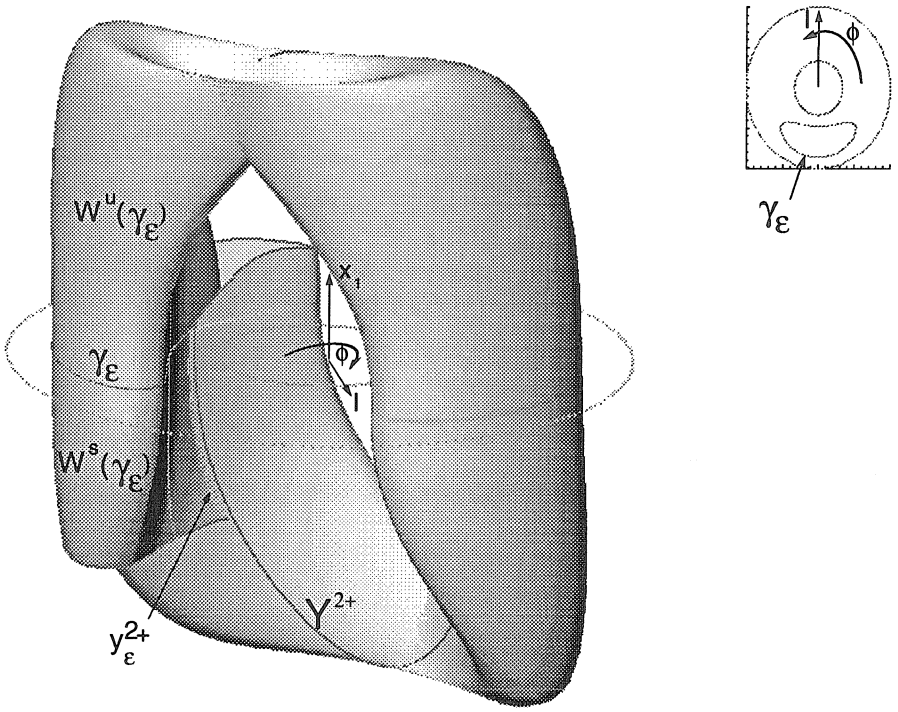

Figure 4.9: Double-pulse orbit homoclinic to a periodic solution in the resonance band

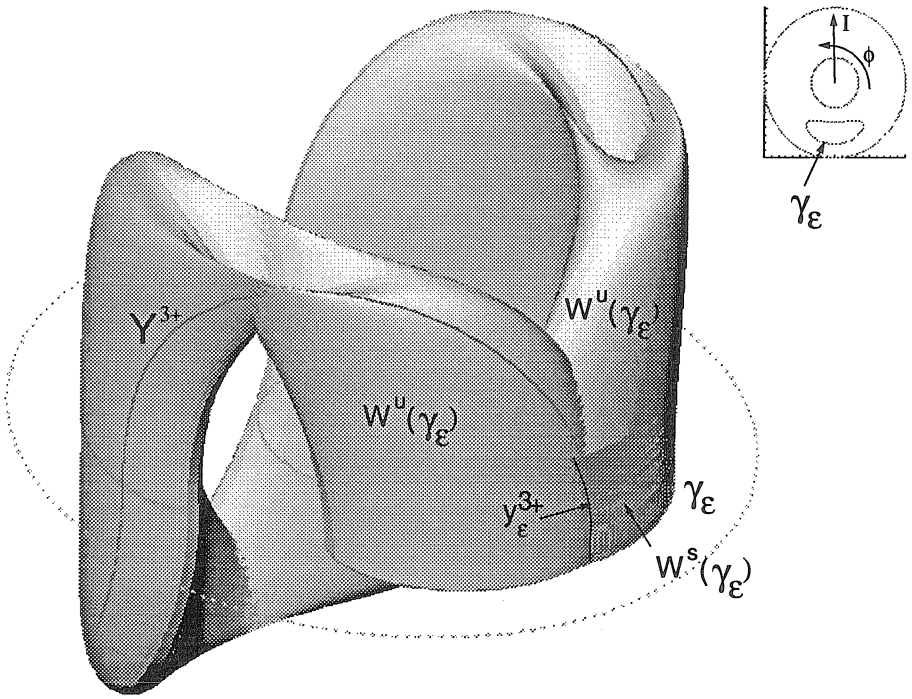

Figure 4.10: Triple-pulse orbit homoclinic to a periodic solution in the resonance band

References

[1] Abraham, R. and Marsden, J.E., *Foundations of Mechanics*, The Benjamin/Cummings Publishing Co. Inc., Reading (1978).

[2] Arnold, V.I., *Mathematical Methods of Classical Mechanics*, Springer-Verlag, New York (1978).

[3] Arnold, V.I., Small denominators and the problem of stability of motion in classical and celestial mechanics, *Russ. Math. Surv.* **18/6** (1963) 85.

[4] Arnold,V.I., Instability of dynamical systems with many degrees of freedom, *Dokl. Akad. Nauk. USSR* **156** (1964) 9.

[5] Arnold,V.I., Kozlov,V.V., and Neishtadt, A.I., *Mathematical Aspects of Classical and Celestial Mechanics* in *Dynamical Systems III*, V.I. Arnold (ed.), Springer-Verlag, New York (1988).

[6] Benettin, G. and Gallavotti, G., Stability of motions near resonances in quasi-integrable Hamiltonian systems, *J. Stat. Phys.* 44 (1986) 293.

[7] Bishop A.R., Forest, M.G., McLaughlin, D.W., and Overman, E.A., A modal representation of chaotic attractors for the driven, damped pendulum chain, Phys. Lett. A **144** (1990) pp. 17-25.

[8] Bishop, A.R., Flesch, R., Forest, M.G., McLaughlin, D.W., and Overman, E.A., Correlations between chaos in a perturbed Sine-Gordon equation and a truncated model system, *SIAM J. Math. Anal.* **21** (1990) pp. 1511-1536.

[9] Chiercia, L. and Gallavotti, G., Drift and diffusion in phase space, Universitá di Roma preprint (1992).

[10] Churchill, R.C., Pecelli, G., and Rod, D.L., A survey of the Henon-Heilies Hamiltonians with applications to related examples, in *Stochastic Behavior in Classical and Quantuum Hamiltonian Systems, Lect. Notes. in Phys.* **93**, Springer-Verlag, New-York (1979).

[11] Churchill, R.C., Kummer, M., and Rod, D.L., On averaging, reduction and symmetry in Hamiltonian systems, *J. Diff. Eqs.* **49** (1983) 359.

[12] Churchill, R.C. and Rod, D.L., Homoclinic and heteroclinic orbits of reversible vectorfields under perturbation, *Proc. Royal Soc. of Ed.* **102A** (1988) 345.

[13] Cushman, R., Notes on the 1:2:2 resonance, unpublished (1985).

[14] Cushman, R., Rod, D.L., The reduction of the 1:1 resonance, *Physica D* **6** 105.

[15] Delshams, A., Por que la difusion de Arnold aparece genericamente en los systemas Hamiltonians con mas de 2 grados de libertad, Ph.D. thesis, Universitat de Barcelona (1984).

[16] Delshams, A., Terera, M., and Seara, M., An asymptotic expression for the splitting of separatrices of the rapidly forced pendulum, U. Politécnice de Catalunya preprint (1991).

[17] Devaney, R., Homoclinic orbits in Hamiltonian systems, *J. Diff. Eqs.* **21** (1976) 431.

[18] Duistermaat, J.J., Non-integrability of the 1: 2: 2 resonance, *Ergod. Theory and Dyn. Sys.* 4 (1984) 553.

[19] Feng, Z.C. and Sethna, P.R., Symmetry breaking bifurcations in resonant surface waves, *J. Fluid Mech.* **199** (1989) pp. 495-518.

[20] Feng, Z.C. and Sethna, P.R., Global bifurcation and chaos in parametrically forced systems with one-one resonance, *Dynamics and Stability of Systems*, **5** (1990) p. 201.

[21] Feng, Z.C. and Sethna, P.R., Global bifurcations in the motion of parametrically excited thin plates, (1992) University of Minnesota preprint.

[22] Feng, Z.C. and Wiggins, S., On the existence of chaos in a class of two-degree-of-freedom, damped, strongly parametrically forced mechanical systems with broken $O(2)$ symmetry, to appear in *ZAMP* (1992).

[23] Fenichel, N., Persistence and smoothness of invariant manifolds for flows, *Ind. Univ. Math. J.* **21** (1971) pp. 193-225.

[24] Fenichel, N., Geometric singular perturbation theory for ordinary differential equations, *J. Diff. Eqs.* **31** (1979) pp. 53-98.

[25] Ford, J., Waters, J., Computer studies of energy sharing and ergodicity for nonlinear oscillator systems, *J. Math. Phys.* **4/10** (1963) 1293.

[26] Ford, J. and Lunsford, G.H., Stochastic behavior of resonant nearly linear oscillator systems in the limit of zero nonlinear coupling, *Phys. Rev. A* **1/1** (1970) 59.

[27] Guckenheimer, J. and Holmes, P., *Nonlinear Oscillations, Dynamical Systems and Bifurcations of Vectorfields*, Springer-Verlag, New York (1983).

[28] Haller, G. and Wiggins, S., Orbits homoclinic to resonances: the Hamiltonian case, to appear in *Physica D* (1992).

[29] Hirsch, M.W., Pugh, C.C., and Shub, M., *Invariant Manifolds*, *Lect. Notes. in Math.* **583**, Springer-Verlag, New York (1975).

[30] Holm, D.D., Notes on reduction of integrable resonant normal forms, unpublished (1989).

[31] Holmes, P. and Marsden, J., Horseshoes in perturbations of Hamiltonian systems with two degrees of freedom, *Comm. Math. Phys.* **82** (1982) pp. 523-544.

[32] Holmes, P., Chaotic motion in a weakly nonlinear model for surface waves, *J. Fluid. Mech.* **162** (1986) pp. 365-388.

[33] Holmes, P., Marsden, J., and Scheurle, J., Exponentially small splittings of separatrices with application to KAM theory and degenerate bifurcations, *Cont. Math.* **81** (1988) 213.

[34] Hoveijn, I. and Verhulst, F., Chaos in the 1:2:3 Hamiltonian normal form, *Physica D* **44** (1990) 397.

[35] Hoveijn, I., Aspects of resonance in dynamical systems, Ph.D. thesis (1992).

[36] Iooss, G., *Bifurcations of Maps and Applications*, North-Holland Publishing Co. (1979).

[37] Ito, H., Long periodic orbits near an equilibrium and the averaging method in higher-order resonances, *J. Diff. Eqs.* **51** (1984) p. 232.

[38] Jones, C.K.R.T. and Kopell, N., Tracking invariant manifolds with differential forms in singularly perturbed systems, to appear in *J. Diff. Eq.* (1992).

[39] Jones, C.K.R.T., Kaper, T.J., and Kopell, N., *ELESE: The exhange lemma with exponentially small error*, preprint (1993).

[40] Kaper, T.J. and Kovačič, G., Multiple-pulse orbits homoclinic to resonance bands, preprint (1993).

[41] Kirchgraber, U., On the existence and geometry of invariant tori in the method of averaging, *Z. Ang. Math* **38** (1987) p. 213.

[42] Kirk, V., Marsden, J., and Silber, M., Spheres and pinched spheres, unpublished notes (1992).

[43] Kopell, N., Invariant manifolds and the initialization problem for some atmospheric equations, *Physica D*, **14** (1985) pp. 203-215.

[44] Kovačič, G. and Wiggins, S., Orbits homoclinic to resonances, with an application to chaos in the damped and forced Sine-Gordon equation, *Physica D* **57** (1992) pp. 185-225.

[45] Kovačič, G., Singular perturbation theory for homoclinic orbits in a class of near-integrable Hamiltonian systems, RPI preprint (1992).

[46] Kovačič, G., Singular perturbation theory for homoclinic orbits in a class of near-integrable dissipative systems, RPI preprint (1992).

[47] Kovačič, G., Hamiltonian dynamics of orbits homoclinic to a resonance band, *Phys. Lett. A* **167** (1992) pp. 137-142.

[48] Kummer, M., An interaction of three resonant modes in a nonlinear lattice, *J. Math. Anal. and Apps.* **52** (1975) 64.

[49] Kummer, M., On resonant classical Hamiltonians with two degrees of freedom near an equilibrium point, in *Stochastic Behavior in Classical and Quantuum Hamiltonian Systems, Lect. Notes in Phys.* **93**, Spriger-Verlag, New-York (1979).

[50] Kummer, M., On resonant Hamiltonian systems with finitely many degrees of freedom, in *Local and global methods of nonlinear Dynamics, Lect. Notes in Phys.* **252**, Springer-Verlag, New York (1986).

[51] Kummer, M., On resonant classical Hamiltonians with n frequencies, *J. Diff. Eqs.* **83** (1990) 220.

[52] de la Llave, R. and Wayne, C.E., Whiskered and low dimensional tori in nearly integrable Hamiltonian systems, (1990) University of Texas, Austin preprint.

[53] Lochak, P., Canonical perturbation theory via simultaneous approximation, D.M.I. preprint (1992).

[54] Martinet, L., Magnenat, P., and Verhulst, F., On the number of isolating integrals in resonant systems with three degrees of freedom, *Celest. Mech.* **29** (1981) 93.

[55] McLaughlin, D., Overman, E.A.II., Wiggins S., and Xiong, C., Homoclinic orbits in a four dimensional model of a perturbed NLS equation: a geometric singular perturbation study, *preprint* (1993).

[56] Mielke, A., Holmes, P., and O'Reilly, O., Cascades of homoclinic orbits to, and chaos near, a Hamiltonian saddle-center, *J. Dyn. and Diff. Eqs.* 4 (1992) pp. 95-126.

[57] Montaldi, J., Roberts, M., and Stewart, I., Existence of nonlinear normal modes of symmetric Hamiltonian systems, *Nonlinearity* **3** (1990) 695.

[58] Montaldi, J., Roberts, M., and Stewart, II., Stability of nonlinear normal modes of symmetric Hamiltonian systems, *Nonlinearity* **3** (1990) 731.

[59] Moser, J., *Stable and Random Motions in Dynamical Systems*, Princeton University Press, Princeton (1973).

[60] Moser, J., Periodic orbits near an equilibrium a theorem by Alan Weinstein, *Comm. Pure Appl. Math* **23** (1970) 609.

[61] Nekhorosev, N.N., An exponential estimate on the time of stabilty of nearly-integrable Hamiltonian systems, *Russ. Math. Surv.* **32** (1977) 1.

[62] Sacker, R.J., A new approach to the perturbation theory of invariant surfaces, *Comm. Pure. Appl. Math* **18** (1965) 717.

[63] Sanders, J.A. and Verhulst, F., *Averaging methods in Nonlinear Dynamical Systems*, Springer-Verlag, New York (1985).

[64] Scheurle, J. and Marsden, J.E., Bifurcation to quasiperiodic tori in the interaction of steady-state and Hopf bifurcations, *SIAM J. Math. Anal.* **15** (1984) 1055.

[65] Silnikov, L.P., A contribution to the problem of the structure of an extended neighborhood of a rough equilibrium state of saddle-focus type, *Math. USSSR Sbornik* **10** (1970) pp. 91-102.

[66] Smale, S., Diffeomorphisms with many periodic points, in *Differential and Combinatorial Topology*, S.S. Cairns (ed.), Princeton Univ. Press, Princeton (1963) pp. 63-80.

[67] Tien, W.-M. and Namachchivaya, N.S., Nonlinear dynamics of a shallow arch under periodic excitation II: 1:1 internal resonance, submitted to the *Int. J. Non-Lin. Mech.* (1992).

[68] Tin, S., On the dynamics of tangent spaces near a normally hyperbolic invariant manifold, preprint (1993).

[69] Van der Aa E. and Sanders, J.A., The 1:2:1 resonance, its periodic orbits and integrals, in *Asymptotic Analysis, Lect. Notes in Math* **711**, Springer-Verlag, New York (1979).

[70] Van der Aa, E., First order resonances in three-degree-of-freedom systems., *Celest. Mech.* **31** (1983) 163.

[71] Van der Aa, E. and Verhulst, F., Asymptotic integrability and periodic solutions of a Hamiltonian system in 1:2:2 resonance, *SIAM J. Math. Anal.* **15** (1984) 890.

[72] Weinstein, A., Lagrangian submanifolds and Hamiltonian systems, *Ann. Math.* **98** (1973) pp. 377-410.

[73] Weinstein, A., Normal modes for nonlinear Hamiltonian systems, *Inv. Math.* **20** (1973) 47.

[74] Wiggins, S., *Global Bifurcations and Chaos-Analytical Methods*, Springer-Verlag, New York (1988).

[75] Yang, X.L. and Sethna, P.R., Non-linear phenomena in forced vibrations of a nearly square plate: antisymmetric case, *J. Sound and Vib.* **155** (1992) pp. 413-441.